Locus coeruleus physiology in physiology in Alzheimer's disease

By

Michael A. Kelberman

Doctor of Philosophy

Graduate Division of Biological and Biomedical Science

Neuroscience

David Weinshenker

Advisor

Shella Keilholz

Committee Member

Annabelle Singer

Committee Member

Elena Vazey

Committee Member

Jay Weiss

Committee Member

Accepted:

Kimberly Jacob Arriola, Ph.D, MPH

Dean of the James T. Laney School of Graduate Studies

Date

Locus coeruleus physiology in physiology in Alzheimer's disease

By

Michael A. Kelberman

B.S. University of Massachusetts Amherst, 2018

Advisor: David Weinshenker, Ph.D.

An abstract of

a dissertation submitted to the Faculty of the

James T. Laney School of Graduate Studies of Emory University

in partial fulfillment of the requirements for the degree of Doctor of Philosophy in Neuroscience

2023

Abstract

Locus coeruleus physiology in Alzheimer's disease

By Michael A. Kelberman

Alzheimer's disease (AD) is the most common form of dementia and is expected to pose a significant societal and financial burden as the population ages. AD is characterized by the aggregation of extracellular amyloid-beta plaques and intracellular tau neurofibrillary tangles. Therapeutic interventions have targeted these two protein aggregates but have failed to yield a cure. Subcortical regions, and specifically the noradrenergic locus coeruleus (LC), are the earliest sites of tau aggregation, occurring decades prior to the onset of cognitive deficits. However, the consequences of such early tau pathology in the LC are not well defined. Specifically, changes in LC activity in AD are inferred by their correlates in human imaging and behaving animals, and the consequences of hyperphosphorylated tau on neuronal activity in other brain regions. In this dissertation, I first described how tau pathology affects LC activity with electrophysiological recordings in wild-type (WT) and TgF344-AD rats, a preclinical model of AD that develops LC tau pathology prior to substantial pathological forebrain deposition. I next explored mechanisms underlying this altered activity by comparing LC gene expression in age-matched WT and TgF344-AD animals. Finally, I expanded previous behavioral characterizations of this rat model by testing measures of anxiety-like phenotypes, arousal, and active/passive coping. I found LC hyperactivity and downregulation of inhibitory markers coincident with the emergence of anxiety-like behaviors in 6-month TgF344-AD rats. Meanwhile, 15-month TgF344-AD rats demonstrate LC hypoactivity and a compensatory upregulation of genes involved in norepinephrine synthesis, packaging, and reuptake in a likely attempt to counteract worsening cognitive deficits at this age. Overall, this dissertation confirms and extends previous models of LC dysfunction along the progression of AD. Namely, that early non-cognitive behavioral phenotypes are consistent and coincident with the appearance of LC hyperphosphorylated tau pathology and increased neuronal firing, while later LC hypoactivity parallels the emergence of disease-typical cognitive impairments. I add potential mechanistic underpinnings by delineating changes in LC molecular signatures that align with observed changes in LC activity and behavior at each stage. These data will be crucial for the rational design and implementation of noradrenergic-based therapies to improve AD symptoms and impede disease progression.

Locus coeruleus physiology in physiology in Alzheimer's disease

By

Michael A. Kelberman

B.S. University of Massachusetts Amherst, 2018

Advisor: David Weinshenker, Ph.D.

A dissertation submitted to the Faculty of the

James T. Laney School of Graduate Studies of Emory University

in partial fulfillment of the requirements for the degree of Doctor of Philosophy in Neuroscience

2023

Acknowledgments

I would like to first thank each of my committee for their unwavering support and guidance throughout my graduate studies. Dr. Elena Vazey was the most influential mentor in my decision to pursue a graduate degree. She gave me the opportunity to join her lab as an undergraduate and exposed me to the locus coeruleus-norepinephrine system. I will be forever grateful for that opportunity and her enduring support, and hope to continue contributing to this field throughout my career. I would also like to thank Dr. Jay Weiss for allowing me to use his colony space for housing our animals and lab space to perform electrophysiology experiments described here. He also taught me how to collect electrophysiology data from anesthetized animals, and without him, Chapter 2 of this dissertation would have been impossible. I would like to thank Dr. Annabelle Singer for her endless supply of tips and recommendations for my experiments and my career plans. I would also like to thank Dr. Shella Keilholz who guided me through the neuroimaging field when I came into graduate school and joined the collaboration between her and David. The work from this project does not appear in this dissertation, but I believe has the potential to be some of the most influential work that will come out of my graduate research. I would also like to thank the various other members of the Keilholz lab for accepting me as one of their lab mates and for their help in developing methods, analyzing, and thinking about the data collected as part of this collaboration.

I would like to thank all the members of the Weinshenker lab for laying the foundation of and assisting me in my dissertation work. I would like to thank Drs. Rachel Tillage, Daniel Lustberg, and Stephanie Foster, who welcomed me into the lab with open arms and guided me in the early days as a graduate student. I would also like to thank Drs. Jacki Rorabaugh and Claire Anderson, who performed experiments that laid the foundation for this dissertation. I also would like to acknowledge the current and future set of trainees who will continue to expand on my work, in addition to exploring their own interests within the lab: Anu Korukonda, Leslie Hassanein, Abigail Galvez, Dr. Brittany Pate, Dr. Maggie Tish, and Alexia Marriott. Next, I would like to thank Dr. Katharine McCann who appears as or will appear as a co-author on nearly every manuscript that I publish from David's lab. She is a jack of all trades and has improved every aspect of my science. Finally, I am eternally grateful to Dr. Alexa Iannitelli, my lab twin and closest friend during graduate school; someone who challenged me to be my best self, both in and out of lab, and was always available to listen and offer advice, especially during coffee breaks. There is no one else I would rather have had next to me during graduate school. Finally, I would like to thank my primary mentor, Dr. David Weinshenker. David's passion for science is, in my opinion, unmatched. His door was always open to discuss data, plan new experiments (including my crazy ideas, some of which made it into this dissertation), and revise papers, grants, and other applications He was indispensable for my successful scientific achievements in graduate school. However, David was also a caring mentor, who offered advice and guidance on topics outside of research. To have a mentor that excels in promoting an environment where either scientific achievement or personal well-being thrives is difficult. Finding someone like David, who was able to balance both, is rare, and has allowed me to develop into the scientist I am today.

From the neuroscience program, I would like to thank Dr. Ellen Woon, who was my guide during my interviews at Emory, and who became my neurobuddy and one of my closest friends once I joined the program. I would also like to thank Nmachi Anumba from the Keilholz lab who works on the collaborative project between our labs. Over the past five years, we have run 150+ fMRI scans totaling over 300 hours in a room with loud noises and no windows. There are few people I could imagine doing this with while being on good terms, but I take it as a sign of our strong friendship.

Finally, I would like to thank my mother, father, and sister for their unconditional love and support throughout my educational endeavors, and their continued support and guidance as I remain in the academic realm. My adopted cat, Lyla, was one of the best decisions I made in graduate school, providing much needed breaks from what sometimes seemed like endless workdays. I want to also thank my partner Taylor, who was my biggest advocate during graduate school. She was understanding of my abnormal work hours that sometimes accompanies graduate school, and was always on hand to offer advice and support about various topics. I could not have completed this work without her and for that I am forever grateful.

This work is dedicated to Kun Lin, my cohort-mate who passed away during graduate school. He had an insatiable thirst for knowledge and was one of the kindest people I have ever met. I hope that this work would have made him proud.

Table of Contents

CHAPTER 1: INTRODUCTION

Parts of this chapter were used verbatim, with permission, from the following publications:

1. Ehrenberg AJ, Kelberman MA, et al. (2023) Priorities for research on neuromodulatory subcortical systems in Alzheimer's disease: Position paper from the NSS PIA of ISTAART. Alzheimers Dement Available at: http://dx.doi.org/10.1002/alz.12937.
2. Kelberman M, Keilholz S, Weinshenker D (2020) What's That (Blue) Spot on my MRI? Multimodal Neuroimaging of the Locus Coeruleus in Neurodegenerative Disease. Frontiers in Neuroscience 14 Available at: http://dx.doi.org/10.3389/fnins.2020.583421.

1.1 THE LOCUS COERULEUS

1.1.1 COMPOSITION, STRUCTURE, AND ORGANIZATION

The locus coeruleus (LC) is the main noradrenergic nucleus in the brain. The LC contains approximately 30,000-50,000 neurons bilaterally in adult humans and 3,000-5,000 neurons bilaterally in rodents (Mouton et al., 1994; Aston-Jones and Cohen, 2005a; Sara, 2009; Kelberman et al., 2020). LC neurons are densely packed within the brainstem, and the LC adopts a tubular shape extending along the dorsal-ventral axis that is apposed to the 4th ventricle (Gilvesy et al., 2022).

Both large multipolar and smaller fusiform cell morphologies have been observed in the LC (Swanson, 1976; Grzanna and Molliver, 1980; Schwarz and Luo, 2015). with the former more common in the ventral region and the latter enriched in dorsal portion of the nucleus (Swanson, 1976). Whether these cells possess different properties (inputs, projections, electrophysiological characteristics) remains to be determined.

The LC has been considered a singular nucleus, where all neurons support common functions through release of NE in target regions. For example, LC axons extend broadly throughout the brain and spinal cord, and individual neurons can innervate multiple regions (Loughlin et al., 1982; Berridge and Waterhouse, 2003). Moreover, LC neurons display firing rates typically between 0.5-2 spikes per second and respond en masse to aversive stimuli like footshock (Ishimatsu and Williams, 1996; Aston-Jones and Cohen, 2005a; Uematsu et al., 2017; Poe et al., 2020).

More recent evidence indicates a more nuanced description of LC function, including substantial heterogeneity at the level of individual neurons (Chandler et al., 2019). For example, LC neurons preferentially project to target sites based on location within the LC core (Kebschull

et al., 2016). Forebrain innervating neurons are concentrated in the anterior-dorsal portions of the LC and thalamic nuclei are innervated by LC neurons located in the posterior-dorsal area, while subcortical, cerebellar, and spinal cord projections arise mostly from the ventral aspects of the LC (Mason and Fibiger, 1979; Loughlin et al., 1986; Schwarz et al., 2015). Evidence suggests that some projections can be exclusive, such as LC neurons projecting exclusively to either the prefrontal or motor cortices (Chandler et al., 2014). Expanding on this evidence, the authors demonstrated that LC neurons projecting to the prefrontal cortex were enriched for excitatory markers and had higher firing rates. Activity of ensembles of LC neurons with specific and exclusive projections can also have differential effects on behavior. For example, amygdala projecting LC neurons promote aversive learning while mPFC projecting LC neurons result in extinguishing these behaviors (Uematsu et al., 2017). Similarly, mPFC projecting LC neurons also serve to produce aversion, anxiety-like phenotypes, and pain, whereas activation of spinal cord projecting LC neurons is antinociceptive (Hirschberg et al., 2017). While populations of LC neurons responded homogeneously to salient aversive stimuli, there is substantial variability to other cues which depended on the state of the animal (Uematsu et al., 2017). Whether LC neurons receive preferential inputs based on anatomical location, projection targets, biochemical nature, or some other factors has been virtually unexplored. Some recent lends support for this theory, as amygdala projecting LC neurons receive stronger innervation from cortical structures while medial prefrontal cortex projecting LC neurons are innervated more heavily by subcortical structures (Sulkes Cuevas et al., 2023). In addition to variable afferent and efferent connections, there is heterogeneity of neuropeptide co-expression within the LC. Up to 80% of LC neurons co-express galanin and a smaller proportion co-express neuropeptide Y, and this expression is anatomically restricted (Holets et al., 1988; Schwarz and Luo, 2015).

Sexual dimorphism adds an extra layer of complexity to LC function. For example, gene expression of male and female LC neurons differs remarkably (Mulvey et al., 2018). One specific gene of focus encoded the prostaglandin E2 receptor EP3. Application of an EP3 agonist suppressed tonic LC activity, but to a greater degree in female mice, and prevented stress-induced anxiety in females. Another study demonstrated that ablation of pituitary adenylate cyclase activating peptide receptors in the LC had opposing effects in males and females by increasing energy expenditure and food intake, respectively (Duesman et al., 2022). Females have more complex dendritic branching and are theorized to have a greater overall number of LC neurons compared to males (Bangasser et al., 2011; Bangasser et al., 2016), though some of these results might be strain dependent (Babstock et al., 1997). The LC in female animals is more responsive to stress and stress-related signaling (Curtis et al., 2006; Bangasser et al., 2010), which is unsurprising given the role of the LC in stress and anxiety and the higher prevalence of stress-related disorders in females (Bangasser et al., 2016).

While the LC is primary source of the neurotransmitter norepinephrine (NE) for the brain, and the sole source for areas such as the hippocampus, it is important to note that there are other noradrenergic nuclei located within the brainstem and pons (A1, A2, A4, A5, and A7) that are composed of fewer neurons and that project less widely (Waterhouse and Chandler, 2016).

1.1.2 NOREPINEPHRINE SYNTHESIS, RELEASE, AND DEGRADATION

1.1.2.1 Norepinephrine Synthesis

NE is produced in axon terminals beginning with the conversion of phenylalanine into L-tyrosine. L-tyrosine is then converted to L-DOPA by the rate-limiting enzyme tyrosine hydroxylase (TH). L-DOPA is converted to dopamine (DA) by aromatic acid decarboxylase (AADC) decarboxylase. All of this takes place in the cytoplasm, but once synthesized, DA is packaged into

synaptic vesicles by the vesicular monoamine transporter 2 (VMAT2). Within vesicles, dopamine β-hydroxylase (DBH) converts DA into NE. NE can also be converted into adrenaline by the enzyme phenylethanolamine N-methyltransferase in adrenergic cells including small nuclei in the pons and peripherally in the adrenal glands.

1.1.2.2 Norepinephrine Release and Receptors

NE is released from small clear and large dense core vesicles in axons that are mostly unmyelinated, primarily via volume transmission/non-synaptic release from varicosities (Aston-Jones et al., 1985; Atzori et al., 2016; Mather et al., 2016; Kelberman et al., 2020), though there is some evidence of synaptic NE release (Aston-Jones and Waterhouse, 2016; Waterhouse and Chandler, 2016). NE acts throughout the neuraxis via three primary G-coupled receptor subtypes: α1, α2, and β. α1 and β receptors are coupled to Gq and Gs, respectively, and function mainly heteroreceptors on NE target cells. Gq-coupled receptors act through phospholipase C to convert phosphatidylinositol 4,5-bisphosphate into diacylglycerol and inositol 1,4,5-trisphosphate. These two signaling molecules release intracellular stores of calcium and active phosphokinase C to promote intracellular signaling cascades. Meanwhile, Gs-coupled receptors primarily activate adenylyl cyclase to convert ATP to cyclic AMP subsequently activating phosphokinase A to promote calcium influx. α2 receptors are primarily located on LC neurons themselves, but are also found on postsynaptic elements. α2 receptors are Gi-coupled and inhibit adenylyl cyclase activity, inducing neuronal inhibition. The population of these receptors that are located on LC neurons are often referred to as inhibitory autoreceptors (i.e. local release of NE binds to α2 receptors on LC neurons). This negative feedback mechanism is hypothesized to be advantageous in preventing over-activation of LC neurons, and is quite potent given that α2 receptors have the highest affinity for NE of any subtype. α1 receptors display intermediate binding affinity for NE while β receptors demonstrate the lowest affinity for NE (Hussain et al.,

2023). With the exception of α2 receptors, all adrenergic receptors have slightly higher or equal affinity for adrenaline as NE.

1.1.2.3 Norepinephrine Reuptake, Recycling, and Degradation

Reuptake of NE is mediated by the NE transporter (NET) which is located along LC axons, terminals, somas, and dendrites. Following reuptake, NE can be repackaged into vesicles by VMAT2 or degraded by monoamine oxidase-A (MAO-A) and catechol-O-methyltransferase (COMT). These enzymes produce the main NE metabolite, MHPG. Proper balance of NE synthesis and degradation is crucial to cell health, as excessive MHPG and other metabolic intermediates (e.g. DOPEGAL) can be toxic to the cell and/or promote aberrant protein folding (Kang et al., 2020; Kang et al., 2021; Kang et al., 2022).

1.1.2.4 Neurotransmitter and neuropeptide co-release

Though the LC is primarily considered a noradrenergic nucleus, some studies have reported co-release of DA and glutamate, which have distinct effects on behavior (Devoto et al., 2005b; Kempadoo et al., 2016; Takeuchi et al., 2016; Yang et al., 2021). Moreover, subsets of LC neurons co-express various combinations of neuropeptides including galanin, neuropeptide Y (NPY), brain-derived neurotrophic factor (BDNF), cocaine and amphetamine-regulated transcript (CART), and dynorphin (Schwarz and Luo, 2015; Poe et al., 2020). Unlike NE, neuropeptides are packaged exclusively into large dense-core vesicles (Lang et al., 2015). The exact mechanism of large dense-core vesicle release is poorly understood but is thought to require elevated neuronal activity and Ca^{+2} influx (Bartfai et al., 1988; Sciolino and Holmes, 2012; Lang et al., 2015; Tillage et al., 2021). These neuropeptides can act acutely, but also serve as neurotrophic factors which act over longer time periods (Weinshenker and Holmes, 2016; Tillage et al., 2021). Long-term

action of neuropeptides as neurotrophic factors is supported by recent evidence from our lab showing the delayed behavioral effects of galanin release from the LC (Tillage et al., 2021).

1.1.3 LOCUS COERULEUS FIRING PATTERNS AND INFLUENCE ON BEHAVIOR

1.1.3.1 Firing Rates, Patterns, and Characteristics

The LC has historically been described to fire in two distinct patterns: tonic and phasic. Tonic activity refers to the intrinsic pacemaker activity of LC neurons that usually fire between 0.5-2 spikes/sec (Ishimatsu and Williams, 1996; Aston-Jones and Cohen, 2005b). Phasic firing, on the other hand, is less well defined. Under some conditions, phasic activity is referred to as brief bursts of activity typically between 15-20 spikes/sec followed by prolonged inhibition in response to external stimuli (Akaike, 1982; Vankov et al., 1995). Others have described phasic activity as transient changes in firing rates (Aston-Jones and Bloom, 1981a; Aston-Jones et al., 1994; Marzo et al., 2014). Still others utilize interspike interval (amount of time between two successive spikes) histograms and base phasic periods on previously defined DA neuron literature (Grace and Bunney, 1984; Iro et al., 2021). Regardless, tonic and phasic LC activity have been shown to differentially impact NE release and subsequent behavioral responses (Florin-Lechner et al., 1996; Aston-Jones and Cohen, 2005a; Bouret and Sara, 2005; Devoto et al., 2005b; Mather et al., 2016). However phasic activity is operationalized, it broadly refers to elevated periods of firing which is thought to release large dense-core vesicles containing neuropeptides and may be a mechanism for NE and neuropeptide co-release.

Classically, the LC has been considered to function as a homogeneous nucleus that broadcasts NE signals globally to promote stereotyped responses. However, this view has come into question recently, as chemical, functional, neuroanatomical, and electrophysiological heterogeneity of LC neurons have been described. For example, field standard criteria for

identifying LC neurons includes broad action potentials, but a recent report demonstrated the presence of both wide and narrow waveforms. Although wide and narrow waveform units displayed similar evoked responses and inhibition by the α2 agonist clonidine, narrow units were located more ventrally and had higher firing rates (Totah et al., 2018). Neighboring LC neurons are also connected by gap junctions, which are thought to drive synchronous activity throughout the nucleus or in distinct ensembles (Christie, 1997; Alvarez et al., 2002; Rash et al., 2007). Engaging different LC ensembles results in distinct cortical states (Noei et al., 2022), though these have yet to be directly linked to behavior. Projection targets also influence LC activity, with prefrontal cortex projecting LC neurons having higher firing rates compared to motor cortex projecting LC neurons (Chandler et al., 2014). In line with this observation, prefrontal cortex projecting LC neurons were found to be enriched for markers of excitability and transmitter release (Chandler et al., 2014). Interestingly, a separate study showed prefrontal cortex projecting LC neurons had lower firing rates and were less responsive to α2-adrenergic receptor mediated inhibition compared to those projecting to the hippocampus (Wagner-Altendorf et al., 2019).

It is also worth mentioning that the size and location of the LC makes recordings from individual neurons in awake behaving animals technically challenging. The field has therefore adopted anesthetized and slice preparations to obtain stable, long duration recordings of single units, under the assumption that firing properties mimic those in awake and *in vivo* situations, respectively. Additional variability between studies comes from differences in choice of anesthetic, model system, sex, age, and other factors that have known or predicted impacts on LC firing rates. Therefore, our understanding of LC firing rates and patterns comes from diverse datasets that have yet to be directly compared, which could impact interpretations of LC function.

Implementation and optimization of newer methods to monitor LC activity and NE release such as calcium imaging and photometry are ongoing. Early reports using these methods have

refined and expanded on the role of the LC sleep, arousal, parenting, and feeding (Breton-Provencher and Sur, 2019; Dvorkin and Shea, 2022; Kjaerby et al., 2022; Sciolino et al., 2022). There is also some debate regarding how LC firing rates at the level of the cell body translate to activity and NE release from LC axons. Combining electrophysiology of LC neurons and fiber photometry of LC axons answering this longstanding question (Breton-Provencher and Sur, 2019).

Compared to preclinical models, there is a dearth of methods that can be used to track LC activity in humans. MRI and PET can be used to probe the integrity of LC axons and cell bodies, in addition to activity (Kelberman et al., 2020) (**Figures 1.1-1.3**). Stimulation of the LC also results in pupil dilation (Liu et al., 2017; Zerbi et al., 2019; Hayat et al., 2020), and some studies have therefore used transient fluctuations in pupil dilation as a reflection of changes in LC activity (Alnaes et al., 2014; Murphy et al., 2014; Joshi et al., 2016; Elman et al., 2017; Kelberman et al., 2020), though other evidence refutes these claims (Megemont et al., 2022). Importantly, the current temporal resolution of MRI does not allow for identification of different types of LC firing patterns, and the involvement of other nuclei in pupil dynamics means that pupillometry lacks LC specificity (Joshi et al., 2016; Reimer et al., 2016; Cazettes et al., 2021; Megemont et al., 2022). Therefore, tracking patterns of LC activity in humans is still an ongoing endeavor but would be useful in bridging findings made in preclinical settings to human populations.

1.1.3.2 Neurochemical Control of Locus Coeruleus Firing Patterns

LC firing rates and patterns are controlled by a complex combination of excitatory, inhibitory, and neuromodulatory inputs. Pacemaker activity is observed in slice preparations (Williams et al., 1984; Alreja and Aghajanian, 1995; Chandler et al., 2014; Downs et al., 2022), indicating that LC neurons are capable of firing with limited inputs. Activation of α2-adrenergic

receptors on LC cell bodies/dendrites leads to cessation of LC activity (McCune et al., 1993; Totah et al., 2018; Wagner-Altendorf et al., 2019; Kelberman et al., 2023). Therefore, local release of NE can autoinhibit LC neurons and neighboring cells. GABAergic inputs arise from the ventrolateral preoptic area and peri-LC to modulate basal LC firing (Chiang and Aston-Jones, 1993a; Nitz and Siegel, 1997; Breton-Provencher and Sur, 2019; Breton-Provencher et al., 2021). Similarly, LC responsiveness to glutamatergic inputs arising from the cortex, lateral habenula, and paragigantocellularis nucleus are also modulated by serotonin (Herkenham and Nauta, 1979; Ennis and Aston-Jones, 1988; Aston-Jones et al., 1991; Chiang and Aston-Jones, 1993b; Jodo and Aston-Jones, 1997). On the other hand, direct application of or engagement circuits releasing hypocretin/orexin or CRF to LC neurons augments tonic activity, typically above the normal range of 0.5-2 spikes/sec, without affecting phasic firing rates (Valentino and Foote, 1988; Horvath et al., 1999; Curtis et al., 2012; Sears et al., 2013; McCall et al., 2015). The LC is supplied with hypocretin/orexin primarily by the lateral hypothalamus while CRF terminals originate from the central nucleus of the amygdala (Horvath et al., 1999; Reyes et al., 2008). Serotonin can also lower tonic LC firing rates, but enhances phasic firing in a manner that is dependent on GABA and simultaneously dampens responsiveness to glutamate (Aston-Jones et al., 1991; Chiang and Aston-Jones, 1993a). Interestingly, though there are robust modulatory effects of both serotonin and CRF on LC activity (Valentino and Foote, 1988; Aston-Jones et al., 1991; Chiang and Aston-Jones, 1993a; Curtis et al., 2006; Curtis et al., 2012; McCall et al., 2015), there is a lack of robust mRNA expression of receptors for either molecule in the LC (see chapter 3). Rather, evidence points to these receptors being located within dendritic fields of LC neurons or the presence of multi-synaptic pathways that modulate excitatory and inhibitory neurotransmission (Aston-Jones et al., 1991; Pompeiano et al., 1992; Chiang and Aston-Jones, 1993a; Van Bockstaele et al., 1996; Reyes et al., 2006). This is also true of the neuropeptide galanin, which has potent inhibitory effects

on LC neurons even though they are largely devoid of galanin receptors (Seutin et al., 1989; Xu et al., 2005; Weinshenker and Holmes, 2016; Foster et al., 2021). Excitatory amino acid transmission via AMPA receptors also is important for phasic LC responses, but also somewhat paradoxically the post-activation inhibition of LC neurons (Zamalloa et al., 2009). A diverse set of opioid (μ, δ, κ) and opioid-related receptors are also located in the LC (Mansour et al., 1994; Connor et al., 1996; Neal et al., 1999; Van Bockstaele et al., 2010; Tkaczynski et al., 2022). δ opioid receptors appear to prevent overactivation of LC neurons in response to stress, while the opioid-related nociception receptor 1 alters conductance through inwardly rectifying potassium channels (Connor et al., 1996; Neal et al., 1999; Tkaczynski et al., 2022). New evidence using transcriptomic approaches in the LC have identified a host of other neuromodulators and receptors that are highly expressed in the LC and influence behavior, but their effects on LC activity and physiology have yet to be characterized (Mulvey et al., 2018; Duesman et al., 2022; Weber et al., 2022). Finally, there is emerging evidence that non-neuronal signatures may modulate LC activity through direct signaling or modulation of excitatory neurotransmission though this idea remains controversial (Lee et al., 1998; Savtchouk and Volterra, 2018; Wahis and Holt, 2021). Circuits between LC neurons and non-neuronal cell types may also be bidirectional, as cells like astrocytes and microglia express adrenergic receptors that are important for cell-type specific functions (Liu et al., 2019; Porter-Stransky et al., 2019; Stowell et al., 2019).

1.1.3.3 Behavior

Decades of work has revealed that the LC influences behaviors including sleep and arousal, stress and anxiety, response to novelty, social behavior, cognition, and memory.

Sleep/Arousal

The influence of the LC on sleep and arousal has been well described. The LC is part of the ascending reticular activating system along with other brainstem and midbrain neuromodulatory nuclei (lateral hypothalamus-orexin/hypocretin, dorsal raphe-serotonin, tuberomammillary nucleus-histamine). LC neurons are tonically active and phasically responsive during periods of wakefulness, gradually reduce their activity during non-REM sleep, and are almost completely silent during REM sleep (Aston-Jones and Bloom, 1981b). These changes in LC firing rates occur prior to sleep-wake transitions (Aston-Jones and Bloom, 1981b). Direct activation of the LC induces wakefulness while genetically ablating NE synthesis increases sleepiness (Kaitin et al., 1986; Hunsley and Palmiter, 2003; Hunsley et al., 2006; Carter et al., 2010; Vazey and Aston-Jones, 2014; Singh et al., 2015). NE levels also vary with stage of sleep, in accordance with activity at the level of LC cell bodies (Osorio-Forero et al., 2022). These variations in LC activity and NE levels are important for mediating arousal levels, particularly in response to salient stimuli. Reducing NE levels or inhibiting LC activity lowered while LC stimulation increased the probability of sound evoked awakenings (Hayat et al., 2020).

Variations in LC-NE levels and activity are partially mediated by GABA signaling, likely emanating from the local GABAergic pool and/or the ventrolateral preoptic area (Nitz and Siegel, 1997; Breton-Provencher and Sur, 2019; Breton-Provencher et al., 2021). Hypocretin/orexin from the hypothalamus also plays a role in how the LC-NE system modulates arousal. Hypocretin/orexin increases LC neuron activity and knockdown of hypocretin/orexin type 1 receptors in the LC increases REM sleep during the dark period (Chen et al., 2010). LC-NE release is also required for increased locomotor-inducing effects of hypocretin/orexin-expressing neuron stimulation (Singh et al., 2015), highlighting the importance of this circuit in arousal.

Based on its role in sleep, the LC is also implicated in and target for sedation and anesthesia. Under most anesthetics, the LC remains tonically active and phasic firing can be

induced by applying salient stimuli (Vazey and Aston-Jones, 2014; West et al., 2015; Noei et al., 2022; Kelberman et al., 2023). Dexmedetomidine and clonidine are two sedatives that more directly affect the LC by activating α2 adrenergic receptors and inhibiting LC activity (Jorm and Stamford, 1993; Totah et al., 2018; Zerbi et al., 2019; Kelberman et al., 2023).

Stress and Anxiety

Stress is a potent activator of LC neurons, and causes elevations in tonic firing above basal levels (3-8 spikes/sec). Acute stress can be adaptive, but chronic elevations in tonic LC firing lead to the expression of anxiety-like behaviors, which has been demonstrated by optogenetic stimulation of LC neurons, administration of pharmacological agents that increase NE transmission, and under conditions that recapitulate naturally stressful situations in rodents (Valentino and Foote, 1988; Bremner et al., 1996; Curtis et al., 2012; McCall et al., 2015; Tillage et al., 2021). In particular, corticotropin releasing factor (CRF) has been shown to potently drive LC neurons at high tonic firing rates under conditions of naturalistic stress such as exposure to predator odors (Valentino and Foote, 1988; Curtis et al., 2012; McCall et al., 2015). In contrast, NE-deficient mice lack typical neophobic and stress induced responses which can be restored by artificially increasing NE signaling (Lustberg et al., 2020a; Lustberg et al., 2020b; Lustberg et al., 2022). These same mice lack footshock-induced anxiety-like behaviors in an elevated zero maze, whereas noradrenergic-derived galanin is not required for the acute expression of anxiety-like phenotypes. Interestingly, restoration of galanin, but not NE, during stress exposure restores anxiety-like behaviors 24 h after the stressor, suggesting that LC-derived NE and galanin are responsible for expression of anxiety on different timescales (Tillage et al., 2021). Furthermore, reducing LC activity or antagonizing NE receptors has anxiolytic properties. Post-mortem human studies also show increased levels of NE and its metabolites, and an upregulation of TH in those with mood disorders. NE also contributes to stress-induced behaviors reminiscent of obsessive-

compulsive disorders in rodents (Lustberg et al., 2020a; Lustberg et al., 2020b; Lustberg et al., 2022). Specifically, NE deficient mice lack stress-induced shredding and digging behavior that can be rescued by restoring NE levels, while application of anti-adrenergic drugs in wild-type mice produces similar deficits in stress-induced repetitive behaviors (Lustberg et al., 2020a; Lustberg et al., 2020b; Lustberg et al., 2022).

Response to Novelty

Rodents exhibit anxiety-like responses to novel environments which gradually evolves into exploratory behavior as the animal becomes familiar with the context. This habituation is adaptive, allowing animals to explore and exploit new environments when no threat is present. The LC is exquisitely responsive and rapidly habituates to novel stimuli, provided that they are non-noxious (Aston-Jones and Bloom, 1981a; Vankov et al., 1995; Omoluabi et al., 2021). Therefore, the LC has been hypothesized to contribute to the behavior transition from anxiety-like phenotypes to exploration in novel environments. Mice lacking NE have a blunted ambulatory activity in response to being exposed to a novel environment. Specifically, these mice show lower activity levels within the first 20 minutes of being exposed to and habituate more rapidly to a novel environment (Lustberg et al., 2020b). These same mice display impaired social discrimination when exposed to a novel animal (Marino et al., 2005). Pharmacological reduction of NE in rats results in identical behavioral deficits in response to environmental novelty (Delini-Stula et al., 1984). The authors went on to show that alterations in novelty response extended to novel object recognition but not behaviors such as grooming, defecation, or other contexts (response to familiar objects in a novel environment). The authors conclude that explorative behaviors in novel environments are most sensitive to NE. Data from our lab supports this hypothesis, as DA signaling appears to control some aspects of response to novelty such as grooming (Lustberg et al., 2022).

Social Behavior

The LC influences specific aspects of social behaviors, including maternal behaviors. Pup retrieval in mice leads to a phasic burst of LC activity that is not due to sensory, motor, or rewarding aspects of the behavior (Dvorkin and Shea, 2022). Meanwhile, changes in tonic LC activity are associated with specific pup-directed actions, such as licking and nesting (Dvorkin and Shea, 2022). In contrast, pharmacologically reducing NE synthesis reduced parental behavior of biparental rodents (Acosta et al., 2022). Similarly, genetic depletion of NE in mothers reduces the number of and increases the latency to gather pups, culminating in high rates of pup mortality (Thomas and Palmiter, 1997). Separate from parental behaviors, the LC is also heavily involved in expression of social behaviors. Genetic ablation of NE caused deficits in social discrimination and abolished aggressive behaviors in a resident intruder task, while leaving social memory largely intact (Marino et al., 2005). Similarly, ablating LC neurons in a mouse model of neurodegeneration induced recognition deficits of a previously encountered conspecific (Heneka et al., 2006).

Cognition, Attention, and Learning and Memory

Historically, forebrain regions have received the most attention in regulating higher order behaviors such as cognition and attention. However, the LC innervates every portion of the cortex allowing modulation of cognition and attention via NE release. There are a few prominent theories of how the LC influences cognition that are worth reviewing. It has been proposed that the LC mainly influences task performance by influencing arousal levels according to a Yerkes-Dodson model (Aston-Jones and Cohen, 2005b; Howells et al., 2012). Low levels of LC activity are associated with low levels of arousal, weak task performance, and inattentiveness. The other end of the spectrum proposes that high levels of LC activity are maladaptive, resulting in distractibility.

Proper balance of tonic and phasic LC activity promotes strong task performance at intermediate levels of arousal. Newer theories of LC involvement in cognition have added nuance to the traditional Yerkes-Dodson model. Specifically, adaptive gain theory is based on an antagonistic relationship between the tonic and phasic firing modes of the LC. Phasic activity is theorized to respond to aspects of task-related decision making and update future behaviors to optimize performance (Aston-Jones and Cohen, 2005b; Howells et al., 2012). Meanwhile, tonic activity is proposed to facilitate disengagement from tasks and support flexible behavioral responses. The Glutamate Amplifies Noradrenergic Effects (GANE) theory of LC activity focuses on the synergistic effects of glutamate and NE in LC target regions to amplify representation of highly salient stimuli and ultimately assist with memory consolidation of these specific stimuli (Mather et al., 2016). Network Reset suggests that phasic LC activity facilitates cognitive shifts by interrupting and reorganizing neural networks (Bouret and Sara, 2005). All the previously mentioned models are supported by literature and are not mutually exclusive, implying that the influence of the LC-NE system on cognition and memory is highly complex and is likely dependent on NE signaling within specific brain regions based on task demands.

For example, the LC plays an important role in fear conditioning, consolidation, and extinction, each of which are regulated by different afferent outputs of the LC (For a comprehensive review, see (Giustino and Maren, 2018)). Cued fear conditioning is dependent upon LC projections to the basolateral amygdala. Pharmacological blockade of NE signaling at β-adrenergic receptors systemically or in the basolateral amygdala, or activating α2-adrenergic receptors prior to training impairs cued fear conditioning (Cole and Koob, 1988; Davies et al., 2004; Bush et al., 2010; Schiff et al., 2017). Opposingly, blocking α1 receptors enhances fear conditioning via induction of long-term potentiation in the lateral amygdala (Lazzaro et al., 2010). Separately, depletion of NE impairs contextual fear conditioning (Neophytou et al., 2001; Ouyang

and Thomas, 2005; Hott et al., 2012). While cued fear consolidation does not appear to rely on LC-NE signaling, increasing or decreasing noradrenergic tone can increase and decrease contextual fear consolidation, respectively (LaLumiere et al., 2003; Murchison et al., 2004; Ouyang and Thomas, 2005; Gazarini et al., 2013; Gazarini et al., 2014). Differences in cued and contextual fear consolidation are hypothesized to involve altered hippocampal long-term potentiation and signaling within the medial prefrontal cortex resulting from noradrenergic manipulations (Giustino and Maren, 2018). Finally, the LC-NE system has a prominent role in both cued and contextual fear extinction. Activating LC projections to the medial prefrontal cortex promotes cued extinction learning (Uematsu et al., 2017). However, these effects may depend on arousal levels, as stress appears to impair cued extinction learning (Fitzgerald et al., 2015; Lin et al., 2016; Maren and Holmes, 2016; Giustino and Maren, 2018). Contextual fear extinction is enhanced by augmenting NE tone in the ventromedial prefrontal cortex, hippocampus, and basolateral amygdala (Berlau and McGaugh, 2006; Do-Monte et al., 2010; Abraham et al., 2012; Chai et al., 2014).

Expanding on the role of LC in hippocampal-dependent memory, long-term depression and potentiation of hippocampal synapses are facilitated by signaling via β-adrenergic receptors (O'Dell et al., 2015; Hagena et al., 2016; Hansen, 2017). Altering β-adrenergic signaling in the hippocampus leads to deficits in object recognition and fear extinction in rats (Goodman et al., 2021). Beyond fear conditioning, there is a wealth of evidence that NE signaling in the hippocampus is crucial for other types of memory. Lesioning or silencing the LC impairs encoding of spatial memory in the T-maze and Morris water maze (Amaral and Foss, 1975; Khakpour-Taleghani et al., 2009; Coradazzi et al., 2016). NE signaling is also crucial for consolidation of novelty-associated memories involving the hippocampus, as inhibition of LC cell bodies and terminals in CA3 prevents encoding of novel contexts (Wagatsuma et al., 2018). It was further demonstrated that inhibition of LC activity during encoding of a novel context disrupts the ability

of CA3 place cells to stably represent areas in space upon re-exposure to an environment. Dopamine release appears to be important for encoding environmental novelty. In a separate study, stimulation of LC axons in the dorsal hippocampus enhanced spatial object recognition that required D1/D5 receptors (Kempadoo et al., 2016). There was an added effect on spatial learning, as stimulation of LC axons accelerated latency to the target chamber in the Barnes Maze. Similarly, stimulating the LC after encoding enhanced spatial memory, and was completely ablated by D1/D5 receptor antagonism in CA1 (Takeuchi et al., 2016). Proper consolidation is partially dependent on NE signaling during sleep. Abnormally activating the LC during sleep alters characteristic EEG signatures and interferes with consolidation in a hippocampal-dependent task (Swift et al., 2018). Similar sleep and behavioral disruptions are observed with application of α2-adrenergic agonists and β-adrenergic following a radial arm maze task (Duran et al., 2023).

It is again worth considering the role of different LC firing rates and patterns in cognition. Electrical stimulation of the LC that mimics bursting activity of the nucleus produces DA release in forebrain regions (Devoto et al., 2005a, b). In addition, the previously referenced memory enhancements following dopamine release from the LC were in response to burst-like LC stimulation (Kempadoo et al., 2016; Takeuchi et al., 2016). Similarly patterned stimulation of the LC in wild-type rats accelerates rates of odor discrimination that is dependent on actions of NE in the piriform cortex (Ghosh et al., 2021). Expressing aberrant tau in the LC of these rats interferes with odor discrimination by reducing LC axonal density and upregulating β-adrenergic receptors in the olfactory cortex (Ghosh et al., 2019). Still, phasic LC stimulation in these rats can prevent deficits in odor discrimination and preserve LC integrity, whereas high tonic firing is associated with anxiety- and depressive-like phenotypes, and worse LC health (Omoluabi et al., 2021). Genetically abolishing NE also results in reduced social discrimination in mice (Marino et al., 2005).

Behavioral flexibility is also heavily influenced by the LC, specifically via its connections to the medial prefrontal and orbitofrontal cortices. Pharmacological ablation and chemogenetic silencing of LC inputs to the orbitofrontal cortex, but not the prelimbic cortex, disrupted animals' ability to update actions to varying outcome contingencies (Cerpa et al., 2023). It is therefore unsurprising that the LC has been heavily implicated in substance use disorders (for a comprehensive review, see (Weinshenker and Schroeder, 2007)). Similarly, silencing LC activity during an attentional set-shifting task led to impairments in reversal learning and extradimensional set shifting, but not tasks that did not require cognitive flexibility (Janitzky et al., 2015). In a path foraging task, elevating LC tonic activity reduced task participation and increased trial omissions and reaction times (Kane et al., 2017). While this at first appears to indicate distractibility, the driver of these behavioral outputs was an increase in tendency to leave the current patch, suggesting induction of behavioral flexibility. Further support for this theory that elevated LC activity promotes behavioral flexibility, LC firing rates were correlated with the speed of rule switching in a tactile-based rule-shift task in mice (McBurney-Lin et al., 2022). We have separately shown that spatial memory deficits in aged rats that develop Aβ and tau pathology can be rescued by stimulating the LC (Rorabaugh et al., 2017). This effect is likely to be dependent on basal LC firing rates, as we have shown that these rats display LC hypoactivity at the ages tested (Kelberman et al., 2023), a topic we discuss further in Chapter 2.

In humans, neuromelanin sensitive MRI sequences are used to localize the LC and provide a measure of the integrity of the nucleus (Kelberman et al., 2020). Preserved LC integrity, is positively associated with cortical thickness (Bachman et al., 2021), better memory performance (Hammerer et al., 2018; Dahl et al., 2019; Olivieri et al., 2019), and preserved cognition (Liu et al., 2020). Post-mortem LC integrity also correlates with cognitive function during health aging (Robertson, 2013; Wilson et al., 2013; Clewett et al., 2016). Specific sets of connections and

signaling between the LC and other brain regions are likely to support cognition. In particular, higher LC-nucleus basalis of Meynert or ventral tegmental area functional connectivity is associated with poorer memory in those over 40 (Jacobs et al., 2018), whereas stronger functional connectivity with the parahippocampal gyrus is associated with better memory performance (Jacobs et al., 2015b). The LC also plays a role in retrieval/recollection of memories that have a salient emotional component (Sterpenich et al., 2006; Il Jacobs et al., 2020). There is also evidence in humans that LC activity patterns are an important predictor of cognitive outcome. Similar to preclinical literature, higher LC response to novelty in healthy populations is associated with resistance to cognitive decline, even in the presence of forebrain AD pathology (Prokopiou et al., 2022).

Together, preclinical and human data show a robust involvement of the LC in arousal, attention, cognition, and learning and memory that are mediated by engagement of different adrenergic receptor subtypes within specific brain regions.

1.2 CONTRIBUTIONS OF LOCUS COERULEUS DYSFUNCTION TO DISEASE

Alterations to normal LC function have been implicated in a multitude of disorders which are covered below.

1.2.1 NEUROPSYCHIATRIC AND NEURODEVELOPMENTAL DISORDERS

Many neuropsychiatric disorders involve adverse stress responses. Given the role of the LC-NE system in stress and anxiety, it is unsurprising that dysfunction of this system is heavily linked with neuropsychiatric disorders. Patients with depression show substantial reduction in LC contrast (Shibata et al., 2007; Shibata et al., 2008), a marker of LC integrity. Lower NET and higher TH levels in the LC have been reported in post-mortem samples from patients with major depression, without changes to overall cell number (Klimek et al., 1997; Zhu et al., 1999). Similar

downregulation of NET in the LC is noted in patients with post-traumatic stress disorder, with an additional hyperresponsiveness of the LC evident in response to salient stimuli (Pietrzak et al., 2013; Naegeli et al., 2018). Dysfunction of the LC-NE system is not surprising, given the preclinical evidence linking NE signaling to all aspects of fear conditioning (Giustino and Maren, 2018). Symptoms of post-traumatic stress disorder can be improved with the α1-adrnergic receptor antagonist prazosin (Raskind et al., 2007; Raskind et al., 2013). Nightmares, hyperarousal, and sleep abnormalities were identified by a meta-review as the primary symptoms that improve with prazosin treatment, and are in agreement with the idea that the LC is hyperactive in these patients (Singh et al., 2016). In schizophrenia, average LC cell body size and total LC volume is increased compared to control subjects, without a change in overall cell number (Marner et al., 2005). The LC is also dysfunctional in neurodevelopmental disorders, such as autism spectrum disorder. No differences in LC cell counts or volume are noted in autism spectrum disorders (Martchek et al., 2006). Both increased and decreased LC functional connectivity are noted in autism spectrum disorder (Huang et al., 2021). However, children with autism spectrum disorder typically display larger resting pupil diameter (Arora et al., 2021), which has been linked to attentional disengagement (Keehn et al., 2021). This putatively implicates augmented tonic LC activity in autism spectrum disorder. In addition, evidence suggests that LC dysfunction might be dependent upon task utility (Bast et al., 2023), but increases in functional connectivity are specific to visual areas (Huang et al., 2021). This indicates that LC dysfunction in autism spectrum disorder may contribute to deficits influenced by vision. Cumulatively, these studies indicate that LC hyperactivity contributes to neuropsychiatric and neurodevelopmental disorders.

1.2.2 SLEEP DISORDERS

Given the wake-promoting effects of LC activity, it is unsurprising that LC dysfunction contributes to symptoms of various sleep disorders. Patients with REM Sleep Behavior Disorder

present with lower LC contrast than healthy controls (Ehrminger et al., 2016; Knudsen et al., 2018). Furthermore, while Parkinson's disease (PD) patients present with reduced LC contrast (Sasaki et al., 2006; Wang et al., 2018a), PD patients with concomitant REM Sleep Behavior Disorder show even lower LC contrast (Sommerauer et al., 2018). Patients with chronic insomnia present with altered patterns of LC functional connectivity that are associated with both disease duration and anxiety scores (Gong et al., 2021). Conversely, one study identified a mutation in the gene encoding the β1-adrenergic receptor found in humans that sleep less (Shi et al., 2019). Introducing this mutation to mice led to shortened sleep behavior and *in vitro* decreased protein stability and agonist sensitivity.

1.2.3 NEURODEGENERATIVE DISORDERS

Alzheimer's disease (AD) and PD are the two most common neurodegenerative disorders in the world. AD is the leading form of dementia, and is characterized by the accumulation of extracellular β-amyloid (Aβ) and intracellular neurofibrillary tangles composed of hyperphosphorylated tau. The main symptom of AD are cognitive and memory deficits that occur during late stages of the disease. Meanwhile, PD patients present with motor impairments that have been attributed to degeneration of the dopaminergic substantia nigra and aggregation of α-synuclein. Although primary symptomology and protein aggregates differ between AD and PD, LC dysfunction is ubiquitous across disease progression (Weinshenker, 2018; Kelberman et al., 2020). In fact, the LC is the first brain region to accumulate hyperphosphorylated tau and α-synuclein in prodromal phases of AD and PD, respectively, which occurs well before other areas that canonically associated with these disorders such as the hippocampus, cortex (AD), and basal ganglia (PD) (Braak et al., 2011; Del Tredici and Braak, 2013; Pletnikova et al., 2018; Gilvesy et al., 2022). Aggregation of these proteins occurs decades prior to primary symptomology associated with each disease, and LC neurons appear to be spared from frank cell death until mid

to late stages of disease, when up to 80% of cell bodies are lost (German et al., 1992; Busch et al., 1997; Theofilas et al., 2017). Despite delays in cell death, the LC experiences volume loss and morphological alterations in the earliest Braak stages (Theofilas et al., 2017; Gilvesy et al., 2022). In addition, LC neuronal loss is greater than that of the nucleus basalis of Mynert and substantia nigra in both AD and PD, respectively (Zarow et al., 2003). Beyond AD and PD, LC dysfunction contributes to aspects of other neurodegenerative diseases including chronic traumatic encephalopathy, frontotemporal dementia, progressive supranuclear palsy, Pick's disease, and more (Weinshenker, 2018; Betts et al., 2019b; Kelberman et al., 2020).

1.3 ALZHEIMER'S DISEASE

1.3.1 EPIDEMIOLOGY AND ETIOLOGY

AD is the most common form of dementia, which is an umbrella term describing impairments in ability to remember, think, or make decisions that significantly impact daily life. AD currently affects over 30 million individuals worldwide, and incidences are expected to rise as the population ages. A majority of AD cases are sporadic, but there are several genetic mutations that are causative (PSEN1, PSEN2, APP) or pose an increased risk (APOE4, TREM2) of developing AD (Karch and Goate, 2015; Yamazaki et al., 2016). Most people are diagnosed with AD after the age of 65, and aging is the highest risk factor for developing AD. However, specific mutations alter disease course by accelerating (early onset) or delaying (late onset) the onset of AD. There are also a variety of other environmental and lifestyle factors that confer resilience or risk of developing AD. Chronic illnesses such as cardiovascular disease, high blood pressure, and diabetes increase the risk for AD whereas exercise, education, and occupational attainment confer resilience (Stern, 2012).

Historically, AD diagnosis could only be confirmed post-mortem by the appearance of the two pathological hallmarks: Aβ and neurofibrillary tangles composed of hyperphosphorylated tau. More recently, a combination of neuroimaging, biomarker assays (blood-based, positron emission tomography, cerebrospinal fluid, plasma, etc.), and comprehensive clinical exams (cognitive, neuropsychological and behavioral questionnaires) can be used to issue a probable AD diagnosis. Genetic testing for mutations associated with familial AD (PSEN1, PSEN2, and APP) and less common variants that pose low to moderate risk (APOE4, TREM2) are now possible, but are used sparingly. The Food and Drug Administration recommends that biomarkers be specific, sensitive, predictive, inexpensive, and easily obtainable, among other criteria (Khoury and Ghossoub, 2019). For AD, a sensitivity and specificity measure above 80% should be achieved (Khoury and Ghossoub, 2019). The National Institute of Aging has categorized AD biomarkers into three categories: Aβ deposits, hyperphosphorylated tau aggregates, and markers of neuronal damage and/or degeneration, collectively termed ATN. All of these biomarkers can currently be assessed in living humans, though each have drawbacks. Cerebrospinal fluid is in direct contact with the brain, perhaps making it the best proxy for changes occurring within the brain. Samples are also easily obtained, though not unintrusive. Changes in cerebrospinal fluid levels of $A\beta_{42}$ occur prior to other emerging diagnostic measures, such as Aβ positron emission tomography (Palmqvist et al., 2016). Total tau and various versions of hyperphosphorylated tau can also be assessed in cerebrospinal fluid (Blennow et al., 2015; Costa et al., 2022). However, during prodromal phases of AD, these markers yield low specificity and sensitivity, in addition to low predictive accuracy for conversion to AD (Ritchie et al., 2014; Cummings, 2019). Instead, recent evidence suggests combining multiple cerebrospinal fluid markers in early AD diagnosis or using $A\beta_{42}/A\beta_{40}$ ratio as a more accurate biomarker (Biscetti et al., 2019). Plasma biomarkers are even easier to obtain, but changes along disease progression and diagnostic accuracy of biomarkers are still in their infancy.

Due to the low level of biomarkers in blood, the sensitivity of these assays must be greater than that of cerebrospinal fluid samples (Khoury and Ghossoub, 2019). However, emerging evidence suggests that $A\beta_{42}/A\beta_{40}$ ratios are lower in patients with AD and correlate with Aβ and tau levels in both cerebrospinal fluid and using positron emission tomography scans (Ovod et al., 2017; Risacher et al., 2019).

Positron emission tomography is a functional imaging procedure that utilizes radioligands to assess changes in metabolism, neurotransmitter levels, and other markers of interest. It has relatively poor spatial resolution, especially for investigating small brain regions such as the LC. However, positron emission tomography remains the only way to probe pathological load directly in the brain of living humans. Pittsburgh Compound-B was the first amyloid positron emission tomography tracer and routinely used today (Klunk et al., 2004). Tau tracers have also been developed and broadly fall into three categories (Saint-Aubert et al., 2017), but have suffered from problems with off-target binding and lack of overlap with validated antibodies (Sander et al., 2016; Marquie et al., 2017; Vermeiren et al., 2018). Sensitivity and specificity of diagnosing AD are mixed using these tracers, and likely depend on disease stage (Zhang et al., 2014; O'Brien and Herholz, 2015; Martinez et al., 2017). Other compounds can be used to assess neuronal health including those that measure inflammation (microglia and astrocytes), cell damage (neurofilament light), and neural activity (glucose metabolism), with the potential for improved sensitivity and specificity when combined with other biomarker assays.

Structural changes can also be assessed using structural MRI, where AD patients showing significant hippocampal and entorhinal cortex atrophy (Golebiowski et al., 1999; Juottonen et al., 1999). However, these changes occur quite late in disease progression, and therefore would produce low predictive value of conversion to AD. Brain regions such as the LC can be visualized using neuromelanin sensitive MRI techniques, and yield measures of integrity that can be

correlated with various other aspects of AD. We have also extensively reviewed other structural and functional imaging techniques to probe LC dysfunction along AD progression, but these methods are still in their infancy and require further refinement for use as diagnostic and predictive biomarkers (Kelberman et al., 2020).

1.3.2 NEUROPATHOLOGY

1.3.2.1 Amyloid-β

Aβ is one of the two pathological hallmarks of AD, and the major target of therapeutic interventions. Normal production of Aβ is produced through cleavage of the transmembrane amyloid precursor protein (APP) by α and γ secretase. Soluble fragments of APP are released bother extra and intracellularly which can act as signaling molecules. Abnormal processing of APP occurs with overactive cleavage by β-secretase which releases soluble Aβ fragments which aggregate extracellularly into plaques. Plaques follow a top-down deposition pattern, accumulating in cortical regions early and spreading to subcortical systems in later stages of AD (Braak and Braak, 1991; Thal et al., 2002). The LC also develops amyloid pathology, first in the form of Aβ oligomers and later as plaques (Cole et al., 1993; Kelly et al., 2021). However, deposition of Aβ pathology occurs in late-stages and in more severe forms of disease. Familial cases of AD are caused by genetic mutations involving the processing of APP, which favors the amyloidogenic pathway. This is also supported by the observation that people with Down Syndrome have higher risk of developing early onset AD, which has been linked to the extra copy of the APP gene located on chromosome 21 (Salehi et al., 2016). Some more common genetic variants pose a lower risk of AD (APOE4, TREM2, SORLA, BIN1), while others (APOE3, CR1), some of which lower Aβ production, are associated with reduced risk of AD (Karch and Goate, 2015; Yamazaki et al., 2016). These observations led to the development of the amyloid cascade

hypothesis, which posits that dysfunction in the balance of Aβ processing is the driving force of disease progression (Hardy and Higgins, 1992). This is supported by the fact that Aβ pathology can induce oxidative stress (Abramov et al., 2004; Karapetyan et al., 2022), inflammation and immune responses (Minter et al., 2016), synapse dysfunction (Walsh et al., 2002; Wang et al., 2002; Tu et al., 2014), behavioral impairments (Trinchese et al., 2004; Leon et al., 2010; Mehla et al., 2019), and tau hyperphosphorylation (Ryan et al., 2009; Jin et al., 2011; Zhang et al., 2020). Despite the large focus on Aβ as the main driver of AD and preclinical trials showing promise of Aβ based antibody therapies, clinical trials have, until recently, failed to delay or prevent the progression of AD using these drugs in human patients.

1.3.2.2 Tau

Tau is encoded by the MAPT gene on chromosome 17q21 and is typically found in complex with microtubules along axons (Boyarko and Hook, 2021). Following transcription, alternative splicing results in the translation of six major isoforms of tau in the human brain (Boyarko and Hook, 2021). These tau isoforms are composed of zero, one, or two N-terminal repeats and three or four C-terminal repeats (Boyarko and Hook, 2021). The C-terminal is positively charged to facilitate its binding to negatively charged microtubules, ultimately assisting with axonal transport and neurite outgrowth (Weingarten et al., 1975; Drubin and Kirschner, 1986; Kadavath et al., 2015). Tau is an intrinsically disordered protein, meaning it does not adopt a stable secondary structure, but is rather flexible (Mukrasch et al., 2005; Jeganathan et al., 2008; Schwalbe et al., 2014), which likely assists in its function of binding to and stabilizing microtubules. Tau can also undergo a variety of post-translational modifications, including phosphorylation (Martin et al., 2011; Wang et al., 2013). Phosphorylation and dephosphorylation is the most relevant for this discussion and is a normal aspect of the life cycle of tau, allowing for axonal flexibility that is crucial for synaptic plasticity (Guo et al., 2017). However, excessive

phosphorylation of tau causes detachment from microtubules and promotes aggregation of tau monomers (Mandelkow and Mandelkow, 2012; Boyarko and Hook, 2021). Without tau, microtubules become destabilized, impairing axonal transport, while the aggregation of tau further impedes processes within neuronal cell bodies (Guo et al., 2017). Surprisingly, tau knockout animals fail to display prominent phenotypes, likely due to compensation from other microtubule-associated proteins (Dawson et al., 2001; Fujio et al., 2007; Wang et al., 2013). Knockouts of multiple microtubule-associated proteins in single animals does induce behavioral phenotypes such as abnormal circadian rhythms, muscle weakness and motor deficits, and impairments in spatial learning (Cantero et al., 2010; Lei et al., 2012; Ma et al., 2014; Lopes et al., 2016).

Although tau is the other pathological hallmark of AD and required for diagnosis, it has often been thought of as secondary to Aβ pathology because familial cases of AD are caused by mutations in amyloid processing and Aβ pathology can induce tau hyperphosphorylation. However, tau and tangle pathology are the principal protein aggregates in the group of diseases known as tauopathies (Williams, 2006). There are many tauopathies, which are separated into groups based on the tau isoforms that compose their aggregates. Moreover, mutations in genes encoding tau have been shown to cause cases of various tauopathies, such as frontotemporal dementia (Goedert and Jakes, 2005). Tau has also gained increased interest in AD given its tight link with emergence of prodromal symptoms and cell death compared to Aβ (Busch et al., 1997; Ehrenberg et al., 2018; Oh et al., 2019; Cassidy et al., 2021; Cassidy et al., 2022; Kelberman et al., 2022).

Tau has been shown to alter neuronal activity, but in a way that is less predictable than the hyperactivity produced by Aβ (Busche and Hyman, 2020). Tau alone has been shown to either increase or decrease neuronal activity (Holth et al., 2013; Busche et al., 2019; Huijbers et al., 2019; Shimojo et al., 2020), suggesting that these effects may be isoform dependent. Combined Aβ and

tau pathology typically induces neuronal hypoactivity to a greater degree than what is seen with tau alone (Busche and Hyman, 2020). Tau deficient mice are also protected against the negative consequences induced by Aβ pathology, which is partially due to its protective role against excitotoxicity (Rapoport et al., 2002; Roberson et al., 2007; Ittner et al., 2010; Shipton et al., 2011). Though the effects of pathogenic tau has been well described in forebrain regions, the consequences of early tau deposition in the LC on physiology, behavior, and other aspects of AD remain to be fully explored.

1.3.3 CLINICAL PRESENTATION

1.3.3.1 Cognition and Memory

AD is perhaps best known for its deleterious effects on cognition and memory. Patients exhibit cognitive and memory impairments across a wide range of categories, including declarative and emotional memory, executive function, language, attention and working memory. These deficits have been typically attributed to atrophy of the hippocampus and higher cortical areas that occur in late stages of disease. Cognitive deficits across as range of domains (attention, executive dysfunction, memory, language, etc.) are most commonly ascertained via questionnaires such as the Mini-Mental State Examination or Montreal Cognitive Assessment (Tsoi et al., 2015). There are other, less common cognitive assessments that are also employed including the Mini-Cog and Eight-Item Informant Interview to Differentiate Aging and Dementia, with each assessment having variable sensitivity and specificity for AD diagnosis (Tsoi et al., 2015).

1.3.3.2 Prodromal Symptomology

A host of other behavioral and psychosocial symptoms emerge decades prior to the appearance of substantial cognitive deficits in AD, and have therefore been termed prodromal

symptoms. The specific sets of prodromal symptoms can vary widely been individuals and can include changes in mood and arousal/sleep, increased stress, anxiety, apathy, and more (Ehrenberg et al., 2018). These are typically assessed using questionnaires such as the mild behavioral impairment checklist or Neuropsychiatric Inventory Questionnaire (Mallo et al., 2018). Many of these symptoms are considered secondary to memory decline and cognitive deficits, but often have a greater impact on quality of life for those with AD. All these phenotypes can be modulated by LC activity and respond to treatment with drugs targeting the LC-NE system (Aston-Jones and Bloom, 1981b; Peskind et al., 2005; Wang et al., 2009; Bangasser et al., 2016; O'Callaghan et al., 2021; Levey et al., 2022). These prodromal symptoms are consistently and specifically correlated with tau burden, and emerge coincident with tau accumulation in the LC (Braak et al., 2011; Ehrenberg et al., 2018; Cassidy et al., 2021; Cassidy et al., 2022; Kelberman et al., 2022).

1.3.4 CONTRIBUTIONS OF LOCUS COERULEUS DYSFUNCTION TO ALZHEIMER'S DISEASE

1.3.4.1 Susceptibility

The LC is one of the most susceptible nuclei to the pathophysiological insults of AD. These insults occur early and are exacerbated as the disease progresses. There are several characteristics of LC neurons that render them susceptible, including long and diffuse axonal projections, pacemaker activity, metabolic demand, and direct contact with blood vessels and ventricles.

First, despite the relatively small number of neurons, the LC projects nearly brain-wide, using highly branched axons to signal with NE. Previous studies have indicated that these axons are unmyelinated, but this has come into question in recent years. Although LC cell bodies develop hyperphosphorylated tau pathology as early as the first decades of life, they only undergo

frank neuronal degeneration in mid- to late-Braak stages. In fact, axon terminals undergo degeneration prior to substantial LC volume or cell loss.

Second, LC neurons have intrinsic pacemaker activity, even in the absence of excitatory inputs. This pacemaker tonic activity allows neurons to set and rapidly shift through behavioral states, but also has consequences. Constant activity is metabolically demanding on cells and can lead to oxidative stress and mitochondrial dysfunction. Moreover, unmyelinated axons transmit neural signals slower than myelinated axons, further increasing LC metabolic demands. Increased activity of the LC can also lead to increased production of NE metabolites. Of note, the NE metabolite DOPEGAL is toxic to LC neurons and indirectly leads to tau cleavage and aggregation via overactivity of asparagine endopeptidase (Kang et al., 2020; Kang et al., 2021). Alternatively, DOPEGAL can directly modify tau at residue 353, also promoting its aggregation and propagation (Kang et al., 2022). LC neurons have derived a mechanism to deal with such toxic compounds. Neuromelanin is a double-layered membrane granule that is thought to form in order to sequester excess catecholamines and byproducts within neurons (Zecca et al., 2001). These granules also chelate heavy metals and bind pesticides, again suggesting a protective role of neuromelanin (Zecca et al., 1992; Zecca et al., 2001; Zecca et al., 2008). However, neurons have no way of breaking down neuromelanin granules, leading to their accumulation during the process of aging (Mann and Yates, 1974; Manaye et al., 1995; Zucca et al., 2006). Over time, it is hypothesized that these granules can be partially broken down by reactive oxygen species, leading to the release of toxic products intracellularly (Shamoto-Nagai et al., 2004; Zecca et al., 2004). In addition, as neurons die, neuromelanin is released and can induce toxicity in neighboring neurons (Zhang et al., 2011).

Third, the LC is located adjacent to and its dendrites contact the 4th ventricle. LC axons also regulate blood-brain barrier permeability, and it is estimated that a single LC neuron

innervates 20 meters of capillaries (Pamphlett, 2014). Innervation of the ventricle and blood vessels permit the LC to contact toxic compounds circulating in cerebrospinal fluid and blood.

1.3.4.2 Dysfunction

As previously covered, the LC is the first brain region to develop AD tau pathology, often decades prior to Aβ or tau deposition in forebrain regions. LC axons and dendrites degenerate early in AD while catastrophic loss of cell bodies occurs starting in mid-stages of disease, suggesting that LC dysfunction could persist for a long time after the appearance of pathology (Gilvesy et al., 2022). Prior to cell body loss and as early as the transition from Braak stage 0 to 1, LC volume decreases ~8% for every increase in Braak stage (Theofilas et al., 2017).

With regards to symptoms, the LC influences every known atypical behavioral phenotype noted throughout the progression of AD. The early accumulation of tau and manifestation of behavioral symptoms have led to the hypothesis that altered LC activity is an important mediator of disease progression (Weinshenker, 2018; Janitzky, 2020). Specifically, sleep disturbances and increased anxiety and stress responses that coincide with accumulation of LC tau pathology suggest hyperactivity in early disease states (Ehrenberg et al., 2018; Weinshenker, 2018; Oh et al., 2019). This is further supported by neuromelanin-sensitive LC imaging, which shows that higher LC integrity is predictive of neuropsychiatric symptom load (Cassidy et al., 2021; Cassidy et al., 2022). Meanwhile, LC volume and cell loss coincides with memory and cognitive impairments that are indicative of hypoactivity (Kelly et al., 2017; Rorabaugh et al., 2017; Theofilas et al., 2017; David et al., 2022; Kelberman et al., 2022).

Most studies report overall decreases in brain NE levels, which correlates with the degree of cognitive impairment. However, NE metabolites and turnover (NE:metabolite ratios), the latter of which is considered a proxy of LC activity, are typically increased in AD patient samples. High

MHPG levels in cerebrospinal fluid is associated with decreased cortical thickness and hippocampal volume, even in the absence of significant Aβ pathology (van Hooren et al., 2021). One study also reports that LC neuron survival is inversely correlated with NE turnover, suggesting elevated LC activity is toxic to LC neurons (Hoogendijk et al., 1999). Others have reported no change or even increased NE levels in cerebrospinal fluid and some brain regions, which also tracks declining cognition (Gannon et al., 2015). Some of these discrepancies could be explained by disease stage, with early compensatory mechanisms resulting in maintenance or increased NE levels which fail at later stages of disease. These compensatory mechanisms include a downregulation of NET sites in projection regions and an upregulation of TH mRNA in the LC (Szot et al., 2006, 2007).

Noradrenergic receptors have also been shown to be dysfunctional and contribute to various aspects of AD. For example, Aβ oligomers hijack normal NE signaling via α2-receptors to promote tau hyperphosphorylation (Zhang et al., 2020), a potential mechanism of early tau deposition in the LC given its high density of α2 receptors and the presence of Aβ oligomers (Kelly et al., 2021; Kelberman et al., 2023). Many changes in receptor function and expression appear to be a compensatory effort in response to the early loss of LC axons and decrease in NE tone. β-adrenergic receptors are hypersensitive in early disease states (Goodman et al., 2021), but the density of adrenergic receptors in forebrain regions appear to decrease as the disease progresses (Szot et al., 2006, 2007). Dendritic sprouting and increased TH mRNA expression is also observed at the level of the LC (Szot et al., 2006), which is thought to represent compensatory mechanisms to upregulate NE signaling as fibers and cell bodies are lost.

NE also regulates immune responses which are important in the context of inflammation and pathological deposition/clearing in AD. Pharmacological depletion of NE in mouse models of AD increases microglia and astrocyte staining in cortical regions, and exacerbates pathological

deposition (Heneka et al., 2006; Chalermpalanupap et al., 2018). Pharmacologically elevating NE levels restores ability of microglia to clear pathology (Heneka et al., 2010). Under normal conditions, microglia surveillance decreases with increasing noradrenergic tone (Liu et al., 2019; Stowell et al., 2019). This observation may be partially responsible for consolidation of memories during sleep, mediated by microglia-induced synaptic plasticity brought about by decreased NE levels.

1.3.4.3 Current State of Noradrenergic Therapies in Alzheimer's Disease

The current FDA approved treatments for AD are cholinesterase inhibitors (galantamine, rivastigmine, and donepezil) and the NMDA antagonist memantine, which are used for mild and moderate to severe AD, respectively. These medications treat symptoms of the disease, such as memory loss, but do not impede disease progression. More recently, the FDA has approved two other drugs, aducanumab and lecanemab which remove amyloid from the brain. These treatments were the first approved by the FDA that were said to delay disease progression, but these effects appear to be marginal and can come with severe side effects, such as brain swelling. As such, more research is needed to identify therapeutic targets for both non-cognitive symptoms of AD, which are more predictive of quality of life, as well as disease modification.

Surprisingly, although LC dysfunction is ubiquitous throughout the progression of AD, use of noradrenergic interventions in AD remains limited. In 2022, there were only four noradrenergic drugs that were being tested for use in AD: prazosin (α1 adrenoreceptor antagonist), CTS-2032 (β2 adrenoreceptor agonist), guanfacine (α2 adrenoreceptor agonist), and BXCL-501 (orally dissolving formulation of dexmedetomidine; α2 adrenoreceptor agonist) (Cummings et al., 2022). Preclinical evidence suggests that augmenting noradrenergic tone can restore cognitive deficits and block declines in LC health (Rorabaugh et al., 2017; Omoluabi et al., 2021). Human literature

also supports the use of noradrenergic therapies in different stages of AD. Adrenergic antagonists have been reported to reduce agitation/aggression and anxiety in subjects with probable or possible AD (Peskind et al., 2005; Wang et al., 2009). Meanwhile, atomoxetine, an NE reuptake inhibitor, had beneficial effects on AD biomarkers in mild cognitive impairment (Levey et al., 2022). Vagus nerve stimulation is in the early stages of testing for use in AD populations (Vargas-Caballero et al., 2022), but has long been shown to modulate LC activity (Takigawa and Mogenson, 1977; Groves et al., 2005). Vagus nerve stimulation has been shown to enhance synaptic transmission in the hippocampus via β-adrenergic receptors (Shen et al., 2012) and can improve various aspects of memory which involve the LC-NE system (Clark et al., 1999; Ghacibeh et al., 2006; Sun et al., 2017; Vazquez-Oliver et al., 2020). Moreover, different patterns of LC activity can be elicited based on different stimulation protocols which is impossible with pharmacological therapies (Farrand et al., 2023). However, there are still questions surrounding the best stimulation protocols and which outcome measures should be used to track target engagement for vagus nerve stimulation (Ludwig et al., 2021). In addition, a lack of understanding of how LC activity changes over the course of the disease represents one of the major roadblocks to current implementation of noradrenergic-based therapies. This presents a nontrivial challenge for preclinical researchers for reasons that will be explained in the next section.

1.4 PRECLINICAL MODELS OF ALZHEIMER'S DISEASE

The AD field has an abundance of models used to study the contributions of Aβ and tau pathology to biochemical/molecular and behavioral dysfunction, and disease progression. This section will cover *in vitro* and *in vivo* models of AD with a specific focus on studies investigating the LC.

1.4.1 IN VITRO MODELS

Due to the small size of the LC, it is challenging to analyze molecular, cellular, and physiological properties *in vivo* although methods are being developed and optimized. *In vitro* models could be particularly useful for defining the effects of AD-type lesions on LC neurons. Bath application of NE dose dependently decreases caspase activity induced by Aβ pathology in cultured cortical neurons, leading to improved neuron survival (Liu et al., 2015). Cultured LC neurons expressing mutant P301S tau show reduced neurite length (Rorabaugh et al., 2017). Furthermore, while these P301S expressing LC neurons show no changes in survival rates (Rorabaugh et al., 2017), they are more susceptible to damage by a selective neurotoxin (personal communication).

Induced pluripotent stem cell, fibroblast-based 2D, and organoid differentiation protocols are being developed to specify noradrenergic neuron fates without having to dissect and culture LC neurons (Pirhajati Mahabadi et al., 2015; Li et al., 2019b). Alternatively, the SH-SY5Y cell line is often used to investigate LC-like neuronal populations in the context of neurodegenerative disorders. In this cell line, the NE metabolite DOPEGAL triggers aggregation of tau and cell death by increasing asparagine endopeptidase activity (Kang et al., 2020). DOPEGAL can also directly interact with tau lysine residue 353, leading to its aggregation, propagation, and cellular toxicity (Kang et al., 2022). Furthermore, the APOE4 allele known to increase AD risk can associate with VMAT2 in SH-SY5Y cells, which leads to the suppression of NE packaging (Kang et al., 2021). Ultimately, this process upregulates DOPEGAL levels, again resulting in tau cleavage and cell death. Unfortunately, the cells generated from existing protocols represent forebrain neuron populations rather than the LC. Given the selective vulnerability of LC and other brainstem neurons to neurodegenerative disorders, developing protocols to generate human cells that reflect these populations is a high priority and would meaningfully complement animal models,

biomarker findings, and neuropathology through high-throughput molecular genetic screens, drug screens, electrophysiological recording, or cell signaling assays.

1.4.2 MODELING ALZHEIMER'S DISEASE WITH PHARMACOLOGY

N-(2-chloroethyl-N-ehtyl-2-bomobenzylamine (DSP-4) is an LC-specific neurotoxin which has long been used to mimic features of LC dysfunction seen in neurodegenerative disorders. In rodents, DSP-4 administration leads to LC terminal loss and NE depletion, like what is observed in human AD patients (Grzanna et al., 1989; Theron et al., 1993; Szot et al., 2010). This loss of LC terminals leads to inflammation in the hippocampus and prefrontal cortex, and mimics neuropsychiatric phenotypes associated with prodromal AD such as increased anxiety-like behavior (Iannitelli et al., 2023a). Moreover, when DSP-4 is administered to transgenic rodent models of AD, it exacerbates pathology, neuroinflammation, and behavioral impairments (Chalermpalanupap et al., 2018; Flores-Aguilar et al., 2022). DSP-4 thus provides a good model of early disease stages when LC axons are damaged, but is limited by the lack of Aβ and tau pathology that defines AD and the involvement of other nuclei as the disease progresses. 6-Hydroxydopamine (6-OHDA) is a similar compound that indiscriminately lesions dopaminergic and noradrenergic neurons, and produces phenotypes akin to PD. Direct injection of 6-OHDA into the LC of mice resulted in noradrenergic denervation and cell body degeneration and reduced forebrain NE tissue content and NET binding sites without altering other NE synthesis and handling genes (Szot et al., 2012).

1.4.3 VIRAL VECTOR AND SEEDING MODELS

Viral vectors have been useful for targeting and manipulating the LC due to the PRSx8 promoter and Cre-lines which allow for cell-type specific, robust expression of viral cargo. These extend beyond opto/chemogenetic manipulations, as viruses have also been used to drive

pathology in the LC. One study utilized a viral vector approach to express pseudophosphorylated tau in the rat LC, leading to axonal degeneration and impaired odor discrimination, which could be rescued by phasic LC stimulation (Ghosh et al., 2019; Omoluabi et al., 2021). Injection of tau in the LC of MAPT mice leads to the propagation and aggregation of tau in regions innervated by the LC (Kang et al., 2020). Furthermore, this tau expression leads to spatial and hippocampal-dependent learning and memory in both MAPT and 3xTg mice. Propagation of tau from the LC and behavioral effects were blunted in mice with genetic deletions of asparagine endopeptidase, the major enzyme targeted by the NE metabolite DOPEGAL. Another study overexpressed the PD-related pathology α-synuclein in the LC, which augmented firing rates of these neurons (Matschke et al., 2022). A separate study that also expressed α-synuclein in the LC resulted in LC fiber damage, increased anxiety-like behavior, and dysregulated sleep, the latter of which was corrected by blocking α-adrenergic receptors (Butkovich et al., 2020). We have also used viral vectors to express wild-type human tau in the LC of AD model rats and wild-type littermates, but found minimal effects of this tau isoform on behavior and pathology (see Chapter 4). These models have utility in understanding the consequences of various types of pathology that are constrained to the LC. These models, like application of DSP-4, do not address the contributions of other brain regions to AD, and are usually limited to a single type of pathology.

Numerous studies have also purified pathological proteins from AD patients and used them to seed pathology in various brain regions (Harper and Lansbury, 1997; Robert et al., 2021; Ulm et al., 2021). K18 synthetic tau fibrils unilaterally injected into the LC led to altered hippocampal EEG signatures despite the absence of tau spread from the LC (Ahnaou et al., 2019). Interestingly, another study also demonstrated a lack of spread to the hippocampus and entorhinal cortex following LC injections of synthetic tau fibrils (Iba et al., 2015). Spreading was noted in other heavily innervated regions like the amygdala, thalamus, and cortex. Though cell death was

observed over the course of 12 months, the LC contralateral to the injected hemisphere was largely spared and gradually cleared tau pathology. Injections of similar tau fibrils into the hippocampus remarkably resulted in appearance of tau pathology in the LC (Iba et al., 2013). Seeding models are also useful for understanding the effects of pathology that is isolated to the LC, and have the additional benefit of delineating the isoform-specific consequences of pathology. Like viral approaches, most studies do not account for both Aβ and tau pathology simultaneously, and cannot asses contributions of multiple brain regions when there is evidence of pathological spreading.

1.4.4 GENETIC MODELS

Introducing genetic mutations to murine species are the most common way of studying AD. There are a plethora of models that have induced AD phenotypes and Aβ pathology in rodents by introducing mutated human APP and PSEN genes that are causative of familial AD. Without the introduction of mutations that are causative of tauopathies, mice do not develop endogenous tau pathology.

Even in the absence of tau pathology, the LC is still affected in these genetic models (Kosel et al., 2020). Aβ oligomers are present in the LC of APP/PS1 mice and dysregulate GABA receptors in the LC, resulting in hyperactivity (Kelly et al., 2021). APP/PS1 mice also display early reductions in LC innervation and mid to late degeneration of LC cell bodies (O'Neil et al., 2007; Liu et al., 2008; Cao et al., 2021). These findings have been corroborated in other preclinical AD models, which again speaks to the susceptibility of the LC-NE system (Guerin et al., 2009; Mehla et al., 2019).

Another popular model is the P301S mouse, which introduces human microtubule-associated protein tau with mutations in the 0N4R or 1N4R isoforms (Allen et al., 2002; Yoshiyama

et al., 2007). P301S mice develop brain-wide tau pathology including the LC and show reduced capacitance and frequency of spontaneous excitatory postsynaptic currents (Zhu et al., 2018; Downs et al., 2023). Chronic sleep disruption exacerbates LC tau pathology and cell loss (Zhu et al., 2018) and ablation of LC neurons exacerbates cognitive deficits, pathology, and lethality in these mice (Chalermpalanupap et al., 2018). Interestingly, introducing familial mutations in the β1-adrenergic receptor that leads humans to require less sleep can restore rapid eye movement sleep and alleviate tau deposition in the LC (Shi et al., 2019; Dong et al., 2023). One drawback of this model is that it does not recapitulate the temporal deposition of tau, as the hippocampal CA1 subregion displays tau aggregates prior to the LC (personal communication).

It is worth briefly mentioning that new models that produce neuromelanin in the LC of rodent models are ongoing in an attempt to probe its protective and deleterious role in aging and disease. Early evidence suggests that neuromelanin expression in the rodent substantia nigra, another region that produces neuromelanin in humans, can be detected with MRI, and induces age-dependent cell loss in parallel with early and persistent dopaminergic dysregulation (Carballo-Carbajal et al., 2019). Preliminary evidence from our lab suggests that the LC is even more susceptible to the detrimental effects of neuromelanin, with accelerated neural degeneration and behavioral alterations (Iannitelli et al., 2023a).

1.4.5 RAT MODELS WITH A FOCUS ON THE TGF344-AD RAT

There are several drawbacks to the previously mentioned preclinical models of AD. These models rely on ubiquitous promoters, which cause expression of pathology throughout the brain, rather than in a region-specific manner (Yoshiyama et al., 2007; Jankowsky and Zheng, 2017; Kelly et al., 2021). Furthermore, most tau models of AD express mutated versions of tau that are more reminiscent of frontotemporal dementia (Yoshiyama et al., 2007; Jankowsky and Zheng,

2017). Finally, mouse models with amyloid mutations causative of AD in humans do not develop spontaneous tau pathology. There could be a number of reasons for this phenomenon including the fact that mice do not express the full complement of tau isoforms in adulthood (Hernandez et al., 2020).

Rats, on the other hand, express the full complement of tau in adulthood albeit in slightly different ratios compared to humans, suggesting that they might provide a more translatable model of AD (Hanes et al., 2009; Hernandez et al., 2020). Compared to mice, there are fewer rat models of AD, but are promising in the fact that some develop endogenous tau pathology while harboring only disease causing Aβ mutations (Leon et al., 2010; Cohen et al., 2013; Rorabaugh et al., 2017). MgCill-R-Thy1-APP transgenic rats express the APP_{751} gene that contains both the Swedish and Indiana mutations under the Thy1.2 promoter (Leon et al., 2010). No study has reported endogenous accumulation of tau in any region of the brain of these rats. However, lesioning the LC with DSP-4 results in similar behavioral deficits and neuroimmune response as we have previously reported in wild-type and P301S mice (Chalermpalanupap et al., 2018; Flores-Aguilar et al., 2022; Iannitelli et al., 2023a). Separately, the TgF344-AD rat model was created by introducing the Swedish mutation of the APP gene and exon 9 deletion of the presenilin gene that are causative of early onset AD (Cohen et al., 2013). We have extensively phenotyped behavior and pathology in these rats (Rorabaugh et al., 2017; Kelberman et al., 2022), which will be the focus of Chapter 4. Briefly, these rats develop Aβ pathology in the forebrain beginning at 12 months of age, endogenous forebrain tau pathology around 15 months (Cohen et al., 2013; Rorabaugh et al., 2017; Kelberman et al., 2022). TgF344-AD rats display prodromal AD symptoms as early as 3-6 months of age that occur in the absence of forebrain pathology, which are followed by late-stage (12-15 months) cognitive impairments (Rorabaugh et al., 2017; Kelberman et al., 2022). Crucially for this dissertation, we have previously shown that these rats develop

endogenous hyperphosphorylated tau in the LC by 6 months of age that is coincident with the emergence of prodromal behavioral symptoms (Rorabaugh et al., 2017; Kelberman et al., 2022). Furthermore, it is well documented that these rats display NE depletion and denervation, especially in the hippocampus, but in the absence of frank LC cell death (Rorabaugh et al., 2017; Goodman et al., 2021; Kelberman et al., 2022). Although NE depletion and denervation occur early, β-adrenergic receptor function is heightened and compensates to promote normal performance in some tasks (Goodman et al., 2021). Aged animals display cognitive deficits, most prominently in reversal learning, which can be restored by augmenting LC activity (Cohen et al., 2013; Rorabaugh et al., 2017; Kelberman et al., 2022). Although DSP-4 has not be utilized in these rats to date, another study used the selective neurotoxin dopamine-β hydroxylase IgG-saporin to lesion LC terminals and noted worse spatial and working memory, increased pathology and inflammation, and blood brain barrier breakdown (Kelly et al., 2019). TgF344-AD rats will be the focus of the current dissertation and arguably represent the preclinical model that most closely recapitulates the human condition. Together, these data suggest disease-state dependent alterations in LC firing rates that contribute to behavioral abnormalities along AD progression that are address comprehensively in Chapters 2 and 4.

1.4.6 NON-HUMAN PRIMATES

One limitation of using rodents to study AD is that they do not develop endogenous Aβ or tau pathology over the course of aging, and even TgF344-AD rats do not display frank LC degeneration (Van Dam and De Deyn, 2006; Rorabaugh et al., 2017). Therefore, certain key aspects of disease progression are lacking in the model that will be comprehensively described in this dissertation. Some non-human primates develop age-related deposition of amyloid and tau, in the absence of genetic mutations (Li et al., 2019a). Non-human primates also produce neuromelanin, which murine models do not, thus expressing a potential vulnerability factor and

allowing for use of neuromelanin-sensitive MRI to investigate LC-related changes (Scherer, 1939; Adler, 1942; Herrero et al., 1993; McCormack et al., 2004). To date, two studies have used pharmacological means in non-human primates to recapitulate LC dysfunction akin to what is observed in human neurodegenerative disorders. The first notes LC volume loss induced by MPTP administration, a pharmacological means to produce PD-like phenotypes, in marmosets (Hikishima et al., 2015). The second showed that DSP-4 reduced LC NE and dopamine-β hydroxylase levels and increased amyloid-β pathology in the forebrain, but in the absence of neuroinflammation (Duffy et al., 2019). In contrast, DSP-4 administration in rodent results in dramatic neuroimmune responses, which reiterates the need to verify preclinical findings across a variety of species to better inform us of the human condition. The paucity of non-human primate imaging studies is likely due to a number of factors including cost, underdeveloped models of neurodegenerative disease and a lack of genetic and opto/chemogenetic tools to selectively manipulate circuits. Development of transgenic non-human primates is nonetheless warranted and ongoing, and could be especially important for understanding genetic contributions to progression of endogenous neuropathology within the LC across aging and disease (Arnsten et al., 2019; Seita et al., 2020).

1.5 PREVIOUS WORK AND GAPS IN THE FIELD

Hypotheses regarding changes in LC activity across the progression of AD are abundant and supported by observed behavioral abnormalities (Weinshenker, 2018; Janitzky, 2020). However, only two studies have directly recorded LC neurons under the influence of AD-relevant pathology, and these were limited by the use of animal models that develop pathology throughout the brain in a pattern that does not recapitulate the “LC-first” hyperphosphorylated tau deposition observed in humans (Kelly et al., 2021; Downs et al., 2022). Therefore, recordings of LC neurons in animal models that develop selective early LC tau pathology are lacking. With the advent of the

TgF344-AD rat, which accumulates hyperphosphorylated tau in the LC prior to tau or amyloid deposition in the rest of the brain, it became possible to study the effects of isolated LC tau pathology on electrophysiological properties (Cohen et al., 2013; Rorabaugh et al., 2017). Similarly, molecular characterization of the LC has been performed, but typically focus on changes in genes involved in NE synthesis and transmission (TH, DβH, NET) in the context of AD or are performed in unperturbed contexts (Szot et al., 2006, 2007; Mulvey et al., 2018; Luskin et al., 2022; Weber et al., 2022; Iannitelli et al., 2023b). Efforts using targeted and bulk transcriptomic and proteomic approaches have been hampered due to the small size of the LC and proximity to other brainstem nuclei but are necessary for identifying molecular targets that underlie LC dysfunction and could be leveraged to normalize LC activity in clinical settings. Finally, while behavioral changes in TgF344-AD rats have been described by us and others, most reports focused on the progression of cognitive deficits (Cohen et al., 2013; Rorabaugh et al., 2017; Munoz-Moreno et al., 2018; Pentkowski et al., 2018; Kreuzer et al., 2020; Sare et al., 2020; Wu et al., 2020; Goodman et al., 2021). Further characterization of prodromal symptoms, such as changes in sleep/arousal and anxiety-like phenotypes, and their link to LC hyperphosphorylated tau aggregation and subsequent dysfunction are indispensable for guiding the use of noradrenergic interventions in AD.

1.6 DISSERTATION AIMS

The goal of this dissertation was to specifically describe LC dysfunction at multiple levels in a rat model that recapitulates the “LC first” pattern of AD pathology deposition. I leveraged the TgF344-AD rat model, the only known preclinical model that fits this specification. Moreover, we phenotyped these rats at both 6-months, representing a preclinical stage of disease where hyperphosphorylated tau is isolated to the LC, and 15-months, a stage akin to mild-cognitive impairment when Aβ and tau pathology are abundant throughout the brain. I first describe how

LC electrophysiological properties are altered in AD in Chapter 2. Next, I identify potential molecular underpinnings of these alterations in Chapter 3. Finally, I explore the behavioral consequences of altered LC activity in Chapter 4 (**Figure 1.4**).

Overall, my comprehensive characterization of LC dysfunction in the TgF344-AD rat lends support to the concept that alterations to LC firing rates and biochemistry contribute to symptoms at each stage of AD. Both young and old TgF344-AD rats demonstrated lower basal firing rates and elevated spontaneous bursting properties. There was an age-dependent effect on sensory-evoked LC firing, where young and old rats showed hyperactivity and hypoactivity, respectively. I next revealed age-dependent molecular changes occurring at the level of gene expression in LC neurons of TgF344-AD rats that were consistent with the observed alterations to LC firing rates. Compared to age-matched WT controls, 6-month TgF344-AD rats expressed lower mRNA levels of Gabra3 and Oprl1, two receptors crucial for inhibitory neurotransmission, while 15-month TgF344-AD rats demonstrated elevated levels of genes involved in NE synthesis (*Th*, *Dbh*), packaging (*Slc18a2*), and reuptake (*Slc6a2*), likely representing a compensatory mechanism to counteract decreased forebrain NE levels and axonal degeneration. A possible unintended consequence of this upregulation in NE tone is the potential for increased somatodendritic release of NE and excessive autoinhibition of LC neurons via α2-adrenergic receptors.

Finally, I tested young and old TgF344-AD rats in a battery of paradigms to understand the contributions of previously identified electrophysiological and molecular phenotypes to disease stage-dependent behavioral deficits (Chapter 4). I also assessed the added consequences of virally-expressed human tau in the LC on behavior, inflammation, and pathology. Overall, I found that effects of viral human tau expression were negligible, and, in many instances, the effects of age were more pronounced than that of genotype. However, I did identify early and persistent anxiety-like phenotypes and cognitive deficits in TgF344-AD rats, both of which are observed in

the human condition. Early emergence of anxiety-like phenotypes and late-stage cognitive deficits are consistent with my finding of LC hyperactivity and hypoactivity, respectively.

Together, these data provide a comprehensive catalog of LC firing rates and patterns in AD, while also linking dysregulated LC activity with the appearance of behavioral abnormalities. Importantly, the use of TgF344-AD rats allowed me to isolate the consequences of LC tau pathology on early disease states for the first time. Because the LC undergoes catastrophic degeneration later in disease, these early findings have important clinical significance, as they mark a point before the LC is irreversibly damaged and when LC-based disease-altering therapeutics may be most beneficial. To this end, my molecular characterization of LC neurons along the progression of AD suggests mechanistic underpinnings of dysregulated LC firing and provides specific therapeutic targets to potentially normalize LC activity in both early and late AD.

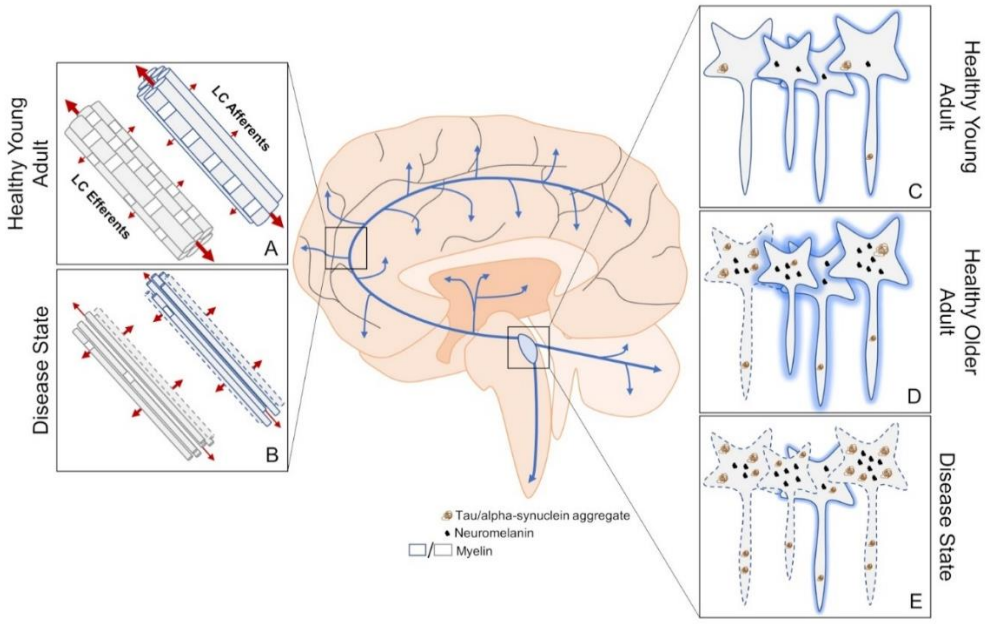

Figure 1.1. An overview of structural MRI approaches to investigate LC dysfunction in neurodegenerative disorders. (A) DTI measures three-dimensional diffusion of water molecules (red arrows where thickness of the arrow represents weight of diffusion) to get readouts of axonal health. Water molecules tend to diffuse along, rather than across, healthy myelinated axons. (B) This structural imaging method has been used to determine changes in innervation, myelination, and axon size between the LC and downstream brain regions in disease states, but cannot distinguish between deficits in efferent or afferent connections. (C) Contrast thought to arise from neuromelanin, high water proton density, and/or other mechanisms allow the LC to be visualized using structural MRI. (D) LC contrast appears to peak in adulthood, which is correlated with neuromelanin levels. At this stage, some hyperphosphorylated tau may be apparent. (E) A decrease in LC contrast is thought to represent compromised LC integrity during disease states, but has yet to be attributed to cell or dendritic field loss. Neurodegeneration may result from the aggregation of hyperphosphorylated tau. Dashed lines indicate degenerating neurons and shading represents relative contrast from each neuron. Blue arrows represent LC-NE release sites throughout the brain and spinal cord.

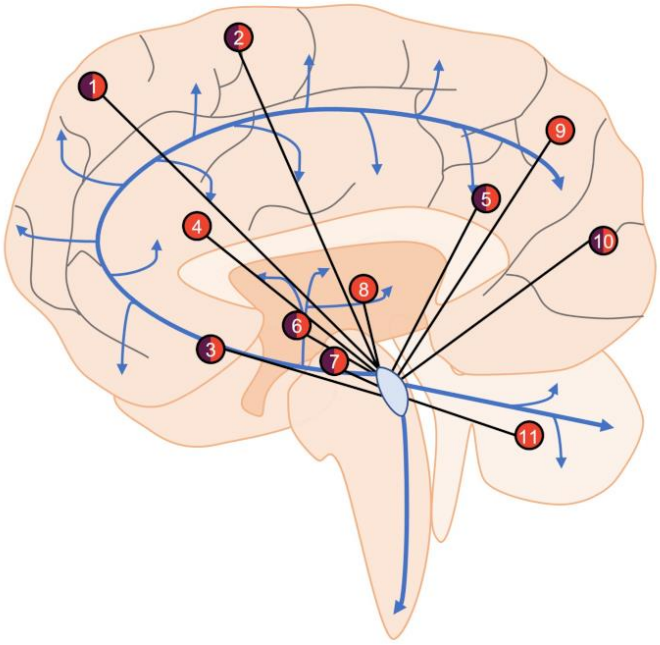

Figure 1.2. An overview of LC functional connectivity obtained using fMRI. Areas with positive (orange), negative (purple), or mixed (both) functional connectivity with the LC include frontal (1) and sensorimotor (2) cortical regions, nucleus basalis of Meynert (3), anterior and posterior cingulate cortices (4, 5), caudate/putamen (6) ventral tegmental area (7), thalamus (8), parietal cortex (9), occipital cortex (10), and cerebellum (11). Areas showing both positive and negative functional connectivity are the result of specific subregions of interest (i.e., in the frontal cortex, the LC is positively connected with superior frontal gyrus but negatively connected with frontopolar regions), changes in connectivity across aging (i.e., nucleus basalis of Meynert), or disparate findings between studies (i.e., occipital cortex). Blue arrows represent LC-NE release sites throughout the brain and spinal cord.

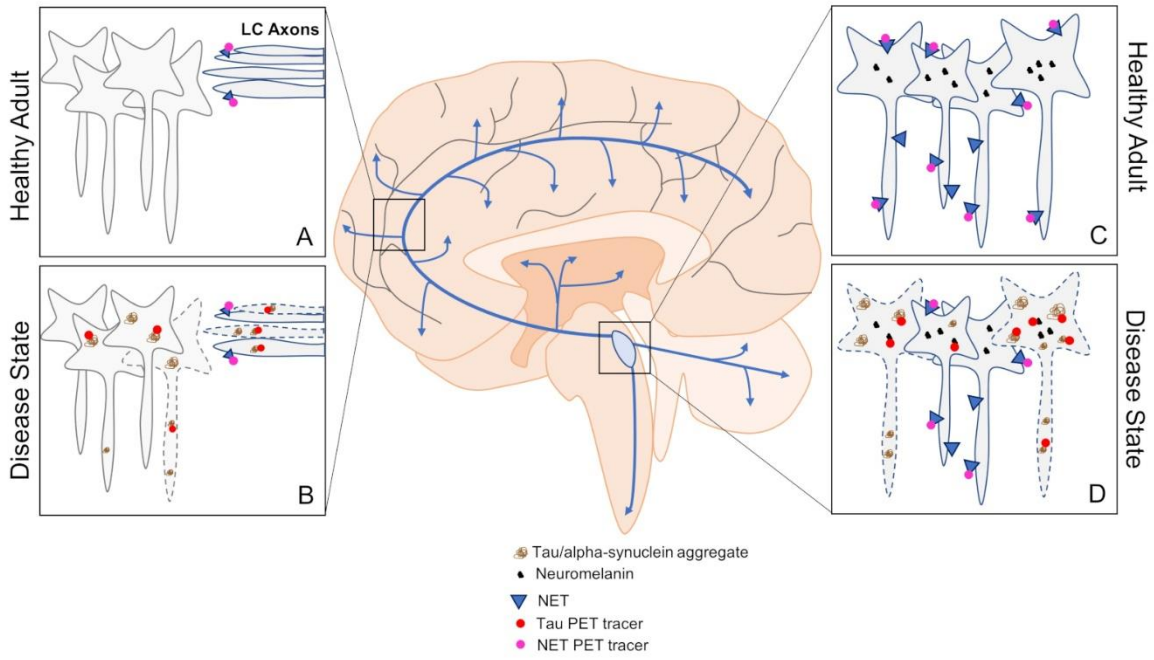

Figure 1.3. An overview of PET approaches to investigating changes in LC dysfunction in neurodegenerative disorders. (A,B) Tau and NET PET can be used to assess pathological load and LC fiber integrity by imaging downstream brain regions in healthy and disease states. (C,D) Imaging the LC using tau and NET PET can also be informative of pathological load and cell body integrity in healthy and disease states. Blue arrows represent LC-NE release sites throughout the brain and spinal cord.

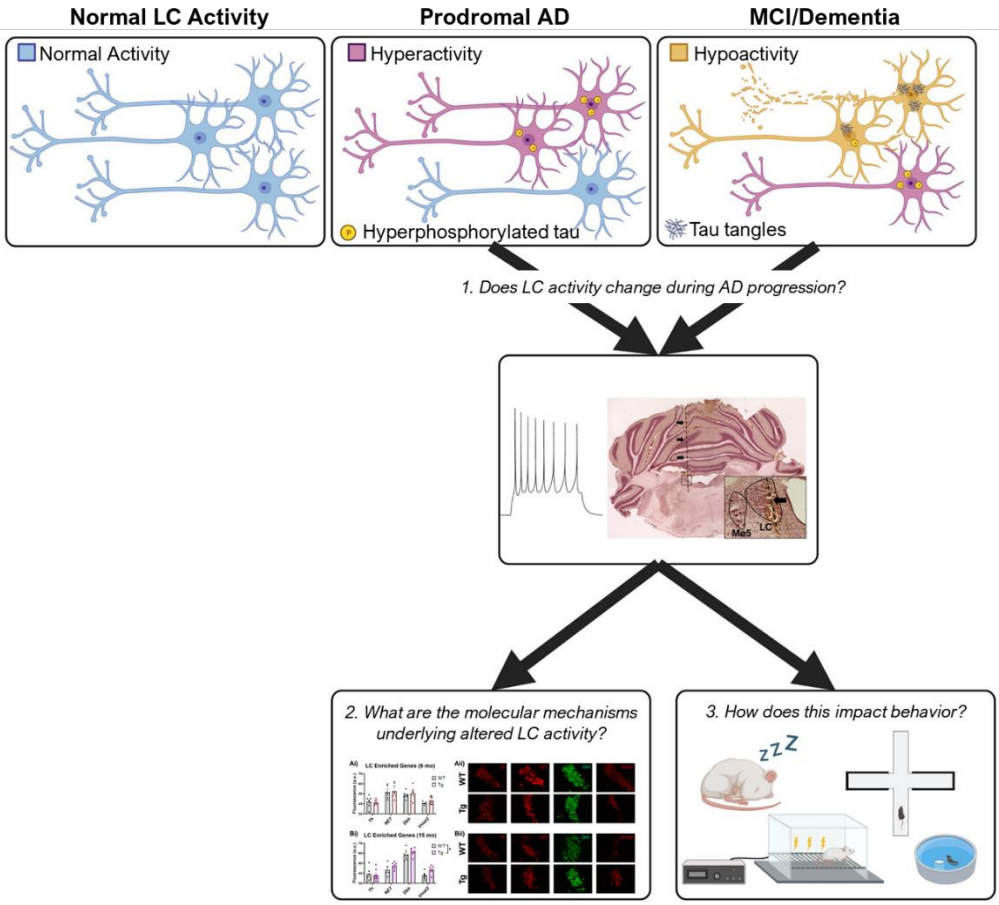

Figure 1.4. An overview of LC dysfunction in Alzheimer's disease and aims of this dissertation. During normal aging, the LC is healthy and exhibits normal tonic and phasic firing patterns. In prodromal phases of AD, hyperphosphorylated tau pathology is noted in some LC neurons which is thought to cause hyperactivity and contribute to non-cognitive behavioral symptoms such as alterations to mood and arousal. In late stages of disease, the LC harbors neurofibrillary tangles, leading to degeneration and presumed hypoactivity of LC neurons that contribute to cognitive deficits. The first goal of this dissertation was to determine disease stage-dependent changes in LC firing rates using the TgF344-AD rat model which develops early hyperphosphorylated tau pathology restricted to the LC, and in late stages develops both amyloid and tau pathology in forebrain regions (1). Next, I sought to uncover molecular mechanisms that contribute to altered LC firing rates that we identified in the previous aim (2). Finally, I

comprehensively characterized the behavioral abnormalities, both non-cognitive and cognitive, in similarly aged rats (3).

CHAPTER 2: AGE-DEPENDENT DYSREGULATION OF LOCUS COERULEUS FIRING IN A TRANSGENIC RAT MODEL OF ALZHEIMER'S DISEASE

Parts of this chapter were used verbatim, with permission, from the following publication:

1. Kelberman MA, Rorabaugh JM, Anderson CR, Marriott A, DePuy SD, Rasmussen K, McCann KE, Weiss JM, Weinshenker D (2023) Age-dependent dysregulation of locus coeruleus firing in a transgenic rat model of Alzheimer's disease. Neurobiology of Aging Available at: http://dx.doi.org/10.1016/j.neurobiolaging.2023.01.016.

Abstract

Hyperphosphorylated tau in the locus coeruleus (LC) is ubiquitous in prodromal Alzheimer's disease (AD), and LC neurons degenerate as AD progresses. Hyperphosphorylated tau alters firing rates in other brain regions, but its effects on LC neurons are unknown. We assessed single unit LC activity in anesthetized wild-type (WT) and TgF344-AD rats at 6 months, which represents a prodromal stage when LC neurons are the only cells containing hyperphosphorylated tau in TgF344-AD animals, and at 15 months when β-amyloid (Aβ) and tau pathology are both abundant in the forebrain. At baseline, LC neurons from TgF344-AD rats were hypoactive at both ages compared to WT littermates but showed elevated spontaneous bursting properties. Differences in footshock-evoked LC firing depended on age, with 6-month TgF344-AD rats demonstrating aspects of hyperactivity, and 15-month transgenic rats showing hypoactivity. Early LC hyperactivity is consistent with appearance of prodromal neuropsychiatric symptoms and is followed by LC hypoactivity which contributes to cognitive impairment. These results support further investigation into disease stage-dependent noradrenergic interventions for AD.

2.1 INTRODUCTION

Accumulation of hyperphosphorylated tau within subcortical nuclei and subsequent dysfunction of these neurons is a nearly ubiquitous feature along Alzheimer's disease (AD) progression (Theofilas et al., 2015; Ehrenberg et al., 2017). A seminal report from Braak and colleagues (Braak et al., 2011), independently replicated by other groups (Elobeid et al., 2012; Theofilas et al., 2017; Pletnikova et al., 2018), positions the noradrenergic locus coeruleus (LC) as the earliest site of pathological tau deposition, well before cortical β-amyloid (Aβ) plaque accumulation or the onset of diagnostic cognitive deficits. During prodromal phases of AD, non-cognitive symptoms consistent with noradrenergic hyperactivity, including sleep disturbances, agitation, and anxiety, emerge coincident with the appearance of hyperphosphorylated tau in the LC (Ehrenberg et al., 2018; Pentkowski et al., 2018; Weinshenker, 2018; Johansson et al., 2021; Kelberman et al., 2022). Cerebrospinal fluid norepinephrine (NE) levels and its turnover are elevated in early AD (Palmer et al., 1987; Elrod et al., 1997; Hoogendijk et al., 1999; Henjum et al., 2022), and a recent neuroimaging study demonstrated that higher LC signal on a neuromelanin-sensitive MRI was predictive of neuropsychiatric symptom severity in AD patients (Cassidy et al., 2022), further supporting the theory of LC hyperactivity during initial stages of disease. At the same time, numerous studies have linked the deterioration of LC integrity to cognitive and structural decline in aging and AD (Wilson et al., 2013; Kelly et al., 2017; Bachman et al., 2021; Jacobs et al., 2021; van Hooren et al., 2021; Prokopiou et al., 2022), suggestive of reduced LC-NE transmission during later stages of the disease.

While neurochemical, neuropathological, and behavioral results are consistent with disease stage-specific alterations in LC activity, direct evidence for changes in LC firing is mostly lacking. Aβ pathology often induces neural hyperactivity (Busche and Hyman, 2020), including in the LC (Kelly et al., 2021), whereas tau pathology typically induces neuronal hypoactivity (Busche

et al., 2019). However, there are other reports of tau-mediated hyperactivity (Holth et al., 2013; Huijbers et al., 2019; Shimojo et al., 2020), suggesting region and/or cell-type specific effects. Given that Aβ only accumulates in the LC during late stages of AD (Cole et al., 1993; Kelly et al., 2021), the dysregulation of LC circuits at the level of the cell bodies is likely dominated by the early accumulation of hyperphosphorylated tau. Therefore, understanding the impact of aberrant tau on LC neural activity is critical for determining the neurobiological underpinnings of prodromal AD symptoms and progression to cognitive impairment. This information could then inform rational development of early biomarkers and therapeutic interventions at various disease stages.

The objective of this study was to delineate the effects of AD-like hyperphosphorylated tau on LC firing rates. Though some studies have begun to track LC activity in humans using functional MRI (Prokopiou et al., 2022), these techniques lack spatial and target specificity for small regions like the LC (Kelberman et al., 2020). We therefore employed the TgF344-AD rat model, which expresses mutant human amyloid precursor protein and presenilin-1 (APP/PS1) that cause autosomal dominant, early-onset AD (Cohen et al., 2013). This model possesses several benefits for our study. These rats demonstrate many of the same behavioral phenotypes that are observed in AD that are influenced by LC activity. These include early anxiety-like behaviors followed later by cognitive impairment that can be reversed by LC activation (Cohen et al., 2013; Rorabaugh et al., 2017; Pentkowski et al., 2018; Kelberman et al., 2022). In addition, TgF344-AD rats, unlike their APP/PS1 transgenic mouse counterparts, develop endogenous tau pathology that first appears in the LC (Rorabaugh et al., 2017). This tau deposition is coincident with the appearance of non-cognitive behavioral abnormalities but prior to tau or Aβ pathology elsewhere in the brain, reminiscent of human disease progression. In the current study, we recorded single unit LC activity from anesthetized TgF344-AD rats and wild-type (WT) littermates at baseline and in response to footshock at 6 months, an age when anxiety-like behavior emerges and

hyperphosphorylated tau in the LC is the only detectable AD-like neuropathology, as well as 15 months, when brain-wide tau and Aβ pathology are evident in combination with deficits in learning and memory.

2.2 METHODS

2.2.1 Animals

This study used a total of 42 TgF344-AD rats and WT littermates on a Fischer background aged 6 or 15 months. TgF344-AD rats were hemizygous for the *APPsw/PS1ΔE9* transgene that contains mutations causative of autosomal dominant early-onset AD (Cohen et al., 2013). Rats were housed in groups of 2-3 on a 12-h light/dark cycle (lights on at 7:00 am) with food and water available *ad libitum*.

All experiments were conducted in accordance with the Institutional Animal Care and Use Committee at Emory University. Male and female rats were assigned to sex-balanced experimental groups, given the lack of prominent sex differences noted in this strain (Cohen et al., 2013; Sare et al., 2020; Kelberman et al., 2022).

2.2.2 Surgery

At two months of age, all rats to be used for electrophysiology underwent stereotaxic surgery. Rats were anesthetized with 5% isoflurane and maintained at 2% throughout surgery. Prior to incision, rats were given ketoprofen (5 mg/kg, s.c.). An AAV9-PRSx8-mCherry-WPRE-rBG virus was infused bilaterally targeting the LC (AP: -3.8 mm, ML: +/- 1.2 mm, DV: -7.0 mm from lambda with the head tilted 15 degrees downward). The injection syringe was left in place for 5 min following the infusion prior to being moved dorsally 1 mm and waiting an additional 2 min to ensure diffusion of virus at the site of injection. This tau-free virus was to be used as a control infusion for a planned experiment that we did not end up pursuing, and nothing further was done

with it in this study. Electrophysiology recordings were performed approximately 4 or 13 months following surgery.

2.2.3 Electrophysiology

At 6 or 15 months, rats were anesthetized with chloral hydrate (400 mg/kg, i.p.) and secured in a stereotaxic frame. An incision was made to expose the skull, which was leveled based on measurements made at bregma and lambda. A 15° head tilt was employed to avoid the sagittal sinus, and bilateral burr holes were drilled over the approximate location of the LC (AP: 3.8-4.0 mm, ML: 0.9-1.3 mm from lambda). 16-channel silicone probes (V1x16-Poly2-10mm-50s-177-V16_100-50, NeuroNexus; Ann Arbor, MI) were connected to a u-series Cereplex headstage (Blackrock Neurotech; Salt Lake City, UT). A 16-channel Cereplex Direct System was used to acquire digitized signals with a 250 Hz-5 kHz bandpass filter and 10 kS/s sampling rate. During electrophysiological recordings, LC units were identified based on field standard criteria, including stereotaxic coordinates, location adjacent to the mesencephalic trigeminal nucleus (Me5), biphasic response to footpinch/footshock, and reduction/cessation of spontaneous activity following injection of the selective α2-adrenergic receptor agonist clonidine (0.1 mg/kg i.p.) (Hirata and Aston-Jones, 1994; Kalwani et al., 2014; Vazey and Aston-Jones, 2014; West et al., 2015; Totah et al., 2018). Each recording began with a 5-min baseline period, which was immediately followed by 10 applications of a contralateral footpinch for LC verification, each separated by 10 s, as described previously (West et al., 2015). Afterwards, 0.5 ms 10 mA footshocks (each separated by 10 s for 5.5 min) were applied to the contralateral hindpaw, followed by the same pattern using 5 ms 10 mA footshocks. Footshocks were delivered by an ISO-Flex stimulus isolator and controlled by a Master-8 (A.M.P. Instruments; Jerusalem, Israel). LC spikes were manually sorted using Blackrock Offline Spike Sorting Software.

Electrophysiology analysis was performed in NeuroExplorer v5 (Nex Technologies; Colorado Springs, CO) or Matlab (R2019a; Mathworks; Natick, MA). To ensure that single units were being analyzed, neurons with >2% of recorded spikes within a predefined 3 ms refractory period were eliminated (Kalwani et al., 2014). The 5-min baseline recording served as the basal firing rate and to calculate the interspike interval for each single unit. Spontaneous bursting properties (number of bursts, percentage of spikes within a burst, burst duration, spikes per burst, interspike interval within a burst, burst rate, and interburst interval) of LC neurons during baseline recordings were also quantified. Spontaneous bursts were defined as two spikes with an interspike interval of <0.08 s and terminated with an interspike interval >0.16s, as previously described (Grace and Bunney, 1983; Iro et al., 2021). Footshock was used to ascertain changes to sensory evoked LC activity. LC response to footshock was divided into three response categories: immediate (0-60 ms), intermediate (60-100 ms), and late (200-400 ms). These periods were based on a previous report demonstrating that altering the length (0.5, 2, and 5 ms) of footshock could elicit both a standard immediate and long latency LC response (Hirata and Aston-Jones, 1994).

2.2.4 Tissue Preparation and Immunohistochemistry

Following completion of electrophysiological recordings, rats were overdosed with isoflurane and perfused with potassium phosphate-buffered saline followed by 4% paraformaldehyde (PFA). Brains were removed and stored in 4% PFA overnight then transferred to 30% sucrose until sectioning. Brain sections containing the LC were sliced at 30 um and either dry mounted or stored in cryoprotectant until being processing for immunohistochemistry.

Dry mounted sections were counterstained with neutral red. Slides were submerged in increasing concentrations of ethanol (70%, 95%, and 100%) for 1 min each, followed by 10 min in

neutral red, dunked 3-5 times in increasing concentrations of ethanol (70%, 95%, and 100%), and finally in xylene for 2 min. Slides were coverslipped with permount and imaged on a Keyence BZ-X700 microscope (KEYENCE; Osaka, Japan).

To confirm that α2-adrenergic receptors (*Adra2a*) are specific to noradrenergic neurons in the LC region and thus the only cells that could respond to clonidine during our recordings, we performed fluorescent *in situ* hybridization using the RNAscope Multiplex Fluorescent V2 Assay (Advanced Cell Diagnostics, Newark, CA, USA) on brainstem sections containing the LC. One 6-month WT male was lightly anesthetized, and the brain was quickly removed and flash frozen in isopentane on dry ice. The brain was stored at -80C until sectioning on a cryostat at 16µm. The RNAscope assay was performed following the manufacturer's protocol, multiplexing tyrosine hydroxylase (*Th*) and *Adra2a*. Images were taken in a 1µm pitch z-stack (10um total) on a Keyence BZ-X700 microscope at 20x and 40x. A representative 2x section was also captured to visualize most of the coronal section containing the LC.

2.2.5 Statistical Analysis:

Figures were made and statistical analyses were performed using GraphPad Prism (v. 9.2.0; San Diego, CA) with the mean ± SEM. A two-way ANOVA was used to identify main effects of age, genotype, or their interaction. When applicable, post-hoc tests were performed across genotypes within an age group using the Holm-Sidak correction. For all analyses, statistical significance was set at $\alpha = 0.05$. Supplemental figures are presented as raincloud plots consisting of a density plot, box-and-whiskers plot, and individual data points that were created in R using modified code from open-source platforms and from (Allen et al., 2019; Xu et al., 2021). All code is available upon reasonable request.

2.3 RESULTS

2.3.1 LC Neural Recording Verification

We used neuroanatomical, sensory, electrophysiological, and pharmacological methods to verify that recordings were from bona fide LC neurons. LC units were located at a similar depth but medial to Me5, which was identified by jaw deflection **(Figure 2.1A)**. Putative LC units displayed a canonical biphasic response to footpinch/footshock, and as previously reported, a subset of these neurons demonstrated a late phase (200-400 ms) response to 5 ms footshock that was not observed in response to 0.5 ms footshock **(Figure 2.1B)**. LC cells, unlike other adjacent nuclei, express high levels of *Adra2a* and are inhibited by the α2-adrenergic receptor agonist clonidine (McCune et al., 1993) **(Figure 2.1C, D)**. Finally, we verified that electrode tracks were in the LC post-recording using a neutral red counterstain **(Figure 2.1E)**.

2.3.2 Alteration of Pacemaker-like LC Firing in TgF344-AD Rats

LC neurons fire with regular pacemaker activity between 0.5-2 Hz under normal conditions that maintains baseline levels of arousal, attention, and noradrenergic tone (Aston-Jones and Cohen, 2005a; Poe et al., 2020). To assess tau pathology- and age-induced changes in tonic firing, we recorded periods of spontaneous activity from 75-120 isolated LC neurons per group (N=8-11 animals). We graphed our data in the main figures using traditional bar graphs which highlight group level differences in firing rates as well as in supplemental figures using raincloud plots to highlight the variability and patterns that are not captured by more traditional visualization methods. There was a significant main effect of genotype ($F_{1, 385} = 4.35$, $p = 0.04$) on baseline firing rates, such that LC neurons of TgF344-AD rats were less active than those from WT littermates (**Figure 2.2A**; **Supplemental Figure 2.1A**). There was no effect of age ($F_{1, 385} = 0.11$, $p = 0.74$) or an age x genotype interaction ($F_{1, 385} = 0.78$, $p = 0.38$). We also quantified interspike interval for units with two or more spikes (N=74-119 neurons/group), defined as the time between successive

action potentials (**Figure 2.2B**; **Supplemental Figure 2.2B**). There was a trend towards a main effect of genotype ($F_{1, 379}$ = 3.55, p = 0.06), where TgF344-AD LC neurons had a shorter time between successive spikes, which was surprising given that tonic firing was lower in the TgF344-AD rats. However, LC neurons can also transiently fire in brief bursts, even in the absence of external stimuli (Aston-Jones and Bloom, 1981b; Akaike, 1982; Finlayson and Marshall, 1988; Safaai et al., 2015; Iro et al., 2021). Therefore, we quantified the spontaneous bursting properties of LC neurons from TgF344-AD and WT rats. Of the neurons exhibiting spontaneous bursts (N=48-88 neurons/group), there was a main effect of genotype on firing rate within a burst ($F_{1, 267}$ = 6.57, p = 0.01) and on interspike interval within a burst ($F_{1, 267}$ = 8.02, p < 0.01). During spontaneous bursts, firing rates were higher in TgF344-AD rats and interspike intervals were lower (**Figures 2.2C, D**; **Supplemental Figure 2.1C, D**). There were no alterations in other aspects of spontaneous bursts (**Table 2.1**). Overall, these changes indicate lower basal firing rates but elevated bursting properties of LC neurons in TgF344-AD rats.

2.3.3 Dysregulated LC Response to Footshock in TgF344-AD Rats

LC neurons fire in transient bursts in awake animals to a variety of salient stimuli, including novelty, tones, pain, and stress (Aston-Jones and Bloom, 1981a; Vankov et al., 1995; Uematsu et al., 2017). We characterized the responsiveness of LC neurons 0-60, 60-100, and 200-400 ms following footshock (10 mA, 0.5 or 5 ms), which maintains its ability to trigger LC bursting under anesthesia, as described (Hirata and Aston-Jones, 1994). For the immediate response phase (**Figure 2.3A, B**; **Supplemental Figure 2.2A, B**), there was a reduction of LC activity in TgF344-AD rats that was specific to the 0.5 ms footshock ($F_{1, 433}$ = 6.06, p = 0.01). There was a significant age x genotype interaction on LC firing rates in the mid-phase response to both 0.5 ms ($F_{1, 433}$ = 6.26, p = 0.01) and 5 ms ($F_{1, 452}$ = 9.56, p < 0.01) footshock (**Figure 2.3C, D**; **Supplemental Figure 2.2C, D**). LC neurons from TgF344-AD rats were hyperactive at 6 months following the 5 ms

footshock (t_{452} = 2.36, p = 0.04), but hypoactive at 15 months following the 0.5 (t_{433} = 2.16, p = 0.03) and 5 ms footshock (t_{452} = 2.03, p = 0.04), compared to age-matched WT littermates. We observed no main effects on late phase response to either 0.5 ms or 5 ms footshock (**Figure 2.3E, F**; **Supplemental Figure 2.2E, F**).

2.4 DISUCSSION

2.4.1 Overview of changes in LC firing and associations with symptoms of AD

The LC is one of the earliest regions to develop AD-related neuropathology in the form of hyperphosphorylated tau and undergoes frank cell death in mid- to late-stage disease (Busch et al., 1997; Braak et al., 2011; Elobeid et al., 2012; Theofilas et al., 2017; Pletnikova et al., 2018). The appearance of hyperphosphorylated tau in the LC is coincident with the emergence of prodromal symptoms of AD such as sleep disturbances, agitation, dysregulated mood, and increased anxiety, which are suggestive of LC hyperactivity (Ehrenberg et al., 2018; Pentkowski et al., 2018; Weinshenker, 2018; Johansson et al., 2021; Kelberman et al., 2022). Early LC hyperactivity is further supported by increases in cerebrospinal fluid NE levels and turnover (Palmer et al., 1987; Elrod et al., 1997; Hoogendijk et al., 1999; Henjum et al., 2022), axonal sprouting and elevated receptor density (Szot et al., 2006, 2007), and adrenergic receptor hypersensitivity (Goodman et al., 2021). By contrast, late-stage AD is characterized by phenotypes consistent with NE deficiency such as apathy and cognitive impairment that are correlated with loss of LC integrity (Matthews et al., 2002; Kelly et al., 2017; David et al., 2022; Hezemans et al., 2022; Ye et al., 2022). These data suggest that early hyperphosphorylated tau triggers compensatory mechanisms that increase LC-NE transmission and maintain function, which eventually fail as LC neurons succumb to more advanced pathology (Szot et al., 2006, 2007;

Goodman et al., 2021). The divergent phenotypes across the progression of AD could be explained, at least in part, by changes in LC firing rates.

Prior to our study, only two investigations tracked changes in LC activity using rodent AD models, one with Aβ and one with mutant P301S tau pathology (Kelly et al., 2021; Downs et al., 2022). Mislocalization of GABA receptors associated with soluble Aβ oligomers in the LC led to hyperactivity, whereas effects of P301S tau expression were minimal. There are limitations in these studies that should be noted. In both cases, only one aspect of AD-like pathology was incorporated, the transgenes were driven by ubiquitous promoters, and LC Aβ and P301S tau are more reminiscent of late-stage AD and frontotemporal dementia, respectively. It is therefore unsurprising that we uncovered different dysregulated tonic and phasic LC firing patterns using an AD model that develops both Aβ and tau pathology (**Figure 2.4**), the latter of which is comprised of endogenous wild-type tau and isolated to the LC at early ages.

In our study, both young and old TgF344-AD animals showed tonic LC hypoactivity but elevated spontaneous bursting properties. Moreover, LC activity in response to footshock stress was elevated in 6-month TgF344-AD rats. Importantly, we and others have reported behavioral abnormalities in young TgF344-AD reminiscent of neuropsychiatric symptoms in prodromal AD (Ehrenberg et al., 2018; Pentkowski et al., 2018; Wu et al., 2020; Johansson et al., 2021; Kelberman et al., 2022). At first glance, reduced pacemaker LC firing is inconsistent with evidence that excessive NE transmission contributes to comorbidities seen in prodromal phases of AD (Weinshenker, 2018). Specifically, elevations in tonic, but not phasic, LC activity are associated with stress and anxiety (Valentino and Foote, 1988; Curtis et al., 2012; McCall et al., 2015). On the other hand, increased phasic LC activity driven by spontaneous bursting and/or environmental stimuli could promote improper transitions through different stages of arousal (Aston-Jones and Bloom, 1981b; Carter et al., 2010; Takahashi et al., 2010), resulting in fractured sleep/wake cycles

that are common in AD (Ehrenberg et al., 2018; Weinshenker, 2018). The importance of distinguishing between different patterns of LC firing across disease stages is highlighted by a recent report that enhancement of phasic LC firing protects LC neurons from deleterious forms of tau, whereas high tonic firing results in AD-associated psychiatric symptoms and worsened neuronal health (Omoluabi et al., 2021). Together, these data are consistent with the idea that a combination of homeostatic mechanisms to maintain LC function in the presence of pathology and damage (e.g. altered LC firing, increased NE turnover, elevated adrenergic receptor sensitivity and density, and axonal sprouting) contributes to prodromal behaviors. These homeostatic/compensatory mechanisms ultimately fail in later disease, as indicated by reduced NE tissue levels, noradrenergic denervation, and frank LC neuron loss (Reinikainen et al., 1988; Nazarali and Reynolds, 1992; Matthews et al., 2002; Rorabaugh et al., 2017; Goodman et al., 2021; Kelberman et al., 2022), and our results showing tonic LC hypoactivity and blunted response to footshock in 15-month TgF344-AD rats. This culminates in a loss of LC-NE transmission and cognitive impairment, which our lab has successfully rescued by selectively augmenting tonic LC firing (Armbruster et al., 2007; Vazey and Aston-Jones, 2014; Rorabaugh et al., 2017).

2.4.2 Potential mechanisms underlying changes in LC firing rates

While the neurobiological mechanisms underlying the changes in LC firing properties we observed remain to be determined, the nature of those changes offers clues. Reductions in tonic firing rates and hypoactivity in aged TgF344-AD rats are unlikely due to cell death because there is no LC neuron loss at this age (Rorabaugh et al., 2017). However, we know that β-adrenergic receptor function in the dentate gyrus is heightened in young TgF344-AD rats, indicating that adrenergic receptor plasticity exists in this model (Goodman et al., 2021). In the pons, α2-adrenergic receptors are abundantly expressed within the LC itself (**Figure 2.1**) and regulate its activity as inhibitory autoreceptors. Changes in the density or sensitivity of these receptors, which

have been noted in the human condition with other subtypes of adrenergic receptors (Szot et al., 2006, 2007; Goodman et al., 2021), could alter LC neuron firing properties. Furthermore, elevated phasic activity may result in greater NE release compared to tonic activity (Florin-Lechner et al., 1996). A surplus of NE at the level of LC cell bodies would culminate in augmented inhibition from neighboring LC neurons, also potentially leading to tonic LC hypoactivity.

Besides its intrinsic pacemaker activity, the LC also receives extensive excitatory, inhibitory, and modulatory (serotonin (5-HT), hypocretin/orexin, corticotropin releasing hormone) input from various cortical and subcortical regions that could contribute to altered firing rates in TgF344-AD rats (Benarroch, 2009; Delaville et al., 2011). GABAergic inputs arising from the ventrolateral preoptic area or the peri-LC region modulate basal noradrenergic tone and have been mainly studied in the context of arousal (Nitz and Siegel, 1997; Lu et al., 2002; Breton-Provencher and Sur, 2019). In addition, given that the LC and peri-LC GABAergic neurons receive a set of non-overlapping innervations (Breton-Provencher and Sur, 2019), it is possible that changes in firing rates are the result of a dysregulated, multi-synaptic pathway. For example, systemic application of a 5-HT receptor agonist lowers tonic but enhances phasic firing of the LC in a GABA-dependent manner (Chiang and Aston-Jones, 1993a). Similarly, 5-HT dampens sensitivity of LC neurons to glutamatergic inputs, which originate from the cortex, lateral habenula, and paragigantocellularis nucleus (Herkenham and Nauta, 1979; Ennis and Aston-Jones, 1988; Aston-Jones et al., 1991; Chiang and Aston-Jones, 1993b; Jodo and Aston-Jones, 1997). Thus, altered serotonergic signaling to the LC represents a singular mechanism that could influence both altered tonic and phasic firing patterns. With respect to footshock-evoked LC activity, the immediate and middle phase responses are also mediated, in part, by excitatory amino acids (Ennis and Aston-Jones, 1988; Chiang and Aston-Jones, 1993b). Changes in excitatory amino acid transmission, receptor expression, or localization could be responsible for various aspects of

dysregulated LC firing. Other neuropeptides, such as hypocretin/orexin and corticotropin releasing factor powerfully activate LC neurons and are both associated with elevations of tonic LC firing and the expression of anxiety-like phenotypes (Valentino and Foote, 1988; Horvath et al., 1999; Curtis et al., 2012; Sears et al., 2013; McCall et al., 2015). The TgF344-AD rats represent an excellent model to further evaluate AD pathology-associated changes in these systems and their influence on LC activity.

2.4.3 Clinical Implications

We have previously posited that LC/NE-based therapies for AD should be guided by disease stage (Weinshenker, 2018). The dysregulated/hyperactive NE transmission that is produced by early AD pathology (e.g. hyperphosphorylated tau) and promotes prodromal symptoms may be best alleviated by therapies that decrease LC firing and/or NE signaling, while reduced LC-NE transmission resulting from advanced pathology and deterioration of LC neurons would benefit from LC-NE stimulation. Our current findings largely support this model. At 6-months of age, TgF344-AD rats have hyperphosphorylated tau in the LC but no degeneration and display phenotypes relevant to neuropsychiatric disorders such as anxiety, and they primarily present with LC hyperactivity (increased firing during bursts and in responses to footshock stress). Meanwhile 15-month transgenic animal have increased tau pathology, some loss of LC fibers/terminals, cognitive impairment, and display LC hypoactivity (reduced baseline and footshock-induced firing). Moreover, we previously reported that deficits in reversal learning in 15-month TgF344-AD rats can be rescued by chemogenetic LC stimulation (Rorabaugh et al., 2017), and we predict that drugs that suppress LC activity or antagonism of adrenergic receptors would be effective at alleviating prodromal phenotypes in young TgF344-AD rats (Weinshenker, 2018). These results provide a foundation for translation to the clinical setting, where promising data already exist. For example, adrenergic antagonists have been reported to reduce

agitation/aggression and anxiety in subjects with probable or possible AD (Peskind et al., 2005; Wang et al., 2009), and our recent phase II study showed beneficial effects of the NE transporter inhibitor atomoxetine, which increases extracellular NE levels, on AD biomarkers in mild cognitive impairment (Levey et al., 2022). Atomoxetine also improves response inhibition in Parkinson's disease patients, with the greatest benefits observed in those with lower LC integrity (O'Callaghan et al., 2021). Whether this is also true in AD has not been determined but will be important for guiding the use of personalized noradrenergic-based interventions.

2.4.4 Limitations

There are several caveats to the current study that are worth discussing. Given the extracellular *in vivo* nature of our recordings, we were unable to determine whether the neurons recorded from TgF344-AD rats were tau positive or negative. However, our previous report demonstrated that essentially all LC neurons stain positive for the CP13 antibody at 6 months of age (Rorabaugh et al., 2017). This staining becomes more intense by 15 months, but does not stain for more mature versions of hyperphosphorylated/aggregated tau (i.e. AT8, MC1, PHF1) (Rorabaugh et al., 2017). Given the extensive gap junctions between LC neurons (Ishimatsu and Williams, 1996; Rash et al., 2007), it is also possible that even the rare tau-negative neurons are dysfunctional in TgF344-AD rats. Furthermore, there is evidence of LC heterogeneity, including different firing rates that are dependent upon projection targets, which may have influenced our results (Chandler et al., 2014). However, this is unlikely given that we recorded LC neurons from a range of coordinates. Follow-up studies using slice electrophysiology coupled with retrograde tracers and tau antibody staining would help determine whether differences in LC firing rates are tau-dependent and/or projection specific, with the latter being particularly interesting given the selective vulnerability of forebrain-projecting LC neurons (Schwarz and Luo, 2015; Weinshenker, 2018; Kelberman et al., 2020). It is possible that Aβ pathology, and not just aberrant tau,

contributed to the changes in LC firing rates in TgF344-AD rats, as a previous report identified the presence of soluble Aβ pathology in LC neurons of postmortem human AD brains, as well as in APP/PS1 transgenic mice that was associated with LC hyperactivity (Kelly et al., 2021). Aβ pathology has not been examined in the LC of TgF344-AD rats, but one caveat is that commonly used antibodies (i.e. 4G8) have off-target binding to the amyloid precursor protein (Kelly et al., 2021), which is ubiquitously overexpressed in these animals (Cohen et al., 2013). In TgF344-AD rats, plaques are minimal in forebrain regions at 6 months of age, evident at 12 months of age, and ubiquitous at 16 months of age (Cohen et al., 2013; Rorabaugh et al., 2017; Kelberman et al., 2022). Therefore, we speculate that early alterations to LC firing rates are likely dominated by the effects of hyperphosphorylated tau, while interactions between tau and Aβ are more likely during late stages of disease. Finally, there may be some concern that viral expression of the fluorescent marker mCherry altered LC firing rates in the current study. However, because all animals in the current report received viral infusions, the effects of mCherry expression would be equivalent across groups. Moreover, the WT rats in our study demonstrated LC firing rates consistent with non-manipulated rats based on previous literature (Aston-Jones and Bloom, 1981a, b; Hirata and Aston-Jones, 1994; Chandler et al., 2014; Vazey and Aston-Jones, 2014; West et al., 2015; Totah et al., 2018), indicating that any effects of the virus were negligible.

2.5 CONCLUSIONS

We have identified disease stage-dependent changes in LC firing patterns in a rat model of AD that accumulates hyperphosphorylated tau in the LC prior to forebrain pathology. These data further support the notion that early LC hyperactivity and late LC hypoactivity contribute to prodromal symptoms and cognitive/memory impairments of AD, respectively. These insights should prove useful for developing noradrenergic-based therapeutics for AD.

Table 2.1. Spontaneous bursting properties of LC neurons.

Measure	Main Effect	F Statistic	p-value	Summary Values [Mean +/- SEM (N)]		
Number of Bursts	**Age**	$F_{1,385}$ = 0.002712	0.9585		**WT**	**Tg**
	Genotype	$F_{1,385}$ = 3.258	0.0719	**6 month**	26.89 ± 6.00 (75)	16.43 ± 3.29 (107)
	Interaction	$F_{1,385}$ = 0.6039	0.4376	**15 month**	23.53 ± 3.58 (120)	19.37 ± 3.45 (87)
Percent of Spikes in a Burst	**Age**	$F_{1,385}$ = 1.649	0.1999		**WT**	**Tg**
	Genotype	$F_{1,385}$ = 0.1737	0.6771	**6 month**	18.41 ± 2.75 (75)	19.64 ± 2.37 (107)
	Interaction	$F_{1,385}$ = 0.8379	0.3606	**15 month**	23.84 ± 2.23 (120)	20.55 ± 2.44 (87)
Burst Duration	**Age**	$F_{1,267}$ = 0.5341	0.4655		**WT**	**Tg**
	Genotype	$F_{1,267}$ = 2.652	0.1046	**6 month**	0.36 ± 0.07 (48)	0.32 ± 0.04 (75)
	Interaction	$F_{1,267}$ = 0.5149	0.4737	**15 month**	0.44 ± 0.06 (88)	0.32 ± 0.02 (60)
Spikes Per Burst	**Age**	$F_{1,267}$ = 0.9097	0.3411		**WT**	**Tg**
	Genotype	$F_{1,267}$ = 0.06193	0.8037	**6 month**	7.46 ± 1.41 (48)	8.61 ± 1.56 (75)
	Interaction	$F_{1,267}$ = 1.356	0.2453	**15 month**	7.72 ± 1.08 (88)	5.94 ± 0.34 (60)
Interburst Interval	**Age**	$F_{1,226}$ = 0.01437	0.9047		**WT**	**Tg**
	Genotype	$F_{1,226}$ = 2.222	0.1375	**6 month**	16.27 ± 3.67 (37)	37.83 ± 8.13 (60)
	Interaction	$F_{1,226}$ = 3.516	0.0621	**15 month**	27.51 ± 5.21 (75)	25.05 ± 5.42 (58)

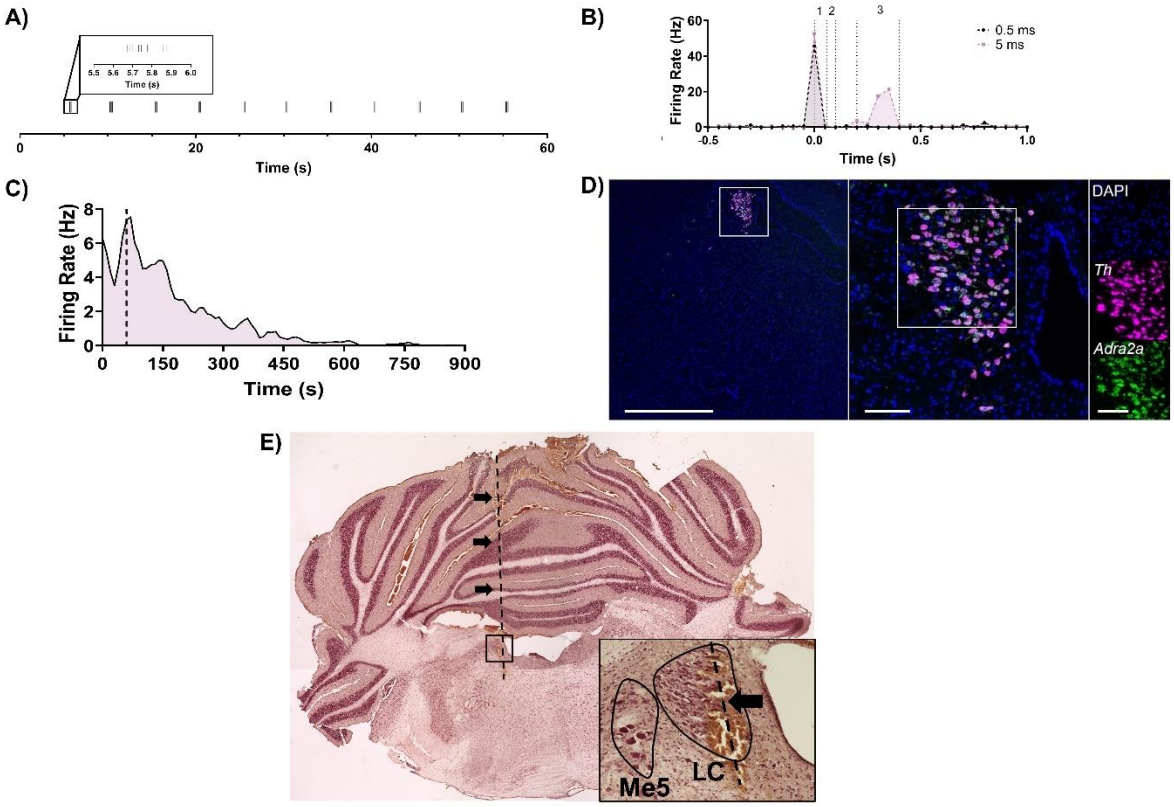

Figure 2.1. Multimodal confirmation of single unit recordings from LC neurons. A) The approximate depth of the LC was estimated by locating Me5 via jaw deflection every 5 s during 1-min long recording. B) Putative LC units displayed a biphasic response to footshock (gray, 0.5 ms; purple, 5 ms; 0.05 ms bins around footshock at time 0 s). Unit responses were also quantified between 0-60 ms (1), 60-100 ms (2), and 200-400 ms (3) following footshock. C) Noradrenergic LC neuron activity is inhibited by the α2-adrenergic receptor clonidine (0.1 mg/kg i.p.; dashed line), and D) RNAscope performed at the level of the LC confirmed that expression of α2-adrenergic receptors (green) is limited to TH-expressing (magenta) LC neurons in this part of the brain. Scale bars: 1 mm at 2x, 100 μm at 20x, and 100 μm at 40x magnification. E) Localization of electrode tracks (arrows and dashed line) in the LC core using neutral red counterstaining. Main image stitched from four images at 2x magnification. Inset taken at 20x magnification with the LC outlined in black and the electrode track marked by an arrow.

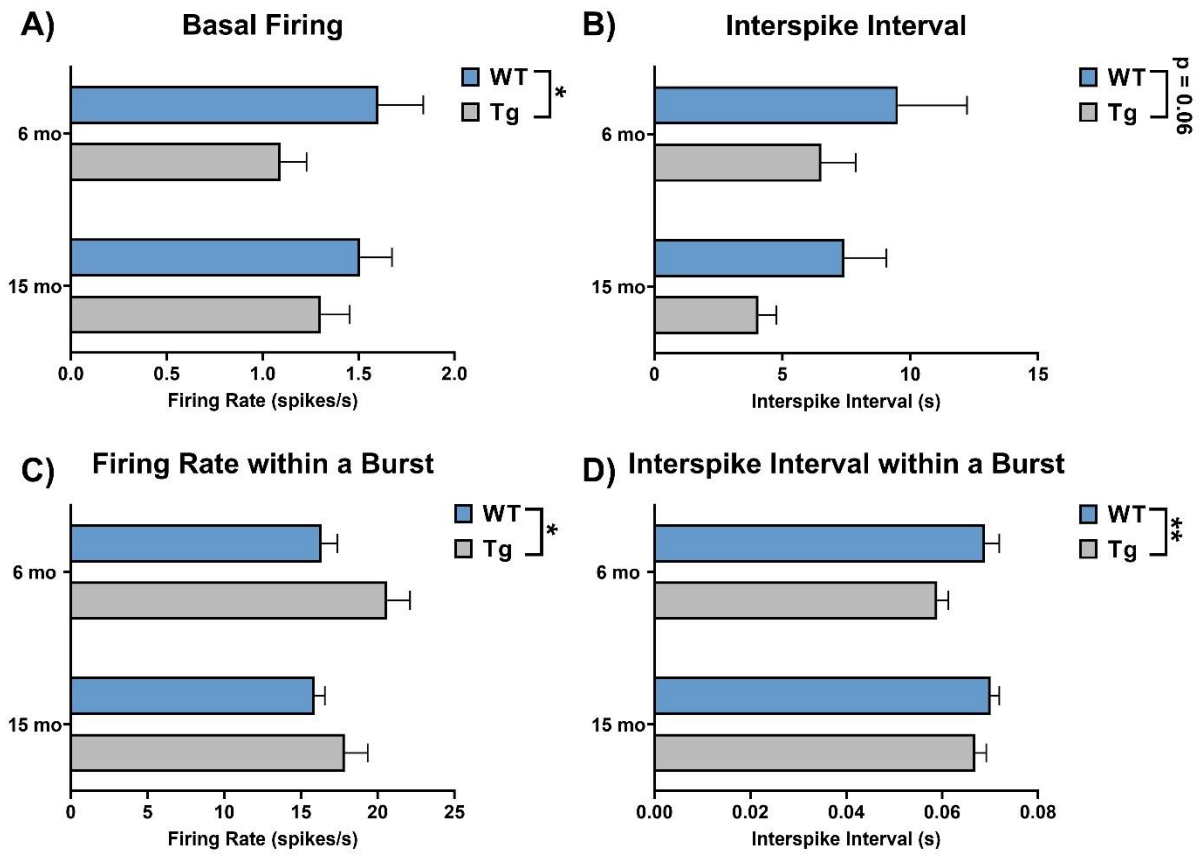

Figure 2.2. Basal firing properties of LC neurons from 6- and 15-month TgF344-AD rats and WT littermates. A) Baseline firing was lower in TgF344-AD rats at both ages. B) There was a trend towards decreased interspike interval in TgF344-AD rats. C) Firing rate during spontaneous bursts was higher in TgF344-AD rats. D) Interspike intervals within a burst were lower in TgF344-AD rats, and there was an additional effect of age where younger rats had lower interspike intervals. N=74-120 neurons/group (N=8-11 animals/group) for A and B. N=48-88 neurons/group (N=8-11 animals/group) for C and D. *$p<0.05$, **$p<0.01$.

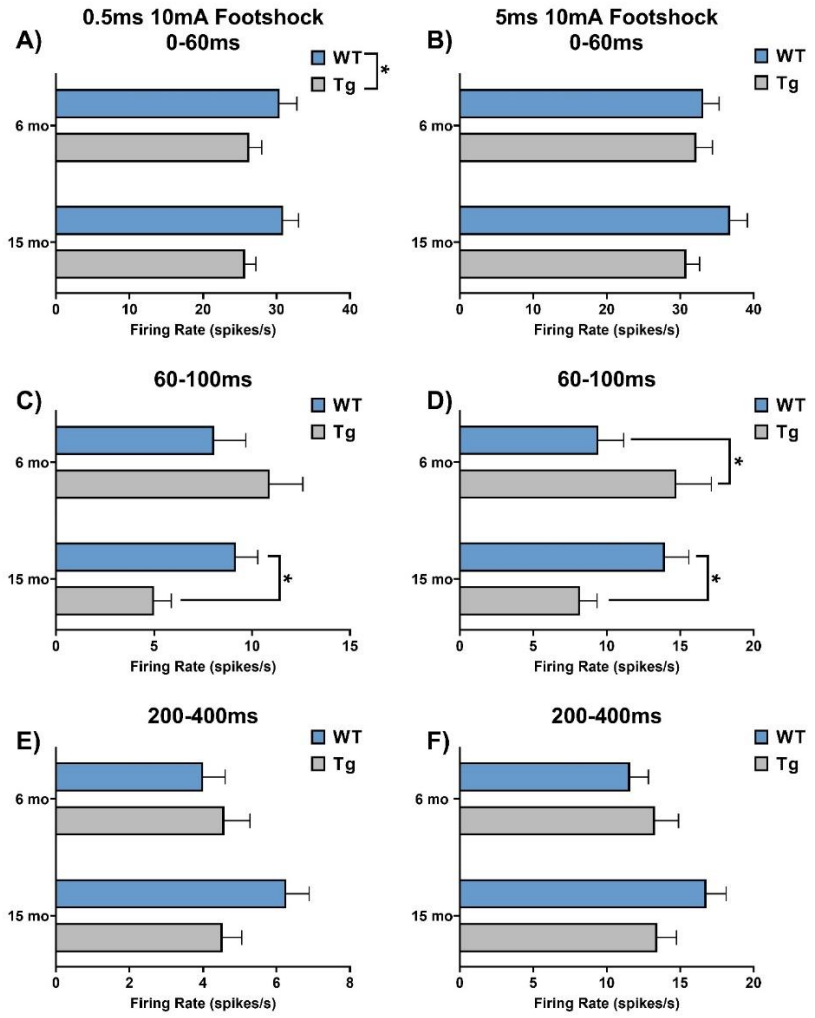

Figure 2.3. Footshock response of LC neurons from 6- and 15-month TgF344-AD rats and WT littermates. A & B) LC neuron firing rate was lower in TgF344-AD rats during the immediate phase in response to 0.5 ms footshock, but this effect was not seen in response to 5 ms footshock. C & D) There was an age x genotype interaction in the intermediate phase of response to both 0.5 and 5 ms footshock. Post-hoc analysis revealed that young TgF344-AD animals demonstrated hyperactivity in response to 5 ms footshock, while aged TgF344-AD animals showed hypoactivity in response to both 0.5 and 5 ms footshock. E & F) There were no differences in late phase response to footshock. N=84-128 neurons/group (N=8-11 animals/group) for A, C, and E. N=94-126 neurons/group (N=8-11 animals/group) for B, D, and F. *$p<0.05$.

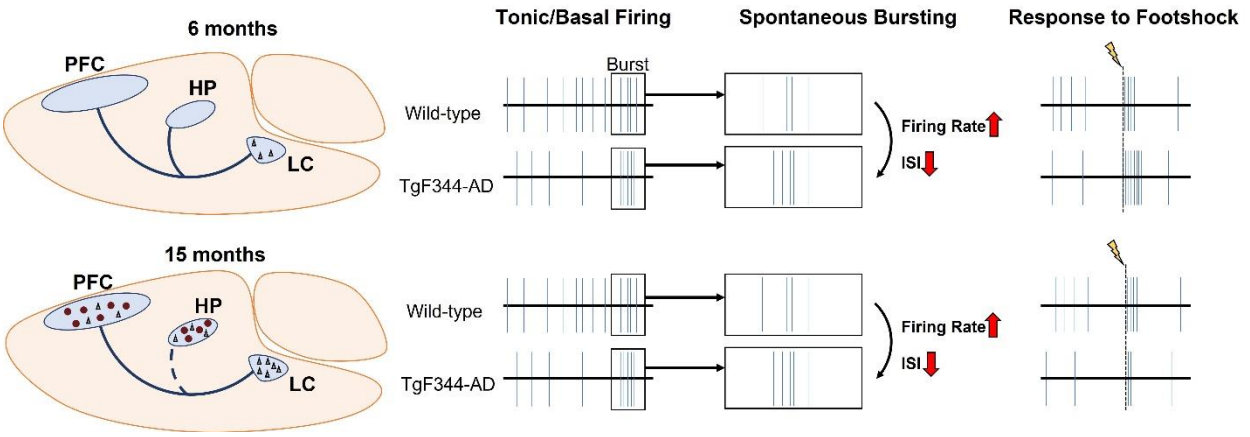

Figure 2.4. Summary of dysregulated LC firing patterns as a function of age in TgF344-AD rats. At 6 months, the LC is the only brain region that displays AD-like neuropathology in the form of hyperphosphorylated tau (black triangles). LC neurons show tonic hypoactivity, but elevated firing rate and shorter interspike intervals during periods of spontaneous bursts. LC response to footshock (lightning bolt/dashed line) at this age is also elevated in TgF344-AD rats. At 15 months, hyperphosphorylated tau pathology in the LC worsens, and tau and Aβ (red circles) pathology are present throughout the forebrain. There is also evidence of noradrenergic denervation, specifically to the hippocampus (dashed blue line). Similar to 6-month TgF344-AD rats, LC neurons again show tonic hypoactivity, and elevated firing rate and lower interspike intervals during periods of spontaneous bursts. However, in contrast to younger rats, 15-month TgF344-AD rats have an impaired, rather than elevated, footshock response.

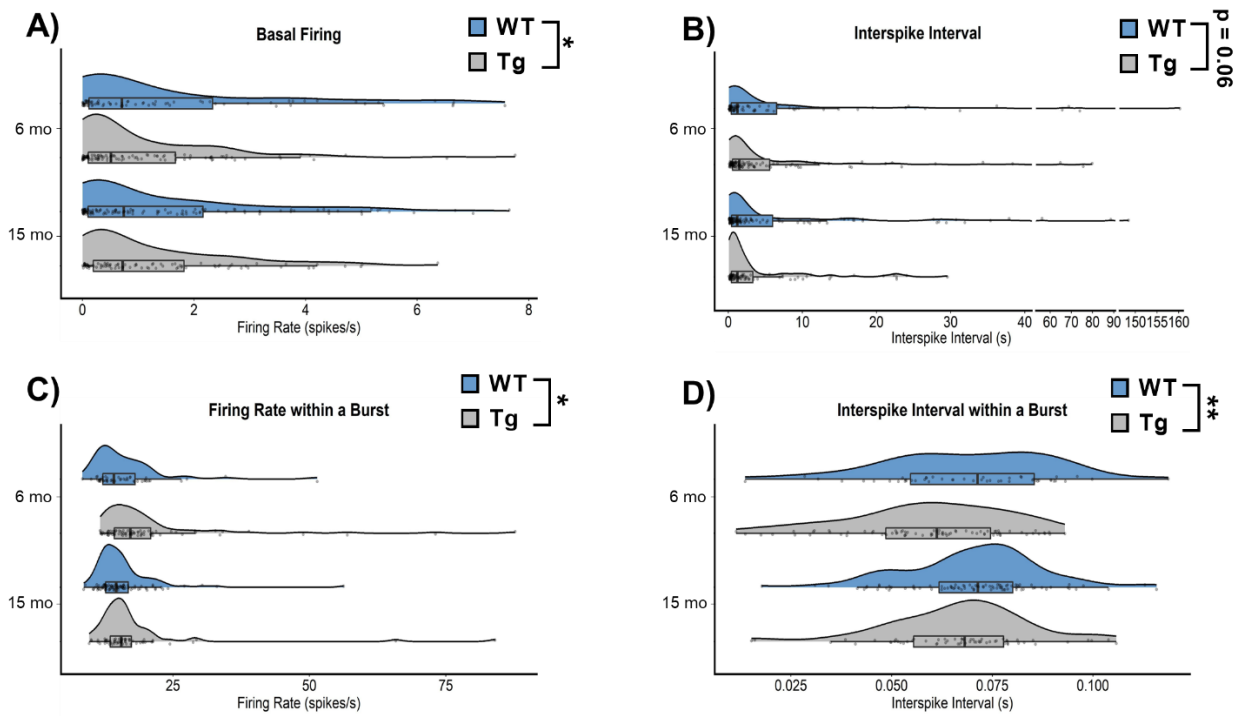

Supplemental Figure 2.1. Basal firing properties of LC neurons from 6- and 15-month TgF344-AD rats and WT littermates. A) Baseline firing was lower in TgF344-AD rats at both ages. B) There was a trend towards decreased interspike interval in TgF344-AD rats. C) Firing rate during spontaneous bursts was higher in TgF344-AD rats. D) Interspike intervals within a burst were lower in TgF344-AD rats, and there was an additional effect of age where younger rats had lower interspike intervals. N=74-120 neurons/group (N=8-11 animals/group) for A and B. N=48-88 neurons/group (N=8-11 animals/group) for C and D. *p<0.05, **p<0.01.

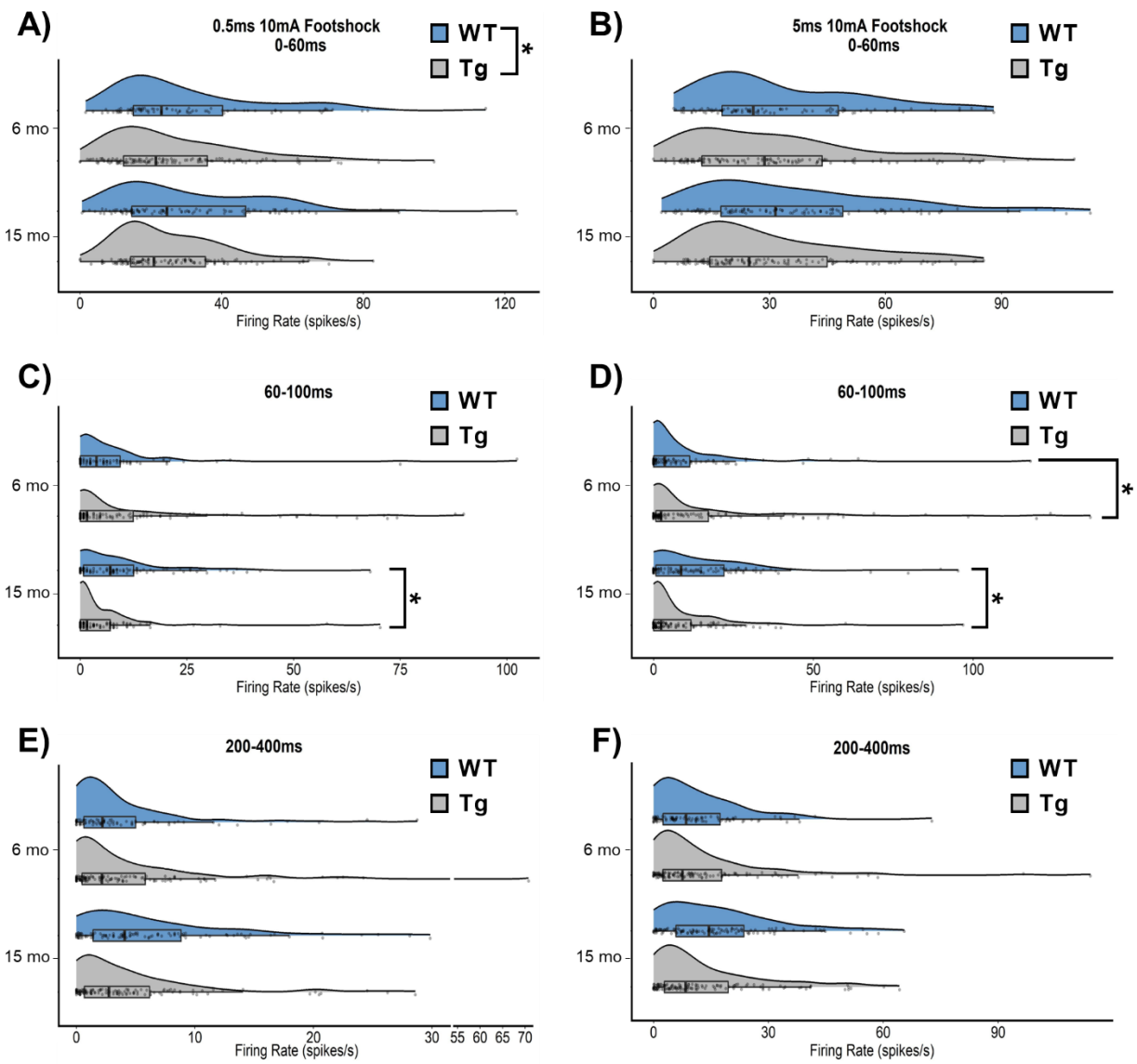

Supplemental Figure 2.2. Footshock response of LC neurons from 6- and 15-month TgF344-AD rats and WT littermates. A & B) LC neuron firing rate was lower in TgF344-AD rats during the immediate phase in response to 0.5 ms footshock, but this effect was not seen in response to 5 ms footshock. C & D) There was an age x genotype interaction in the intermediate phase of response to both 0.5 and 5 ms footshock. Post-hoc analysis revealed that young TgF344-AD animals demonstrated hyperactivity in response to 5 ms footshock, while aged TgF344-AD animals showed hypoactivity in response to both 0.5 and 5 ms footshock. E & F) There were no differences in late phase response to footshock. N=84-128 neurons/group (N=8-11

animals/group) for A, C, and E. N=94-126 neurons/group (N=8-11 animals/group) for B, D, and F. *p<0.05.

CHAPTER 3: DISRUPTED GENE EXPRESSION SIGNATURES OF LOCUS COERULEUS NEURONS IN A RAT MODEL OF ALZHEIMER'S DISEASE

Abstract

The noradrenergic locus coeruleus (LC) is one of the earliest and most impacted nuclei during the progression of Alzheimer's disease (AD). The early behavioral symptoms, including sleep disturbances, alterations to mood, and exaggerated stress and anxiety are concomitant with hyperphosphorylated tau deposition in the LC, while LC neuronal loss parallels the development of cognitive deficits in later disease stages. Using the TgF344-AD rat model of AD, we recently demonstrated that the LC is hyperactive in young animals, when hyperphosphorylated tau is present in the nucleus, while aged transgenic rats display LC hypoactivity. However, a mechanism underlying these age-dependent changes in LC activity is lacking. We sought to identify mechanisms leading to altered LC activity using a targeted gene expression approach in age-matched TgF344-AD rats. We found decreased mRNA for *Gabra3* (α3 subunit of the GABA-A receptor) and the *opioid-related nociception receptor 1* (nociception receptor) in the LC of 6-month TgF344-AD animals, which is consistent with the hyperactive phenotype of these neurons at this age. We further observed an increase in a group of transcripts that encode proteins important for NE synthesis, packaging, and reuptake in 15-month TgF344-AD animals, which we hypothesize reflect compensatory mechanisms to counteract the loss of forebrain norepinephrine (NE) and axons noted in aged TgF344-AD rats. These results identify potential mechanisms underlying altered LC activity and function across the progression of AD, as well as plausible targets for LC-NE based therapeutics for AD.

3.1 INTRODUCTION

Alzheimer's disease (AD) is characterized by the accumulation of extracellular amyloid-β (Aβ) plaques and intracellular hyperphosphorylated tau neurofibrillary tangles. Past and current therapies largely target Aβ pathology but have only yielded marginal clinical benefits, which may be partially due to the late stages at which Aβ is targeted. On the other hand, subcortical hyperphosphorylated tau accumulation occurs prior to Aβ deposition and decades before hallmark cognitive deficits in AD (Ehrenberg et al., 2023). Specifically, the noradrenergic locus coeruleus (LC) is the consistently reported as the earliest site in the brain to accumulate tau pathology (Braak et al., 2011; Elobeid et al., 2012; Theofilas et al., 2017; Pletnikova et al., 2018; Gilvesy et al., 2022). Although tau pathology is predictive of neuronal loss in AD, there is a delay between pathological tau accumulation and LC degeneration (Theofilas et al., 2017). Consequently, tau-induced LC dysfunction prior to frank cell death could contribute to symptoms and advancement of AD throughout the entirety of disease course.

The LC is the main central norepinephrine (NE) producing nucleus and projects nearly brain-wide to influence arousal, attention, cognition, stress response, and mood (Poe et al., 2020). The influence of the LC-NE system on behaviors has been partially attributed to different firing rates and patterns exhibited by these neurons. LC neurons fire with pacemaker activity between 0.5-2 Hz that facilitates general arousal and behavioral flexibility, while high tonic rates (3-8 Hz) are induced by stress and promote anxiety-like behaviors (Foote et al., 1980; Aston-Jones and Bloom, 1981b; Grant et al., 1988; Valentino and Foote, 1988; Sara and Segal, 1991; Curtis et al., 1997; Aston-Jones et al., 1999; Page and Abercrombie, 1999; Curtis et al., 2012; McCall et al., 2015). Phasic activity has been defined by transient elevations in firing rates or brief bursts of activity followed by prolonged inhibition that occurs in response to relevant environmental stimuli (Aston-Jones and Bloom, 1981a; Florin-Lechner et al., 1996; Aston-Jones and Cohen, 2005a;

Bouret and Sara, 2005). Phasic firing is associated with behavioral adaptation by facilitating cognitive shifts and filter task-related stimuli (Aston-Jones and Cohen, 2005a; Bouret and Sara, 2005; Mather et al., 2016). Proper combinatorial patterns of tonic and phasic firing are required for optimal attention (Aston-Jones and Cohen, 2005a; Howells et al., 2012). Many behaviors influenced by LC activity go awry in prodromal stages of AD, including disrupted sleep/wake cycles, exaggerated stress responses and anxiety, and altered mood (Ehrenberg et al., 2018; Johansson et al., 2021). Early behavioral alterations are coincident with accumulation of LC tau pathology (Ehrenberg et al., 2018; Johansson et al., 2021; Kelberman et al., 2022), and subsequent cognitive deficits and forebrain structural decline parallel LC degeneration (Wilson et al., 2013; Olivieri et al., 2019; Bachman et al., 2021; Jacobs et al., 2021; van Hooren et al., 2021), suggesting changes in LC firing rates could be a key driver of AD symptomology and progression. Thus, we have posited that the LC is hyperactive early in disease, leading to increased anxiety and other prodromal symptoms, and hypoactive in late stages of disease, contributing to cognitive decline (Weinshenker, 2018). We have recently observed these changes in firing patterns over the course of disease in the TgF344-AD rat model (Weinshenker, 2018). Specifically, phasic LC hyperactivity was noted at 6 months and both tonic and phasic LC hypoactivity at 15 months, which parallels the emergence of early behavioral symptoms (i.e. anxiety-like phenotypes) and cognitive deficits in these rats, respectively (Cohen et al., 2013; Rorabaugh et al., 2017; Kelberman et al., 2022; Kelberman et al., 2023). Notably and akin to the human condition, the TgF344-AD rats develop early LC hyperphosphorylated tau pathology beginning at 6 months and prior to any forebrain accumulation of amyloid or tau pathology (Cohen et al., 2013; Rorabaugh et al., 2017; Kelberman et al., 2022).

There are a variety of molecular mechanisms that could affect LC firing rates, and the nature of changes identified in the TgF344-AD rat could offer insights into their origin. LC neurons

are molecularly defined by expression of genes such as *Th* (tyrosine hydroxylase), *Dbh* (dopamine β-hydroxylase), *Slc18a2* (vesicular monoamine transporter 2), and *Slc6a2* (plasma membrane NE transporter), which are critical for NE synthesis, packaging, and reuptake (Mulvey et al., 2018; Iannitelli et al., 2023b). In AD patients, expression of these genes is augmented or unchanged in surviving LC neurons, suggesting a compensatory increase in NE transmission in response to neuronal loss (Szot et al., 2000; Szot et al., 2006, 2007; McMillan et al., 2011). The LC receives excitatory, inhibitory, and modulatory inputs from cortical and subcortical regions that facilitate aspects of both tonic and phasic LC activity (Herkenham and Nauta, 1979; Ennis and Aston-Jones, 1988; Jodo and Aston-Jones, 1997; Aston-Jones et al., 2004; Sara and Bouret, 2012; Schwarz and Luo, 2015; Breton-Provencher and Sur, 2019; Breton-Provencher et al., 2021). For example, corticotropin releasing factor (CRF) and hypocretin/orexin augment LC tonic activity (Valentino and Foote, 1988; Horvath et al., 1999; Curtis et al., 2012; Sears et al., 2013; McCall et al., 2015), while inhibition is mediated locally via peri-LC GABAergic inputs and through action of NE on autoinhibitory α2-adrenergic receptors (McCune et al., 1993; Aston-Jones et al., 2004; Totah et al., 2018; Breton-Provencher and Sur, 2019; Breton-Provencher et al., 2021; Kelberman et al., 2023). Further inhibition of tonic LC activity is achieved by opioid signaling through various GPCR receptor subtypes (Connor et al., 1996; Van Bockstaele et al., 2010). Phasic firing is mediated by excitatory and inhibitory neurotransmission, and LC responsiveness to such signaling is further refined by neuromodulators like serotonin (Aston-Jones et al., 1991; Chiang and Aston-Jones, 1993a). Changes in the innervation pattern of afferents to the LC and receptor expression or localization could underlie changes in LC activity beyond direct effects of hyperphosphorylated tau pathology.

Despite the well-defined modulators of, and having previously revealed age-dependent alterations in, LC firing rates, a mechanistic underpinning of these changes in AD that could be

the target of therapeutic interventions is still lacking. We therefore sought to characterize the molecular landscape of LC neurons at the gene expression level along AD progression in TgF344-AD rats, with a specific focus on identifying signatures that could drive altered LC firing rates that we previously identified (Kelberman et al., 2023).

3.2 MATERIAL AND METHODS

3.2.1 Animals:

32 male and female TgF344-AD rats and WT littermates aged 6 or 15 months were used for this study. TgF344-AD rats were hemizygous for the *APPsw/PS1ΔE9* transgene carrying mutations causative of autosomal-dominant early-onset AD. Rats were housed in groups of 2-3 on a 12-h light/dark cycle (lights on at 7:00 am) with freely available food and water. All experiments were conducted in accordance with the Institutional Animal Care and Use Committee at Emory University.

3.2.2 Tissue Collection:

Animals were rapidly decapitated under isoflurane between 1:00-4:00 pm (6-9 h after lights on) and brains were flash-frozen in isopentane on dry ice. Brains were stored at -80ºC until being sectioned on a cryostat at 16 µm.

3.2.3 In Situ Hybridization, Imaging, and Analysis:

We performed fluorescent *in situ* hybridization using the RNAscope Multiplex Fluorescent V2 Assay (Advanced Cell Diagnostics, Newark, CA, USA) according to the manufacturer's protocol. Information regarding probes used in this study is located in Table 3.1. Images were obtained in a 1µm pitch z-stack (10µm total) on a Keyence BZ-X700 microscope (Osaka, Japan) at 2x, 20x, and 40x using uniform exposure parameters for each marker. Analysis of puncta was

performed in Halo® Imaging Analysis Platform (Indica Labs, Albuquerque, NM, USA) using the Multiplex IF/FISH module of 40x images. Analysis of the LC markers *Th*, *Slc6A2*, *Dbh*, and *Slc18a2* did not appear as individual puncta and were instead classified in HALO as immunofluorescence markers. These mRNAs were further analyzed by measuring fluorescence levels in ImageJ using 20x images. A common threshold (Otsu) was applied, and a region of interest was outlined using the "Create Selection" function. Fluorescence intensity limited to the region of interest from the original image was then measured. Puncta of all other probes were measured as puncta per cell, with "cell" being defined as positive for the co-labeled LC marker (*Th, Dbh, Slc6a2,* or *Slc18a2*). Parameters for FISH analysis and probe groups can be found in Table 3.2. 1-3 LC sections from the right hemisphere were quantified and averaged per animal per marker.

3.2.4 Statistical Analysis:

Figures were made and statistical analyses were performed using GraphPad Prism (v. 9.2.0; San Diego, CA, USA) using the mean ± SEM. Given limitations in the number of samples we could run in-tandem and that previously identified differences in LC firing rates were most prominent within an age, we focused our RNAscope analyses on effects of genotype within each age group. First, outliers were removed based on the Grubb's method with $\alpha = 0.001$. NE neurotransmission (i.e. synthesis and handling) genes were grouped and analyzed as a two-way ANOVA considering gene and genotype as factors. All other transcripts were analyzed using a student's t-test to compare WT and TgF344-AD animals at 6 or 15 months with Welch's corrections used when variances differed between groups. Non-normally distributed data were analyzed with a Mann-Whitney test. For all analyses, statistical significance was set at $\alpha = 0.05$.

3.3 RESULTS

We have previously shown that LC axonal damage in the absence of AD-like neuropathology or cell body degeneration reduces expression of mRNAs that define noradrenergic neuron identity (Iannitelli et al., 2023b), while others have reported an upregulation in noradrenergic transcripts in post-mortem AD samples (Szot et al., 2006). Given TgF344-AD rats display both AD-like neuropathology and a progressive loss of LC fibers akin to the human condition (Rorabaugh et al., 2017), we first investigated whether levels of mRNAs involved in NE synthesis and handling (*Th, Dbh, Slc6a2*, *Slc18a2*) were altered at 6 or 15 months. We found a significant effect of gene (Two-way ANOVA: $F_{3, 47} = 15.36$, $p < 0.0001$), but no effect of genotype (Two-way ANOVA: $F_{1, 47} = 0.66$, $p = 0.42$) or a gene x genotype interaction (Two-way ANOVA: $F_{3, 47} = 0.34$, $p = 0.80$) on fluorescence level in 6-month animals (**Figure 3.1Ai and Aii**). In 15-month animals there was a similar significant effect of gene (Two-way ANOVA: $F_{3, 42} = 51$, $p < 0.0001$) and no gene x genotype interaction either (Two-way ANOVA: $F_{3, 42} = 0.76$, $p = 0.52$), but at this age a significant effect of genotype emerged (Two-way ANOVA: $F_{1, 42} = 4.53$, $p = 0.04$) (**Figure 3.1Bi and Bii**), revealing elevated levels of noradrenergic genes in TgF344-AD rats. We also examined expression of the α2-adrenergic receptor, which is responsible for local autoinhibition of LC neurons (McCune et al., 1993; Totah et al., 2018; Kelberman et al., 2023), but found no differences in the number of *Adra2a* copies per cell at either 6 (**Figure 3.1Ci**; $t = 0.59$, $df = 13$, $p = 0.57$) or 15 months (**Figure 3.1Cii**; $t = 1.29$, $df = 11$, $p = 0.22$).

The LC receives extensive glutamatergic innervation from the cortex, lateral habenula, and paragigantocellularis nucleus (Herkenham and Nauta, 1979; Ennis and Aston-Jones, 1988; Jodo and Aston-Jones, 1997), which drive various aspects of LC firing (Aston-Jones et al., 1991; Chiang and Aston-Jones, 1993a, b). We therefore probed whether there were any changes in mRNAs corresponding to excitatory amino acid transmission by examining *Grin1* (**Figure 3.2Ai and Aii**), *Grm3* (**Figure 3.2Bi and Bii**), and *Gria2* (**Figure 3.2Ci and Cii**) expression. These transcripts were

chosen to encompass the glutamatergic receptor subunits expressed in the LC (Noriega et al., 2007). There were no differences in the number of *Grin1* (6 months: t = 0.09, df = 13, p = 0.93; 15 months: t = 1.98, df = 11, p = 0.07), *Grm3* (6 months: t= 0.07, df = 11, p = 0.94; 15 months: Welch-corrected t = 1.31, df = 5.08, p = 0.25), or *Gria2* (6-months: t = 0.64, df = 10, p = 0.54; 15-months (t = 1.06, df = 10, p = 0.32) copies per cell at either age.

Inhibitory control of LC activity is mediated distally by areas such as the ventrolateral preoptic area and locally by peri-LC GABAergic neurons that are particularly important for modulating arousal (Lu et al., 2002; Aston-Jones et al., 2004; Breton-Provencher and Sur, 2019; Breton-Provencher et al., 2021). The LC expresses high levels of $GABA_A$ α3 receptors across species, but low levels of other GABA receptor subunits (Waldvogel et al., 2010; Corteen et al., 2011; Kelly et al., 2021). Mislocalization of $GABA_A$ α3 receptors in the LC is associated with LC hyperactivity in the APP-PS1 mouse model of AD that produces Aβ oligomers but not hyperphosphorylated tau, and is also observed in the LC of human AD subjects (Kelly et al., 2021). Therefore, we next characterized the expression of the $GABA_A$ α3 receptor subunit (*Gabra3*) in the LC of TgF344-AD and control rats (**Figure 3.2Di and Dii**). In 6-month TgF344-AD animals, there was a decrease in *Gabra3* copies per cell compared to WT littermates (t = 2.75, df = 10, p = 0.02), but no effect of genotype in 15-month animals (t = 0.93, df = 8, p = 0.38).

LC firing is also controlled by various neuromodulators and neuropeptides including orexin/hypocretin (Hagan et al., 1999; Horvath et al., 1999; Inutsuka and Yamanaka, 2013), CRF (Bangasser and Valentino, 2012; Valentino et al., 2012), pituitary adenylate cyclase-activating peptide (PACAP) (Duesman et al., 2022), serotonin (Aston-Jones et al., 1991; Chiang and Aston-Jones, 1993a), and endogenous opioids (Mansour et al., 1994; Connor et al., 1996; Neal et al., 1999; Van Bockstaele et al., 2010; Tkaczynski et al., 2022). Despite the robust modulatory effects of serotonin and CRF on LC activity (Valentino and Foote, 1988; Aston-Jones et al., 1991; Chiang

and Aston-Jones, 1993a; Curtis et al., 1997; McCall et al., 2015), we did not detect substantial expression of either the serotonin 1a (*Htr1a*) or CRF1 receptors (*Crfr1*) in the LC (**Supplemental Figure 3.1**). Indeed, a previous reports failed to localize *Htr1a* or *Crfr1* mRNA in the LC (Pompeiano et al., 1992; Luskin et al., 2022; Weber et al., 2022) and these markers were not further pursued.

Few studies have investigated PACAP modulation of the LC but suggest that it is important for metabolism (Duesman et al., 2022) and, in regions other than the LC, is crucial for mediating anxiety-like behaviors (Hammack et al., 2009; Boucher et al., 2022). We found high transcript levels of *Adcyap1r1* in the LC but no significant difference between genotypes at either age (**Figure 3.3Ai and Aii**; 6 months: $t = 0.47$, $df = 10$, $p = 0.65$; 15 months: Mann-Whitney $U = 11$, $p = 0.31$).

Opioid signaling in the LC occurs through μ, δ, κ, and other receptor subtypes (Mansour et al., 1994; Connor et al., 1996; Neal et al., 1999; Van Bockstaele et al., 2010; Tkaczynski et al., 2022). Regardless of pre-/post-synaptic localization or mechanism of action of these receptors, all have potent inhibitory effects on LC activity (Connor et al., 1996; Van Bockstaele et al., 2010). Behaviorally, overexpression of δ opioid receptors in the LC reduces anxiety-like phenotypes (Tkaczynski et al., 2022). The stress-dependent increase in LC firing rate was also blocked by δ opioid receptor overexpression in the LC. Given the alterations in LC firing and robust anxiety-like phenotypes observed in TgF344-AD rats at both ages (Kelberman et al., 2022; Kelberman et al., 2023), we determined whether there were differences in mRNA expression of the δ opioid receptor (*Oprd1*) in the LC of TgF344-AD rats and WT littermates (**Figure 3.3Bi and Bii**). There were no differences at either age in copies per cell of *Oprd1* at either age (6 months: $t = 0.60$, $df = 11$, $p = 0.56$; 15 months: Mann-Whitney $U = 14$, $p = 0.59$). *Oprl1* is also highly expressed in the LC and inhibits firing and NE release through an inwardly rectifying potassium conductance

(Connor et al., 1996; Neal et al., 1999; Okawa et al., 2001; Kawahara et al., 2004; Yoshitake et al., 2013). While we observed no difference in *Oprl1* copies per cell in 15-month TgF344-AD rats ($t = 0.55$, $df = 8$, $p = 0.60$), there was a significant decrease in 6-month TgF344-AD rats ($t = 2.61$, $df = 10$, $p = 0.03$) (**Figure 3.3Ci and Cii**).

3.4 DISCUSSION

The LC is vulnerable to pathological insults in the form of hyperphosphorylated tau deposition well before clinical AD diagnosis (Braak et al., 2011; Gilvesy et al., 2022; Ehrenberg et al., 2023). As the disease progresses, LC axons degenerate, LC volume decreases, and frank neuronal loss is observed (Wilson et al., 2013; Theofilas et al., 2017; Goodman et al., 2021; Jacobs et al., 2021; van Hooren et al., 2021; Kelberman et al., 2022). Using the TgF344-AD rat model of AD that recapitulates the "LC first" pattern of hyperphosphorylated tau deposition observed in humans, we recently showed that dysfunctional LC firing rates are disease stage-dependent, with hyperactivity being noted in young animals that transitions to hypoactivity in later stages of disease (Kelberman et al., 2023). LC hyperactivity appears coincident with early behavioral impairments, while the transition to hypoactivity parallels the emergence of cognitive deficits observed in AD (Rorabaugh et al., 2017; Jacobs et al., 2021; Johansson et al., 2021; van Hooren et al., 2021; Kelberman et al., 2022; Kelberman et al., 2023). While these data suggest that lowering and increasing noradrenergic tone in early and late AD, respectively, may provide symptomatic relief (Weinshenker, 2018), a more comprehensive understanding of the molecular mechanisms resulting in altered LC is required for more targeted therapies. We therefore molecularly characterized LC neurons in TgF344-AD rats at the transcript level using in situ hybridization, with a specific focus on markers that could influence LC activity.

The LC is molecularly defined by a core set of genes that confer noradrenergic identity and transmission (Mulvey et al., 2018; Iannitelli et al., 2023b). While there were no differences in these transcripts in 6-month animals, they were upregulated as a group in 15-month animals. Expression of *Th* is elevated in surviving LC neurons in AD patients, while expression of other noradrenergic genes are either increased or unchanged (Szot et al., 2000; Szot et al., 2006, 2007; McMillan et al., 2011). TgF344-AD rats do not display frank LC cell loss at ages tested here (Rorabaugh et al., 2017), suggesting that compensatory upregulation of noradrenergic genes precedes cell death. This is at odds with our recent report showing downregulation of these same mRNAs in the LC of mice treated with the selective LC neurotoxin, N-(2-chloroethyl)-N-ethyl-2-bromobenzylamine (DSP-4) at a dose and time point that almost entirely ablates axons and leaves cell bodies injured but intact (Iannitelli et al., 2023b). We suspect that the substantial, acute damage to LC axons and cell bodies caused by DSP-4 drives LC neurons into a survival mode where many "non-essential" genes are downregulated, including those that define the neurotransmitter phenotype. This is in contrast to the gradual, chronic nature of disease in TgF344-AD rats and human AD subjects that allows time for the engagement of compensatory mechanisms designed to maintain NE homeostasis in the face of accumulating pathology. For example, there are region-specific decreases in NE content in the forebrain and reductions in LC activity of aged TgF344-AD animals (Rorabaugh et al., 2017; Kelberman et al., 2023). Thus, upregulation of genes involved in synthesis (*Th*, *Dbh*), packaging (*Slc18a2*), and reuptake (*Slc6a2*) of NE may be an attempt to augment NE tone in response to deteriorating transmission. However, this upregulation could also have consequences for LC activity. For instance, the LC is enriched in inhibitory α2-adrenergic autoreceptors (McCune et al., 1993; Totah et al., 2018; Kelberman et al., 2023), the expression of which was unaltered at either age. The upregulation of noradrenergic tone at 15-months, when coupled with degeneration of LC axons (Rorabaugh et al., 2017;

Goodman et al., 2021; Kelberman et al., 2022), could lead to more somatodendritic NE release, culminating in excessive negative feedback onto LC neurons.

We observed no changes in glutamatergic receptor gene expression in noradrenergic LC neurons of TgF344-AD rats at either age. There are other glutamatergic receptor subunits expressed in the LC at lower levels that could be altered in TgF344-AD rats, such as *Grin2a*, *Gria4*, and *Grm5* (Noriega et al., 2007) that may also be worth exploring. Notably, glutamate promotes phasic LC responses which are followed by post-activation inhibition, with the inhibition phase partially mediated by AMPA receptors (Zamalloa et al., 2009). Alterations to other glutamatergic receptor subunit expression, localization, or function that have not been described here could therefore impact both tonic and phasic LC activity.

Compared to the diversity of glutamatergic receptor subunits expressed in the LC, GABAergic transmission mainly occurs through the $GABA_A$ α3 subunit (Waldvogel et al., 2010; Corteen et al., 2011; Kelly et al., 2021). We further focused on this receptor because of a previous report demonstrating downregulation of $GABA_A$ α3 receptor subunits in the LC of APP/PS1 mice, which was associated with LC hyperactivity (Kelly et al., 2021). $GABA_A$ α3 immunoreactivity was also mislocalized to the cytoplasm instead of the plasma membrane in LC neurons from human AD subjects (Kelly et al., 2021). We observed downregulation of *Gabra3* mRNA that was specific to 6-month TgF344-AD rats, which is consistent with the LC hyperactivity we observe at this age (Kelberman et al., 2023). Interestingly, the downregulation of $GABA_A$ α3 receptor subunits in the LC of APP/PS1 mice was related to Aβ oligomer pathology, and knocking out this subunit in WT mice recapitulated the LC hyperactivity observed in the mutant mice (Kelly et al., 2021). TgF344-AD rats accumulate hyperphosphorylated tau in the LC at 6 months, but no tau or plaque pathology elsewhere in the brain at this age (Rorabaugh et al., 2017). The presence of Aβ oligomers in the LC of TgF344-AD rats has not been determined, although it is plausible given

that the APP/PS1 transgenes in the two models are identical. Some notable differences exist between the LC hyperactivity in APP/PS1 mice (increased tonic firing) and TgF344-AD rats (increased firing during spontaneous and evoked bursts) (Kelly et al., 2021; Kelberman et al., 2023). The reasons for these differences are unclear, but could involve the type of AD pathology present in the LC, in addition to other complex changes in gene expression described here (e.g. *Oprl1*) or that has yet to be uncovered. Despite these differences, both studies together suggest that LC $GABA_A$ α3 receptor subunits are especially vulnerable to AD pathology and could be an early point of therapeutic intervention.

We also confirmed the high expression of *Adcyap1r1* transcripts in LC neurons. While these receptors are generally involved in stress/anxiety and neuroinflammation and likely influence LC activity (Vaudry et al., 2005; Ohtaki et al., 2006; Hammack et al., 2009; Szakaly et al., 2011; Matsumoto et al., 2016; Bozadjieva-Kramer et al., 2021; Boucher et al., 2022; Duesman et al., 2022), we found no effect of genotype on expression of *Adcyap1r1* mRNA. Therefore, it is unlikely that these receptors contribute to phenotypes of TgF344-AD rats at the level of mRNA.

Opioids are potent modulators of LC activity and function, signaling through various subtypes of receptors (Mansour et al., 1994; Connor et al., 1996; Neal et al., 1999; Van Bockstaele et al., 2010; Tkaczynski et al., 2022). We quantified the expression of two of these subtypes within the LC, *Oprd1* and *Oprl1*. There was relatively low expression of *Oprd1* transcripts in the LC, and there were no differences in expression between WT and TgF344-AD rats at either age. However, we found a reduction in *Oprl1* transcripts in 6-month TgF344-AD rats. Because Gαi/o signaling through these receptors promotes inhibitory tone via activation of inwardly rectifying potassium channels (Connor et al., 1996), a decrease in their expression is consistent with the LC hyperactivity observed at this age (Kelberman et al., 2023). Interestingly, the signaling peptide pronociceptin is co-expressed in peri-LC GABAergic neurons, which are responsive to odor,

feeding, and aversive stimuli like footshock (Luskin et al., 2022). Specifically, pronociceptin co-expressing GABAergic neurons are activated immediately after footshock (0-5 s) and inhibited at longer durations (5-20 s). Given the alterations we observed to spontaneous and evoked phasic LC activity in 6-month animals (Kelberman et al., 2023), an altered pronociceptin-Oprl1 signaling pathway via peri-LC GABAergic population is possible. When combined with the reduced expression of *Gabra3* that we also identified at this age, these results suggest that impaired inhibitory transmission from peri-LC neurons contributes to LC hyperactivity in young TgF344-AD rats. While this is consistent with observed phasic LC hyperactivity, it is inconsistent with tonic hypoactivity that is also seen at this age (Kelberman et al., 2023). Because stimulating the LC at phasic frequencies is known to release more NE than tonic frequencies (Florin-Lechner et al., 1996), it is possible that autoinhibition via local release of NE contributes to tonic LC hypoactivity, while altered inhibitory signaling contributes to hyperactive phasic firing. By 15-months of age, differences in *Gabra3* and *Oprl1* expression are not evident, indicating that LC neurons would be subjected to similar levels of inhibitory input at a time when they are releasing excessive local NE, culminating in LC hypoactivity.

How can we reconcile what we know about AD-like neuropathology, changes in gene expression, and altered firing rates in the LC of young and aged TgF344-AD rats and develop a comprehensive model of AD progression in the noradrenergic system? LC neurons have an incredible capacity for plasticity, using changes in gene expression and protein abundance to tune NE transmission in response to environmental or internal challenges. The ability of LC neurons to adapt to tonic inhibition, chronic stress, or reuptake blockade is well described, and can often result in pathophysiology (e.g. during opioid withdrawal) (Maldonado, 1997; Nestler et al., 1999; Weinshenker et al., 2002; Benmansour et al., 2004). In AD brains, changes in expression of NE biosynthesis and handling genes have been noted in LC neurons, while adrenergic receptor

expression is altered in LC targets (Szot et al., 2000; Szot et al., 2006, 2007; McMillan et al., 2011; Goodman et al., 2021). In the earliest stages of AD, both clinically and in TgF344-AD rats, hyperphosphorylated tau is the dominant pathology in the LC (Braak et al., 2011; Rorabaugh et al., 2017; Gilvesy et al., 2022). In other types of neurons, tau pathology typically decreases neuronal activity (Gomez-Isla et al., 1997; Theofilas et al., 2018; Busche et al., 2019; Marinkovic et al., 2019; Busche and Hyman, 2020; Kang et al., 2020), and indeed, tonic LC firing is lower in both young and aged TgF344-AD rats (Kelberman et al., 2023). Inhibiting LC activity can invoke transient elevations in firing rates post-inhibition (Marzo et al., 2014), which is consistent with the tonic hypoactivity and phasic hyperactivity (spontaneous and evoked in 6-month, and spontaneous only in 15-month TgF344-AD rats). However, it appears that there are two distinct phases of LC compensation that yield different outcomes. Downregulation of *Gabra3* and *Oprl1* expression may serve to disinhibit noradrenergic transmission and counteract neuronal hypoactivity. While both these inhibitory signaling mechanisms are reported to affect tonic LC activity (Chiang and Aston-Jones, 1993a; Connor et al., 1996; Okawa et al., 2001; Kawahara et al., 2004; Yoshitake et al., 2013; Kelly et al., 2021), we observed a selective increase in spontaneous and evoked firing during phasic burst (Kelberman et al., 2023). However, a recent report suggests that blocking GABAergic signaling to the LC can enhance phasic-like activity in slice (Kuo et al., 2020). Meanwhile, although Oprl1 inhibition is GPCR-based, these mechanisms are also known to activate various other intracellular signaling cascades that may have complex effects on electrophysiological properties of LC neurons (Toll et al., 2016). For example, nociception signaling can dampen response to glutamate via indirect effects on glutamatergic receptor subunits (Wang et al., 1996; Shu et al., 1998). Changes in expression of *Oprl1* may therefore upregulate phasic LC activity by increasing responsiveness to excitatory amino acid transmission (Ennis and Aston-Jones, 1988; Aston-Jones et al., 1991; Chiang and Aston-Jones, 1993b). At 15

months, tau pathology in the LC worsens, the genotype differences in *Gabra3* and *Oprl1* wane, and the stimulus-evoked LC hyperactivity is replaced by hypoactivity (Rorabaugh et al., 2017; Kelberman et al., 2023). These changes are accompanied by increased expression of NE synthesis and transmission genes, which are also indicative of later stage AD. Levels of CSF NE and turnover can be higher in AD subjects (Palmer et al., 1987; Elrod et al., 1997; Hoogendijk et al., 1999; Henjum et al., 2022), which may be driven by one or both of these compensatory mechanisms, but it is not enough to overcome the overall deficiency in normal LC-NE transmission. Overall, LC inhibition mechanisms are targeted during phase I (early) compensation and result in dysregulated LC firing that may contribute to prodromal symptoms including anxiety. By contrast, noradrenergic-specific genes are targeted during phase II (late) compensation, permitting LC hypoactivity to dominate both at baseline and in response to relevant stimuli, likely contributing to cognitive decline.

There are several caveats to the current study that can be addressed with follow-up studies that are worth discussing. The LC is a sexually dimorphic structure (Babstock et al., 1997; Bangasser et al., 2011; Bangasser et al., 2016; Duesman et al., 2022; Sulkes Cuevas et al., 2023), including in gene expression (Mulvey et al., 2018). Our groups were unbalanced and underpowered to detect sex differences, and there were some trends suggesting an influence of sex on some of the markers studied here (see *Th*, *Adra2a*, and *Grm3* in **Figure 3.1Bi**, **Cii**, and **Figure 3.2Bi**, respectively). Along with this, there is evidence that the LC is modular with respect to electrophysiological properties, biochemical makeup, and afferent/efferent connections (Sara and Bouret, 2012; Chandler et al., 2014; Schwarz and Luo, 2015; Chandler et al., 2019; Wagner-Altendorf et al., 2019; Poe et al., 2020). Rostral and middle portions of the LC preferentially project to hippocampal and cortical structures and are particularly susceptible in AD (German et al., 1992; Sara and Bouret, 2012; Schwarz and Luo, 2015; Theofilas et al., 2017; Betts et al., 2019a; Gilvesy

et al., 2022). It is therefore possible that changes in gene or protein expression are dependent upon location within the LC that we were unable to parse out in the current study.

Similarly, although there appeared to be an effect of age on gene expression (see *Dbh*, *Adra2a, Grin1*, and *Oprl1* as examples), we were unable to statistically compare transcript levels across ages due to potential variability between RNAscope runs. Comparisons were instead made between age-matched TgF344-AD rats and WT littermates because we previously identified genotype as the main contributor to aberrant LC activity (Kelberman et al., 2023). However, we have separately shown that aging can impair spatial memory, associative learning, arousal, and anxiety-like behaviors (Kelberman et al., 2022). It is also clear that variations in LC gene expression can impact behavior (Mulvey et al., 2018). Therefore, it is possible that there are changes in LC gene expression during the course of aging that may have functional consequences that we were unable to detect in the present study.

We chose to examine mRNAs because specific antibodies suitable for immunohistochemistry are not available for many of the molecules we wanted to quantify. However, a limitation of this approach is that we were unable to interrogate aspects of receptor localization. In the hippocampus of APP/PS1 mice, there are no changes in AMPA receptor subunit density, but there is evidence of increased receptor internalization (Martin-Belmonte et al., 2020). Meanwhile, $GABA_A$ α3 receptor subunits in the LC of these mice are similarly mislocalized to the cytoplasm (Kelly et al., 2021). Future studies should therefore investigate localization of these receptors and how they may impact LC activity. This may require the development of new antibodies and/or animals with tagged proteins. Our study also does not address the complex interplay between different receptor subtypes and signaling. For example, serotonin is involved in modulating LC responses to both glutamate and GABA (Aston-Jones et al., 1991; Chiang and Aston-Jones, 1993a) and could impact signaling through these receptors in

the absence of changes in expression levels. Moreover, serotonergic modulation of LC activity impacts both tonic and phasic LC firing in a manner that phenocopies aspects of LC neurons recorded from both 6- and 15-month TgF344-AD rats (Aston-Jones et al., 1991; Chiang and Aston-Jones, 1993a; Kelberman et al., 2023). Combining patch-clamp electrophysiology and pharmacology could further elucidate any abnormalities beyond expression levels, such as receptor subunit function and excitatory/inhibitory balance.

There are a host of other neuromodulators of LC activity, including hypocretin/orexin, galanin, neuropeptide Y, and substance P which were not probed here due to limitations in available probes and number of available samples (Luskin et al., 2022; Weber et al., 2022). We therefore focused on markers that were likely to cause changes in LC activity if expression was disrupted. Single cell/single nucleus RNA sequencing of the LC is challenging due to its fragility and small size, but would be useful for obtaining a holistic and unbiased view of changes in the LC transcriptome and then mapping them onto enrichment pathways for further analysis. There can also be significant discordance between expression at the level of RNA versus protein, leaving an open question as to how our results would translate to the LC proteome.

3.5 CONCLUSIONS

We identified changes in the LC gene expression profile that could sensibly contribute to altered LC activity over the course of AD (**Figure 3.4**). Specifically, hyperactivity at 6-months is associated with reduced expression of *Gabra3* and *Oprl1* while hypoactivity at 15 months is paralleled by an upregulation of genes involved in NE synthesis, packaging, and turnover. Still, these results further support the idea of disease-stage dependent dysregulation of LC activity (Weinshenker, 2018) while adding further nuance and identify potential molecular targets for therapeutic interventions targeting the LC-NE system. Preclinical reports suggest that increasing

glycinergic neurotransmission to the LC may be a valid way of reducing hyperactivity of LC neurons (Kelly et al., 2021). Meanwhile, studies in human populations indicate that noradrenergic blockers provide non-cognitive symptomatic relief (Peskind et al., 2005; Wang et al., 2009). When cognitive deficits are present, augmenting noradrenergic tone should be considered, and has already been shown to be beneficial for cognitive deficits preclinically and improve signatures of disease in patients with mild-cognitive impairment (Rorabaugh et al., 2017; Levey et al., 2022).

Table 3.1. Probes used for RNAscope

Transcript Category	Target [Reference]	Gene	Probe catalog #
NE Synthesis and Transmission	Tyrosine hydroxylase (Mulvey et al., 2018; Iannitelli et al., 2023b)	*Th*	314651-C2
	Dopamine-β hydroxylase (Mulvey et al., 2018; Iannitelli et al., 2023b)	*Dbh*	316421-C1
	Norepinephrine transporter (NET) (Mulvey et al., 2018; Iannitelli et al., 2023b)	*Slc6a2*	497031-C2
	α2-adrenergic receptor (McCune et al., 1993; Kelberman et al., 2023)	*Adra2a*	519451-C1
	Vesicular monoamine transporter 2 (Vmat2) (Mulvey et al., 2018)	*Slc18a2*	311971-C2
Excitatory Neurotransmission	Glutamate metabotropic receptor 3 (Noriega et al., 2007)	*Grm3*	317741-C2
	Glutamate ionotropic receptor AMPA type subunit 2 (Noriega et al., 2007)	*Gria2*	505321-C1
	Glutamate ionotropic receptor NMDA type subunit 1 (Noriega et al., 2007)	*Grin1*	317021-C3
Inhibitory Neurotransmission	Gamma-aminobutyric acid type A receptor subunit α3 (Waldvogel et al., 2010; Corteen et al., 2011; Kelly et al., 2021)	*Gabra3*	411611-C1
Neuromodulatory Transmission	Pituitary adenylate cyclase-activating polypeptide type 1 receptor (Hashimoto et al., 1996; Duesman et al., 2022)	*Adcyap1r1*	466981-C3

	Opioid receptor delta 1 (Mansour et al., 1994; Van Bockstaele et al., 2010; Tkaczynski et al., 2022)	*Oprd1*	536061-C3
	Opioid related nociception receptor 1 (Connor et al., 1996; Neal et al., 1999)	*Oprl1*	576011-C3
	Serotonin 1a receptor (Aston-Jones et al., 1991; Chiang and Aston-Jones, 1993a)	*5htr1a*	404801-C2
	Corticotropin releasing hormone receptor 1 (Van Bockstaele et al., 1996; Reyes et al., 2006)	*Crhr1*	318911-C3

Table 3.2. HALO® Analysis Parameters

Nuclear Settings							
	DAPI Nucleus Weight	*Nuclear Contrast Threshold*	*Minimum Nuclear Intensity*	*Nuclear Segmentation Aggressiveness*	*Fill Nuclear Holes*	*Nuclear Size*	*Minimum Nuclear Roundness*
Probe Set 1	1	0.505	10	0	True	0,1000	0
Probe Set 2	1	0.506	23	-5	True	0,1000	0
Probe Set 3	1	0.5002	6	-5	True	10,1000	0
Probe Set 4	1	0.506	14	-6	True	0,1000	0

Cytoplasm Settings				
	Maximum Cytoplasm Radius	*Membrane Segmentation Aggressiveness*	*Cell Size*	*DAPI membrane segmentation*
Probe Set 1	13	0	10,1000	True
Probe Set 2	13	0	10,1000	True
Probe Set 3	10	0	10,1000	True
Probe Set 4	11	0	10,1000	True

Immunofluorescence Settings						
	DAPI Nucleus Positive Threshold	*DAPI Cytoplasm Positive Threshold*	*DAPI Membrane Positive Threshold*	*LC marker Nucleus Positive Threshold*	*LC marker Cytoplasm Positive Threshold*	*LC marker Membrane Positive Threshold*
Probe Set 1	1	255	255	*Th*: 12	*Th*: 16.2	*Th*: 12
Probe Set 2	1	255	255	*Slc6a2*: 27	*Slc6a2*: 18	*Slc6a2*: 20
Probe Set 3	1	255	255	*Dbh*: 10	*Dbh*: 30	*Dbh*: 12
Probe Set 4	1	255	255	*Slc18a2*: 20	*Slc18a2*: 25	*Slc18a2*: 30

FISH Scoring					
	Contrast Threshold	*Signal Minimum Intensity*	*Spot Size*	*Copy Intensity*	*Spot Segmentation Aggressiveness*
Probe Set 1: Adra2a	0.505	10	0.5,30	38.25	1
Probe Set 1: Grin	0.51	10	0.5,30	38.25	1
Probe Set 2: Gria	0.505	18	0.5,30	38.25	1
Probe Set 2: Pac1r	0.505	11	0.5,30	38.25	1
Probe Set 3: Grm3	0.511	5	0.5,30	38.25	1
Probe Set 3: Oprd1	0.508	1	0.5,30	38.25	1

Probe Set 4: Gabr3	0.508	5	0.5,30	38.25	1
Probe Set 4: Oprl1	0.513	5	0.5,30	38.25	1

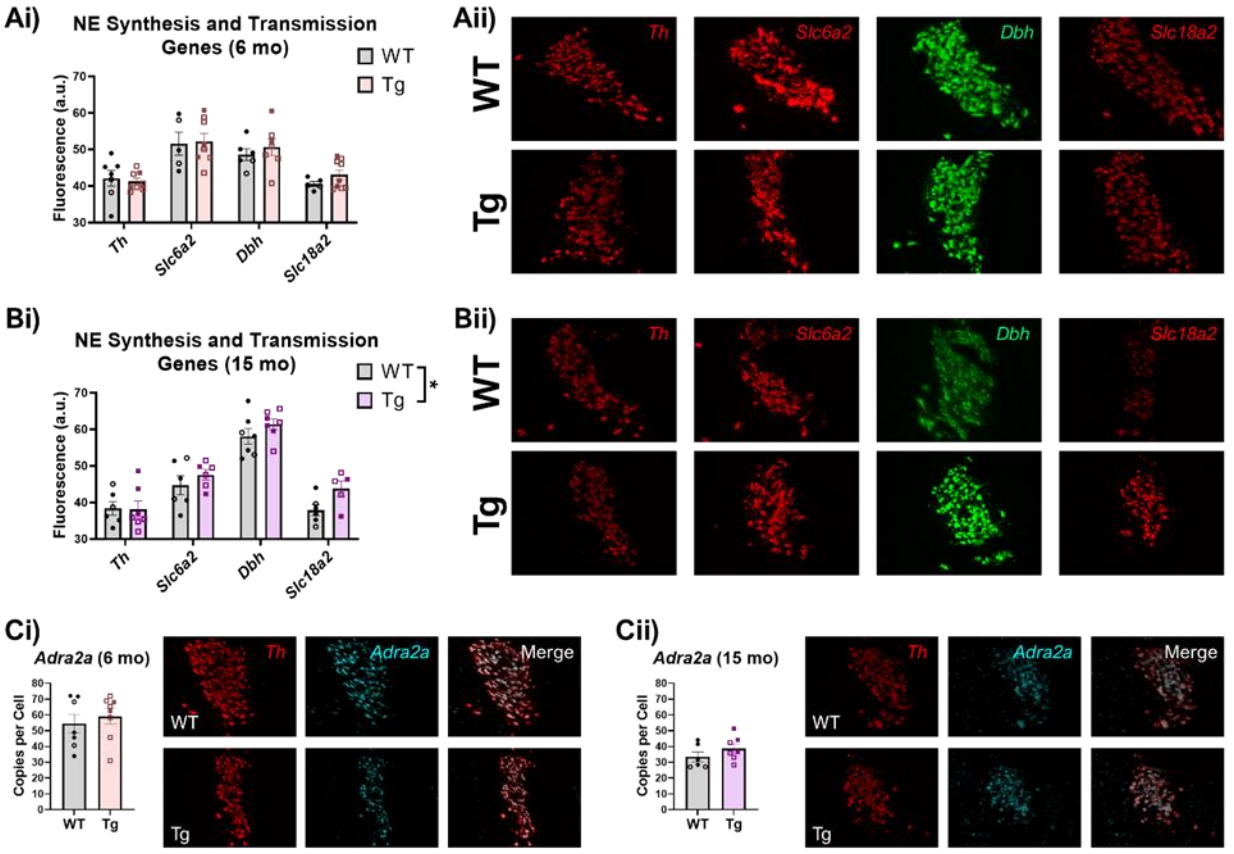

Figure 3.1. Quantification of NE synthesis and transmission transcript expression in 6- and 15-month TgF344-AD rats and WT littermates. Ai) Quantification of *Th*, *Slc6a2*, *Dbh*, and *Slc18a2* transcript fluorescence in the LC of 6-month animals. Aii) Representative images of *Th* (red), *Slc6a2* (red), *Dbh* (green), and *Slc18a2* (red) transcript fluorescence in the LC of 6-month animals. Bi) Quantification of *Th*, *Slc6a2*, *Dbh*, and *Slc18a2* transcript fluorescence in the LC of 15-month animals. Bii) Representative images of *Th* (red), *Slc6a2* (red), *Dbh* (green), and *Slc18a2* (red) transcript fluorescence in the LC of 15-month animals. Ci) Quantification and representative images of *Adra2a* transcript copies per cell (cyan) in the LC (marked by *Th* in red) of 6-month animals. Cii) Quantification and representative images of *Adra2a* transcript copies per cell (cyan) in the LC (marked by *Th* in red) of 15-month animals. N = 5-9 animals per group. Males and females represented by closed and open symbols, respectively. Images taken at 20x. *p<0.05

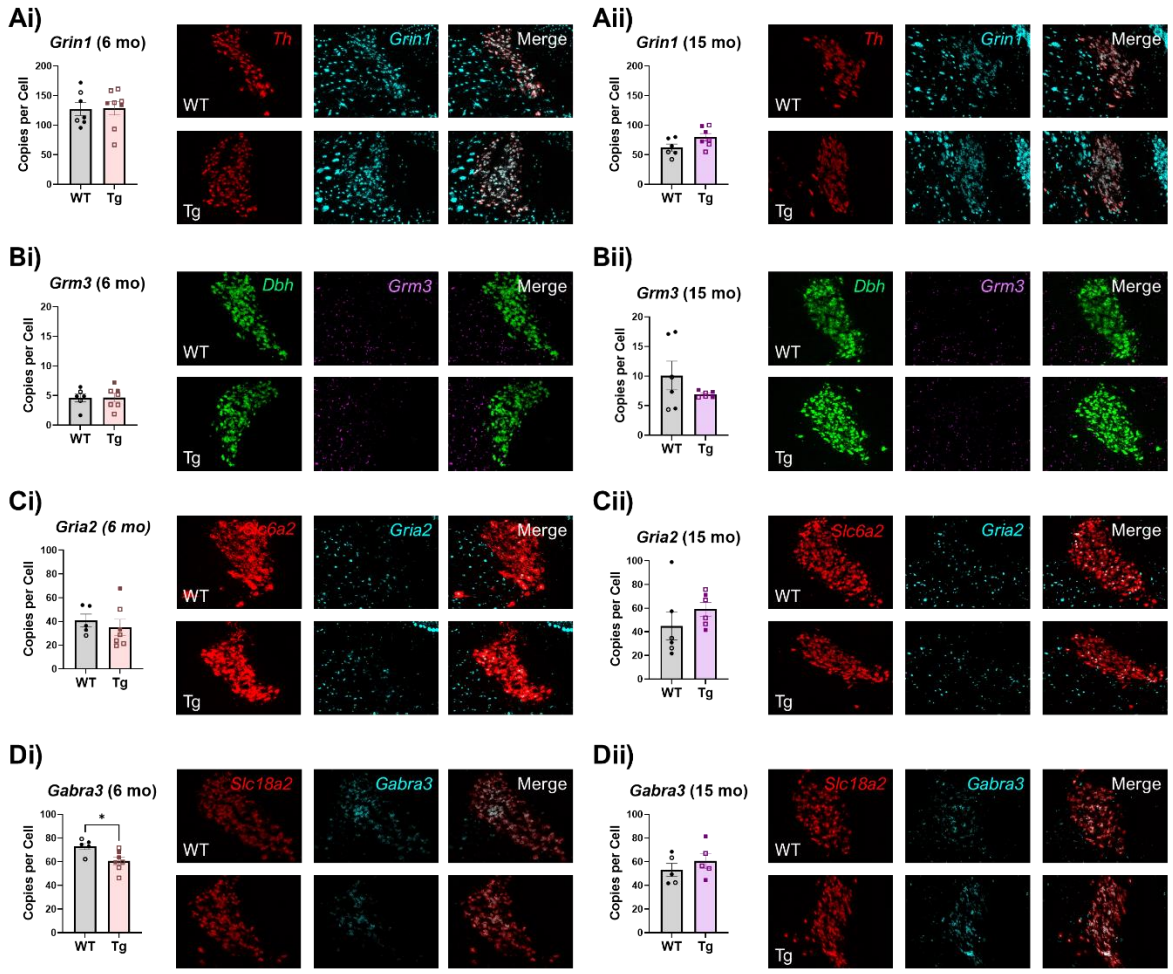

Figure 3.2. Quantification of glutamatergic and GABAergic receptor subunit transcript expression in the LC of 6- and 15-month TgF344-AD rats and WT littermates. Ai) Quantification and representative images of *Grin1* transcript copies per cell (cyan) in the LC (marked by *Th* in red) of 6-month animals. Aii) Quantification and representative images of *Grin1* transcript copies per cell (cyan) in the LC (marked by *Th* in red) of 15-month animals. Bi) Quantification and representative images of *Grm3* transcript copies per cell (purple) in the LC (marked by *Dbh* in green) of 6-month animals. Bii) Quantification and representative images of *Grm3* transcript copies per cell (purple) in the LC (marked by *Dbh* in green) of 15-month animals. Ci) Quantification and representative images of *Gria2* transcript copies per cell (cyan) in the LC (marked by *NET* in red) of 6-month animals. Cii) Quantification and representative images of *Gria2*

transcript copies per cell (cyan) in the LC (marked by *NET* in red) of 15-month animals. Di) Quantification and representative images of *Gabra3* transcript copies per cell (cyan) in the LC (marked by *Slc18a2* in red) of 6-month animals. Dii) Quantification and representative images of *Gabra3* transcript copies per cell (cyan) in the LC (marked by *Slc18a2* in red) of 15-month animals. N = 5-8 animals per group. Males and females represented by closed and open symbols, respectively. Images taken at 20x. *$p<0.05$

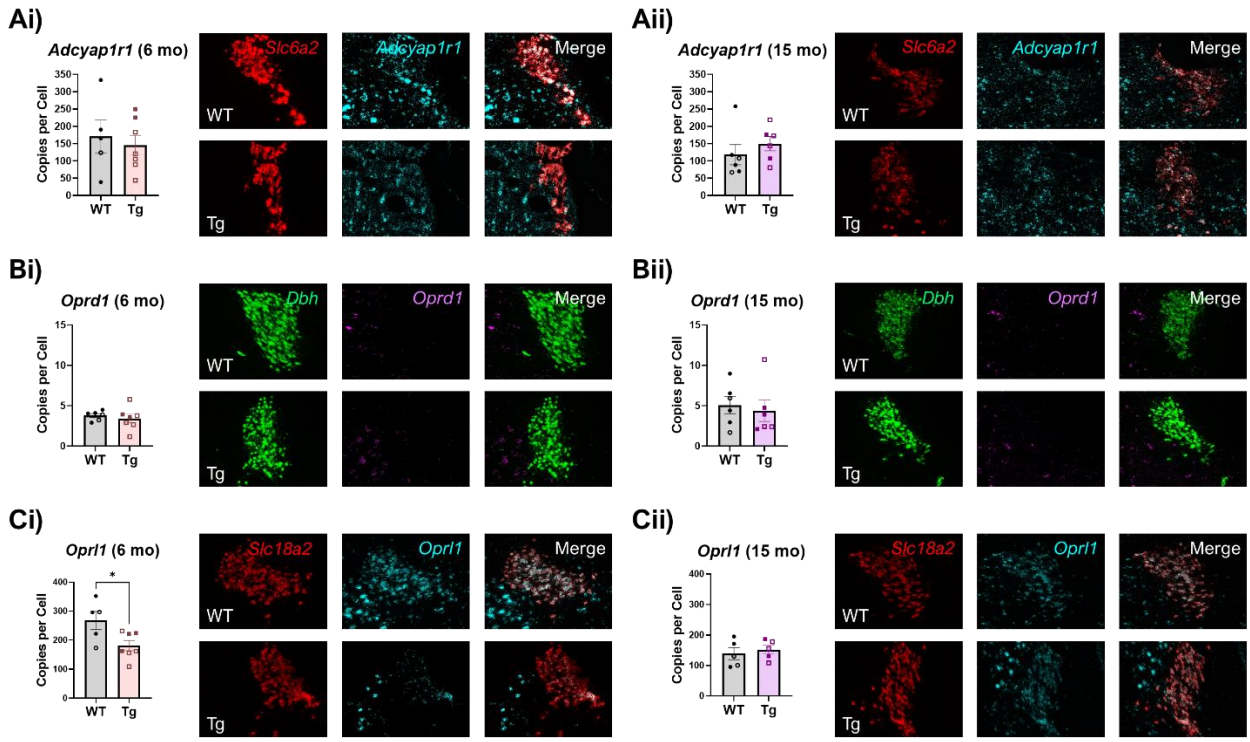

Figure 3.3. Quantification of neuromodulatory receptor transcript expression in the LC of 6- and 15-month TgF344-AD rats and WT littermates. Ai) Quantification and representative images of *Adcyap1r1* transcript copies per cell (cyan) in the LC (marked by *Slc6a2* in red) of 6-month animals. Aii) Quantification and representative images of *Adcyap1r1* transcript copies per cell (cyan) in the LC (marked by *Slc6a2* in red) of 15-month animals. Bi) Quantification and representative images of *Oprd1* transcript copies per cell (purple) in the LC (marked by *Dbh* in green) of 6-month animals. Bii) Quantification and representative images of *Oprd1* transcript copies per cell (purple) in the LC (marked by *Dbh* in green) of 15-month animals. Ci) Quantification and representative images of *Oprl1* transcript copies per cell (cyan) in the LC (marked by *Slc18a2* in red) of 6-month animals. Cii) Quantification and representative images of *Oprl1* transcript copies per cell (cyan) in the LC (marked by *Slc18a2* in red) of 15-month animals. N = 5-8 animals per group. Males and females represented by closed and open symbols, respectively. Images taken at 20x. *p<0.05

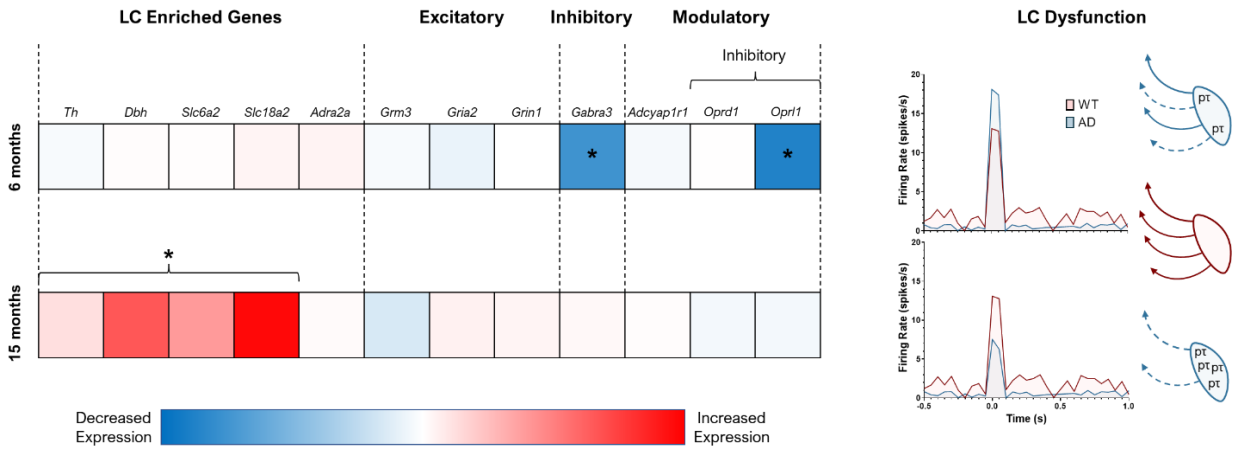

Figure 3.4. Summary of altered gene expression in and dysfunction of LC neurons in 6- and 15-month TgF344-AD rats. At 6 months, TgF344-AD rat LC neurons demonstrate normal expression of noradrenergic-specific, excitatory and most neuromodulatory receptor mRNAs, but show downregulated expression of inhibitory mRNAs (*Gabra3 and Oprl1*). These changes coincide with the appearance of phosphorylated tau (pτ) in the LC, axonal damage (dashed arrows), tonic hypoactivity, and phasic hyperactivity. At 15 months, TgF344-AD rat LC neurons have normal expression of excitatory, inhibitory, and neuromodulatory receptor mRNAs, but exhibit upregulation of mRNAs involved in NE synthesis (*Th, Dbh*), packaging (*Slc18a2*), and reuptake (*Slc6a2*). LC neuropathology and denervation is worsened alongside hypoactivity of both tonic and phasic firing.

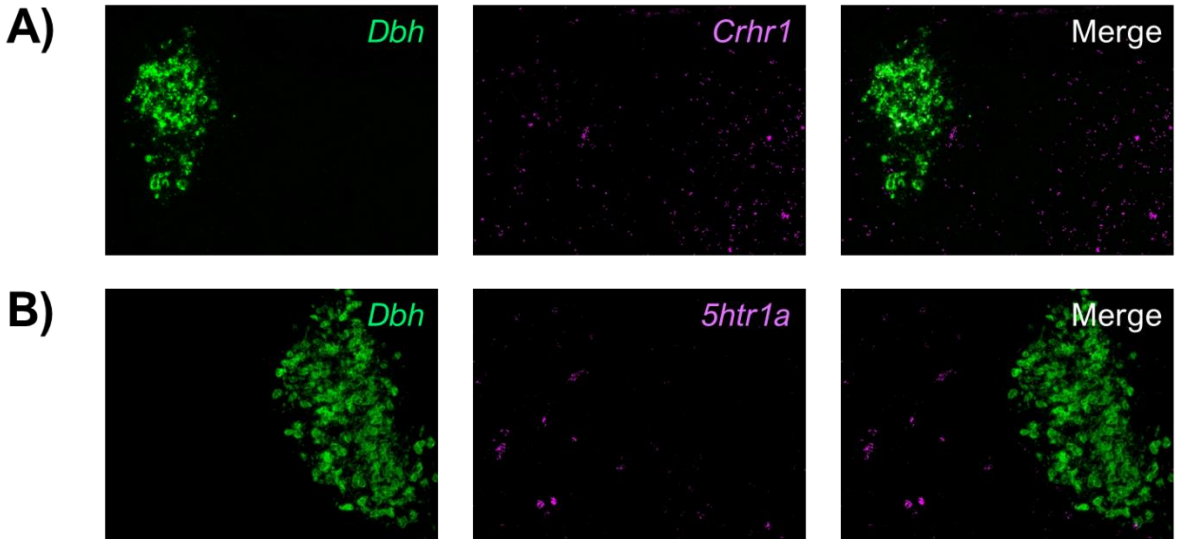

Supplemental Figure 3.1. Expression of *Crhr1* and *5htr1a* in the LC. Representative images of RNAscope for *Crhr1* (A) and *5htr1a* (B) reveal low levels of both mRNA in the LC (marked by *Dbh* in green).

CHAPTER 4: CONSEQUENCES OF HYPERPHOSPHORYLATED TAU IN THE LOCUS COERULEUS ON BEHAVIOR AND COGNITION IN A RAT MODEL OF ALZHEIMER'S DISEASE

Parts of this chapter were used verbatim, with permission, from the following publication:

Kelberman MA*, Anderson CR*, Chlan E, Rorabaugh JM, McCann KE, Weinshenker D (2022) Consequences of Hyperphosphorylated Tau in the Locus Coeruleus on Behavior and Cognition in a Rat Model of Alzheimer's Disease. Journal of Alzheimer's Disease:1–23 Available at: http://dx.doi.org/10.3233/jad-215546.

**Denotes equal contribution*

Abstract

Background: The locus coeruleus (LC) is one of the earliest brain regions to accumulate hyperphosphorylated tau, but a lack of animal models that recapitulate this pathology has hampered our understanding of its contributions to Alzheimer's disease (AD) pathophysiology.

Objective: We previously reported that TgF344-AD rats, which overexpress mutant human amyloid precursor protein and presenilin-1, accumulate early endogenous hyperphosphorylated tau in the LC. Here, we used TgF344-AD rats and a wild-type (WT) human tau virus to interrogate the effects of endogenous hyperphosphorylated rat tau and human tau in the LC on AD-related neuropathology and behavior.

Methods: Two-month old TgF344-AD and WT rats received bilateral LC infusions of full-length WT human tau or mCherry control virus driven by the noradrenergic-specific PRSx8 promoter. Rats were subsequently assessed at 6 and 12 months for arousal (sleep latency), anxiety-like behavior (open field, elevated plus maze, novelty-suppressed feeding), passive coping (forced swim task), and learning and memory (Morris water maze and fear conditioning). Hippocampal microglia, astrocyte, and AD pathology were evaluated using immunohistochemistry.

Results: In general, the effects of age were more pronounced than genotype or treatment; older rats displayed greater hippocampal pathology, took longer to fall asleep, had reduced locomotor activity, floated more, and had impaired cognition compared to younger animals. TgF344-AD rats showed increased anxiety-like behavior and impaired learning and memory. The tau virus had negligible influence on most measures.

Conclusion: Effects of hyperphosphorylated tau on AD-like neuropathology and behavioral symptoms were subtle. Further investigation of different forms of tau is warranted.

4.1 INTRODUCTION

Alzheimer's disease (AD) is the most common neurodegenerative disorder in the world and is characterized by two protein aggregates: amyloid-β (Aβ) plaques and neurofibrillary tangles composed of hyperphosphorylated and misfolded tau. Initiation of AD has been attributed to Aβ (Hardy and Higgins, 1992), which subsequently leads to tau hyperphosphorylation (Busciglio et al., 1995; Jin et al., 2011; Zhang et al., 2020), oxidative stress and mitochondrial dysfunction (Caspersen et al., 2005; Chauhan and Chauhan, 2006; Manczak et al., 2006; Mao and Reddy, 2011; Leuner et al., 2012), and synaptic impairments (Walsh et al., 2002; Lacor et al., 2007; Lauren et al., 2009). However, antibody treatments targeting late-stage Aβ deposition have been largely unsuccessful and/or controversial, highlighting the pressing need to investigate other therapeutic avenues that focus on earlier stages of disease prior to catastrophic neuronal loss and significant cognitive impairment.

Neurofibrillary tangles (NFT) have garnered increasing attention in recent years because tau load is consistently reported as a better predictor of cognitive decline and neuronal degeneration compared with Aβ (Arriagada et al., 1992; Gomez-Isla et al., 1997; Fagan et al., 2007). Although Aβ plaques appear prior to NFT, recent evidence places the deposition of "pretangle" hyperphosphorylated tau prior to both pathologies. Specifically, Braak and colleagues identified the locus coeruleus (LC) as the first brain region to accumulate hyperphosphorylated tau (Braak et al., 2011), a finding that has since been independently confirmed by other groups (Theofilas et al., 2017; Pletnikova et al., 2018). The LC is the primary source of norepinephrine (NE) in the brain, which has potent anti-inflammatory/neuroprotective properties and regulates attention, arousal, and stress responses (Aston-Jones and Cohen, 2005a; Sara, 2009; Chandler et al., 2019; Poe et al., 2020), all of which often go awry in AD (Teri et al., 1999; Hamann et al., 2000; Yesavage et al., 2004; Berardi et al., 2005; Ju et al., 2013; Pietrzak et al., 2015; Winsky-

Sommerer et al., 2019). Although tau pathology can cause cell death and there is evidence for some early reduction of LC volume (which likely corresponds to loss of proximal axons/dendrites) (Wittmann et al., 2001; Gendron and Petrucelli, 2009; Theofilas et al., 2017; Ghosh et al., 2019), frank LC cell body degeneration is not evident until mid- to late-stages of AD (Busch et al., 1997; Arendt et al., 2015; Theofilas et al., 2017). Thus, detrimental effects of hyperphosphorylated tau pathology on LC function could persist for years or even decades, and may contribute to behavioral abnormalities in prodromal AD. Indeed, aggregation of hyperphosphorylated tau in the LC coincides with the emergence of non-cognitive behavioral impairments commonly observed in prodromal AD that are consistent with LC dysfunction (Arendt et al., 2015; Ehrenberg et al., 2018; Matchett et al., 2021). Lower LC integrity as measured with MRI contrast has been linked with depression, sleep disorders, and impaired cognition at stages when hyperphosphorylated tau is expected in the LC but few other regions (Shibata et al., 2007; Shibata et al., 2008; Ehrminger et al., 2016; Knudsen et al., 2018; Olivieri et al., 2019). LC post-mortem integrity and tangle load (Wilson et al., 2013; Kelly et al., 2017) and BOLD activation/functional connectivity (Jacobs et al., 2015a; Jacobs et al., 2018; Del Cerro et al., 2020; Jacobs et al., 2020; Grueschow et al., 2021) have also been implicated in cognitive reserve and/or behavioral abnormalities, highlighting a central role for the LC in their dysregulation. One study even identified the LC as the origin of functional connectivity deficits in AD patients (Zhao et al., 2017). Separately, tau abundance in cerebrospinal fluid and positron emission tomography levels have been associated with non-cognitive behavioral impairments in healthy adults and in populations at risk for developing AD (Gatchel et al., 2017; d'Oleire Uquillas et al., 2018; Babulal et al., 2020; Johansson et al., 2021; Pichet Binette et al., 2021). Together, these data suggest an association between the development of LC tau neuropathology and behavioral impairments in early AD, but a causal link remains

speculative due to limitations in the ability for imaging techniques to localize and quantify pathology in small nuclei such as the LC (Kelberman et al., 2020).

Animal models are valuable tools for establishing mechanistic relationships between pathology and behavior in AD. These models have provided crucial information regarding the consequences of LC perturbations in the context of disease that are largely congruent with human studies. For example, neurotoxic LC lesions exacerbate AD neuropathology, neurodegeneration, inflammation, lethality, and/or cognitive impairment in transgenic rodent AD models (Heneka et al., 2006; Jardanhazi-Kurutz et al., 2010; Chalermpalanupap et al., 2018). Even in the absence of experimental LC lesions, noradrenergic denervation, altered NE signaling, and LC cell loss have been reported in these models (O'Neil et al., 2007; Liu et al., 2008; Rorabaugh et al., 2017; Mehla et al., 2019; Cao et al., 2021), but there are important limitations to consider. Amyloidosis models generally fail to recapitulate tau pathology in the LC. Even the P301S mouse, which does accumulate hyperphosphorylated tau in the LC, employs a ubiquitous promoter and a mutant form of tau that causes frontotemporal dementia that simultaneously produces tau pathology all over the brain and more closely mimics pure tauopathies (Yoshiyama et al., 2007; Chalermpalanupap et al., 2018). To isolate the effects of aberrant tau in the LC, we and others have used viral vectors to express various forms of tau specifically in the LC of mice and rats (Ghosh et al., 2019; Kang et al., 2020), which triggers LC degeneration, transsynaptic tau spread, and cognitive deficits. These manipulations, however, were not performed in the context of Aβ, primarily utilized mutant forms of tau not known to occur in AD, and did not assess behaviors reminiscent of non-cognitive prodromal AD symptoms.

Our lab has previously demonstrated that the TgF344-AD rat, which overexpresses mutant human amyloid precursor protein and presenilin-1 (APP/PS1), develops endogenous, age-related accumulation of hyperphosphorylated tau in the LC prior to appreciable plaque or tangle

pathology in the forebrain (Rorabaugh et al., 2017). This model provides a unique resource for understanding the consequences of hyperphosphorylated tau in the LC in the earliest phases of AD because the tau pathology (1) is triggered by AD-causing mutant Aβ, (2) is endogenous (i.e. there is no human tau transgene), and (3) follows a spatial pattern of appearance reminiscent of human disease. Dysregulation of the noradrenergic system in TgF344-AD rats is evidenced by forebrain denervation and reduced NE levels in the absence of frank neuronal loss. Behavioral characterizations of these rats have shown impaired learning and memory, hyposmia, and anxiety-like phenotypes (Cohen et al., 2013; Rorabaugh et al., 2017; Munoz-Moreno et al., 2018; Pentkowski et al., 2018; Sare et al., 2020), and we have shown that chemogenetic LC activation rescues reversal learning deficits (Rorabaugh et al., 2017). However, few studies have comprehensively tested this strain on behaviors influenced by the LC along disease progression, beginning with the appearance of tau in the LC (~6 months) and at more advanced stages, when forebrain pathology is present (~12 months). Moreover, LC tau in this model is limited to a mild hyperphosphorylated state reminiscent of prodromal AD, limiting our understanding of how more mature forms of tau affect LC function.

The goals of this study were two-fold: (1) to expand the characterization of TgF344-AD rats across a battery of AD- and LC-relevant behaviors at time points where hyperphosphorylated tau in the LC is the only detectable AD-like neuropathology (6 months) and when Aβ and tau pathology is evident in the forebrain (12 months), and (2) to assess whether viral-mediated expression of wild-type (WT) human tau in the LC that is prone to more advanced states of hyperphosphorylation exacerbates AD-like behavioral phenotypes and pathology.

4.2 MATERIALS AND METHODS

4.2.1 Animals:

TgF344-AD rats hemizygous for the *APPsw/PS1ΔE9* transgene and WT littermates were housed in the animal facilities at Emory University. Rats were housed in groups of 2-3 on a 12-h light/dark cycle (lights on at 7:00 am) and given *ad libitum* access to food and water except during behavioral testing or otherwise specified. All procedures were approved by the Institutional Animal Care and Use Committee of Emory University.

4.2.2 Stereotaxic Injections:

At two months of age, rats underwent stereotaxic, sterile-tip surgery. Rats were anesthetized with isoflurane and given meloxicam or ketoprofen (2 mg/kg or 5 mg/kg, s.c., respectively) prior to receiving bilateral injections (1.3 ul/hemisphere) of virus expressing either full-length wild-type human tau under control of a noradrenergic-specific promoter (AAV9-PRSx8-hTau(WT)-WPRE-SV40) or mCherry control (AAV9-PRSx8-mCherry-WPRE-rBG) targeting the LC (AP: -3.8, ML: +/-1.2mm, DV: -7.0mm from lambda with a 15 degree downward head-tilt). Viral expression was driven by the noradrenergic-specific PRSx8 promoter (Hwang et al., 2001). Following the infusion, the injection syringe was left in place for 5 min before being moved dorsally 1mm and waiting 2 additional min to ensure diffusion of the virus at the site of injection. Behavioral assays were conducted 4 or 10 months following surgery (i.e. at 6 or 12 months of age).

4.2.3 Behavioral Assays

4.2.3.1 General:

A variety of assays were chosen to assess changes in behaviors commonly associated with prodromal and later stage AD including arousal (sleep latency), general activity levels (23-h locomotor activity), anxiety-like behaviors (open field, elevated plus maze, and novelty-suppressed feeding), passive coping that may reflect aspects of depression (forced swim test), and learning and memory (Morris water maze, cue- and context-dependent-fear conditioning).

Rats were tested on behavioral tasks in the following order, from least to most stressful/invasive: sleep latency, 23-h locomotor activity, open field, elevated plus maze, forced swim task, Morris water maze, novelty-suppressed feeding, and fear conditioning. Rats were singly-housed 3-7 days before sleep latency and subsequently re-paired following completion of the 23-h locomotor test. Behavioral tests were separated by at least 1 day. All behavioral tests were conducted during the light phase under white light, unless otherwise reported.

4.2.3.2 Sleep latency:

Approximately 2-3 hrs following lights on, rats were gently handled for 2-3 s and placed back into their home cage for 4 h and recorded with video cameras mounted above the home cage. Latency to fall asleep was quantified as the duration of time (min) until the rat had its first sleep bout. Sleep bouts were defined as periods of time that rats exhibited a sleep position for at least 75% of a 10 min time period that began with at least 2 mins of uninterrupted sleep, as previously described (Hunsley and Palmiter, 2004), which our lab has validated with EEG (Porter-Stransky et al., 2019).

4.2.3.3 23-h locomotor activity:

Rats were placed into a clean cage with free access to food and water for 23 h. Cages were surrounded with 11.5 x 20” Photobeam Activity System-Home Cage infrared beams to measure locomotor activity. Total number of ambulations were binned in 30-min intervals over the 23 h testing period. Testing for all cohorts began between 9:15-10:15 am. Analyses were performed on novelty-induced locomotion, defined as occurring within the first 30 min interval, locomotion during the light and dark phases, and total locomotion over the entire 23-h period.

4.2.3.4 Open field:

Rats were individually placed into the center of a 39” outer diameter circular arena with plastic floors and 12” gray plexiglass walls and allowed to freely explore the arena for 5 min. Activity was measured and recorded with a ceiling-mounted camera and TopScan software. Analyses focused on the duration of time spent in the inner 50% of the circle area, total velocity, and latency to exit the inner circle. Time spent in the inner circle is interpreted as lower anxiety-like behavior.

4.2.3.5 Elevated plus maze:

Rats were individually placed into the center of an elevated plus maze (Harvard Apparatus) with two arms enclosed by 50 cm high walls and two open arms with no walls (each 50 cm x 10 cm) and allowed to freely explore for 5 min. Activity was measured and recorded with a ceiling-mounted camera and TopScan software. Rats were tested during the light phase under red lighting. Analyses focused on the time spent in the open and closed arms and total velocity. Time spent in the open arms is interpreted as lower anxiety-like behavior.

4.2.3.6 Forced swim test:

Rats were individually placed in a clear plastic cylinder filled two-thirds with water at 25°C for 10 min. Behavior was recorded by video cameras, and immobility, defined as when the rats made only those movements necessary to keep their heads above water, was manually scored using BORIS software (Friard and Gamba, 2016). Immobility is indicative of passive coping behavior and was calculated using the average of scores from two blinded experimenters.

4.2.3.7 Morris water maze:

Acquisition – Rats underwent four training sessions in which they were placed in a different quadrant of a 75” diameter plastic circular arena surrounded by several extra-maze cues and filled with opaque water, with a hidden platform just below the surface of the water. The platform

remained in the same location throughout the acquisition sessions. Rats remained in the water until locating the platform or 60 s had elapsed, whichever came first. If 60 s elapsed, the rat was placed on the platform for 10 s. Rats completed four training sessions every day for four consecutive days. Behavior was tracked and recorded by a ceiling-mounted camera and TopScan software. Analyses were performed on distance travelled, latency to find the hidden platform, and total velocity averaged across training sessions for each day.

Acquisition Probe – The day following the final acquisition training day, rats were placed into the circular arena with no platform for 60 s. Analyses were performed on time spent and distance travelled in the quadrant of the maze where the platform was located during acquisition training.

Reversal Training – Rats underwent the same training they received during the acquisition training, but the hidden platform was moved to a different quadrant.

Reversal Probe – Following reversal training, rats underwent a reversal probe under identical conditions to the acquisition probe.

4.2.3.8 Novelty-suppressed feeding:

Rats were food-deprived for 24 h and then placed in a 24 x 12 x 12” rectangular arena that contained a pre-weighed food pellet at the center of the arena during the light phase under red lighting. The session ended when the rat picked up and bit into the pellet, or when 15 min elapsed, whichever came first. Rats were subsequently placed into their home cages with the same pellet. The primary outcome measure was latency to eat in the novel environment. Shorter latency to eat the pellet in a novel environment was interpreted as lower anxiety-like behavior. To control for the possibility that there were group differences in overall hunger levels or motivation to consume

food, latency to eat in the home cage immediately following the experimental session and the amount of pellet consumed after 1 h was recorded.

4.2.3.9 Fear conditioning:

Testing was performed over three consecutive days. After each session, rats were returned to their home cage. Freezing levels for each session were recorded with FreezeFrame software.

Training – For the training phase, rats were placed in a sound-enclosed metal chamber illuminated with a single light with stainless-steel bar flooring capable of delivering footshocks. Rats were allowed to habituate to the chamber for 3 min which was followed by a 2000 Hz, 80 dB tone for 20 s that co-terminated with a 2 s, 0.5 mA shock. This procedure was repeated three times with inter-tone intervals set at 60 s. Chambers were cleaned with RB10 between sessions.

Contextual fear conditioning – To test memory for the shock-context pairing, 24 h after Training rats were placed in the original chamber where they received training for 8 min in the absence of tone or footshock.

Cued fear conditioning – To test memory for the association between the cue-shock pairing, 24 h after contextual fear conditioning rats were placed in a novel chamber with a different texture (metal grid flooring) and odor (chambers cleaned with 70% ethanol before and after each session). After 1 min, rats were played the same tone from the training sessions a total of three times, with 60 s intertrial intervals in the absence of footshocks.

Primary outcome measures were freezing levels throughout contextual and cued fear conditioning. Higher freezing levels are indicative of better memory for the association between the original context and/or cue-shock pairing.

4.2.4 Tissue Preparation & Immunohistochemistry:

Following the conclusion of behavioral testing, rats were overdosed with isoflurane and perfused with ice cold potassium phosphate-buffered saline (KPBS) followed by 4% paraformaldehyde. Brains were removed and stored overnight in 4% PFA before being transferred to 30% sucrose until sectioning. Brains were sectioned at 40 um and stored in cryoprotectant until staining.

All antibody information can be found in **Table 4.1**. Sections from the LC were stained with anti-norepinephrine transporter (NET) and anti-AT8 or dsRED antibodies to confirm viral expression. Sections from the hippocampus were stained for AT8 and 4G8 immunoreactivity to assess AD-related pathology. Both LC and hippocampal sections were stained with anti-ionixed calcium binding adaptor molecule 1 (IBA1) and anti-glial fibrillary acidic protein (GFAP) antibodies to mark microglia and astrocytes, respectively. Hippocampal sections were also stained with anti-NET antibody to assess LC innervation. Briefly, sections were washed 3x5 min in 0.1 M PBS and then incubated for 1 h at room temperature in blocking solution (2% normal goat serum, 1% bovine serum albumin in 0.1% Triton PBS). Sections were then incubated for 24 h at 4 degrees Celsius in blocking solution with a 1:1000 dilution of primary antibody. Sections were subsequently washed 3x5 min in PBS and incubated for 1 h at room temperature in blocking solution with an appropriate secondary antibody (1:500 dilution of goat anti-rabbit 568 for IBA1 and GFAP in the hippocampus, and dsRED, goat anti-rabbit 633 for IBA1 and GFAP in the LC, goat anti-mouse 488 for AT8, 4G8, and NET). Sections were washed 3x5 min in PBS, mounted on SuperFrost+ slides, and coverslipped with DAPI+fluoromount.

4.2.5 Image Analysis:

For each rat, 2-3 brain sections were stained, analyzed, averaged for each animal, and subsequently averaged with animals of the same age, genotype, and virus to obtain group means. All image analysis was performed in ImageJ by blinded experimenters. In hippocampal regions a threshold was applied (Otsu), and a region of interest (ROI) of a standard size across sections (95381 pixels^2) was used to count AT8-, IBA1-, and GFAP-positive cells in CA1, CA3, and the dentate gyrus (DG) using the analyze particles function. Plaques were analyzed as a percent area in a hippocampal subregion following thresholding. NET images were processed and analyzed as previously described (Sathyanesan et al., 2012; Rorabaugh et al., 2017). Briefly, the FeatureJ Hessian plugin was used to process the image, selecting the largest eigenvalue of hessian tensor, absolute eigenvalue comparison, and a smoothing scale of 0.5. An ROI of standard size (2970 pixels^2) was used to assess the mean and standard deviation background fluorescent intensity. Two lines that were perpendicular in orientation and of standard length (208.75 pixels) were used to find peaks using the plot profile and find peaks function, which corresponded to NET fibers. Peaks were defined as fluorescent intensity values greater than the mean plus two standard deviations above background. For the LC, rolling-ball background subtraction was used to mitigate autofluorescence before quantifying IBA1 and GFAP-positive cells as described for the hippocampus. Since the size of the LC varied per section, IBA1 and GFAP-positive cells were normalized and expressed as the number of positive cells for either marker per area.

4.2.6 Statistics and Analysis:

All data are reported as mean ± SEM and were analyzed using a 3-way ANOVA with age, genotype, and virus as factors. When interactions between the main effects were present, post-hoc analyses with Šidák correction were performed between groups differing by a single factor (age, genotype, or virus) with statistical significance set at $\alpha = 0.05$. All statistical information regarding main and interaction effects for behavior and immunohistochemistry are available in

Tables 4.2 and **4.3**, respectively. Meanwhile, significant effects are noted in-text and bolded in Tables. Information for significant post-hoc comparisons, when appropriate, are also noted in-text and appear in **Table 4.4**. Statistical analysis was performed, and data were graphed using Gaphpad Prism. For 23-h locomotion, Morris water maze, and fear conditioning, initial analyses considered interval/time period/training day as a factor. The area under the curve function in GraphPad prism was used to compare across ages with a 3-way ANOVA for novelty-induced, light, and dark phase in the 23-h locomotion paradigm, Morris water maze acquisition and reversal acquisition, and cued and contextual fear condition training and test days.

4.3 RESULTS

4.3.1 Confirmation of viral expression:

We confirmed robust expression of WT hTau and the mCherry control virus in the LC of WT and TgF344-AD rats at 6 and 12 months of age (**Figure 4.1**). Rats that did not show mCherry expression in either hemisphere were categorized as control animals. Rats that demonstrated unilateral expression of WT hTau animals were designated as such, and there were no animals that did not have at least unilateral expression of WT hTau. There was a main effect of genotype of AT8 fluorescence levels, where WT hTau injected TgF344-AD rats had elevated AT8 staining at both ages (**Figure 4.2**). As previously reported (Rorabaugh et al., 2017), the LC of mCherry-infected TgF344-AD rats did not stain positive utilizing the AT8 antibody, but robust AT8 immunoreactivity was observed in both WT and TgF344-AD rats that received the WT hTau virus (**Figure 4.1**).

4.3.2 General Arousal and Locomotion

4.3.2.1 Sleep Latency:

Sleep disturbances are common in AD, and often emerge coincident with tau pathology in the LC (Yesavage et al., 2004; Ju et al., 2013; Ehrenberg et al., 2018; Winsky-Sommerer et al., 2019). We first sought to determine whether age, genotype, virus, or their interactions influenced wakefulness/arousal by measuring latency to fall asleep after gentle handling, and found a main effect of age, where older animals took longer to fall asleep (**Figure 6.3A**). There was also an age x genotype x virus interaction (**Figure 6.3A**); at 12 months, hTau virus appeared to increase sleep latency in WT rats and decrease sleep latency in TgF344-AD rats compared to their mCherry-expressing counterparts, but no post hoc tests were significant.

4.3.2.2 23-h locomotion:

We next used chambers equipped with photobeams to assess overall arousal and locomotor activity patterns over a full day. There was a main effect of time on locomotor activity in both 6- and 12-month rats, indicating that rats had normal circadian rhythms across the light/dark cycle. While there were no main effects of genotype, virus, or an interaction on ambulations in 6-month animals (**Figure 4.3B**), we did detect a main effect of virus and a virus x time interaction on locomotor activity in 12-month animals (**Figure 4.3C**). We next performed an area under the curve analysis to include age as a variable. A main effect of age and an age x virus interaction was apparent for locomotion over the full 23-h period (**Figure 4.3D**). Parsing the data by light/dark phase, there were no main effects during the light period (**Figure 4.3E**), but there was a main effect of age and an age x virus interaction during the dark period (**Figure 4.3F**). While no comparisons survived post-hoc correction, there was a consistent pattern for 12-month mCherry rats of both genotypes to show decreased locomotor activity compared with 6-month animals (**Figure 4.3D**), whereas 12-month hTau rats either maintained or even increased ambulations compared to the younger rats. Finally, we assessed novelty-induced locomotion (**Figure 4.3G**), defined as the number of amublations within the first 30 min following placement

in the chambers, and found a main effect of age and an age x virus interaction. Older rats generally moved less than younger animals, but only WT mCherry injected rats met statistical significance in post-hoc analysis.

4.3.3 Anxiety- and active/passive coping-like behavior

4.3.3.1 Open field:

We investigated anxiety-like behavior, which can be induced by augmenting LC activity (Valentino and Foote, 1988; Curtis et al., 1997; Page and Abercrombie, 1999; Curtis et al., 2012; McCall et al., 2015), using a battery of canonical tests beginning with the open field test. There was a significant main effect of genotype on percent of time spent in the inner 50% of an open field, which was primarily driven by younger TgF344-AD rats (**Figure 4.4A**), indicative of increased anxiety-like behavior (Pentkowski et al., 2021). There was also a significant effect of age on total distance traveled in the open field, where older animals moved less compared with their younger counterparts (**Figure 4.4B**), similar to results we obtained in the locomotor activity experiment (**Figure 4.3**).

4.3.3.2 Elevate plus maze:

We next tested rats on the elevated plus maze. There were no main effects on percent time spent in the open arms (**Figure 4.4C**) or distance traveled (**Figure 4.4D**).

4.3.3.3 Novelty-suppressed feeding:

Novelty-suppressed feeding (NSF) pits a hungry animal's appetitive drive against its fear of exposure in unfamiliar open spaces, and longer latencies to eat are interpreted as increased anxiety-like behavior (Dulawa and Hen, 2005; Lustberg et al., 2020b). Importantly, our lab has recently shown this task to be especially sensitive to dysregulation of LC-NE transmission

(Lustberg et al., 2020b). There were significant main effects of age and genotype, where it took longer for older and TgF344-AD animals to eat the food pellet in a novel cage (**Figure 4.4E**). To control for possible differences in hunger, we recorded the latency to eat a food pellet in the home cage (**Figure 4.4F**) and amount of pellet eaten within 1 h (**Figure 4.4G**). There were no main effects of age, genotype, or virus on either measure. These data are consistent with increased anxiety-like behavior in TgF344-AD rats and in older animals in general.

4.3.3.4 Forced swim test:

The forced swim test is thought to reflect passive (floating) vs active (struggling or swimming) behavior under conditions of inescapable stress (de Kloet and Molendijk, 2016; Commons et al., 2017). There were no main effects on percent of time struggling or swimming in the forced swim test (data not shown). There was a significant effect of age on percent of time spent floating whereby older animals floated less than younger animals (**Figure 4.4H**).

4.3.4 Learning and Memory

4.3.4.1 Morris water maze:

We have previously reported that 6- and 16-month TgF344-AD rats exhibit modest deficits in acquisition of spatial learning in the Morris water maze but have profound impairments in reversal learning (Rorabaugh et al., 2017). We again employed this task to assess hippocampal-dependent learning and memory in WT and TgF344-AD rats with and without hTau expression in the LC. During acquisition, a main effect of day on distance travelled to find the hidden platform was apparent in 6- (**Figure 4.5A**) and 12-month animals (**Figure 4.5B**), indicating that animals of both ages were able to learn the location of the hidden platform with training. 6-month animals also displayed a significant effect of genotype, with impaired learning in TgF344-AD rats (**Figure 4.5A**). For 12-month animals, a main effect of virus indicated that hTau expression was associated

with reduced performance (**Figure 4.5B**). Collapsing across training days and factoring in age revealed no main effects of age, genotype, virus, or interactions on distance travelled (**Figure 4.5C**). For the probe trial, there was a main effect of age, where older animals spent less time in the target quadrant compared with younger animals (**Figure 4.5D**).

For reversal acquisition, main effects of day were again present in both 6- and 12-month animals on distance travelled to find the hidden platform (**Figure 4.5E & F**), with rats improving over training. Consistent with our previous study, reversal learning was impaired in TgF344-AD rats at both 6- (**Figure 4.5E**) and 12-months (**Figure 4.5F**). No differences were observed after collapsing days (**Figure 4.5G**) or during the probe trial (**Figure 4.5H**).

4.3.4.2 Fear conditioning:

To determine whether the impairment in spatial cognition we observed in the TgF344-AD rats in the Morris water maze extended to associative learning and memory, we performed cued and contextual fear conditioning experiments. During shock-tone pairing, a main effect of interval was apparent for both 6- and 12- month rats (**Figure 4.6A & B**), demonstrating that all animals learned to associate the application of a tone with shock. An effect of genotype and a genotype x interval interaction were also apparent in 12-month animals, with TgF344-AD animals freezing less during the tone/shock pairings compared with WT animals. No post-hoc tests were significant, and no differences were apparent when groups were compared across age (**Figure 4.6C**). During subsequent exposure to the shock-paired context in the absence of the tone, there was a main effect of interval in both 6- and 12-month rats (**Figure 4.6D & E**). Likewise, there was a main effect of interval present in 6- and 12-month rats when presented with the shock-paired tone cue in a novel environment (**Figure 4.6G & H**). These results demonstrate maintenance of the association between context/cue and shock regardless of genotype or virus group, and there were no other

main effects on freezing behavior to either the context (**Figure 4.6D & E**) or cue (**Figure 4.6G & H**). Area under the curve analysis indicated a significant effect of age on freezing, where older animals froze less than younger ones under both context (**Figure 4.6F**) and cue (**Figure 4.6I**) conditions.

4.3.5 Hippocampus Pathology:

AD-like neuropathology has previously been reported in the hippocampus of TgF344-AD rats (Cohen et al., 2013; Rorabaugh et al., 2017). To expand on these analyses and determine the effect of hTau expression in the LC, we performed immunohistochemistry for Aβ (4G8), hyperphosphorylated tau (AT8), and neuroinflammation (GFAP and IBA1). Representative images of amyloid pathology in the DG, CA3, and CA1 are shown in **Figure 4.7A** and in Supplemental Fig. 4.1A & B. There were main effects of age, genotype, and an age x genotype interaction on the percentage of plaque-positive area in all three hippocampal subregions (**Figure 4.7B-D**). Post-hoc analyses indicated 12-month TgF344-AD rats had elevated plaque burden when compared with 6-month TgF344-AD rats and age- and virus-matched WT littermates across all hippocampal subregions. There were no effects of hTau expression on plaque pathology across age or genotype.

To assess potential contribution of hTau expression in the LC to hippocampal tau pathology, AT8 was used to visualize hyperphosphorylated tau. Representative images of AT8 pathology in the DG CA3, and CA1 are shown in **Figure 4.8A** and in Supplemental Fig. 4.2A & B. There was a main effect of genotype in the DG, where TgF344-AD rats had higher levels of hyperphosphorylated tau pathology compared with their WT littermates (**Figure 4.8B**), as well as an age x genotype interaction in CA3, where older TgF344-AD rats had elevated AT8 staining compared to their WT littermates (**Figure 4.8C**). However, for CA3, no significant differences were

evident during post-hoc comparisons. In CA1, there was a main effect of age and an age x genotype interaction (**Figure 4.8D**). Post-hoc comparisons revealed increased AT8+ cells in 12-month mCherry injected TgF344-AD animals compared with their 6-month TgF344-AD counterparts. Similar to plaque pathology, there were no effects of hTau expression on AT8 immunoreactivity across age or genotype.

We next assessed neuroinflammatory astrocyte (GFAP) and microglia (IBA1) markers that are noted in AD. Representative images of GFAP staining in the DG, CA3, and CA1 are shown in **Figure 4.9A** and in Supplemental Fig. 4.3A & B. There was a main effect of age, genotype, and an age x genotype interaction on number of GFAP+ cells in the DG (**Figure 4.9B**), CA3 (**Figure 4.9C**), and CA1 (**Figure 4.9D**). Post-hoc analysis of the DG revealed elevated GFAP+ cells in 12-month mCherry and hTau injected TgF344-AD rats compared with their 6-month counterparts. In addition, 12-month mCherry and hTau injected TgF344-AD rats had elevated GFAP+ cells in the DG compared with their WT age-matched littermates. Similarly, 12-month mCherry and hTau injected TgF344-AD rats showed increased GFAP+ cells in CA3 compared with 6-month animals. 12-month mCherry and hTau injected TgF344-AD rats also demonstrated elevated GFAP+ cells in the CA3 compared with WT age-matched littermates. Within CA1, 12-month mCherry injected TgF344-AD rats had more GFAP+ cells compared with 6-month TgF344-AD rats and 12-month WT controls.

Representative images of IBA1 staining in the DG, CA3, and CA1 are shown in **Figure 4.10A** and in Supplemental Fig. 4.4A and B. There was a main effect of genotype in the DG, where transgenic animals had more IBA1+ cells than their WT littermates (**Figure 4.10B**). No main effects of age, genotype, or virus were observed on IBA1+ cells in CA3 (**Figure 4.10C**). There was a main effect of age on IBA1+ cells in CA1 (**Figure 4.10D**).

4.3.6 Hippocampus NE Innervation:

Noradrenergic projections from the LC to the hippocampus, particularly the DG, deteriorate over time in TgF344-AD rats, which contributes to cognitive impairment (Rorabaugh et al., 2017; Goodman et al., 2021). Here, we used NET+ fiber density to assess noradrenergic innervation to the distinct hippocampal subfields. Representative images of NET staining in the DG, CA3, and CA1 are shown in **Figure 6.11A** and in Supplemental Fig. 4.5A & B. There was a significant effect of genotype in the DG (**Figure 6.11B**). In CA3, there was a main effect of age, where older animals generally had lower NET fiber density compared to younger animals (**Figure 6.11C**), while there were no main effects in CA1 (**Figure 6.11D**). These data confirm the loss of LC innervation to the hippocampus in TgF344-AD rats, with the DG exhibiting the highest susceptibility.

4.4 DISCUSSION

The LC is one of the first brain regions that accumulates hyperphosphorylated "pretangle" tau pathology at a time when notable behavioral changes begin to emerge, years or even decades prior to cognitive impairment. In this study, we set out to determine the effects of age, Aβ-triggered endogenous rat tau pathology, and virally-induced WT human tau pathology in the LC on AD-relevant behavioral phenotypes, pathology, and neuroinflammation. We observed significant effects of age and TgF344-AD genotype on behavioral and pathological markers of AD, whereas WT hTau expression in the LC was mostly inert. In general, older rats took longer to fall asleep, had reduced locomotor activity, mixed phenotypes in tests of anxiety-like behavior and passive coping, and impaired learning and memory compared with younger animals. The presence of AD-like neuropathology tended to increase anxiety-like behavior and impair cognitive performance. There are mixed reports on sex differences in behavioral phenotypes in these rats,

and we were underpowered to detect differences based on sex. However, beyond differences in general locomotion, where females appeared to move more than males (see **Figures 4.3G and Figure 4.4B, D**), we did not observe obvious trends in other behavioral measures.

Changes in arousal and sleep disturbances are nearly ubiquitous in AD (Yesavage et al., 2004; Ju et al., 2013; Winsky-Sommerer et al., 2019). A previous study reported that 17-month TgF344-AD rats exhibited atypical EEG sleep/wake features compared to age-matched controls (Kreuzer et al., 2020), but did not include a younger cohort for comparison. We chose to perform the sleep latency test which is an EEG-validated measure of arousal sensitive to noradrenergic manipulation (Hunsley and Palmiter, 2004; Porter-Stransky et al., 2019; Butkovich et al., 2020). We observed a main effect of age (older animals took longer to fall asleep) and a complex interaction between age, genotype, and virus on sleep latency of questionable physiological significance due to its modest influence. We also observed effects of age on 23-h locomotion over the total time of the task, similar to a previous report (Sare et al., 2020), and within the first 30-min. Together, results indicate that 12-month animals took longer to fall asleep but were generally less mobile. Moreover, in 12-month animals specifically, the presence of WT hTau induced an increase in locomotor activity over the entire light/dark cycle, one of the few viral-expression induced phenotypes we identified. This phenotype mimics those reported in mouse models of tauopathy (Scattoni et al., 2010; Jul et al., 2016; Wang et al., 2018b), indicating these effects may be isoform- and/or time-specific or depend on additional influence of forebrain pathology.

Anxiety and depression are highly prevalent in the prodromal phase of disease and increase risk of developing AD (Teri et al., 1999; Pietrzak et al., 2015; Becker et al., 2018; Ehrenberg et al., 2018; Rasmussen et al., 2018). When testing for anxiety-like phenotypes, we observed that 6-month TgF344-AD rats spent less time in the center of an open field compared with littermate controls, while no differences were observed in time spent in the open arms of the

elevated plus maze. It has previously been reported that TgF344-AD rats show increased anxiety-like behaviors at 12, but not 2 months of age in these tasks (Wu et al., 2020). However, these canonical tests of anxiety-like behaviors assume that rodents are motivated to explore novel environments. A lack of anxiety-like phenotypes in these tasks could be masked by differences in exploratory behavior and/or general locomotion, which we and others have observed over the course of aging and in TgF344-AD rats (Sare et al., 2020; Wu et al., 2020). We therefore employed the NSF task, where the main conflict is fear of a novel environment versus drive to consume food in a hungry animal. The NSF task has previously been validated as a NE-sensitive anxiety-like task by our lab using dopamine-β hydroxylase knockout mice, which lack phenotypes in canonical exploration-based anxiety paradigms (Lustberg et al., 2020b). We observed that both older and transgenic rats took longer to eat the food pellet in a novel environment compared with younger and age-matched WT littermates, respectively. These effects are unlikely to be mediated by differences in hunger levels because rats did not differ in the total amount of pellet eaten or latency to eat the pellet in their home cage. Therefore, accumulating evidence from our lab suggests that NSF may be particularly useful at gauging noradrenergic-specific impacts on anxiety-like behaviors.

In the forced swim task, we observed that 12-month rats spent less time spent floating than younger animals. Given the acute nature of this paradigm and the fact that older rats generally moved less in land-based locomotion assays, these results support the notion of an increase in active coping behaviors in older rats (de Kloet and Molendijk, 2016; Commons et al., 2017). A previous report demonstrated an increase in immobility in TgF344-AD rats at 12 months of age (Wu et al., 2020), which is opposite of the effects reported here. Differences may be attributed to multiple exposures to forced swim, influences of sex, or other factors known to

influence coping-like phenotypes in the forced swim task (Bogdanova et al., 2013; Commons et al., 2017).

Spatial learning and memory deficits, which are hallmark behavioral phenotypes of AD, presented here are largely congruent with previous studies of the TgF344-AD strain, where the most robust genotype differences arise in reversal learning (Cohen et al., 2013; Rorabaugh et al., 2017). These differences were primarily observed in acquisition of reversal learning and were exacerbated by age in TgF344-AD rats. Interestingly, we also detected deficits in initial acquisition in 6-month TgF344-AD rats, and hTau virus induced acquisition deficits in 12-month WT rats that were reminiscent of those we observed in 6-month transgenic rats. In both of those cases (6-month Tg rats and 12-month WT rats with hTau), the main detectable AD-like neuropathology present in the brains was hyperphosphorylated tau in the LC, suggesting a causal relationship. We sought to further categorize the nature and anatomical specificity of these deficits by testing these rats on cued and contextual fear conditioning, which are associative learning tasks as opposed to spatial. Additionally, cued fear conditioning is non-hippocampal dependent, unlike both the Morris water maze and contextual fear conditioning. During training, 12-month TgF344-AD rats froze less than WT animals, but genotype differences were not observed during cued or contextual fear conditioning, indicating that recall of these associations once formed was intact. Main effects of age were evident where older animals froze less to both the cue and the context than younger counterparts, suggesting a modest age-related impairment of associative memory.

In this study, we expanded on our previous work demonstrating that TgF344-AD rats have progressive noradrenergic fiber loss (Rorabaugh et al., 2017) by also showing lower NET+ fiber density in TgF344-AD rats, specifically in the dentate gyrus. Recent studies further confirm a reduction in LC innervation to the dentate gyrus (Goodman et al., 2021), suggesting selective vulnerability of NE fibers within this hippocampal subfield. We also reaffirmed an age-dependent

decrease in NE fibers within CA3, 4 months earlier than previously reported (Rorabaugh et al., 2017), in addition to confirming a lack of change in NE innervation to CA1. Given the loss of DBH+ fibers and reduction in NE content in the hippocampus, a loss of NET+ fibers could be indicative of compensatory mechanisms downregulating NE reuptake to increase noradrenergic signaling, in addition to an outright degeneration of forebrain LC fibers. Indeed, other noradrenergic compensatory changes, including enhanced β adrenergic receptor function and axonal sprouting, have been noted in TgF344-AD rats (Goodman et al., 2021) and human AD/dementia cases (Szot et al., 2006, 2007).

We did observe some amyloid deposition beginning at 6 months in TgF344-AD rats across hippocampal subregions, which is slightly earlier than previously reported (Cohen et al., 2013; Sare et al., 2020). By contrast, there were low levels of endogenous hyperphosphorylated tau across all hippocampal subregions and lack of support for transsynaptic spread of hTau from the LC. This was somewhat surprising, given the synergistic effects of amyloid and tau deposition (Busche and Hyman, 2020). We based our viral expression and testing paradigm on previous literature, where pseudophosphorylated tau demonstrated transsynaptic spread and induced cognitive deficits 7 months post-injection in ~10 month old WT rats (Ghosh et al., 2019). The viral form of tau used here (WT hTau) is a milder version from a pathological perspective compared to that reported previously (pseudophosphorylated at 14 sites), and the endogenous LC tau pathology in TgF344-AD rats is an even milder form that only reacts with the CP13 antibody (Ser202) and does not mature into more toxic species observed in the typical progression of AD (Rorabaugh et al., 2017). Although we observed no differences in level of hTau expression within the LC between 6- and 12-month rats, it is possible that longer expression time (e.g. 14 or more months post-infusion) or initial injection of the virus into aged rats is necessary to trigger appreciable effects on behavior and pathology. Indeed, we did observe a potential “seeding”

effect, whereby TgF344-AD rats developed more AT8 pathology in the LC compared to WT littermates.

Behavioral differences between genotypes are likely attributable to development of AD-like neuropathology and inflammation over the course of aging. The effects of tau pathology on neural activity are mixed, as both hyper- and hypo-activity have been reported (Crimins et al., 2012; Holth et al., 2013; Busche et al., 2019; Huijbers et al., 2019). These are also supported by our account of the consequences of hyperphosphorylated tau on LC activity as described in Chapter 2. However, some of these effects likely depend on specific tau species, which have yet to be extensively characterized. Furthermore, the TgF344-AD rats harbor the same mutations as the APP/PS1 mouse counterpart, and APP/PS1 mice develop intraneuronal Aβ oligomers within the LC that are associated with noradrenergic neuron hyperactivity (Kelly et al., 2021). Given that the transgenes are expressed under the same promoter in TgF344-AD rats (Cohen et al., 2013), they also likely develop Aβ oligomers. The additional accumulation of hyperphosphorylated tau within the LC could lead to a complex interaction between the two AD-like pathologies (Busche and Hyman, 2020). Thus, it will be important for future studies to chronicle the time course of AD-like neuropathology accumulation within the LC of TgF344-AD rats.

In Chapter 2, we characterized age-dependent abnormalities in LC firing rates in TgF344-AD rats that were of a similar age to the ones tested here. Young TgF344-AD rats demonstrated LC hyperactivity which transitioned to hypoactivity as the rats aged. Generally, anxiety-like behaviors are promoted by augmented basal LC firing (3-5 Hz) (Valentino and Foote, 1988; Curtis et al., 1997; Page and Abercrombie, 1999; Curtis et al., 2012; McCall et al., 2015). In addition, the LC responds with phasic discharge to novelty (Herve-Minvielle and Sara, 1995; Vankov et al., 1995), and probable/confirmed AD patients show impaired novelty processing and perform worse on tasks incorporating novelty (Daffner et al., 1999; Fritsch et al., 2005; Amanzio et al., 2008).

Similarly, aged TgF344-AD rats also demonstrate reduced ability to distinguish novel objects (Cohen et al., 2013), which may be influenced by novelty-induced anxiety-like phenotypes, as indicated by the NSF task. The blunted phasic response of TgF344-AD LC neurons noted at this age may also contribute to deficits in novel object recognition (Kelberman et al., 2023). Recent evidence also suggests that lower LC response to novelty in cognitively unimpaired individuals is associated with steeper Aβ-related cognitive decline (Prokopiou et al., 2022). The opposite effect is observed in young TgF344-AD rats, which present with enhanced novelty detection that is mediated by β-adrenergic receptors (Goodman et al., 2021) and is in line with the observed heightened spontaneous and evoked phasic LC activity in 6 month TgF344-AD rats (Kelberman et al., 2023). Overall, results from the NSF task are consistent with observed age- and AD-like neuropathology-dependent alterations in LC activity in TgF344-AD rats (Weinshenker, 2018; Kelberman et al., 2023). Furthermore, in young rats, enhanced signal-to-noise ratio (phasic:tonic firing) could support maintenance of novelty detection, but may lead to anxiety-like phenotypes. This effect may be reversed in 12-month rats, where signal-to-noise ratio of the LC is diminished, resulting in reduced novelty detection, and while anxiety-like phenotypes are instead driven by accumulation of pathology in and dysfunction of forebrain regions. This phenotype might be masked in other canonical tasks, such as the open field and elevated plus maze, due to differences in exploratory behavior and general locomotion, which we and others have observed over the course of aging and in TgF344-AD rats (Cohen et al., 2013; Sare et al., 2020). We have previously reported that TgF344-AD rats have impaired reversal learning in the Morris water maze (Rorabaugh et al., 2017), and here demonstrate impairments in training during fear conditioning, but only in 12-month TgF344-AD rats. However, we observed no deficits in probe trials of the Morris water maze or freezing in the contextual and cued fear conditioning paradigms, suggesting intact memory retrieval systems. TgF344-AD rats present with region-specific decreased

noradrenergic forebrain innervation early in disease (Rorabaugh et al., 2017; Goodman et al., 2021). Spatial and associative hippocampal-dependent and independent learning and memory are supported by LC-NE release and are sensitive to noradrenergic perturbations (Hansen and Manahan-Vaughan, 2015; Hagena et al., 2016; Giustino and Maren, 2018; Goodman et al., 2021). The loss of forebrain LC fibers could engage compensatory mechanisms such as increased β-adrenergic receptor function, and increased firing, especially phasic tone, could support the maintenance of certain cognitive functions in prodromal phases of AD. For example, heightened β-adrenergic receptor function facilitates extinction learning and novel object recognition in younger (6-9 month) TgF344-AD rats (Goodman et al., 2021), but these studies should be expanded to additional paradigms.

Independent of genotype effects, we observed aging effects on behavior that are suggestive of altered LC activity. 12-month rats spent less time floating in the forced swim test, indicative of an increase in active coping behaviors in response to stress. Wistar-Kyoto rats, a common rodent model of depression, display increased immobility and enhanced LC activity when tested in the forced swim paradigm (Rittenhouse et al., 2002; Nam and Kerman, 2016). Moreover, coping behaviors mediated by the LC may be partially dependent on galanin co-release (Tillage et al., 2020b), which is expressed in most LC neurons (Holets et al., 1988). Eliminating galanin from the LC promotes active coping behaviors in mice (Tillage et al., 2020b), an effect that is mimicked in older rats tested in the forced swim task. Although we cannot completely rule out frank LC cell loss over the course of aging, 16-month TgF344-AD rats do not exhibit LC degeneration compared with WT littermates (Rorabaugh et al., 2017). Given that galanin co-expressing LC neurons are protected in AD (Miller et al., 1999), we instead theorize that changes in firing rates could reduce galanin co-release and promote active coping behaviors. Although we did not observe changes in sleep latency as would be expected by abnormal tonic and

spontaneous phasic LC firing, other arousal systems that have yet to be explored in these rats could compensate for LC-specific abnormalities. Alternatively, there is evidence for decreased LC activity with aging (Olpe and Steinmann, 1982), but the effects may be strain-dependent as evidenced by our results in Chapter 2. We also stress that other brain regions likely contribute to performance in these tasks and could similarly be impacted by aging.

Our results expand the characterization of behavior and AD-like neuropathology in the TgF344-AD rat that reflect preclinical and prodromal AD. Further studies are necessary to investigate more subtle behavioral phenotypes such as detailed sleep architecture. Impaired impulse control and agitation are also commonly observed in prodromal AD (Ehrenberg et al., 2018; Johansson et al., 2021), and can be improved by anti-adrenergic drugs (Peskind et al., 2005; Wang et al., 2009), which warrants further study in TgF344-AD rats. Age-dependent behavioral impairments in TgF344-AD rats align with known alterations in LC activity and the progression of AD-like neuropathology, beginning with hyperphosphorylated tau in the LC and expanding in later stages to the forebrain. Current AD therapeutics target late-stage pathology, but targeting prodromal stages with drugs that modulate activity or signaling of early affected structures, such as the LC-NE system, may be more effective at slowing the progression of AD. A recent study reported that atomoxetine, a NE reuptake inhibitor, normalized multiple biomarkers of AD in a cohort of patients with mild cognitive impairment (Levey et al., 2021). With the new understanding of changes in LC firing rates (Chapter 2), molecular signatures (Chapter 3), and behavior (Chapter 4) along the progression of AD, the field is now well suited to implement therapeutics targeting the LC-NE system to alleviate disease burden.

Table 4.1. Antibody Information

Primary Antibody	Supplier (Product #)	Dilution	Secondary Antibody	Supplier (Product #)	Dilution
Mouse anti-AT8	ThermoFisher Scientific (MN1020)	1:1000	Goat anti-mouse 488	ThermoFisher Scientific (A-110001)	1:500
Mouse anti-4G8	Biolegend (800709)	1:1000	Goat anti-mouse 488	ThermoFisher Scientific (A-110001)	1:500
Mouse anti-NET	MAB Technologies (NET05-2)	1:1000	Goat anti-mouse 488	ThermoFisher Scientific (A-110001)	1:500
Chicken anti-TH	abcam (ab76442)	1:1000	Goat anti-chicken 633	ThermoFisher Scientific (A-21103)	1:500
Rabbit anti-GFAP	abcam (ab7260)	1:1000	Goat anti-rabbit 568	ThermoFisher Scientific (A-11011)	1:500
Rabbit anti-IBA1	FUJIFILM Wako Pure Chemical Corporation (019-19741)	1:1000	Goat anti-rabbit 568	ThermoFisher Scientific (A-11011)	1:500
Rabbit anti-dsRED	Takara (632496)	1:1000	Goat anti-rabbit 568	ThermoFisher Scientific (A-11011)	1:500

Table 4.2. Behavior Statistics

Behavior	Measure	Interaction	Main Effect	F(DFn, DFd) value	p value
Sleep Latency	Latency to Fall Asleep	Age x Genotype		F (1, 72) = 0.3298	P=0.5676
		Age x Virus		F (1, 72) = 0.2709	P=0.6043
		Genotype x Virus		F (1, 72) = 2.329	P=0.1313
		Age x Genotype x Virus		**F (1, 72) = 4.218**	**P=0.0436**
			Age	**F (1, 72) = 9.284**	**P=0.0032**
			Genotype	F (1, 72) = 0.2349	P=0.6294
			Virus	F (1, 72) = 0.3153	P=0.5762
Locomotion	Ambulations, 6 mo - 23 h	Time interval x Genotype		F (45, 1665) = 0.8895	P=0.6807
		Time interval x Virus		F (45, 1665) = 0.6977	P=0.9363
		Genotype x Virus		F (1, 37) = 0.08733	P=0.7692
		Time interval x Genotype x Virus		F (45, 1665) = 0.6056	P=0.9823
			Time interval	**F (11.84, 437.9) = 31.97**	**P<0.0001**
			Genotype	F (1, 37) = 0.007367	P=0.9321
			Virus	F (1, 37) = 1.019	P=0.3193
	Ambulations, 12 mo - 23 h	Time Interval x Genotype		F (45, 1575) = 1.118	P=0.2750
		Time Interval x Virus		**F (45, 1575) = 1.427**	**P=0.0339**
		Genotype x Virus		F (1, 35) = 0.5669	P=0.4565
		Time Interval x		F (45, 1575) = 0.8914	P=0.6772

	Genotype x Virus			
		Time Interval	**F (10.64, 372.3) = 21.61**	**P<0.0001**
		Genotype	F (1, 35) = 0.3077	P=0.5826
		Virus	**F (1, 35) = 5.880**	**P=0.0206**
Ambulations, 6 and 12 mo - 23 h	Age x Genotype		F (1, 72) = 0.1888	P=0.6652
	Age x Virus		**F (1, 72) = 6.304**	**P=0.0143**
	Genotype x Virus		F (1, 72) = 0.6688	P=0.4162
	Age x Genotype x Virus		F (1, 72) = 0.1316	P=0.7179
		Age	**F (1, 72) = 4.592**	**P=0.0355**
		Genotype	F (1, 72) = 0.1743	P=0.6776
		Virus	F (1, 72) = 1.336	P=0.2516
Ambulations 6 and 12 mo - Light Phase	Age x Genotype		F (1, 72) = 0.2883	P=0.5930
	Age x Virus		F (1, 72) = 0.8304	P=0.3652
	Genotype x Virus		F (1, 72) = 0.3768	P=0.5412
	Age x Genotype x Virus		F (1, 72) = 0.1767	P=0.6755
		Age	F (1, 72) = 0.3634	P=0.5485
		Genotype	F (1, 72) = 0.001673	P=0.9675
		Virus	F (1, 72) = 0.2538	P=0.6160
Ambulations 6 and 12 mo - Dark Phase	Age x Genotype		F (1, 72) = 0.4434	P=0.5076
	Age x Virus		**F (1, 72) = 4.435**	**P=0.0387**
	Genotype x Virus		F (1, 72) = 0.1508	P=0.6989
	Age x Genotype x Virus		F (1, 72) = 0.2927	P=0.5902
		Age	**F (1, 72) = 4.821**	**P=0.0313**
		Genotype	F (1, 72) = 0.7463	P=0.3905

			Virus	F (1, 72) = 0.9755	P=0.3266
	Ambulations 6 and 12 mo - Novelty (30 min)	Age x Genotype		F (1, 72) = 1.781	P=0.1862
		Age x Virus		**F (1, 72) = 3.981**	**P=0.0498**
		Genotype x Virus		F (1, 72) = 0.05367	P=0.8174
		Age x Genotype x Virus		F (1, 72) = 0.7437	P=0.3913
			Age	**F (1, 72) = 31.87**	**P<0.0001**
			Genotype	F (1, 72) = 0.5952	P=0.4429
			Virus	F (1, 72) = 2.433	P=0.1232
Open Field	Percent Time in Inner Circle	Age x Genotype		F (1, 73) = 1.205	P=0.2759
		Age x Virus		F (1, 73) = 3.050	P=0.0849
		Genotype x Virus		F (1, 73) = 0.5330	P=0.4677
		Age x Genotype x Virus		F (1, 73) = 0.2155	P=0.6439
			Age	F (1, 73) = 0.3690	P=0.5454
			Genotype	**F (1, 73) = 4.651**	**P=0.0343**
			Virus	F (1, 73) = 3.414	P=0.0687
	Total Distance	Age x Genotype		F (1, 73) = 0.2590	P=0.6124
		Age x Virus		F (1, 73) = 0.004513	P=0.9466
		Genotype x Virus		F (1, 73) = 0.006385	P=0.9365
		Age x Genotype x Virus		F (1, 73) = 0.05753	P=0.8111
			Age	**F (1, 73) = 14.57**	**P=0.0003**
			Genotype	F (1, 73) = 0.4169	P=0.5205
			Virus	F (1, 73) = 0.1072	P=0.7443
Elevated Plus Maze	Percent Time in Open Arms	Age x Genotype		F (1, 70) = 0.2621	P=0.6103
		Age x Virus		F (1, 70) = 0.8899	P=0.3488

		Genotype x Virus		F (1, 70) = 0.001751	P=0.9667
		Age x Genotype x Virus		F (1, 70) = 1.009	P=0.3186
			Age	F (1, 70) = 2.075	P=0.1542
			Genotype	F (1, 70) = 0.6081	P=0.4381
			Virus	F (1, 70) = 1.009	P=0.3186
	Total Distance	Age x Genotype		F (1, 70) = 1.241	P=0.2691
		Age x Virus		F (1, 70) = 0.02635	P=0.8715
		Genotype x Virus		F (1, 70) = 0.09059	P=0.7643
		Age x Genotype x Virus		F (1, 70) = 0.08218	P=0.7752
			Age	F (1, 70) = 0.08442	P=0.7723
			Genotype	F (1, 70) = 0.6866	P=0.4101
			Virus	F (1, 70) = 0.8085	P=0.3716
Novelty Suppressed Feeding	Latency in a Novel Cage	Age x Genotype		F (1, 73) = 0.1833	P=0.6698
		Age x Virus		F (1, 73) = 0.1495	P=0.7001
		Genotype x Virus		F (1, 73) = 0.04426	P=0.8340
		Age x Genotype x Virus		F (1, 73) = 0.007685	P=0.9304
			Age	**F (1, 73) = 9.691**	**P=0.0026**
			Genotype	**F (1, 73) = 11.12**	**P=0.0013**
			Virus	F (1, 73) = 0.02327	P=0.8792
	Latency in Home Cage	Age x Genotype		F (1, 73) = 1.144	P=0.2883
		Age x Virus		F (1, 73) = 6.831e-006	P=0.9979
		Genotype x Virus		F (1, 73) = 1.782	P=0.1861
		Age x Genotype x Virus		F (1, 73) = 0.09143	P=0.7632

			Age	F (1, 73) = 0.1776	P=0.6747
			Genotype	F (1, 73) = 1.454	P=0.2317
			Virus	F (1, 73) = 0.08312	P=0.7739
	Pellet Weight Eaten	Age x Genotype		F (1, 73) = 1.405	P=0.2397
		Age x Virus		F (1, 73) = 0.8978	P=0.3465
		Genotype x Virus		F (1, 73) = 2.302	P=0.1335
		Age x Genotype x Virus		F (1, 73) = 1.183	P=0.2803
			Age	F (1, 73) = 0.02367	P=0.8781
			Genotype	F (1, 73) = 1.405	P=0.2397
			Virus	F (1, 73) = 0.6447	P=0.4246
Forced Swim Test	Percent Time Spent Floating	Age x Genotype		F (1, 72) = 0.1784	P=0.6740
		Age x Virus		F (1, 72) = 0.004712	P=0.9455
		Genotype x Virus		F (1, 72) = 0.1063	P=0.7453
		Age x Genotype x Virus		F (1, 72) = 0.8174	P=0.3690
			Age	**F (1, 72) = 6.904**	**P=0.0105**
			Genotype	F (1, 72) = 0.01323	P=0.9087
			Virus	F (1, 72) = 0.05062	P=0.8226
Morris Water Maze - Acquisition	Distance to Platform, 6 mo - Training	Day x Genotype		F (3, 111) = 2.289	P=0.0824
		Day x Virus		F (3, 111) = 2.188	P=0.0935
		Genotype x Virus		F (1, 37) = 0.8334	P=0.3672
		Day x Genotype x Virus		F (3, 111) = 2.102	P=0.1040
			Day	**F (2.759, 102.1) = 44.77**	**P<0.0001**
			Genotype	**F (1, 37) = 6.080**	**P=0.0184**
			Virus	F (1, 37) = 0.03508	P=0.8524

	Distance to Platform, 12 mo - Training	Day x Genotype		F (3, 108) = 1.123	P=0.3431
		Day x Virus		F (3, 108) = 0.3593	P=0.7825
		Genotype x Virus		F (1, 36) = 0.06028	P=0.8074
		Day x Genotype x Virus		F (3, 108) = 0.1379	P=0.9372
			Day	**F (2.173, 78.23) = 70.02**	**P<0.0001**
			Genotype	F (1, 36) = 2.709	P=0.1085
			Virus	**F (1, 36) = 5.618**	**P=0.0233**
	Distance to Platform, 6 and 12 mo - Training	Age x Genotype		F (1, 73) = 0.1201	P=0.7299
		Age x Virus		F (1, 73) = 0.3228	P=0.5717
		Genotype x Virus		F (1, 73) = 0.03278	P=0.8568
		Age x Genotype x Virus		F (1, 73) = 0.1442	P=0.7053
			Age	F (1, 73) = 0.05859	P=0.8094
			Genotype	F (1, 73) = 1.556	P=0.2163
			Virus	F (1, 73) = 0.6485	P=0.4233
	Distance to Platform, 6 and 12 mo - Probe	Age x Genotype		F (1, 73) = 0.07450	P=0.7857
		Age x Virus		F (1, 73) = 0.01041	P=0.9190
		Genotype x Virus		F (1, 73) = 1.727	P=0.1930
		Age x Genotype x Virus		F (1, 73) = 0.02698	P=0.8700
			Age	**F (1, 73) = 5.336**	**P=0.0237**
			Genotype	F (1, 73) = 2.193	P=0.1430
			Virus	F (1, 73) = 0.9538	P=0.3320
Morris Water Maze – Reverse Acquisition	Distance to Platform, 6 mo - Training	Day x Genotype		F (3, 111) = 1.592	P=0.1954
		Day x Virus		F (3, 111) = 1.272	P=0.2875

	Genotype x Virus		F (1, 37) = 0.1116	P=0.7402
	Day x Genotype x Virus		F (3, 111) = 1.317	P=0.2724
		Day	**F (1.793, 66.33) = 35.49**	**P<0.0001**
		Genotype	**F (1, 37) = 4.999**	**P=0.0315**
		Virus	F (1, 37) = 0.01777	P=0.8947
Distance to Platform, 12 mo - Training	Day x Genotype		F (3, 108) = 0.5176	P=0.6711
	Day x Virus		F (3, 108) = 1.054	P=0.3720
	Genotype x Virus		F (1, 36) = 0.007100	P=0.9333
	Day x Genotype x Virus		F (3, 108) = 0.4378	P=0.7264
		Day	**F (3, 108) = 22.96**	**P<0.0001**
		Genotype	**F (1, 36) = 9.539**	**P=0.0039**
		Virus	F (1, 36) = 0.09099	P=0.7647
Distance to Platform, 6 and 12 mo - Training	Age x Genotype		F (1, 73) = 0.3419	P=0.5606
	Age x Virus		F (1, 73) = 0.04507	P=0.8325
	Genotype x Virus		F (1, 73) = 0.01787	P=0.8940
	Age x Genotype x Virus		F (1, 73) = 0.002743	P=0.9584
		Age	F (1, 73) = 2.103	P=0.1513
		Genotype	F (1, 73) = 3.363	P=0.0708
		Virus	F (1, 73) = 0.02998	P=0.8630
Distance to Platform, 6 and 12 mo - Probe	Age x Genotype		F (1, 72) = 0.3775	P=0.5409
	Age x Virus		F (1, 72) = 0.03185	P=0.8588
	Genotype x Virus		F (1, 72) = 0.1740	P=0.6778
	Age x Genotype x Virus		F (1, 72) = 0.1609	P=0.6895

			Age	F (1, 72) = 0.09493	P=0.7589
			Genotype	F (1, 72) = 0.3182	P=0.5745
			Virus	F (1, 72) = 0.02243	P=0.8814
Fear Conditioning	Percent Freezing, 6 mo - Training	Interval x Genotype		F (6, 222) = 0.08349	P=0.9978
		Interval x Virus		F (6, 222) = 1.189	P=0.3128
		Genotype x Virus		F (1, 37) = 0.8051	P=0.3754
		Interval x Genotype x Virus		F (6, 222) = 0.2719	P=0.9497
			Interval	**F (3.948, 146.1) = 43.74**	**P<0.0001**
			Genotype	F (1, 37) = 0.0003098	P=0.9861
			Virus	F (1, 37) = 0.08955	P=0.7664
	Percent Freezing, 12 mo - Training	**Interval x Genotype**		**F (6, 216) = 2.203**	**P=0.0438**
		Interval x Virus		F (6, 216) = 0.3948	P=0.8819
		Genotype x Virus		F (1, 36) = 0.1900	P=0.6655
		Interval x Genotype x Virus		F (6, 216) = 0.5728	P=0.7517
			Interval	**F (3.702, 133.3) = 20.58**	**P<0.0001**
			Genotype	**F (1, 36) = 7.184**	**P=0.0110**
			Virus	F (1, 36) = 0.006733	P=0.9351
	Percent Freezing, 6 and 12 mo - Training	Age x Genotype		F (1, 73) = 0.8330	P=0.3644
		Age x Virus		F (1, 73) = 0.03674	P=0.8485
		Genotype x Virus		F (1, 73) = 0.08266	P=0.7745
		Age x Genotype x Virus		F (1, 73) = 0.4622	P=0.4987
			Age	F (1, 73) = 3.268	P=0.0748
			Genotype	F (1, 73) = 0.9175	P=0.3413
			Virus	F (1, 73) = 0.04438	P=0.8337

Percent Freezing, 6 mo - Context	Interval x Genotype		F (6, 222) = 0.9182	P=0.4826
	Interval x Virus		F (6, 222) = 0.3481	P=0.9105
	Genotype x Virus		F (1, 37) = 1.365	P=0.2502
	Interval x Genotype x Virus		F (6, 222) = 0.1483	P=0.9893
		Interval	**F (3.852, 142.5) = 10.78**	**P<0.0001**
		Genotype	F (1, 37) = 3.179	P=0.0828
		Virus	F (1, 37) = 0.4996	P=0.4841
Percent Freezing, 12 mo - Context	Interval x Genotype		F (6, 216) = 0.4350	P=0.8550
	Interval x Virus		F (6, 216) = 0.6593	P=0.6826
	Genotype x Virus		F (1, 36) = 0.01554	P=0.9015
	Interval x Genotype x Virus		F (6, 216) = 0.3688	P=0.8982
		Interval	**F (3.265, 117.6) = 9.797**	**P<0.0001**
		Genotype	F (1, 36) = 0.005031	P=0.9438
		Virus	F (1, 36) = 0.4573	P=0.5032
Percent Freezing, 6 and 12 mo - Context	Age x Genotype		F (1, 73) = 0.8824	P=0.3506
	Age x Virus		F (1, 73) = 0.01794	P=0.8938
	Genotype x Virus		F (1, 73) = 0.2401	P=0.6256
	Age x Genotype x Virus		F (1, 73) = 0.4999	P=0.4818
		Age	**F (1, 73) = 6.434**	**P=0.0133**
		Genotype	F (1, 73) = 0.5668	P=0.4540
		Virus	F (1, 73) = 0.6819	P=0.4116
Percent Freezing, 6 mo - Cue	Interval x Genotype		F (6, 222) = 0.4628	P=0.8354
	Interval x Virus		F (6, 222) = 1.016	P=0.4158

	Genotype x Virus		F (1, 37) = 2.207	P=0.1459
	Interval x Genotype x Virus		F (6, 222) = 1.289	P=0.2632
		Interval	**F (3.489, 129.1) = 100.7**	**P<0.0001**
		Genotype	F (1, 37) = 0.5109	P=0.4792
		Virus	F (1, 37) = 0.09123	P=0.7643
Percent Freezing, 12 mo - Cue	Interval x Genotype		F (6, 216) = 1.914	P=0.0797
	Interval x Virus		F (6, 216) = 1.723	P=0.1168
	Genotype x Virus		F (1, 36) = 0.4232	P=0.5195
	Interval x Genotype x Virus		F (6, 216) = 0.1969	P=0.9774
		Interval	**F (3.348, 120.5) = 49.29**	**P<0.0001**
		Genotype	F (1, 36) = 0.1270	P=0.7237
		Virus	F (1, 36) = 0.7414	P=0.3949
Percent Freezing, 6 and 12 mo - Cue	Age x Genotype		F (1, 73) = 0.3804	P=0.5393
	Age x Virus		F (1, 73) = 0.5732	P=0.4514
	Genotype x Virus		F (1, 73) = 1.120	P=0.2935
	Age x Genotype x Virus		F (1, 73) = 0.1419	P=0.7075
		Age	**F (1, 73) = 4.431**	**P=0.0387**
		Genotype	F (1, 73) = 0.0001671	P=0.9897
		Virus	F (1, 73) = 0.1547	P=0.6952

Table 4.3. Immunohistochemistry Statistics

Stain (Antibody)	Region	Interaction	Main Effect	F(DFn, DFd) value	p value
Hyperphosphorylated Tau (AT8)	LC	Age x Genotype		F (1, 34) = 0.1946	P=0.6619
			Age	F (1, 34) = 0.6288	P=0.4333
			Genotype	**F (1, 34) = 4.857**	**P=0.0344**
Amyloid (4G8)	DG	**Age x Genotype**		**F (1, 38) = 34.32**	**P<0.0001**
		Age x Virus		F (1, 38) = 1.561	P=0.2192
		Genotype x Virus		F (1, 38) = 0.01764	P=0.8950
		Age x Genotype x Virus		F (1, 38) = 1.665	P=0.2048
			Age	**F (1, 38) = 34.36**	**P<0.0001**
			Genotype	**F (1, 38) = 92.88**	**P<0.0001**
			Virus	F (1, 38) = 0.03064	P=0.8620
	CA3	**Age x Genotype**		**F (1, 38) = 69.32**	**P<0.0001**
		Age x Virus		F (1, 38) = 0.2623	P=0.6115
		Genotype x Virus		F (1, 38) = 0.08914	P=0.7669
		Age x Genotype x Virus		F (1, 38) = 0.2377	P=0.6287
			Age	**F (1, 38) = 69.53**	**P<0.0001**
			Genotype	**F (1, 38) = 101.1**	**P<0.0001**
			Virus	F (1, 38) = 0.07557	P=0.7849
	CA1	**Age x Genotype**		**F (1, 38) = 47.14**	**P<0.0001**
		Age x Virus		F (1, 38) = 0.1195	P=0.7315
		Genotype x Virus		F (1, 38) = 0.5785	P=0.4516
		Age x Genotype x Virus		F (1, 38) = 0.1011	P=0.7523
			Age	**F (1, 38) = 46.15**	**P<0.0001**
			Genotype	**F (1, 38) = 73.95**	**P<0.0001**
			Virus	F (1, 38) = 0.6275	P=0.4332
Hyperphosphorylated Tau (AT8)	DG	Age x Genotype		F (1, 33) = 2.311	P=0.1380
		Age x Virus		F (1, 33) = 0.1241	P=0.7269
		Genotype x Virus		F (1, 33) = 0.1311	P=0.7196
		Age x Genotype x Virus		F (1, 33) = 0.3596	P=0.5528
			Age	F (1, 33) = 0.2829	P=0.5983
			Genotype	**F (1, 33) = 4.467**	**P=0.0422**
			Virus	F (1, 33) = 3.391	P=0.0746
	CA3	**Age x Genotype**		**F (1, 38) = 6.305**	**P=0.0164**
		Age x Virus		F (1, 38) = 2.211	P=0.1453
		Genotype x Virus		F (1, 38) = 0.5920	P=0.4464
		Age x Genotype x Virus		F (1, 38) = 0.1392	P=0.7112
			Age	F (1, 38) = 1.593	P=0.2145
			Genotype	F (1, 38) = 2.225	P=0.1441
			Virus	F (1, 38) = 2.137	P=0.1520
	CA1	**Age x Genotype**		**F (1, 38) = 7.596**	**P=0.0089**

		Age x Virus		F (1, 38) = 2.817	P=0.1015
		Genotype x Virus		F (1, 38) = 0.7051	P=0.4063
		Age x Genotype x Virus		F (1, 38) = 0.01587	P=0.9004
			Age	**F (1, 38) = 8.648**	**P=0.0055**
			Genotype	F (1, 38) = 3.273	P=0.0783
			Virus	F (1, 38) = 0.7262	P=0.3995
Astrocytes (GFAP)	DG	**Age x Genotype**		**F (1, 38) = 12.04**	**P=0.0013**
		Age x Virus		F (1, 38) = 0.1457	P=0.7048
		Genotype x Virus		F (1, 38) = 0.4881	P=0.4890
		Age x Genotype x Virus		F (1, 38) = 0.04013	P=0.8423
			Age	**F (1, 38) = 21.56**	**P<0.0001**
			Genotype	**F (1, 38) = 36.66**	**P<0.0001**
			Virus	F (1, 38) = 1.334	P=0.2553
	CA3	**Age x Genotype**		**F (1, 38) = 14.11**	**P=0.0006**
		Age x Virus		F (1, 38) = 0.2107	P=0.6488
		Genotype x Virus		F (1, 38) = 0.3115	P=0.5800
		Age x Genotype x Virus		F (1, 38) = 0.1110	P=0.7408
			Age	**F (1, 38) = 27.91**	**P<0.0001**
			Genotype	**F (1, 38) = 31.43**	**P<0.0001**
			Virus	F (1, 38) = 0.2094	P=0.6499
	CA1	**Age x Genotype**		**F (1, 38) = 4.730**	**P=0.0359**
		Age x Virus		F (1, 38) = 0.5784	P=0.4516
		Genotype x Virus		F (1, 38) = 0.07893	P=0.7803
		Age x Genotype x Virus		F (1, 38) = 3.977	P=0.0533
			Age	**F (1, 38) = 23.76**	**P<0.0001**
			Genotype	**F (1, 38) = 5.528**	**P=0.0240**
			Virus	F (1, 38) = 0.2605	P=0.6127
Microglia (IBA1)	DG	Age x Genotype		F (1, 38) = 0.001233	P=0.9722
		Age x Virus		F (1, 38) = 0.09385	P=0.7610
		Genotype x Virus		F (1, 38) = 1.090	P=0.3030
		Age x Genotype x Virus		F (1, 38) = 0.7188	P=0.4019
			Age	F (1, 38) = 0.9495	P=0.3360
			Genotype	**F (1, 38) = 8.596**	**P=0.0057**
			Virus	F (1, 38) = 0.01557	P=0.9014
	CA3	Age x Genotype		F (1, 39) = 0.8946	P=0.3501
		Age x Virus		F (1, 39) = 0.3941	P=0.5338
		Genotype x Virus		F (1, 39) = 0.2941	P=0.5907
		Age x Genotype x Virus		F (1, 39) = 0.5531	P=0.4615
			Age	F (1, 39) = 3.960	P=0.0536
			Genotype	F (1, 39) = 3.108	P=0.0857
			Virus	F (1, 39) = 3.379	P=0.0736
	CA1	Age x Genotype		F (1, 37) = 0.006922	P=0.9341

		Age x Virus		F (1, 37) = 1.323	P=0.2575
		Genotype x Virus		F (1, 37) = 0.5493	P=0.4633
		Age x Genotype x Virus		F (1, 37) = 0.2734	P=0.6042
			Age	**F (1, 37) = 24.81**	**P<0.0001**
			Genotype	F (1, 37) = 0.7212	P=0.4012
			Virus	F (1, 37) = 0.9558	P=0.3346
Norepinephrine Transporter (NET)	DG	Age x Genotype		F (1, 38) = 0.05830	P=0.8105
		Age x Virus		F (1, 38) = 0.9959	P=0.3246
		Genotype x Virus		F (1, 38) = 1.277	P=0.2655
		Age x Genotype x Virus		F (1, 38) = 1.814	P=0.1860
			Age	F (1, 38) = 0.01035	P=0.9195
			Genotype	**F (1, 38) = 16.36**	**P=0.0002**
			Virus	F (1, 38) = 0.4586	P=0.5024
	CA3	Age x Genotype		F (1, 40) = 0.9422	P=0.3376
		Age x Virus		F (1, 40) = 0.6420	P=0.4277
		Genotype x Virus		F (1, 40) = 2.169	P=0.1487
		Age x Genotype x Virus		F (1, 40) = 0.9345	P=0.3395
			Age	**F (1, 40) = 8.286**	**P=0.0064**
			Genotype	F (1, 40) = 0.4147	P=0.5233
			Virus	F (1, 40) = 2.742	P=0.1056
	CA1	Age x Genotype		F (1, 37) = 1.074	P=0.3068
		Age x Virus		F (1, 37) = 1.183	P=0.2837
		Genotype x Virus		F (1, 37) = 2.548	P=0.1189
		Age x Genotype x Virus		F (1, 37) = 0.4558	P=0.5038
			Age	F (1, 37) = 1.305	P=0.2607
			Genotype	F (1, 37) = 1.846	P=0.1825
			Virus	F (1, 37) = 0.6171	P=0.4371

Table 4.4. Significant Post-Hoc Comparison Statistics

Behavior/Stain (Antibody)	Measure/Brain Region	Comparison	t (df) value	p value	Figure
Locomotion	Amublations - Novelty	6 mo. WT mCherry vs. 12 mo. WT mCherry	t (72) = 4.784	P=0.0001	4.3G
Amyloid (4G8)	DG	6 mo. AD mCherry vs. 12 mo. AD mCherry	t (38) = 4.719	P = 0.0004	4.7B
		6 mo. AD hTau vs. 12 mo. AD hTau	t (38) = 7.228	P < 0.0001	4.7B
		12 mo. WT mCherry vs. 12 mo. AD mCherry	t (38) = 7.371	P < 0.0001	4.7B
		12 mo. WT hTau vs. 12 mo. AD hTau	t (38) = 8.441	P < 0.0001	4.7B
	CA3	6 mo. AD mCherry vs. 12 mo. AD mCherry	t (38) = 8.053	P < 0.0001	4.7C
		6 mo. AD hTau vs. 12 mo. AD hTau	t (38) = 8.954	P < 0.0001	4.7C
		12 mo. WT mCherry vs. 12 mo. AD mCherry	t (38) = 9.054	P < 0.0001	4.7C
		12 mo. WT hTau vs. 12 mo. AD hTau	t (38) = 9.716	P < 0.0001	4.7C
	CA1	6 mo. AD mCherry vs. 12 mo. AD mCherry	t (38) = 6.681	P < 0.0001	4.7D
		6 mo. AD hTau vs. 12 mo. AD hTau	t (38) = 7.260	P < 0.0001	4.7D
		12 mo. WT mCherry vs. 12 mo. AD mCherry	t (38) = 8.178	P < 0.0001	4.7D
		12 mo. WT hTau vs. 12 mo. AD hTau	t (38) = 7.615	P < 0.0001	4.7D
Hyperphosphorylated Tau (AT8)	CA1	6 mo. AD mCherry vs. 12 mo. AD mCherry	t (38) = 3.689	P=0.0084	4.8D
Astrocytes (GFAP)	DG	6 mo. AD mCherry vs. 12 mo. AD mCherry	t (38) = 4.077	P=0.0027	4.9B
		6 mo. AD hTau vs. 12 mo. AD hTau	t (38) = 4.204	P=0.0018	4.9B
		12 mo. WT mCherry vs. 12 mo. AD mCherry	t (38) = 4.640	P=0.0005	4.9B
		12 mo. WT hTau vs. 12 mo. AD hTau	t (38) = 5.080	P=0.0001	4.9B
	CA3	6 mo. AD mCherry vs. 12 mo. AD mCherry	t (38) = 5.040	P=0.0001	4.9C
		6 mo. AD hTau vs. 12 mo. AD hTau	t (38) = 4.180	P=0.002	4.9C
		12 mo. WT mCherry vs. 12 mo. AD mCherry	t (38) = 5.271	P<0.0001	4.9C
		12 mo. WT hTau vs. 12 mo. AD hTau	t (38) = 4.294	P=0.0014	4.9C
	CA1	6 mo. AD mCherry vs. 12 mo. AD mCherry	t (38) = 5.040	P=0.0001	4.9D
		12 mo. WT mCherry vs. 12 mo. AD mCherry	t (38) = 3.208	P=0.0321	4.9D

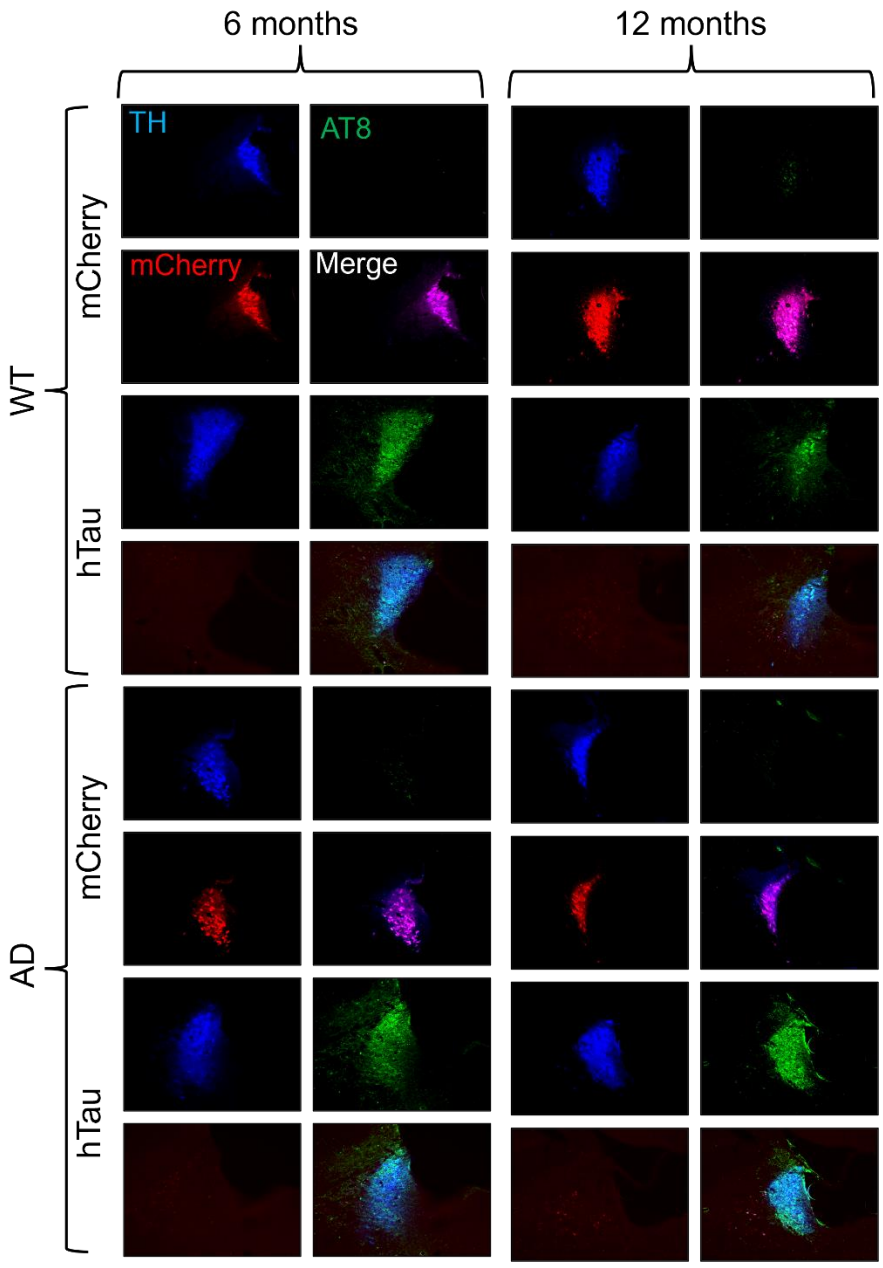

Figure 4.1. Verification of viral-mediated hTau and mCherry expression in the rat LC. Wild-type (WT) and TgF344-AD (AD) rats were injected bilaterally into the LC with AAV-PRSx8-hTau (hTau) or AAV-PRSx8-mCherry (mCherry) at 2 months of age and assessed for hTau and mCherry expression by immunohistochemistry at 6 months or 12 months. Shown are representative 10x immunofluorescent images for the LC marker tyrosine hydroxylase (TH; blue), the hyperphosphorylated tau marker AT8 (green), mCherry (red), and merged signals.

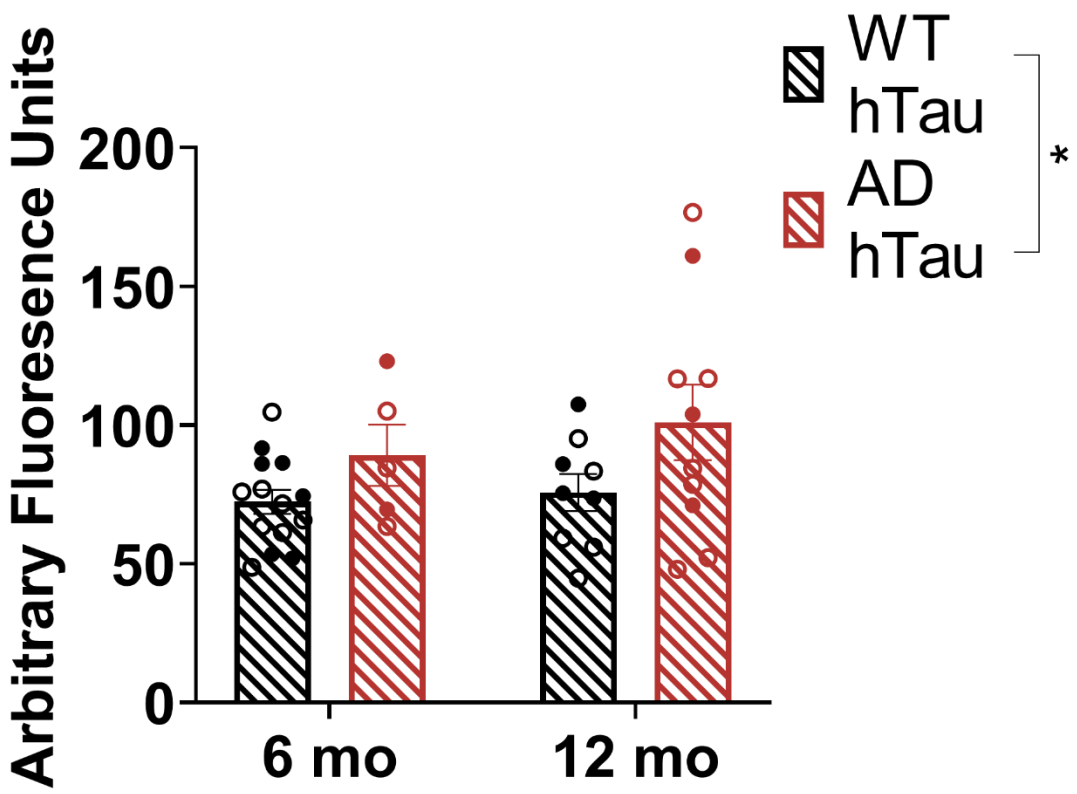

Figure 4.2. Quantification of AT8 pathology in the LC of WT and TgF344-AD littermates. Wild-type (WT, black) and TgF344-AD (AD, red) rats were injected bilaterally into the LC with AAV-PRSx8-hTau (hTau, hashed) at 2 months of age, and AT8 pathology was quantified at 6 months and 12 months. *$p<0.05$. Males are represented by closed circles, females by open circles.

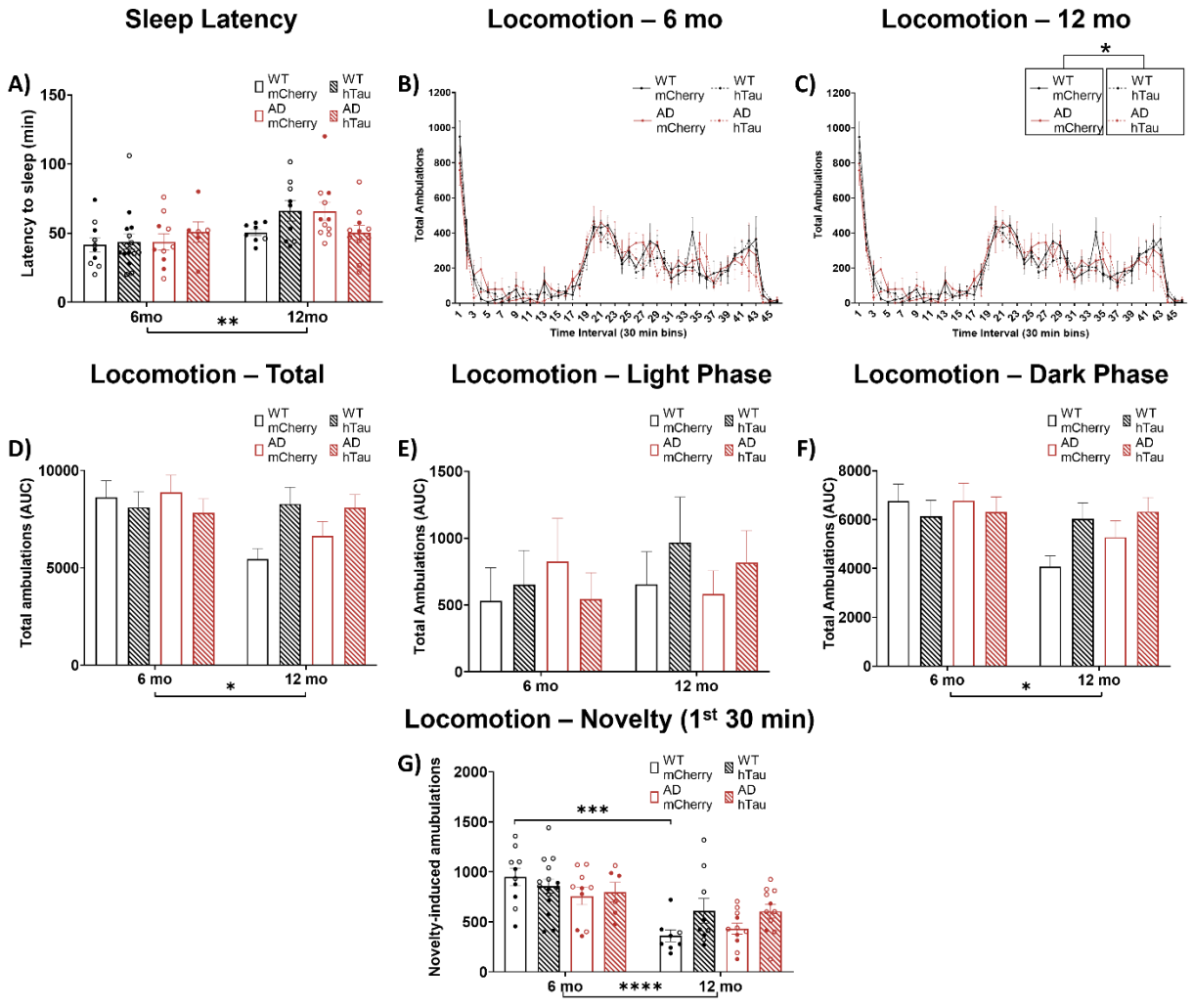

Figure 4.3. Assessment of arousal and locomotor activity. Wild-type (WT, black) and TgF344-AD (AD, red) rats were injected bilaterally into the LC with AAV-PRSx8-hTau (hTau, hashed) or AAV-PRSx8-mCherry (mCherry, solid) at 2 months of age, and assessed for sleep latency and locomotor activity at 6 months or 12 months. Shown are latency to fall asleep after gentle handling (A), time course of 23-h locomotor activity in 6 (B) and 12 (C) month rats, total ambulations (D), light phase ambulation (E), dark phase ambulation (F), and novelty-induced locomotion during the first 30 min of the test (G). *p<0.05, **p<0.01, ***p<0.001, ****p<0.0001. Males are represented by closed circles, females by open circles.

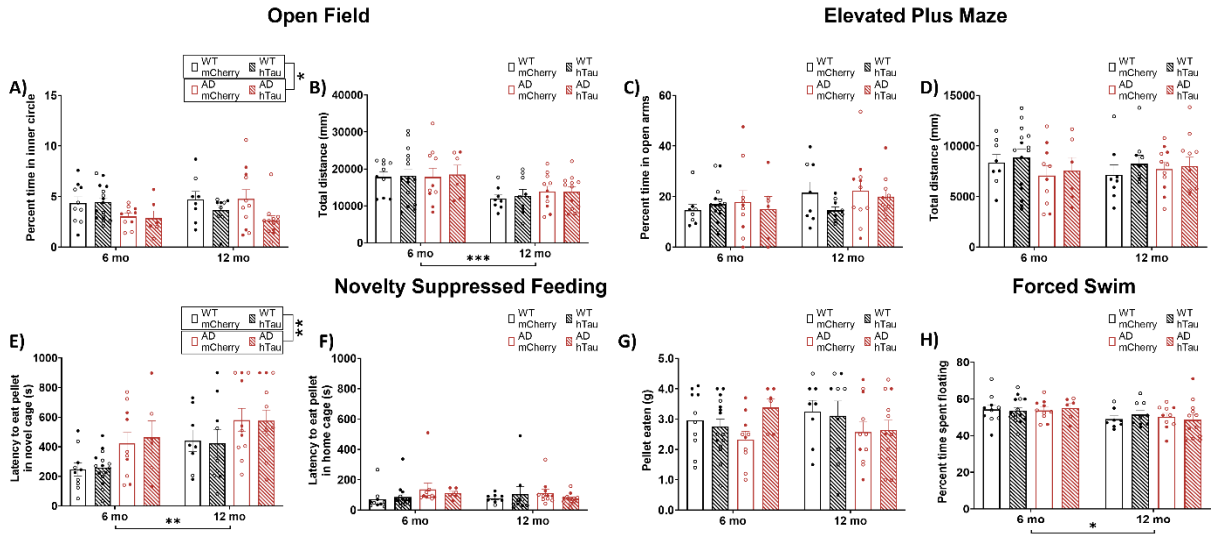

Figure 4.4. Assessment of anxiety-like behaviors and coping strategies. Wild-type (WT, black) and TgF344-AD (AD, red) rats were injected bilaterally into the LC with AAV-PRSx8-hTau (hTau, hashed bars) or AAV-PRSx8-mCherry (mCherry, solid) at 2 months of age, and assessed for open field, elevated plus maze, novelty-suppressed feeding, and forced swim at 6 months or 12 months. Shown is percent time in the inner portion (A) and total distance travelled (B) in the open field test, percent time in the open arms (C) and total distance travelled (D) in the elevated plus maze, latency to eat in a novel (E) or home/familiar (F) cage and amount of food consumed (G) in the novelty-suppressed feeding test, and time spent floating (H) in the forced swim test. *p<0.05, **p<0.01, ***p<0.001. Males are represented by closed circles, females by open circles.

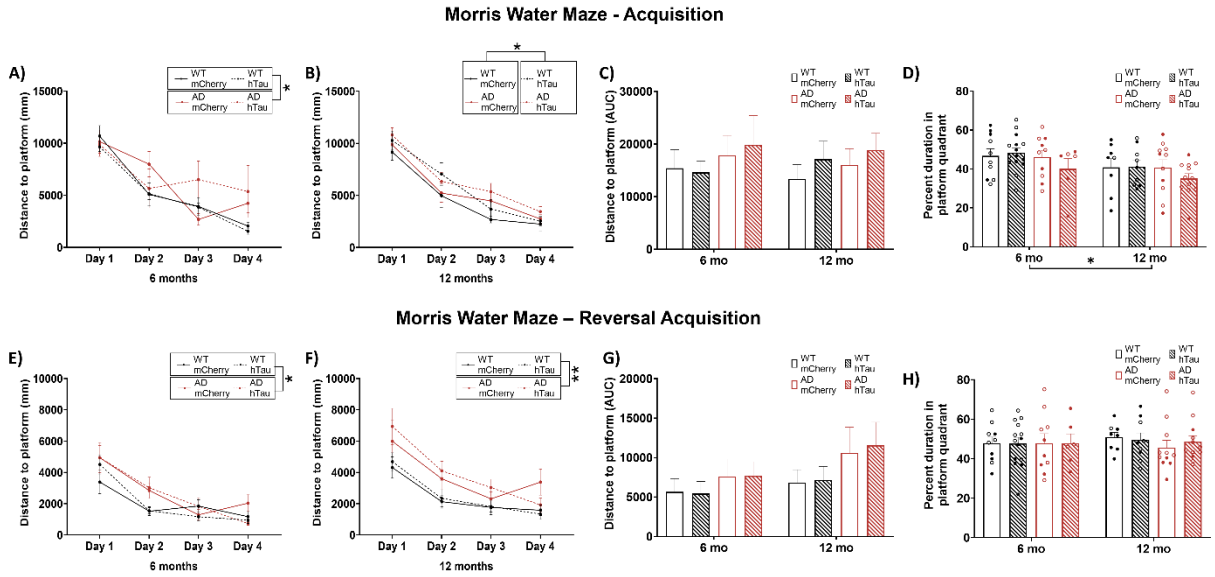

Figure 4.5. Assessment of hippocampal-dependent spatial learning and memory in the Morris water maze. Wild-type (WT, black) and TgF344-AD (AD, red) rats were injected bilaterally into the LC with AAV-PRSx8-hTau (hTau, hashed) or AAV-PRSx8-mCherry (mCherry, solid) at 2 months of age, and assessed for performance in the Morris water maze at 6 months or 12 months. Shown are total distance to find the hidden platform by day at 6 months (A) and 12 months (B), total area under the curve distance collapsed across days at both ages (C), percent time spent in target quadrant during the probe trial (D), total distance during reversal learning at 6 months (E) and 12 months (F), total area under the curve distance during reversal learning collapsed across days at both ages (G), and percent time spent in target quadrant during the probe trial after reversal learning (H). *p<0.05, **p<0.01. Males are represented by closed circles, females by open circles.

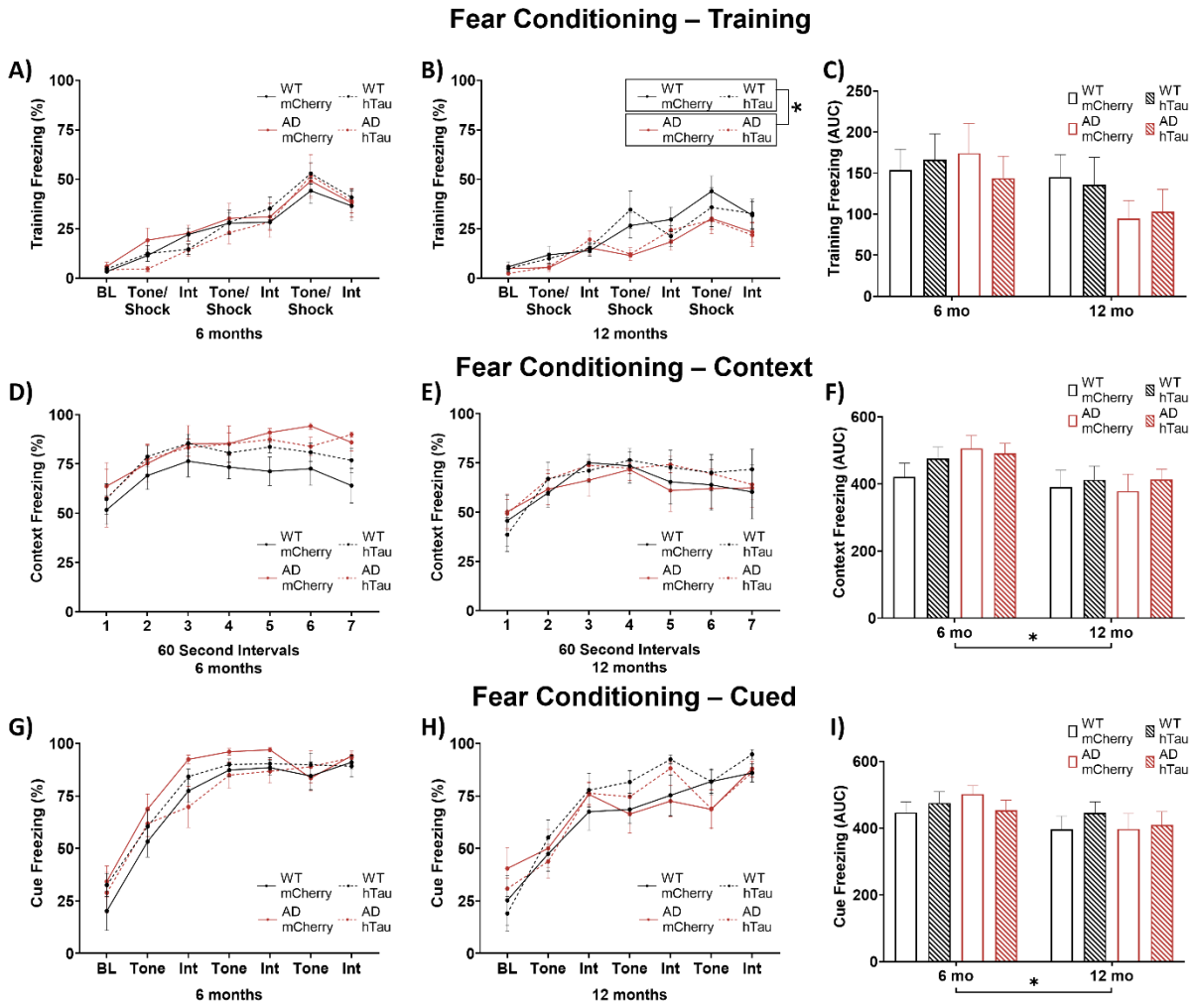

Figure 4.6. Assessment of contextual and cued fear conditioning. Wild-type (WT, black) and TgF344-AD (AD, red) rats were injected bilaterally into the LC with AAV-PRSx8-hTau (hTau, hashed) or AAV-PRSx8-mCherry (mCherry, solid) at 2 months of age, and assessed for contextual and cued fear conditioning at 6 months or 12 months. Shown is % freezing during shock-tone pairing in 6-month (A) and 12-month (B) rats, area under the curve collapsed across both ages (C), during subsequent context exposure in 6-month (D) and 12-month (E) rats, area under the curve collapsed across both ages (F), during subsequent cue exposure in 6-month (G) and 12-month (H) rats, and area under the curve collapsed across both ages (I). *p<0.05.

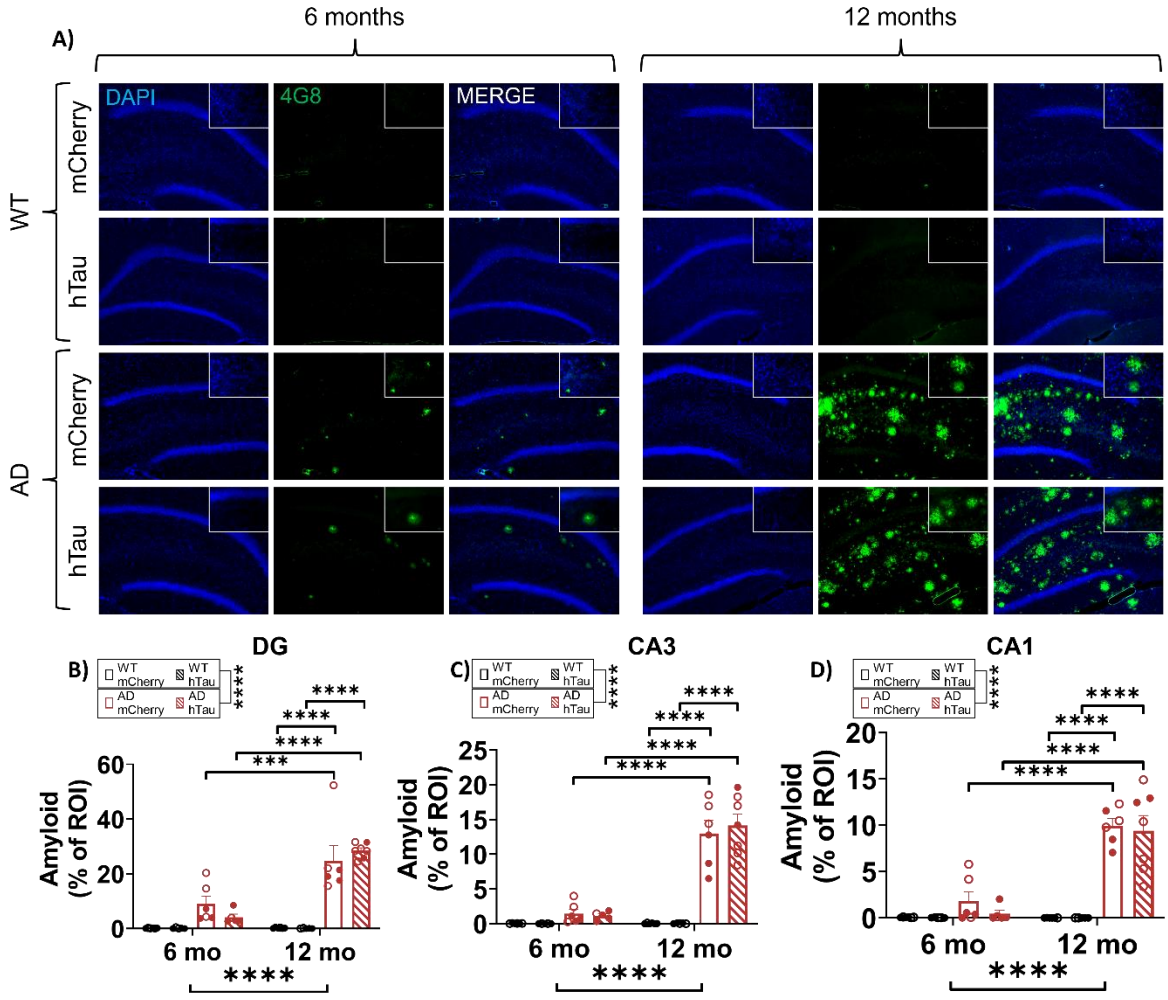

Figure 4.7. Assessment of amyloid pathology in the hippocampus. Wild-type (WT, black) and TgF344-AD (AD, red) rats were injected bilaterally into the LC with AAV-PRSx8-hTau (hTau, hashed) or AAV-PRSx8-mCherry (mCherry, solid) at 2 months of age, and assessed for 4G8 (i.e., Aβ) immunoreactivity at 6 months or 12 months. Shown are representative images of amyloid pathology in the DG subregion of the hippocampus (A), and quantification of amyloid pathology in the DG (B), CA3 (C), and CA1 (D) expressed as % region of interest (ROI). Main images and insets taken at 10x and 40x magnification, respectively. ***p<0.001, ****p<0.0001. Males are represented by closed circles, females by open circles.

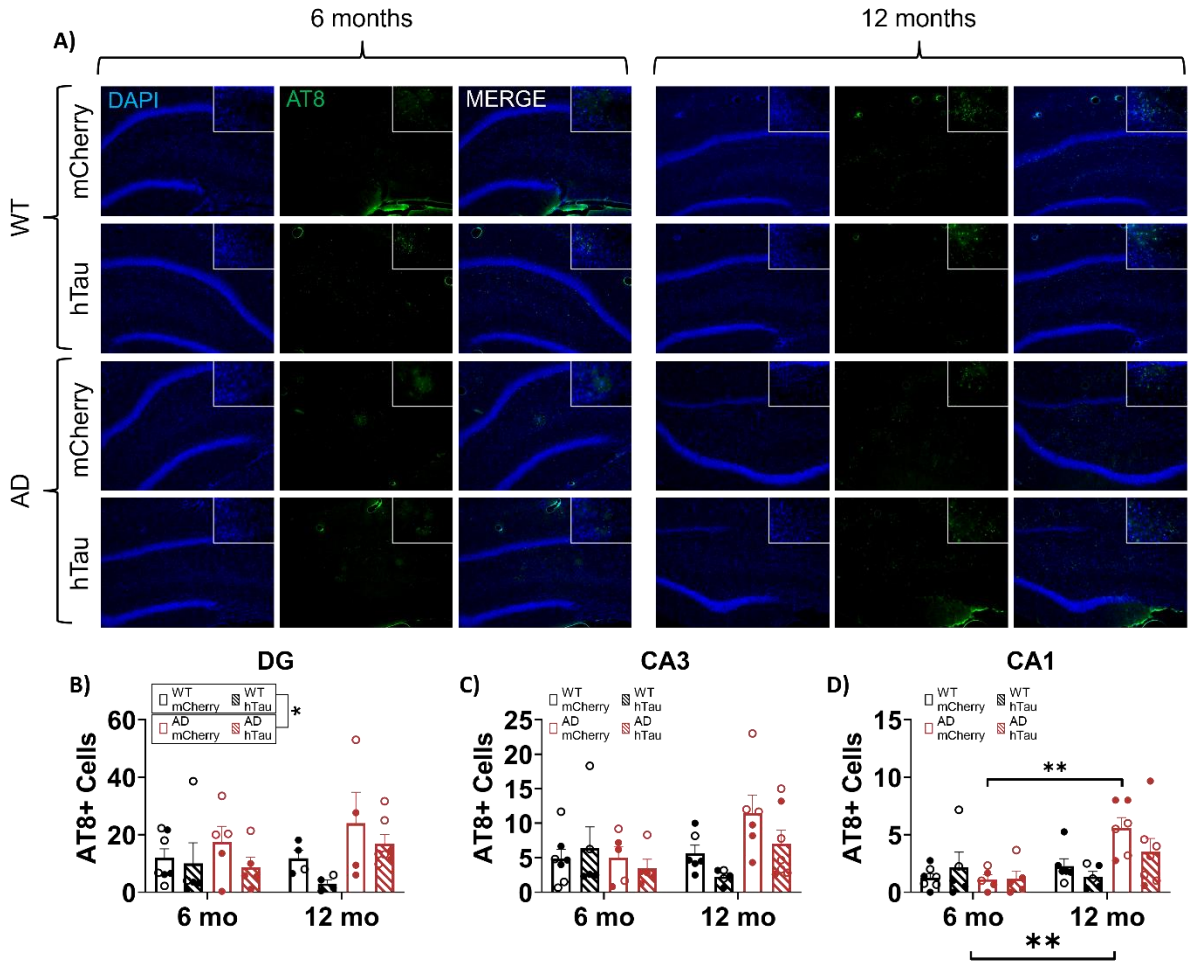

Figure 4.8. Assessment of hyperphosphorylated tau in the hippocampus. Wild-type (WT, black) and TgF344-AD (AD, red) rats were injected bilaterally into the LC with AAV-PRSx8-hTau (hTau, hashed) or AAV-PRSx8-mCherry (mCherry, solid) at 2 months of age, and assessed for AT8 (i.e., hTau) immunoreactivity at 6 months or 12 months. Shown are representative images of hyperphosphorylated tau pathology in the DG subregion of the hippocampus (A), and quantification of hyperphosphorylated tau pathology in the DG (B), CA3 (C), and CA1 (D) expressed as the number of AT8+ cells. Main images and insets taken at 10x and 40x magnification, respectively. *p<0.05, **p<0.01. Males are represented by closed circles, females by open circles.

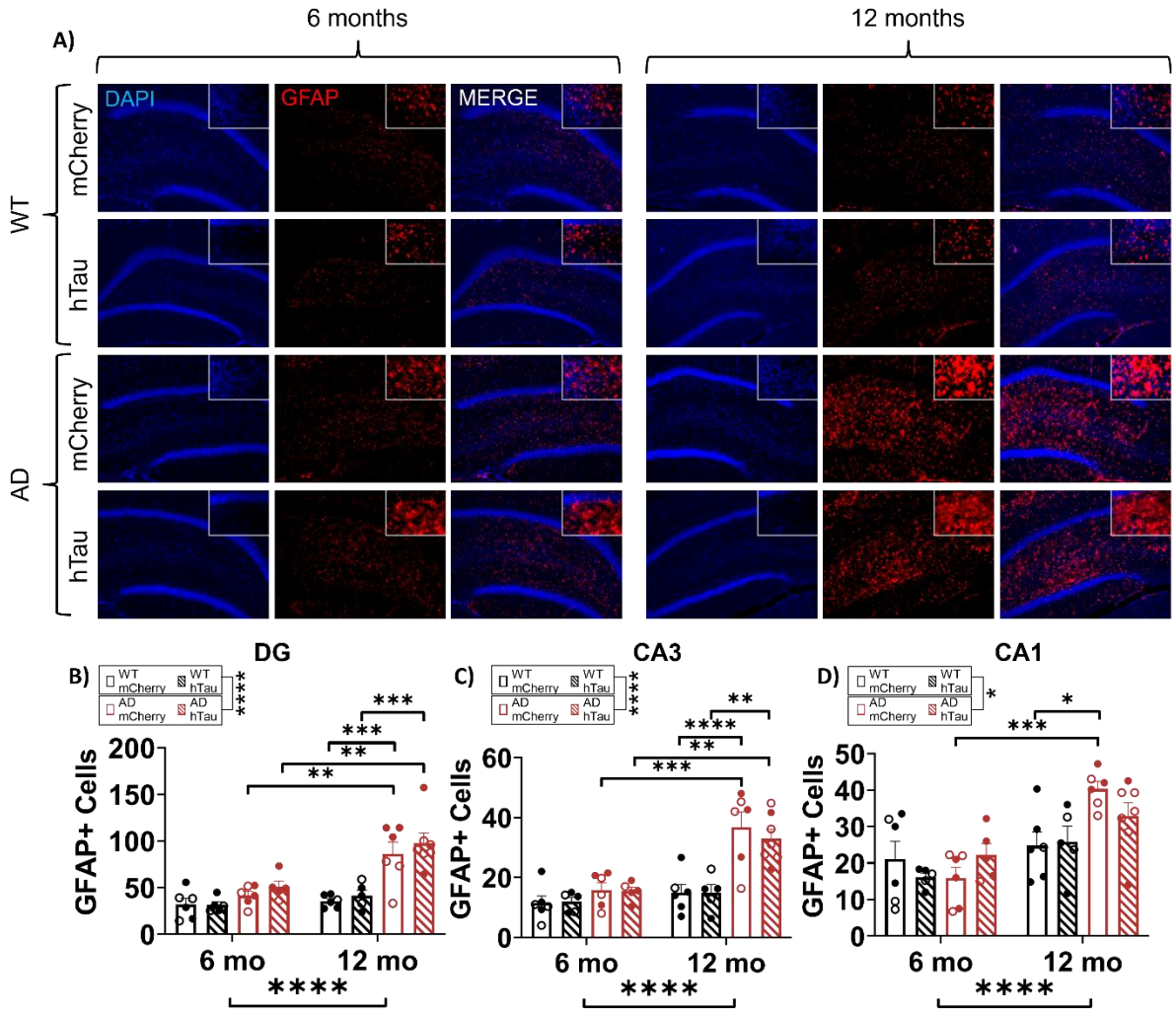

Figure 4.9. Assessment of astrocyte inflammation in the hippocampus. Wild-type (WT, black) and TgF344-AD (AD, red) rats were injected bilaterally into the LC with AAV-PRSx8-hTau (hTau, hashed) or AAV-PRSx8-mCherry (mCherry, solid) at 2 months of age, and assessed for GFAP immunoreactivity at 6 months or 12 months. Shown are representative images of astrocyte inflammation in the DG subregion of the hippocampus (A), and quantification of astrocyte inflammation in the DG (B), CA3 (C), and CA1 (D) expressed as the number of GFAP+ cells. Main images and insets taken at 10x and 40x magnification, respectively. *p<0.05, **p<0.01, ***p<0.001, ****p<0.0001. Males are represented by closed circles, females by closed circles.

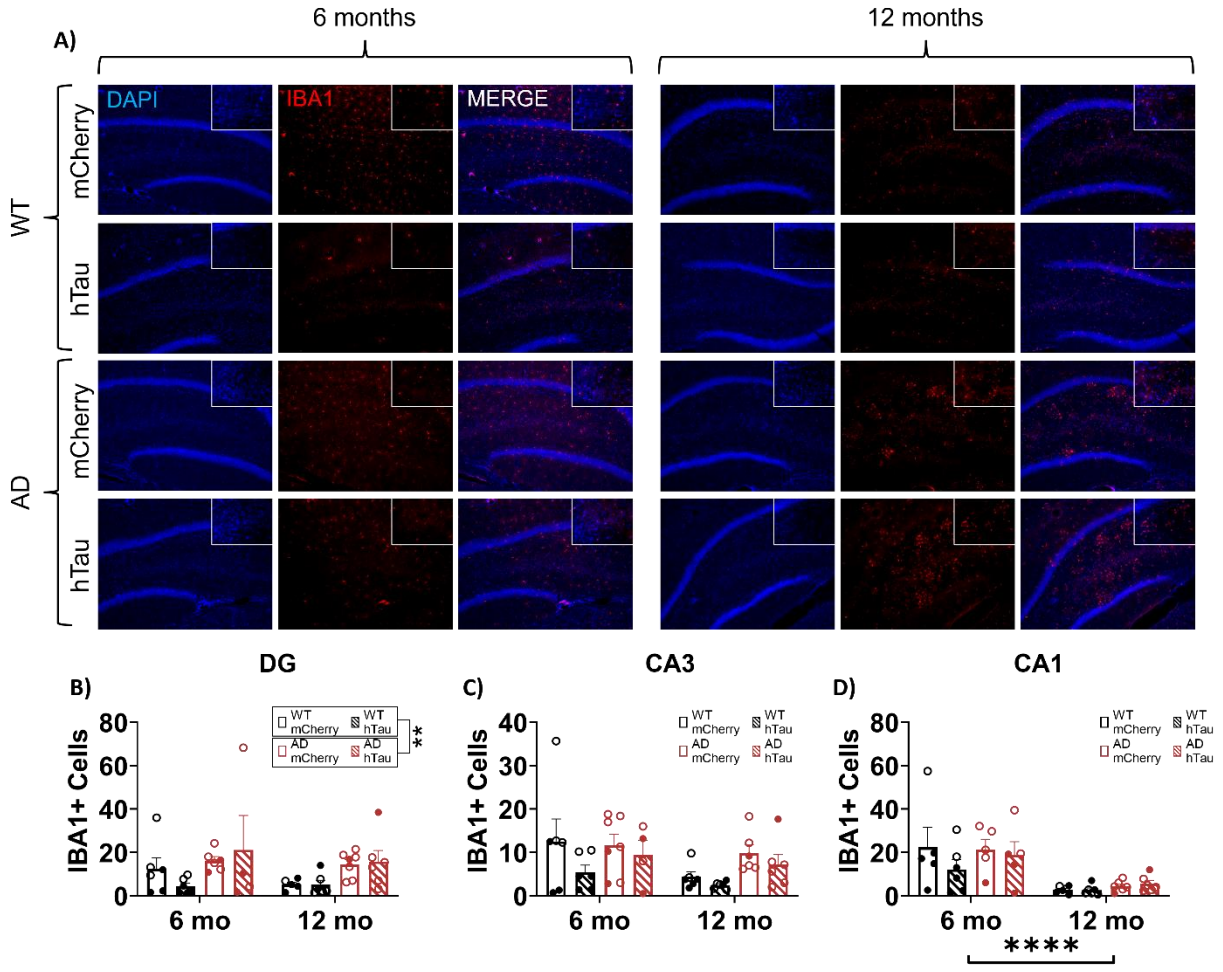

Figure 4.10. Assessment of microglial inflammation in the hippocampus. Wild-type (WT, black) and TgF344-AD (AD, red) rats were injected bilaterally into the LC with AAV-PRSx8-hTau (hTau, hashed) or AAV-PRSx8-mCherry (mCherry, solid) at 2 months of age, and assessed for IBA1 immunoreactivity at 6 months or 12 months. Shown are representative images of microglial inflammation in the DG subregion of the hippocampus (A), and quantification of astrocyte inflammation in the DG (B), CA3 (C), and CA1 (D) expressed as the number of IBA1+ cells. Main images and insets taken at 10x and 40x magnification, respectively. Males are represented by closed circles, females by open circles.

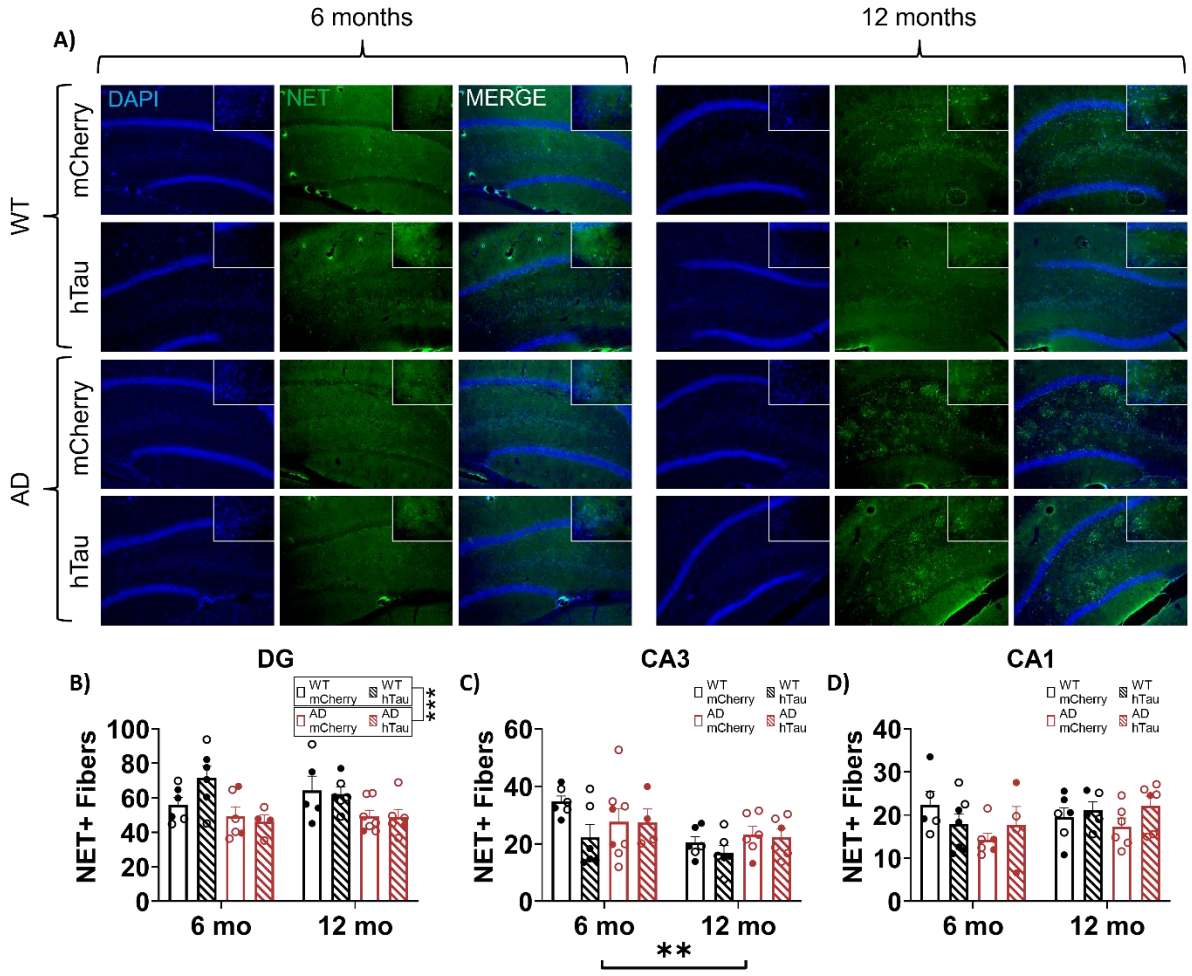

Figure 4.11. Assessment of LC fiber density in the hippocampus. Wild-type (WT, black) and TgF344-AD (AD, red) rats were injected bilaterally into the LC with AAV-PRSx8-hTau (hTau, hashed) or AAV-PRSx8-mCherry (mCherry, solid) at 2 months of age, and assessed for NET immunoreactivity at 6 months or 12 months. Shown are representative images in the DG subregion of the hippocampus (A), and quantification in the DG (B), CA3 (C), and CA1 (D) expressed as the number of NET+ fibers. (D). Main images and insets taken at 10x and 40x magnification, respectively. **p<0.01, ***p<0.001. Males are represented by closed circles, females by open circles.

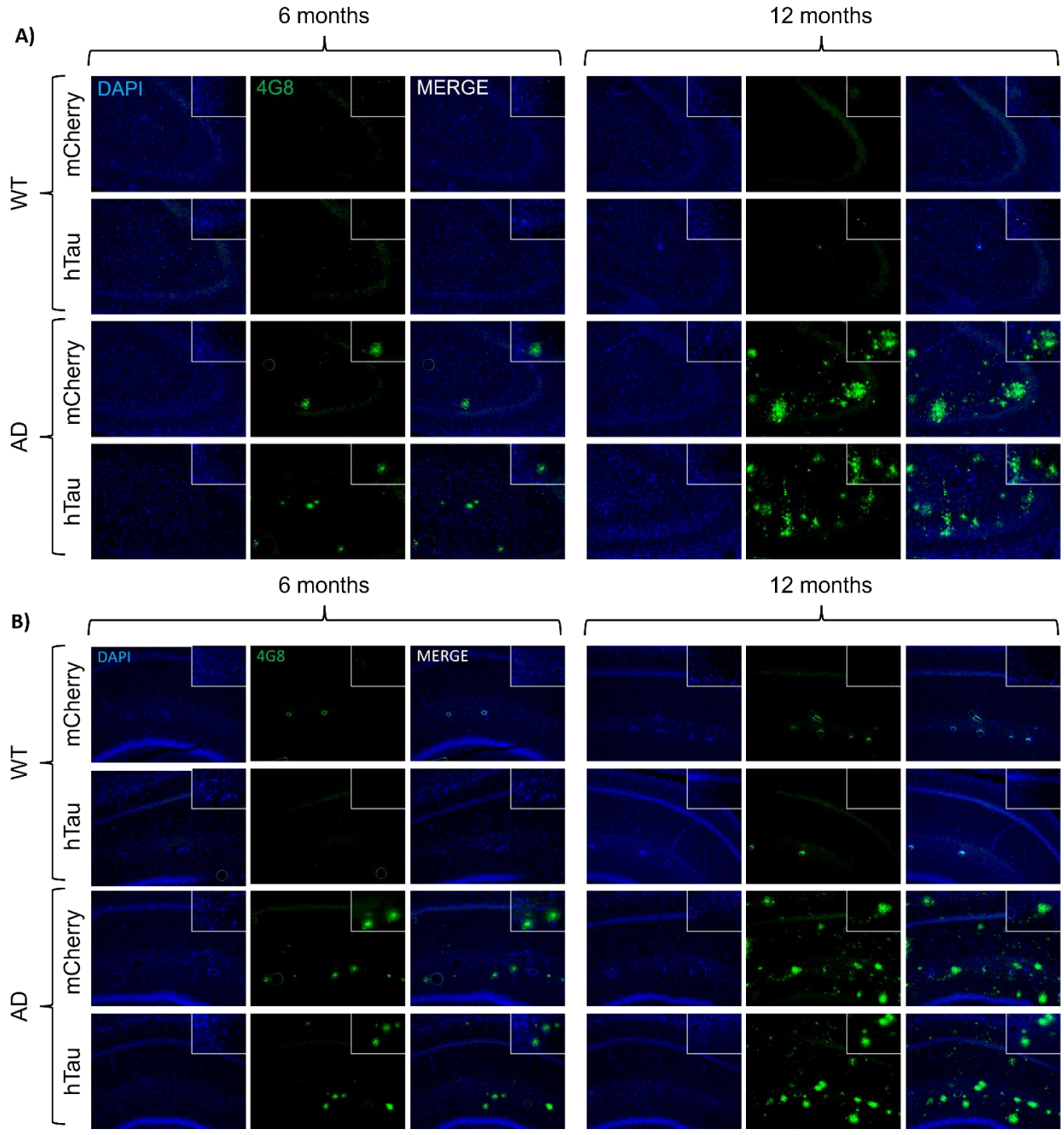

Supplemental Figure 4.1. Representative images of amyloid pathology in the CA3 (A) and CA1 (B) subregions of the hippocampus. Main images and insets taken at 10x and 40x magnification, respectively.

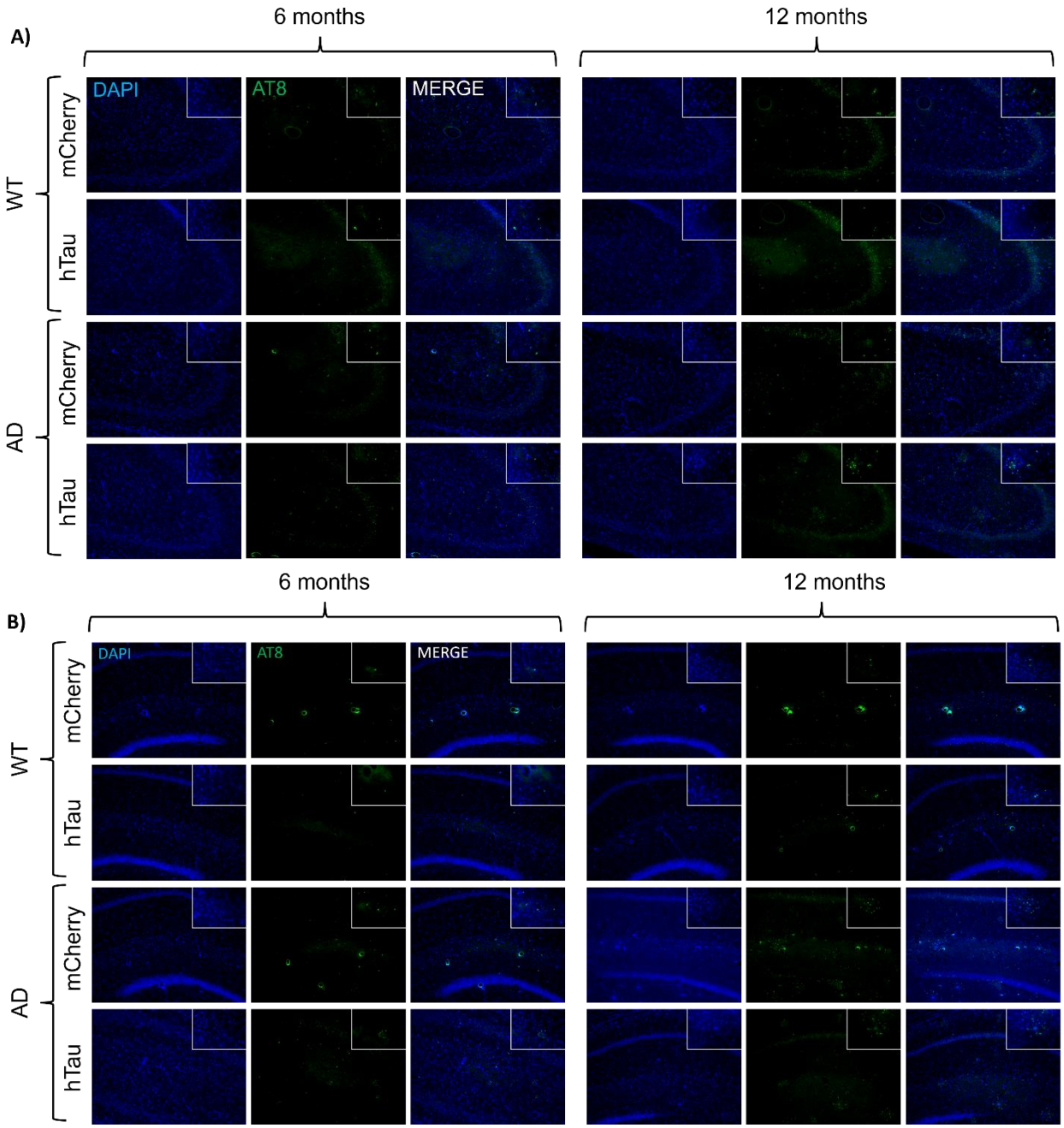

Supplemental Figure 4.2. Representative images of tau pathology (AT8) in the CA3 (A) and CA1 (B) subregions of the hippocampus. Main images and insets taken at 10x and 40x magnification, respectively.

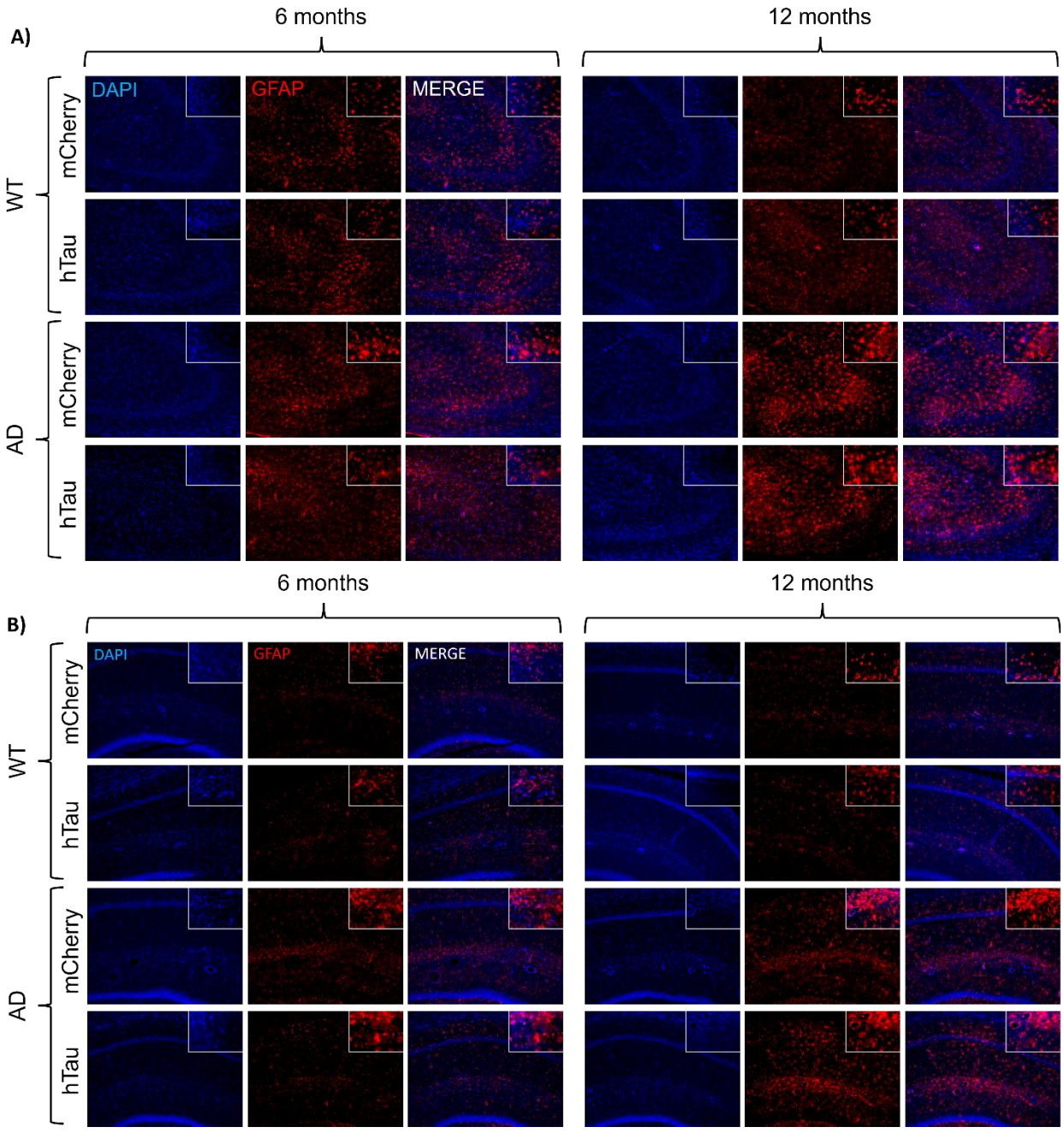

Supplemental Figure 4.3. Representative images of neuroinflammatory astrocytic marker GFAP in the CA3 (A) and CA1 (B) subregions of the hippocampus. Main images and insets taken at 10x and 40x magnification, respectively.

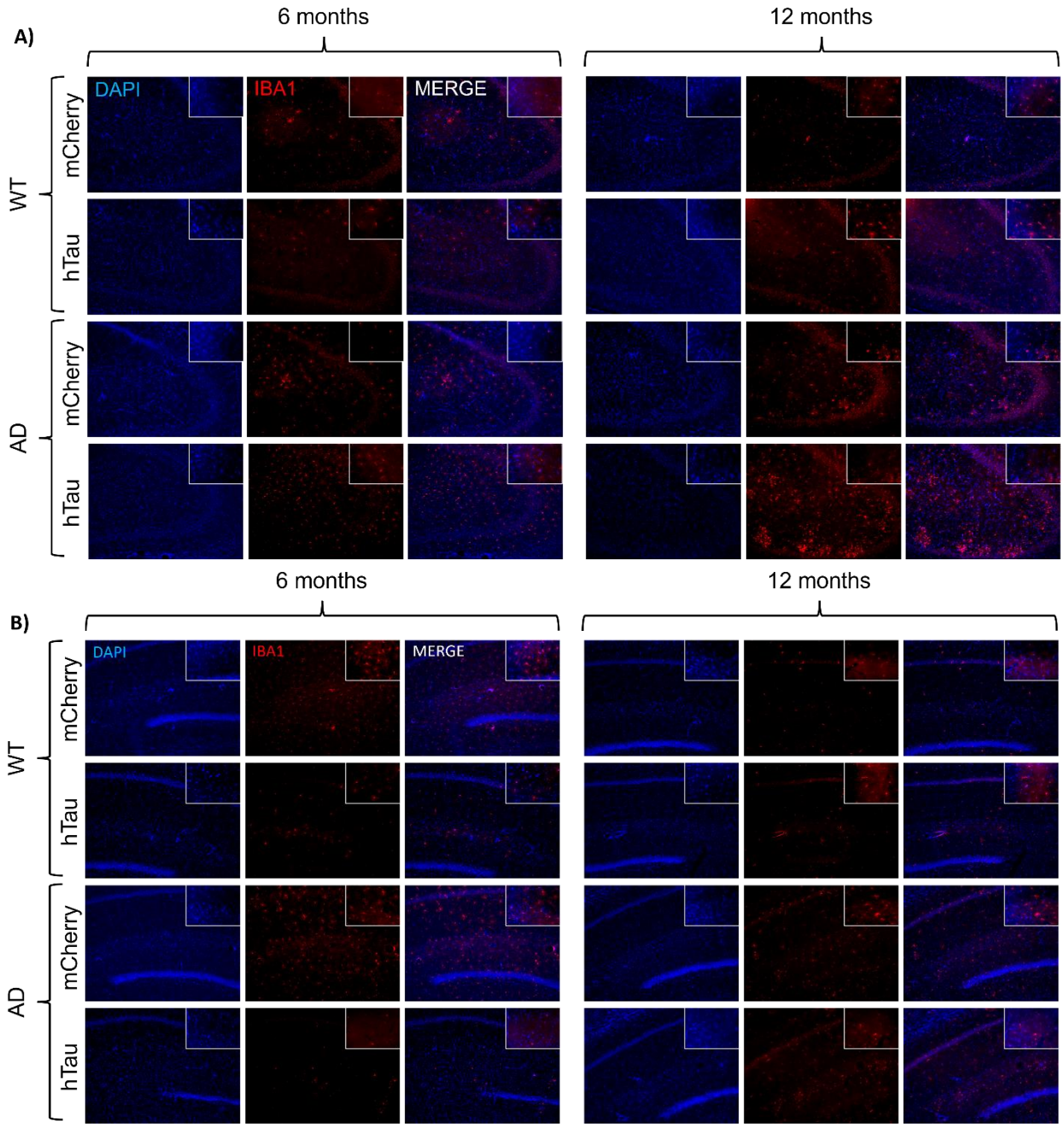

Supplemental Figure 4.4. Representative images of neuroinflammatory microglial marker IBA1 in the CA3 (A) and CA1 (B) subregions of the hippocampus. Main images and insets taken at 10x and 40x magnification, respectively.

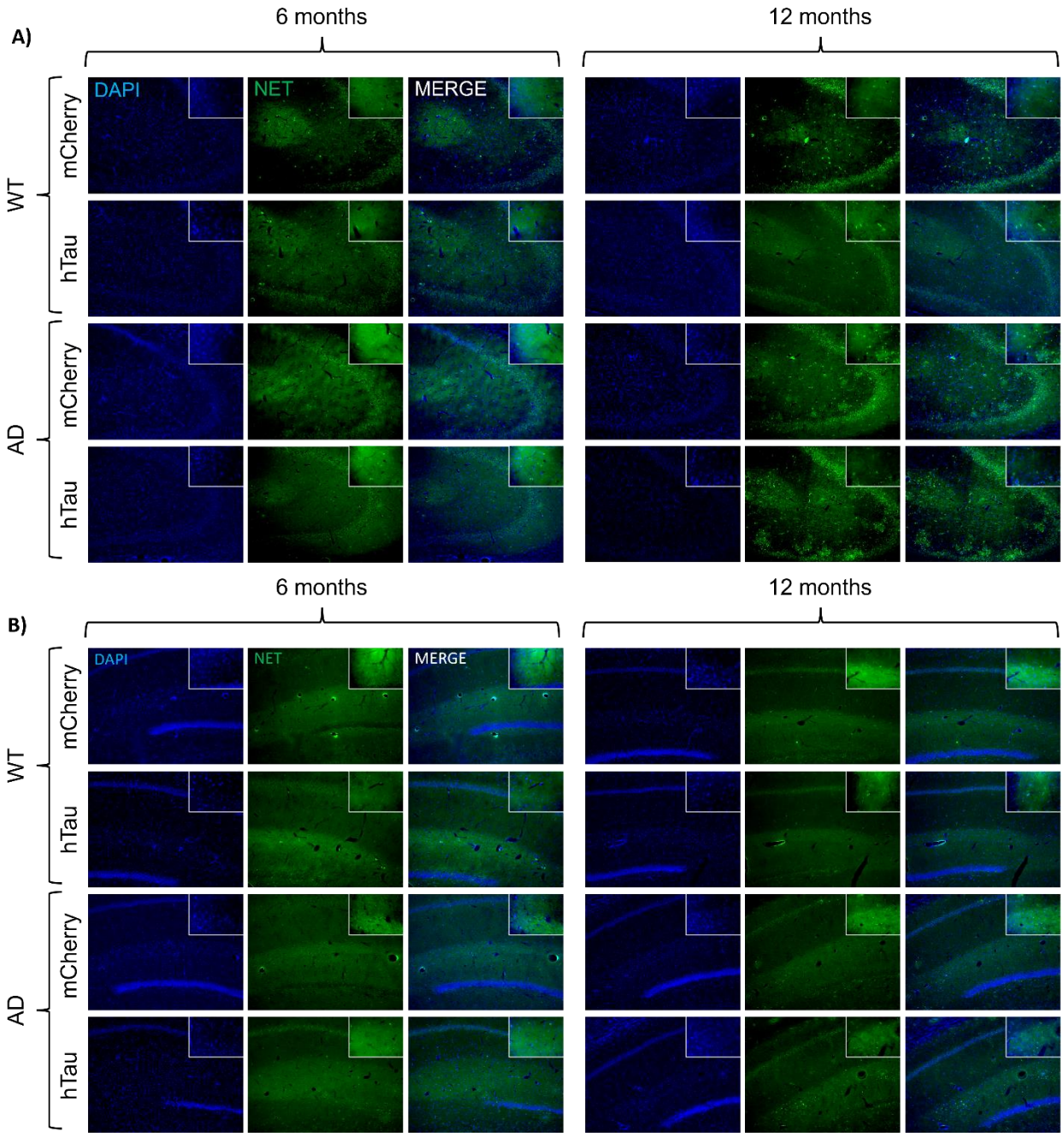

Supplemental Figure 4.5. Representative images of NET staining in the CA3 (A) and CA1 (B) subregions of the hippocampus. Main images and insets taken at 10x and 40x magnification, respectively.

CHAPTER 5: DISCUSSION AND FUTURE DIRECTIONS

5.1 SUMMARY AND INTEGRATION OF KEY FINDINGS

The LC is the primary noradrenergic nucleus in the brain, and decades of work have demonstrated its influence on sleep/wake cycles and arousal, stress and anxiety, response to novelty, social behaviors, cognition, learning, and memory. Dysfunction of the LC-NE system contributes to neuropsychiatric, neurodevelopmental, sleep/arousal, and neurodegenerative disorders. The focus of this dissertation was changes in LC-NE function in AD, the most common form of dementia in the world that first impacts the LC in the form of hyperphosphorylated tau deposition. Although LC dysfunction is noted throughout the progression of AD, fundamental questions regarding its activity, which are important for understanding the mechanisms underlying dysfunction and informing therapeutics targeting this system, were previously unresolved due to the lack of appropriate models and difficulty in targeting using electrophysiology. Nevertheless, changes in LC activity were predicted based on stereotypical effects of pathology on neural activity in other brain regions, the progression of behavioral symptoms at different stages of disease, neurochemical changes in the brain and CSF, and imaging data. However, the lack of direct measurements of LC activity and paradoxes have hampered simple interpretations of the existing information. For example, stimulating the LC at high tonic rates induces anxiety-like phenotypes in rodents akin to mild behavior impairment observed in the human condition (Valentino and Foote, 1988; Curtis et al., 2012; McCall et al., 2015; Omoluabi et al., 2021), but tau pathology typically leads to hypoactivity in other types of neurons (Busche et al., 2019; Marinkovic et al., 2019; Busche and Hyman, 2020). Furthermore, investigating alterations in the molecular composition of the LC in AD has been limited due to difficulty in isolating a sufficient quantity of neurons to accurately profile transcripts and proteins, as well as issues with cell-type specificity. In addition, previously available rodent models fail to recapitulate LC hyperphosphorylated tau pathology, which occurs at a critical early time point for therapeutic interventions aimed at slowing

the progression of AD. Given the development of early LC tau pathology and our in-depth characterization of altered LC firing rates and their relation to behavior in TgF344-AD rats, this model was ideal for delineating the changes in LC biochemistry along AD progression. We used targeted gene expression profiling by RNAscope fluorescence in situ hybridization to identify potential mechanisms underlying and therapeutic targets of altered LC activity in TgF344-AD rats.

In Chapters 2 and 3, I systematically interrogated LC-NE dysfunction in AD by characterizing differences in LC firing rates and potential underlying gene expression in a rat model of AD that recapitulates the temporal pattern of Aβ and tau deposition observed in humans (Rorabaugh et al., 2017). I subsequently linked these abnormalities to behavioral deficits in similarly aged animals in Chapter 4. Previous studies have demonstrated mixed effects of AD-like neuropathology on LC physiology, but had important caveats to consider (Kelly et al., 2021; Downs et al., 2022). The Swinny lab reported LC hyperactivity in mice in the presence of soluble Aβ oligomer pathology due to mislocalization of $GABA_A$ α3 receptor subunits (Kelly et al., 2021). However, Aβ pathology in the LC is more prevalent in late stage and severe forms of AD (Cole et al., 1993; Kelly et al., 2021). Another study recorded LC neurons from P301S mice that express pathogenic tau ubiquitously throughout the brain and found a reduction in spontaneous excitatory post-synaptic potentials (Chalermpalanupap et al., 2018; Zhu et al., 2018; Downs et al., 2023). Limitations common to both of these models are that they express either Aβ or tau pathology but not both, used a slice preparation instead of *in vivo* recording, and did not analyze phasic LC firing. It is thus unsurprising that we identified changes in LC firing rates that were slightly different than those observed in each of these studies.

Consistent with tau-induced hypoactivity observed in other neuronal populations (Busche et al., 2019; Marinkovic et al., 2019; Busche and Hyman, 2020), both 6- and 15-month TgF344-AD rats demonstrated tonic LC hypoactivity (**Figure 2.2 and 2.3**). However, LC neurons are highly

plastic and have adaptive mechanisms for maintaining homeostasis of NE signaling in response to perturbation (Maldonado, 1997; Nestler et al., 1999; Weinshenker et al., 2002; Benmansour et al., 2004). We found that the nature of the compensatory mechanisms engaged differed between 6- and 15-month animals, and aligned with stereotypical behavioral deficits noted in early (mild behavioral impairment) and late (cognitive deficits) AD. Specifically, young TgF344-AD animals with isolated LC tau pathology displayed elevated spontaneous and evoked phasic firing rates (**Figure 2.2 and 2.3**). At a molecular level, 6-month animals showed a significant reduction in mRNA levels of *Gabra3* (encodes the α3 subunit of the GABA-A receptor) and *Oprl1* (encodes the G protein-coupled nociceptin receptor), which are crucial for inhibition of the LC (**Figure 3.2Di and 3.2Ci**). Although the relationship between gene expression and changes in LC firing are merely associations, the reduction in *Gabra3* is likely to be causal because knocking out this gene results in LC hyperactivity (Kelly et al., 2021). Increased activity of LC neurons is consistent with our finding of enhanced anxiety-like phenotypes in both the open field and novelty-suppressed feeding (**Figure 4.4**). 6-month TgF344-AD rats also display slightly impaired cognitive ability in distance travelled to the platform during acquisition of reversal learning in the Morris water maze (**Figure 4.5E**). We did not observe effects of genotype on sleep latency, locomotor activity, or forced swim in 6-month animals (**Figure 4.3**). While changes in sleep/arousal are nearly ubiquitous in AD patients, in-depth phenotyping of these characteristics in TgF344-AD animals is lacking. Locomotor activity and sleep latency were used as gross proxies of arousal (Porter-Stransky et al., 2019), but no differences were found (**Figure 4.3**). A separate report demonstrated that 17-month TgF344-AD rats had an increased number of sleep-wake transitions, shorter bouts of REM and non-REM sleep, and alterations to EEG spectral power (Kreuzer et al., 2020). Use of EEG in younger animals is warranted given our finding of early isolated tau pathology in, and altered activity of, the LC, a critical node of the arousal system.

In contrast to young animals, aged TgF344-AD animals with abundant forebrain Aβ and tau pathology demonstrated a reduction in evoked phasic LC activity (**Figure 2.3**). Consistent with LC hypoactivity, aged rats displayed a worsening of cognitive deficits, as indicated by a longer latency and distance travelled to the platform in reversal acquisition of the Morris water maze (**Figure 4.5B and F**; latency data not shown), in addition to deterioration of performance in other learning and memory tasks as noted by others (Cohen et al., 2013; Sare et al., 2020; Goodman et al., 2021). In response to significant reductions in noradrenergic tone, we observed upregulation of genes involved in NE synthesis, packaging, and reuptake at the level of the LC, similar to what has been observed in later stage AD patients (**Figure 3.1Bi**) (Szot et al., 2000; Szot et al., 2006, 2007).

We argue that ages tested here represent different timepoints in disease progression and are attempts by the LC-NE system to maintain normal function in the face of pathological insult. In phase I, pathological consequences of hyperphosphorylated tau are met with a downregulation of inhibitory neurotransmission to maintain LC activity. Ultimately, these changes likely contribute to LC hyperactivity noted at this age, which are expressed behaviorally as elevated anxiety-like phenotypes. In phase II, worsening tau pathology and denervation of LC axons contribute to LC hypoactivity that are counteracted by elevations in genes promoting NE synthesis and neurotransmission. Engagement of these mechanisms are ultimately ineffective, as evidenced by the tonic and evoked LC hypoactivity (**Figure 2.2 and 2.3**) and worsening of cognitive deficits (Cohen et al., 2013; Sare et al., 2020; Goodman et al., 2021). In fact, an unintended consequence of upregulated NE transmission at this stage is the possibility of excessive somatodendritic NE release and autoinhibiton via α2-adrenergic receptors, but that needs to be tested empirically.

5.2 CLINICAL IMPLICATIONS

We have argued that the nature of LC dysfunction varies by disease stage (Weinshenker, 2018). Specifically, prodromal AD is marked by deposition of hyperphosphorylated tau pathology in the LC that is coincident with the emergence of non-cognitive behavioral impairments. Changes in arousal and mood, and exaggerated stress and anxiety responses imply early LC hyperactivity. This has also been supported by reported increases in cerebrospinal fluid NE levels and turnover, axonal sprouting, and elevated adrenergic receptor density and sensitivity (Palmer et al., 1987; Elrod et al., 1997; Hoogendijk et al., 1999; Szot et al., 2000; Szot et al., 2006, 2007; Goodman et al., 2021; Henjum et al., 2022). We have confirmed LC hyperactivity by directly recording from LC neurons in rats with isolated LC tau pathology. Specifically, while tonic LC activity was decreased, both spontaneous and evoked phasic activity were increased. This occurred in conjunction with reduced expression of inhibitory receptor mRNAs, namely *Gabra3* and *Oprl1*. Given that the GABAergic neurons within the peri-LC space provide both GABA and pronociceptin inhibitory inputs to the LC (Aston-Jones et al., 2004; Breton-Provencher and Sur, 2019; Luskin et al., 2022), investigating whether modulation of these neurons can normalize LC hyperactivity is warranted. Furthermore, there are some preliminary reports that these GABAergic neurons are also glycinergic (Luskin et al., 2022). Although we did not analyze glycine receptors in the LC of TgF344-AD rats, expression and function of these receptors are normal in APP/PS1 mice, and their activation is sufficient to curb LC hyperactivity (Kelly et al., 2021). Therefore, it would be worth exploring the glycinergic system in the LC of TgF344-AD rats and whether activation of these receptors is similarly effective at normalizing LC hyperactivity in 6-month rats. Use of chemogenetic, optogenetic, or pharmacological approaches to inhibit LC neurons in TgF344-AD rats, along with simultaneous recording of LC neurons, would be useful for determining interventions that are most efficacious at normalizing LC activity. Once a treatment is identified that normalizes LC activity, the next step would be testing whether these interventions improve

the prodromal symptoms observed in TgF344-AD rats, such as anxiety-like phenotypes. In clinical populations, interventions targeting LC hyperactivity in prodromal phases of disease are already being investigated. Specifically, adrenergic antagonists reduce agitation and anxiety in subjects with probable or possible AD (Peskind et al., 2005; Wang et al., 2009).

Meanwhile, an 8% decrease in LC volume is noted when transitioning through each Braak stage starting at stage 0-1, and cognitive impairment is correlated with loss of LC integrity (Wilson et al., 2013; Kelly et al., 2017; Theofilas et al., 2017; Jacobs et al., 2021; van Hooren et al., 2021; Prokopiou et al., 2022). At the corresponding stage in TgF344-AD rats, we showed that LC neurons still display elevated spontaneous phasic bursting, but blunted tonic and evoked phasic activity. In a follow up study, we further demonstrated that genes involved in synthesis, packaging, and reuptake of NE are upregulated at this time point. We believe that these are compensatory mechanisms to enhance NE tone that is lost due to tau-induced LC denervation of forebrain regions and LC hypoactivity. We further posit that the loss of LC axons results in excessive somatodendritic NE release, which contributes to the hypoactive phenotype at this age via α2-adrenergic receptor-mediated autoinhibition of LC neurons. These results would suggest that direct stimulation of LC neurons might not be as efficacious as treatments that directly stimulate receptors in forebrain regions, although a previous study in TgF344-AD rats did show beneficial effects of chemogenetic LC stimulation on spatial memory deficits (Rorabaugh et al., 2017). It is important to note that some of the pro-cognitive effects of LC activation may be due to spared mPFC-projecting axons in this model (Rorabaugh et al., 2017). Preventing NE reuptake with atomoxetine in those with mild-cognitive impairment reduced CSF levels of total and phospho-tau, and improved biomarker panels assessing synaptic function and neuroinflammation and brain connectivity and metabolism (Levey et al., 2021). In patients with Parkinson's disease,

atomoxetine also improved response inhibition, most prominently in those with lower LC integrity (O'Callaghan et al., 2021).

Similarly, preclinical evidence suggests that LC firing rates, patterns, and timing are important to consider. Specifically, rats virally expressing pseudophosphorylated tau in the LC show reduced LC axon density and cell counts that were associated with impaired odor discrimination (Ghosh et al., 2019). Follow-up experiments revealed that phasic LC stimulation prevented decline in odor discrimination and LC integrity, whereas tonic stimulation increased measure of anxiety and depression, while exacerbating deterioration of LC health (Omoluabi et al., 2021). Interestingly, these results contrast our own evidence that DREADD-induced LC stimulation, which increases tonic firing rates (Vazey and Aston-Jones, 2014; Zerbi et al., 2019), improves spatial reversal learning deficits in TgF344-AD rats (Rorabaugh et al., 2017). It is important to note that LC stimulation in the former study was performed chronically (daily for 6 weeks) and occurred 2-4 months prior to behavioral testing, rather than on a more acute timescale concurrent with behavior, which could explain some of the differences in the outcomes between the two studies. While electrophysiology experiments were not conducted in the pseudophosphorylated tau study, LC cell degeneration in these 15-month animals suggests that this represents a late-stage phenotype that may mimic the LC hypoactivity that we have observed in aged TgF344-AD rats. Future studies should clarify which type of LC stimulation yields immediate and sustained benefits on cognition and biomarkers of AD. We are actively exploring some of these possibilities by optogenetically stimulating the LC during fMRI in TgF344-AD rats to determine which patterns yield the most benefits on functional connectivity.

Despite the wealth of evidence implicating LC-NE dysfunction in AD and other neurodegenerative disorders, therapeutic interventions targeting this system are still in their infancy. As of 2022, there were only four pharmacological agents being assessed through clinical

trials for use as AD therapeutics (Cummings et al., 2022). These include BXCL-501, CST-2032, prazosin, and guanfacine. BXCL-501, a sublingual version of the selective α2-adrenergic receptor agonist dexmedetomidine, is being investigated in a phase II trial for agitation in mild-to-moderate dementia. The α1-adrenergic receptor antagonist prazosin is being tested in phase II for curbing agitation in mild-to-moderate dementia. CST-2032 is a brain penetrant β2-adrenergic receptor agonist in phase II being explored for cognitive enhancement in prodromal populations. Guanfacine is another α2-adrenergic receptor agonist being tested for use as a cognitive enhancer in mild-to-moderate dementia. These pharmacological approaches deserve discussion in the context of the new data presented in this dissertation. Prazosin has already shown efficacy in AD patients with agitation (Wang et al., 2009) and is approved for the treatment of nightmares in PTSD (Paiva et al., 2021). While it is true that dexmedetomidine benefits agitation symptoms in those with schizophrenia and bipolar disorder, these studies are acute (Citrome et al., 2022; Preskorn et al., 2022). In contrast, agitation in AD is more chronic (Carrarini et al., 2021), and agonizing α2 receptors may further exacerbate LC hypoactivity if prescribed to patients presenting with mild cognitive impairment. Furthermore, preclinical and clinical evidence is mixed on the effects of α2 receptor agonists on cognition (Choi et al., 2006; Gannon et al., 2015; Giustino and Maren, 2018). Meanwhile, targeting β2-adrenergic receptors shows some promise preclinically and clinically on cognition and even has the potential of lowering risk of developing AD and other neurodegenerative disorders (Li et al., 2013; Chai et al., 2016; Mittal et al., 2017; Giustino and Maren, 2018; Hutten et al., 2022). Future use of pharmacological interventions in AD targeting the LC-NE system should be guided by the findings made here on disease-stage dependent alterations in neuronal activity. Successful implementation of such therapies will require further refinement of techniques used to assess LC function in human patients through the use of MRI, PET, and CSF and plasma biomarkers (Kelberman et al., 2020). Non-

pharmacological methods of modulating LC activity are also worth exploring. For example, vagus nerve stimulation, which indirectly activates the LC via a relay from the nucleus tractus solitarius (Ruffoli et al., 2011), demonstrates target engagement and ability to improve cognition (Takigawa and Mogenson, 1977; Clark et al., 1999; Groves et al., 2005; Ghacibeh et al., 2006; Sun et al., 2017; Vazquez-Oliver et al., 2020). Moreover, varying stimulation protocols can differentially impact LC activity (Hulsey et al., 2017; Farrand et al., 2023), meaning that vagus nerve stimulation can be retuned along the entirety of disease course for efficacy.

Exercise is another interesting intervention to consider. AD is commonly referred to as type 3 diabetes because of the high risk that diabetes and impaired metabolic homeostasis pose to the development of AD (Nguyen et al., 2020; Hamze et al., 2022; Michailidis et al., 2022). It is therefore unsurprising that exercise is considered a neuroprotective factor to lower AD risk. The contributions of metabolic dysfunction to disease progression in TgF344-AD rats is not well described (Srivastava et al., 2023), but we note that TgF344-AD rats typically weigh more than age-matched WT littermates (data not shown) despite having similar motivation for food and appetite levels (**Figure 4.4F and G**). The beneficial effects of exercise likely occur throughout the body, but also have profound effects on LC physiology. Galanin is a highly expressed neuropeptide in the LC important for its neuroprotective roles and behaviorally conferring stress resilience (Counts et al., 2010; Schwarz and Luo, 2015; Tillage et al., 2020a). In fact, galanin co-expressing LC neurons are preferentially spared in AD (Miller et al., 1999). Exercise is known to augment galanin expression within the LC (O'Neal et al., 2001; Holmes et al., 2006; Murray et al., 2010; Sciolino et al., 2012; Tillage et al., 2020a). Given that galanin signaling occurs primarily through Gi/o inhibitory pathways, it is likely that the upregulation of galanin by exercise leads to long-term inhibition of LC neurons. This is supported by other evidence that direct application of galanin to LC neurons leads to their inhibition (Seutin et al., 1989; Bai et al., 2018). In TgF344-AD

rats, exercise alleviates accumulation of pathology, neuronal damage, and both cognitive and non-cognitive decline (Yang et al., 2022). Importantly, while assays were performed in 10-month animals, exercise training began at 2 months of age. This timepoint may precede pathological tau deposition in and hyperactivity of LC neurons. A similar study in aged TgF344-AD rats is warranted as exercise is known to activate the LC-NE system acutely (Pagliari and Peyrin, 1995; Chatterton et al., 1996; Segal et al., 2012), which may be beneficial for correcting late-stage hypoactivity. However, the potential long-term effects of galanin acting as a neurotrophic factor should be considered (Weinshenker and Holmes, 2016; Tillage et al., 2020a; Tillage et al., 2021).

Finally, there is an emerging field exploring the effects of daily heart rate variability biofeedback training on measures of LC health. In younger adults, biofeedback training reduces LC contrast, which is typically interpreted as LC dysfunction (Kelberman et al., 2020; Shelby et al., 2022). However, similar training leads to increased cortical volume that is associated with lower levels of mood disturbances (Yoo et al., 2022). Moreover, biofeedback increases LC-targeted hippocampal volume, specifically in older adults (Hyun Joo et al., 2023). Further experiments are required to understand the mechanism of how heart rate variability biofeedback training exerts its beneficial effects on cortical volume and LC physiology, and whether these effects translate to clinical AD populations. Clarifying the biological relevance of LC contrast and being able to track LC activity in humans would be especially valuable in this respect (Kelberman et al., 2020).

Although we have explored changes in LC activity, its molecular landscape, and behavior in aged TgF344-AD animals, there are two aspects that are not captured by this model that would be useful in a clinical context. While these animals develop hyperphosphorylated tau pathology in the LC, this pathology does not appear to progress to more mature versions of tau pathology such as neurofibrillary tangles. These rats also do not display frank LC cell loss up to 16 months of age, a prominent feature of the human condition. Therefore, rats at the ages tested are more

reminiscent of early-to-mid Braak stages. Introducing more mature or mutant versions of tau via seeding or viral infusion would be useful in determining whether LC function is further altered during the progression from mild-cognitive impairment to late-stage dementia.

5.3 FUTURE DIRECTIONS

This dissertation focused on properties and dysfunction of the LC-NE system in AD, mostly focused at the level of the cell bodies and downstream effects on behavior. While we observed no differences in LC firing rates based on sex or age in Chapter 2, we are currently leveraging a large dataset to explore the effects of state (awake, anesthetized, slice), species, sex, and age on LC firing rates in WT animals. Our preliminary analyses suggest complex effects of these factors and their interactions on LC firing rates. Prior evidence has also revealed impacts of sex on LC morphology, gene expression, and response to stress-related signaling (Curtis et al., 2006; Bangasser et al., 2010; Bangasser et al., 2011; Bangasser et al., 2016; Mulvey et al., 2018; Sulkes Cuevas et al., 2023). Two other studies of altered LC activity in AD models, both of which were performed in slice, indicate that Aβ pathology induces hyperactivity while P301S mutant tau causes hypoactivity, which are slightly different from our own findings (Kelly et al., 2021; Downs et al., 2022). Therefore, future studies should expand the characterization of LC firing rates under different conditions in an AD-relevant context, including recording LC neurons containing different forms of Aβ and tau pathology, using different model organisms, and obtaining data from awake behaving animals.

There is considerable evidence for LC dysfunction in projection regions, including axonal damage, sprouting, and receptor hypersensitivity (Szot et al., 2000; Szot et al., 2006, 2007; Goodman et al., 2021). One characteristic that has not been addressed is whether NE release dynamics are altered in AD. Applying classical and new technologies, such as microdialysis, fast

scan cyclic voltammetry, and $GRAB_{NE}$ fiber photometry, is warranted to obtain a holistic view of altered NE transmission in AD. This will be particularly important for determining the potential efficacy of noradrenergic interventions given the complex changes in LC-NE system function along the progression of AD. Moreover, while we uncovered genes that potentially contribute to early LC hyperactivity and later-stage hypoactivity, casual relationships remain to be established and there are likely other molecular changes occurring that we were unable to detect to the limited number of samples we were able to run. These changes would be better captured by unbiased bulk, single cell, or spatial sequencing techniques at the mRNA or protein level. We have collected punches of the LC from 6- and 15-month TgF344-AD rats and littermate controls, which we are currently processing for proteomic analysis. This in-depth characterization of the LC will be invaluable at identifying other abnormalities in the molecular makeup of LC neurons along the progression of AD.

Recent evidence indicates that the LC is a complex and heterogeneous modulatory system. As previously stated, we did not detect sex differences in firing rates of LC neurons in WT or TgF344-AD rats, but our groups for molecular and behavioral characterizations were unbalanced and insufficiently powered to detect sex differences. This is despite the well documented influence of sex on LC morphology and function (Babstock et al., 1997; Bangasser et al., 2011; Bangasser et al., 2016; Mulvey et al., 2018; Duesman et al., 2022; Sulkes Cuevas et al., 2023). Similarly, electrophysiological properties, biochemical makeup, and afferent/efferent connections of the LC exhibit modularity (Sara, 2009; Chandler et al., 2014; Schwarz and Luo, 2015; Mulvey et al., 2018; Chandler et al., 2019; Wagner-Altendorf et al., 2019; Poe et al., 2020; Sulkes Cuevas et al., 2023). We did not address such modularity in these studies, but AD more heavily impacts the rostral and middle portions of the LC that project preferentially to the hippocampus and cortex (German et al., 1992; Sara, 2009; Schwarz and Luo, 2015; Theofilas et

al., 2017; Betts et al., 2019a; Gilvesy et al., 2022). Selective recording, molecular characterization, and behavioral phenotyping with and without interventions would assist in delineating the contributions of specific dysfunctional circuits arising from the LC, rather than viewing the nucleus as a single unit.

Another interesting possibility is normalizing the expression of gene targets identified in Chapter 3 aimed at correcting LC activity. Both specific and non-specific alterations to molecular LC profiles can lead to changes in physiology and behavior (Mulvey et al., 2018; Tillage et al., 2020a; Duesman et al., 2022; Tkaczynski et al., 2022). Young TgF344-AD rats may benefit from selective overexpression of *Gabra3* or *Oprl1* in the LC, which can be tested for efficacy with electrophysiology and behavior. However, these types of genetic interventions will likely require more foundation prior to implementation, such as understanding the link between changes in mRNA levels and protein expression, localization, and function. For example, downregulating noradrenergic-specific genes in aged TgF344-AD rats may further exacerbate noradrenergic tone, but these animals might benefit from modulation of a currently unidentified molecular abnormality (galanin, hypocretin/orexin, etc.).

With respect to our behavioral characterization of TgF344-AD rats, compared to age and genotype, the effects of virally expressing WT human tau in the LC was minimal. Part of the rationale at introducing human tau in this model was because TgF344-AD rats develop a mild form of hyperphosphorylated tau that does not progress to more insidious forms (Rorabaugh et al., 2017). Viral expression of pseudophosphorylated tau in the LC also induced cognitive deficits and gradual decline in LC health, but did not incorporate Aβ or more advanced forms of tau pathology (Ghosh et al., 2019; Omoluabi et al., 2021). P301S and APP/PS1 mouse models do develop severe behavioral deficits, but these cannot be specifically attributed to LC dysfunction given the ubiquitous expression of the transgenes. Therefore, introducing more advanced forms of tau

pathology into the LC is necessary for understanding the consequences of aggregated tau on LC function in late Braak stages. Expanding the behavioral characterization of the TgF344-AD rat is also warranted. Specifically, interpretation of the forced swim test is hotly contested. Anhedonia can be investigated using a sucrose preference test, while active and passive coping may be better interpreted by quantifying darting behavior during fear conditioning or shock probe burying. Pain is another important response that is heavily influenced by the LC, and chronic pain is considered a risk factor for AD (Cao et al., 2019). The changes in *Oprl1* gene expression in the LC further suggest that there could be altered pain processing in these rats. Testing TgF344-AD rats on various pain assays (Von Frey, tail flick, hot plate, etc.) is thus warranted. At its core, AD is a disease that affects social relationships. We are currently employing behavioral tasks for assessing social recognition and memory that are akin to the deficits displayed in the human condition. However, changes in mood can be a large driver of caregiver burden and are not well modeled preclinically due to the lack of strong bonds formed between murine pairs. Prairie voles, like mice and rats, display empathic behaviors and a greater capacity for social memory, but unlike other murine species form monogamous partnerships that would allow for the investigation of complex inter-pair dynamics and how they are affected along disease course. There are also a host of other behavioral tasks such as the two-alternative forced choice task, five choice serial reaction time task, Y-maze or T-maze, 8-arm radial maze, passive/active avoidance, and others that can probe other aspects of cognition and executive function including compulsivity/impulsivity, working memory, and attention that are worth pursuing.

Finally, while the primary focus of this work has been the LC-NE system, early accumulation of hyperphosphorylated tau, subsequent dysfunction, and ultimate degeneration of other subcortical nuclei is nearly ubiquitous in AD (Braak et al., 2011; Theofilas et al., 2015; Ehrenberg et al., 2017; Oh et al., 2019; Engels-Dominguez et al., 2023). In particular, these

neuromodulatory subcortical systems influence many of the same behaviors as the LC, which often go awry in prodromal phases of disease (Ehrenberg et al., 2023). Interrogating the contribution of other dysfunctional subcortical systems to AD symptoms and progression is therefore warranted.

5.4 FINAL REMARKS

This dissertation comprehensively catalogs LC dysfunction along AD progression in the TgF344-AD rat model that recapitulates early, isolated LC hyperphosphorylated tau pathology. I first recorded from LC neurons to ascertain pathology-induced alterations to LC activity along the course of AD. Next, I molecularly characterized the LC of age-matched animals to uncover signatures potentially underlying altered LC activity. Finally, I extensively phenotyped these animals behaviorally and pathologically, with a specific focus on prodromal phases of disease and incorporating aspects of non-cognitive deficits. These data substantiate both long-standing and updated theories of disease-stage dependent changes to LC activity in AD and their link to behavioral abnormalities, both cognitive and non-cognitive. 6-month TgF344-AD rats display isolated LC hyperphosphorylated tau pathology, LC hyperactivity, downregulation of inhibitory receptor mRNA expression, and anxiety-like phenotypes. As the disease progresses and pathology spreads, the LC becomes hypoactive, inhibitory genes are normalized while those that promote noradrenergic transmission are upregulated, and cognitive deficits worsen as noted in 15-month rats. The comprehensive assessment of LC dysfunction along the progression of AD should be used as a guide to inform treatments at each stage of disease, in addition to laying the foundation for future studies to expand on these findings.

REFERENCES

Abraham AD, Cunningham CL, Lattal KM (2012) Methylphenidate enhances extinction of contextual fear. Learn Mem 19:67-72.

Abramov AY, Canevari L, Duchen MR (2004) Beta-amyloid peptides induce mitochondrial dysfunction and oxidative stress in astrocytes and death of neurons through activation of NADPH oxidase. J Neurosci 24:565-575.

Acosta MC, Tillage RP, Weinshenker D, Saltzman W (2022) Acute inhibition of dopamine beta-hydroxylase attenuates behavioral responses to pups in adult virgin California mice (Peromyscus californicus). Horm Behav 137:105086.

Adler A (1942) Melanin pigment in the brain of the gorilla. Journal of Comparative Neurology 76:501-507.

Ahnaou A, Walsh C, Manyakov NV, Youssef SA, Drinkenburg WH (2019) Early Electrophysiological Disintegration of Hippocampal Neural Networks in a Novel Locus Coeruleus Tau-Seeding Mouse Model of Alzheimer's Disease. Neural Plasticity 2019.

Akaike T (1982) Periodic bursting activities of locus coerulleus neurons in the rat. Brain Res 239:629-633.

Allen B, Ingram E, Takao M, Smith MJ, Jakes R, Virdee K, Yoshida H, Holzer M, Craxton M, Emson PC, Atzori C, Migheli A, Crowther RA, Ghetti B, Spillantini MG, Goedert M (2002) Abundant tau filaments and nonapoptotic neurodegeneration in transgenic mice expressing human P301S tau protein. J Neurosci 22:9340-9351.

Allen M, Poggiali D, Whitaker K, Marshall TR, Kievit RA (2019) Raincloud plots: a multi-platform tool for robust data visualization. Wellcome Open Res 4:63.

Alnaes D, Sneve MH, Espeseth T, Endestad T, van de Pavert SH, Laeng B (2014) Pupil size signals mental effort deployed during multiple object tracking and predicts brain activity in the dorsal attention network and the locus coeruleus. J Vis 14.

Alreja M, Aghajanian GK (1995) Use of the Whole-Cell Patch-Clamp Method in Studies on the Role of Camp in Regulating the Spontaneous Firing of Locus-Coeruleus Neurons. J Neurosci Meth 59:67-75.

Alvarez VA, Chow CC, Van Bockstaele EJ, Williams JT (2002) Frequency-dependent synchrony in locus ceruleus: role of electrotonic coupling. Proc Natl Acad Sci U S A 99:4032-4036.

Amanzio M, Geminiani G, Leotta D, Cappa S (2008) Metaphor comprehension in Alzheimer's disease: novelty matters. Brain Lang 107:1-10.

Amaral DG, Foss JA (1975) Locus coeruleus lesions and learning. Science 188:377-378.

Arendt T, Bruckner MK, Morawski M, Jager C, Gertz HJ (2015) Early neurone loss in Alzheimer's disease: cortical or subcortical? Acta Neuropathol Commun 3:10.

Armbruster BN, Li X, Pausch MH, Herlitze S, Roth BL (2007) Evolving the lock to fit the key to create a family of G protein-coupled receptors potently activated by an inert ligand. Proc Natl Acad Sci U S A 104:5163-5168.

Arnsten AFT, Datta D, Leslie S, Yang ST, Wang M, Nairn AC (2019) Alzheimer's-like pathology in aging rhesus macaques: Unique opportunity to study the etiology and treatment of Alzheimer's disease. Proc Natl Acad Sci U S A 116:26230-26238.

Arora I, Bellato A, Ropar D, Hollis C, Groom MJ (2021) Is autonomic function during resting-state atypical in Autism: A systematic review of evidence. Neurosci Biobehav R 125:417-441.

Arriagada PV, Growdon JH, Hedley-Whyte ET, Hyman BT (1992) Neurofibrillary tangles but not senile plaques parallel duration and severity of Alzheimer's disease. Neurology 42:631-639.

Aston-Jones G, Bloom FE (1981a) Norepinephrine-containing locus coeruleus neurons in behaving rats exhibit pronounced responses to non-noxious environmental stimuli. J Neurosci 1:887-900.

Aston-Jones G, Bloom FE (1981b) Activity of norepinephrine-containing locus coeruleus neurons in behaving rats anticipates fluctuations in the sleep-waking cycle. J Neurosci 1:876-886.

Aston-Jones G, Cohen JD (2005a) An integrative theory of locus coeruleus-norepinephrine function: adaptive gain and optimal performance. Annu Rev Neurosci 28:403-450.

Aston-Jones G, Cohen JD (2005b) An integrative theory of locus coeruleus-norepinephrine function: Adaptive gain and optimal performance. Annual Review of Neuroscience 28:403-450.

Aston-Jones G, Waterhouse B (2016) Locus coeruleus: From global projection system to adaptive regulation of behavior. Brain Res 1645:75-78.

Aston-Jones G, Foote SL, Segal M (1985) Impulse conduction properties of noradrenergic locus coeruleus axons projecting to monkey cerebrocortex. Neuroscience 15:765-777.

Aston-Jones G, Rajkowski J, Cohen J (1999) Role of locus coeruleus in attention and behavioral flexibility. Biol Psychiatry 46:1309-1320.

Aston-Jones G, Zhu Y, Card JP (2004) Numerous GABAergic afferents to locus ceruleus in the pericerulear dendritic zone: possible interneuronal pool. J Neurosci 24:2313-2321.

Aston-Jones G, Akaoka H, Charlety P, Chouvet G (1991) Serotonin selectively attenuates glutamate-evoked activation of noradrenergic locus coeruleus neurons. J Neurosci 11:760-769.

Aston-Jones G, Rajkowski J, Kubiak P, Alexinsky T (1994) Locus coeruleus neurons in monkey are selectively activated by attended cues in a vigilance task. J Neurosci 14:4467-4480.

Atzori M, Cuevas-Olguin R, Esquivel-Rendon E, Garcia-Oscos F, Salgado-Delgado RC, Saderi N, Miranda-Morales M, Trevino M, Pineda JC, Salgado H (2016) Locus Ceruleus Norepinephrine Release: A Central Regulator of CNS Spatio-Temporal Activation? Front Synaptic Neurosci 8:25.

Babstock D, Malsbury CW, Harley CW (1997) The dorsal locus coeruleus is larger in male than in female Sprague-Dawley rats. Neurosci Lett 224:157-160.

Babulal GM, Roe CM, Stout SH, Rajasekar G, Wisch JK, Benzinger TLS, Morris JC, Ances BM (2020) Depression is Associated with Tau and Not Amyloid Positron Emission Tomography in Cognitively Normal Adults. J Alzheimers Dis 74:1045-1055.

Bachman SL, Dahl MJ, Werkle-Bergner M, Duzel S, Forlim CG, Lindenberger U, Kuhn S, Mather M (2021) Locus coeruleus MRI contrast is associated with cortical thickness in older adults. Neurobiology of Aging 100:72-82.

Bai YF, Ma HT, Liu LN, Li H, Li XX, Yang YT, Xue B, Wang D, Xu ZD (2018) Activation of galanin receptor 1 inhibits locus coeruleus neurons via GIRK channels. Biochem Biophys Res Commun 503:79-85.

Bangasser DA, Valentino RJ (2012) Sex differences in molecular and cellular substrates of stress. Cell Mol Neurobiol 32:709-723.

Bangasser DA, Wiersielis KR, Khantsis S (2016) Sex differences in the locus coeruleus-norepinephrine system and its regulation by stress. Brain Research 1641:177-188.

Bangasser DA, Zhang X, Garachh V, Hanhauser E, Valentino RJ (2011) Sexual dimorphism in locus coeruleus dendritic morphology: a structural basis for sex differences in emotional arousal. Physiol Behav 103:342-351.

Bangasser DA, Curtis A, Reyes BAS, Bethea TT, Parastatidis I, Ischiropoulos H, Van Bockstaele EJ, Valentino RJ (2010) Sex differences in corticotropin-releasing factor receptor

signaling and trafficking: potential role in female vulnerability to stress-related psychopathology. Mol Psychiatr 15:896-904.

Bartfai T, Iverfeldt K, Fisone G, Serfozo P (1988) Regulation of the release of coexisting neurotransmitters. Annu Rev Pharmacol Toxicol 28:285-310.

Bast N, Boxhoorn S, Super H, Helfer B, Polzer L, Klein C, Cholemkery H, Freitag CM (2023) Atypical Arousal Regulation in Children With Autism but Not With Attention-Deficit/Hyperactivity Disorder as Indicated by Pupillometric Measures of Locus Coeruleus Activity. Biol Psychiatry Cogn Neurosci Neuroimaging 8:11-20.

Becker E, Orellana Rios CL, Lahmann C, Rucker G, Bauer J, Boeker M (2018) Anxiety as a risk factor of Alzheimer's disease and vascular dementia. Br J Psychiatry 213:654-660.

Benarroch EE (2009) The locus ceruleus norepinephrine system: functional organization and potential clinical significance. Neurology 73:1699-1704.

Benmansour S, Altamirano AV, Jones DJ, Sanchez TA, Gould GG, Pardon MC, Morilak DA, Frazer A (2004) Regulation of the norepinephrine transporter by chronic administration of antidepressants. Biol Psychiatry 55:313-316.

Berardi AM, Parasuraman R, Haxby JV (2005) Sustained attention in mild Alzheimer's disease. Dev Neuropsychol 28:507-537.

Berlau DJ, McGaugh JL (2006) Enhancement of extinction memory consolidation: the role of the noradrenergic and GABAergic systems within the basolateral amygdala. Neurobiol Learn Mem 86:123-132.

Berridge CW, Waterhouse BD (2003) The locus coeruleus-noradrenergic system: modulation of behavioral state and state-dependent cognitive processes. Brain Res Brain Res Rev 42:33-84.

Betts MJ, Cardenas-Blanco A, Kanowski M, Spottke A, Teipel SJ, Kilimann I, Jessen F, Duzel E (2019a) Locus coeruleus MRI contrast is reduced in Alzheimer's disease dementia and correlates with CSF Abeta levels. Alzheimers Dement (Amst) 11:281-285.

Betts MJ et al. (2019b) Locus coeruleus imaging as a biomarker for noradrenergic dysfunction in neurodegenerative diseases. Brain 142:2558-2571.

Biscetti L, Salvadori N, Farotti L, Cataldi S, Eusebi P, Paciotti S, Parnetti L (2019) The added value of A beta 42/A beta 40 in the CSF signature for routine diagnostics of Alzheimer's disease. Clin Chim Acta 494:71-73.

Blennow K, Dubois B, Fagan AM, Lewczuk P, de Leon MJ, Hampel H (2015) Clinical utility of cerebrospinal fluid biomarkers in the diagnosis of early Alzheimer's disease. Alzheimers & Dementia 11:58-69.

Bogdanova OV, Kanekar S, D'Anci KE, Renshaw PF (2013) Factors influencing behavior in the forced swim test. Physiol Behav 118:227-239.

Boucher MN, Aktar M, Braas KM, May V, Hammack SE (2022) Activation of Lateral Parabrachial Nucleus (LPBn) PACAP-Expressing Projection Neurons to the Bed Nucleus of the Stria Terminalis (BNST) Enhances Anxiety-like Behavior. J Mol Neurosci 72:451-458.

Bouret S, Sara SJ (2005) Network reset: a simplified overarching theory of locus coeruleus noradrenaline function. Trends Neurosci 28:574-582.

Boyarko B, Hook V (2021) Human Tau Isoforms and Proteolysis for Production of Toxic Tau Fragments in Neurodegeneration. Front Neurosci 15:702788.

Bozadjieva-Kramer N, Ross RA, Johnson DQ, Fenselau H, Haggerty DL, Atwood B, Lowell B, Flak JN (2021) The Role of Mediobasal Hypothalamic PACAP in the Control of Body Weight and Metabolism. Endocrinology 162.

Braak H, Braak E (1991) Neuropathological stageing of Alzheimer-related changes. Acta Neuropathol 82:239-259.

Braak H, Thal DR, Ghebremedhin E, Del Tredici K (2011) Stages of the pathologic process in Alzheimer disease: age categories from 1 to 100 years. J Neuropathol Exp Neurol 70:960-969.

Bremner JD, Krystal JH, Southwick SM, Charney DS (1996) Noradrenergic mechanisms in stress and anxiety: I. Preclinical studies. Synapse 23:28-38.

Breton-Provencher V, Sur M (2019) Active control of arousal by a locus coeruleus GABAergic circuit. Nat Neurosci 22:218-228.

Breton-Provencher V, Drummond GT, Sur M (2021) Locus Coeruleus Norepinephrine in Learned Behavior: Anatomical Modularity and Spatiotemporal Integration in Targets. Front Neural Circuits 15:638007.

Busch C, Bohl J, Ohm TG (1997) Spatial, temporal and numeric analysis of Alzheimer changes in the nucleus coeruleus. Neurobiol Aging 18:401-406.

Busche MA, Hyman BT (2020) Synergy between amyloid-beta and tau in Alzheimer's disease. Nat Neurosci 23:1183-1193.

Busche MA, Wegmann S, Dujardin S, Commins C, Schiantarelli J, Klickstein N, Kamath TV, Carlson GA, Nelken I, Hyman BT (2019) Tau impairs neural circuits, dominating amyloid-beta effects, in Alzheimer models in vivo. Nat Neurosci 22:57-64.

Busciglio J, Lorenzo A, Yeh J, Yankner BA (1995) beta-amyloid fibrils induce tau phosphorylation and loss of microtubule binding. Neuron 14:879-888.

Bush DE, Caparosa EM, Gekker A, Ledoux J (2010) Beta-adrenergic receptors in the lateral nucleus of the amygdala contribute to the acquisition but not the consolidation of auditory fear conditioning. Front Behav Neurosci 4:154.

Butkovich LM, Houser MC, Chalermpalanupap T, Porter-Stransky KA, Iannitelli AF, Boles JS, Lloyd GM, Coomes AS, Eidson LN, De Sousa Rodrigues ME, Oliver DL, Kelly SD, Chang J, Bengoa-Vergniory N, Wade-Martins R, Giasson BI, Joers V, Weinshenker D, Tansey MG (2020) Transgenic Mice Expressing Human alpha-Synuclein in Noradrenergic Neurons Develop Locus Ceruleus Pathology and Nonmotor Features of Parkinson's Disease. J Neurosci 40:7559-7576.

Cantero JL, Hita-Yanez E, Moreno-Lopez B, Portillo F, Rubio A, Avila J (2010) Tau protein role in sleep-wake cycle. J Alzheimers Dis 21:411-421.

Cao S, Fisher DW, Yu T, Dong HX (2019) The link between chronic pain and Alzheimer's disease. J Neuroinflamm 16.

Cao S, Fisher DW, Rodriguez G, Yu T, Dong H (2021) Comparisons of neuroinflammation, microglial activation, and degeneration of the locus coeruleus-norepinephrine system in APP/PS1 and aging mice. J Neuroinflammation 18:10.

Carballo-Carbajal I, Laguna A, Romero-Gimenez J, Cuadros T, Bove J, Martinez-Vicente M, Parent A, Gonzalez-Sepulveda M, Penuelas N, Torra A, Rodriguez-Galvan B, Ballabio A, Hasegawa T, Bortolozzi A, Gelpi E, Vila M (2019) Brain tyrosinase overexpression implicates age-dependent neuromelanin production in Parkinson's disease pathogenesis. Nat Commun 10:973.

Carrarini C, Russo M, Dono F, Barbone F, Rispoli MG, Ferri L, Di Pietro M, Digiovanni A, Ajdinaj P, Speranza R, Granzotto A, Frazzini V, Thomas A, Pilotto A, Padovani A, Onofrj M, Sensi SL, Bonanni L (2021) Agitation and Dementia: Prevention and Treatment Strategies in Acute and Chronic Conditions. Front Neurol 12:644317.

Carter ME, Yizhar O, Chikahisa S, Nguyen H, Adamantidis A, Nishino S, Deisseroth K, de Lecea L (2010) Tuning arousal with optogenetic modulation of locus coeruleus neurons. Nat Neurosci 13:1526-1533.

Caspersen C, Wang N, Yao J, Sosunov A, Chen X, Lustbader JW, Xu HW, Stern D, McKhann G, Yan SD (2005) Mitochondrial Abeta: a potential focal point for neuronal metabolic dysfunction in Alzheimer's disease. FASEB J 19:2040-2041.

Cassidy C, Therriault J, Pascoal T, Cheung V, Chamoun M, Sibahi A, Gandhi R, Tardif C, Ismail Z, Gauthier S, Rosa-Neto P (2021) Association of a Novel MRI-Based Measure of Locus Coeruleus-Norepinephrine System Integrity With Braak Stage and Neuropsychiatric Symptom Severity in Alzheimer's Disease. Neuropsychopharmacology 46:77-77.

Cassidy CM, Therriault J, Pascoal TA, Cheung V, Savard M, Tuominen L, Chamoun M, McCall A, Celebi S, Lussier F, Massarweh G, Soucy JP, Weinshenker D, Tardif C, Ismail Z, Gauthier S, Rosa-Neto P (2022) Association of locus coeruleus integrity with Braak stage and neuropsychiatric symptom severity in Alzheimer's disease. Neuropsychopharmacology 47:1128-1136.

Cazettes F, Reato D, Morais JP, Renart A, Mainen ZF (2021) Phasic Activation of Dorsal Raphe Serotonergic Neurons Increases Pupil Size. Curr Biol 31:192-197 e194.

Cerpa JC, Piccin A, Dehove M, Lavigne M, Kremer EJ, Wolff M, Parkes SL, Coutureau E (2023) Inhibition of noradrenergic signalling in rodent orbitofrontal cortex impairs the updating of goal-directed actions. Elife 12.

Chai GS, Wang YY, Yasheng A, Zhao P (2016) Beta 2-adrenergic receptor activation enhances neurogenesis in Alzheimer's disease mice. Neural Regen Res 11:1617-1624.

Chai N, Liu JF, Xue YX, Yang C, Yan W, Wang HM, Luo YX, Shi HS, Wang JS, Bao YP, Meng SQ, Ding ZB, Wang XY, Lu L (2014) Delayed noradrenergic activation in the dorsal

hippocampus promotes the long-term persistence of extinguished fear. Neuropsychopharmacology 39:1933-1945.

Chalermpalanupap T, Schroeder JP, Rorabaugh JM, Liles LC, Lah JJ, Levey AI, Weinshenker D (2018) Locus Coeruleus Ablation Exacerbates Cognitive Deficits, Neuropathology, and Lethality in P301S Tau Transgenic Mice. Journal of Neuroscience 38:74-92.

Chandler DJ, Gao WJ, Waterhouse BD (2014) Heterogeneous organization of the locus coeruleus projections to prefrontal and motor cortices. Proc Natl Acad Sci U S A 111:6816-6821.

Chandler DJ, Jensen P, McCall JG, Pickering AE, Schwarz LA, Totah NK (2019) Redefining Noradrenergic Neuromodulation of Behavior: Impacts of a Modular Locus Coeruleus Architecture. J Neurosci 39:8239-8249.

Chatterton RT, Jr., Vogelsong KM, Lu YC, Ellman AB, Hudgens GA (1996) Salivary alpha-amylase as a measure of endogenous adrenergic activity. Clin Physiol 16:433-448.

Chauhan V, Chauhan A (2006) Oxidative stress in Alzheimer's disease. Pathophysiology 13:195-208.

Chen L, McKenna JT, Bolortuya Y, Winston S, Thakkar MM, Basheer R, Brown RE, McCarley RW (2010) Knockdown of orexin type 1 receptor in rat locus coeruleus increases REM sleep during the dark period. Eur J Neurosci 32:1528-1536.

Chiang C, Aston-Jones G (1993a) A 5-hydroxytryptamine2 agonist augments gamma-aminobutyric acid and excitatory amino acid inputs to noradrenergic locus coeruleus neurons. Neuroscience 54:409-420.

Chiang C, Aston-Jones G (1993b) Response of locus coeruleus neurons to footshock stimulation is mediated by neurons in the rostral ventral medulla. Neuroscience 53:705-715.

Choi Y, Novak JC, Hillier A, Votolato NA, Beversdorf DQ (2006) The effect of alpha-2 adrenergic agonists on memory and cognitive flexibility. Cogn Behav Neurol 19:204-207.

Christie MJ (1997) Generators of synchronous activity of the locus coeruleus during development. Semin Cell Dev Biol 8:29-34.

Citrome L, Risinger R, Rajachandran L, Robison H (2022) Sublingual Dexmedetomidine for Agitation Associated with Schizophrenia or Bipolar Disorder: A Post Hoc Analysis of Number Needed to Treat, Number Needed to Harm, and Likelihood to be Helped or Harmed. Adv Ther 39:4821-4835.

Clark KB, Naritoku DK, Smith DC, Browning RA, Jensen RA (1999) Enhanced recognition memory following vagus nerve stimulation in human subjects. Nature Neuroscience 2:94-98.

Clewett DV, Lee TH, Greening S, Ponzio A, Margalit E, Mather M (2016) Neuromelanin marks the spot: identifying a locus coeruleus biomarker of cognitive reserve in healthy aging. Neurobiology of Aging 37:117-126.

Cohen RM, Rezai-Zadeh K, Weitz TM, Rentsendorj A, Gate D, Spivak I, Bholat Y, Vasilevko V, Glabe CG, Breunig JJ, Rakic P, Davtyan H, Agadjanyan MG, Kepe V, Barrio JR, Bannykh S, Szekely CA, Pechnick RN, Town T (2013) A transgenic Alzheimer rat with plaques, tau pathology, behavioral impairment, oligomeric abeta, and frank neuronal loss. J Neurosci 33:6245-6256.

Cole BJ, Koob GF (1988) Propranolol antagonizes the enhanced conditioned fear produced by corticotropin releasing factor. J Pharmacol Exp Ther 247:902-910.

Cole G, Neal JW, Singhrao SK, Jasani B, Newman GR (1993) The distribution of amyloid plaques in the cerebellum and brain stem in Down's syndrome and Alzheimer's disease: a light microscopical analysis. Acta Neuropathol 85:542-552.

Commons KG, Cholanians AB, Babb JA, Ehlinger DG (2017) The Rodent Forced Swim Test Measures Stress-Coping Strategy, Not Depression-like Behavior. ACS Chem Neurosci 8:955-960.

Connor M, Vaughan CW, Chieng B, Christie MJ (1996) Nociceptin receptor coupling to a potassium conductance in rat locus coeruleus neurones in vitro. Br J Pharmacol 119:1614-1618.

Coradazzi M, Gulino R, Fieramosca F, Falzacappa LV, Riggi M, Leanza G (2016) Selective noradrenaline depletion impairs working memory and hippocampal neurogenesis. Neurobiol Aging 48:93-102.

Corteen NL, Cole TM, Sarna A, Sieghart W, Swinny JD (2011) Localization of GABA-A receptor alpha subunits on neurochemically distinct cell types in the rat locus coeruleus. Eur J Neurosci 34:250-262.

Costa A, Pais M, Loureiro J, Stella F, Radanovic M, Gattaz W, Forlenza O, Talib L (2022) Decision tree-based classification as a support to diagnosis in the Alzheimer's disease continuum using cerebrospinal fluid biomarkers: insights from automated analysis. Braz J Psychiat 44:370-377.

Counts SE, Perez SE, Ginsberg SD, Mufson EJ (2010) Neuroprotective role for galanin in Alzheimer's disease. Exp Suppl 102:143-162.

Crimins JL, Rocher AB, Luebke JI (2012) Electrophysiological changes precede morphological changes to frontal cortical pyramidal neurons in the rTg4510 mouse model of progressive tauopathy. Acta Neuropathol 124:777-795.

Cummings J (2019) The National Institute on Aging-Alzheimer's Association Framework on Alzheimer's disease: Application to clinical trials. Alzheimers & Dementia 15:172-178.

Cummings J, Lee G, Nahed P, Kambar M, Zhong K, Fonseca J, Taghva K (2022) Alzheimer's disease drug development pipeline: 2022. Alzheimers Dement (N Y) 8:e12295.

Curtis AL, Bethea T, Valentino RJ (2006) Sexually dimorphic responses of the brain norepinephrine system to stress and corticotropin-releasing factor. Neuropsychopharmacology 31:544-554.

Curtis AL, Lechner SM, Pavcovich LA, Valentino RJ (1997) Activation of the locus coeruleus noradrenergic system by intracoerulear microinfusion of corticotropin-releasing factor: effects on discharge rate, cortical norepinephrine levels and cortical electroencephalographic activity. J Pharmacol Exp Ther 281:163-172.

Curtis AL, Leiser SC, Snyder K, Valentino RJ (2012) Predator stress engages corticotropin-releasing factor and opioid systems to alter the operating mode of locus coeruleus norepinephrine neurons. Neuropharmacology 62:1737-1745.

d'Oleire Uquillas F, Jacobs HIL, Biddle KD, Properzi M, Hanseeuw B, Schultz AP, Rentz DM, Johnson KA, Sperling RA, Donovan NJ (2018) Regional tau pathology and loneliness in cognitively normal older adults. Transl Psychiatry 8:282.

Daffner KR, Mesulam MM, Cohen LG, Scinto LF (1999) Mechanisms underlying diminished novelty-seeking behavior in patients with probable Alzheimer's disease. Neuropsychiatry Neuropsychol Behav Neurol 12:58-66.

Dahl MJ, Mather M, Duzel S, Bodammer NC, Lindenberger U, Kuhn S, Werkle-Bergner M (2019) Rostral locus coeruleus integrity is associated with better memory performance in older adults. Nat Hum Behav 3:1203-1214.

David MCB, Del Giovane M, Liu KY, Gostick B, Rowe JB, Oboh I, Howard R, Malhotra PA (2022) Cognitive and neuropsychiatric effects of noradrenergic treatment in Alzheimer's

disease: systematic review and meta-analysis. J Neurol Neurosurg Psychiatry 93:1080-1090.

Davies MF, Tsui J, Flannery JA, Li X, DeLorey TM, Hoffman BB (2004) Activation of alpha2 adrenergic receptors suppresses fear conditioning: expression of c-Fos and phosphorylated CREB in mouse amygdala. Neuropsychopharmacology 29:229-239.

Dawson HN, Ferreira A, Eyster MV, Ghoshal N, Binder LI, Vitek MP (2001) Inhibition of neuronal maturation in primary hippocampal neurons from tau deficient mice. J Cell Sci 114:1179-1187.

de Kloet ER, Molendijk ML (2016) Coping with the Forced Swim Stressor: Towards Understanding an Adaptive Mechanism. Neural Plast 2016:6503162.

Del Cerro I, Martinez-Zalacain I, Guinea-Izquierdo A, Gascon-Bayarri J, Vinas-Diez V, Urretavizcaya M, Naval-Baudin P, Aguilera C, Rene-Ramirez R, Ferrer I, Menchon JM, Soria V, Soriano-Mas C (2020) Locus coeruleus connectivity alterations in late-life major depressive disorder during a visual oddball task. Neuroimage Clin 28:102482.

Del Tredici K, Braak H (2013) Dysfunction of the locus coeruleus-norepinephrine system and related circuitry in Parkinson's disease-related dementia. J Neurol Neurosurg Psychiatry 84:774-783.

Delaville C, Deurwaerdere PD, Benazzouz A (2011) Noradrenaline and Parkinson's disease. Front Syst Neurosci 5:31.

Delini-Stula A, Mogilnicka E, Hunn C, Dooley DJ (1984) Novelty-oriented behavior in the rat after selective damage of locus coeruleus projections by DSP-4, a new noradrenergic neurotoxin. Pharmacol Biochem Behav 20:613-618.

Devoto P, Flore G, Saba P, Fa M, Gessa GL (2005a) Stimulation of the locus coeruleus elicits noradrenaline and dopamine release in the medial prefrontal and parietal cortex. J Neurochem 92:368-374.

Devoto P, Flore G, Saba P, Fa M, Gessa GL (2005b) Co-release of noradrenaline and dopamine in the cerebral cortex elicited by single train and repeated train stimulation of the locus coeruleus. BMC Neurosci 6:31.

Do-Monte FH, Kincheski GC, Pavesi E, Sordi R, Assreuy J, Carobrez AP (2010) Role of beta-adrenergic receptors in the ventromedial prefrontal cortex during contextual fear extinction in rats. Neurobiol Learn Mem 94:318-328.

Dong Q, Ptacek LJ, Fu YH (2023) Mutant beta(1)-adrenergic receptor improves REM sleep and ameliorates tau accumulation in a mouse model of tauopathy. Proc Natl Acad Sci U S A 120:e2221686120.

Downs AM, Catavero CM, Kasten MR, McElligott ZA (2022) Tauopathy and alcohol consumption interact to alter locus coeruleus excitatory transmission and excitability in male and female mice. Alcohol.

Downs AM, Catavero CM, Kasten MR, McElligott ZA (2023) Tauopathy and alcohol consumption interact to alter locus coeruleus excitatory transmission and excitability in male and female mice. Alcohol 107:97-107.

Drubin DG, Kirschner MW (1986) Tau protein function in living cells. J Cell Biol 103:2739-2746.

Duesman SJ, Shetty S, Patel S, Ogale N, Mohamed F, Sparman N, Rajbhandari P, Rajbhandari AK (2022) Sexually dimorphic role of the locus coeruleus PAC1 receptors in regulating acute stress-associated energy metabolism. Front Behav Neurosci 16:995573.

Duffy KB, Ray B, Lahiri DK, Tilmont EM, Tinkler GP, Herbert RL, Greig NH, Ingram DK, Ottinger MA, Mattison JA (2019) Effects of Reducing Norepinephrine Levels via DSP4 Treatment

on Amyloid-beta Pathology in Female Rhesus Macaques (Macaca Mulatta). J Alzheimers Dis 68:115-126.

Dulawa SC, Hen R (2005) Recent advances in animal models of chronic antidepressant effects: the novelty-induced hypophagia test. Neurosci Biobehav Rev 29:771-783.

Duran E, Pandinelli M, Logothetis NK, Eschenko O (2023) Altered norepinephrine transmission after spatial learning impairs sleep-mediated memory consolidation in rats. Sci Rep 13:4231.

Dvorkin R, Shea SD (2022) Precise and Pervasive Phasic Bursting in Locus Coeruleus during Maternal Behavior in Mice. J Neurosci 42:2986-2999.

Ehrenberg AJ, Suemoto CK, Franca Resende EP, Petersen C, Leite REP, Rodriguez RD, Ferretti-Rebustini REL, You M, Oh J, Nitrini R, Pasqualucci CA, Jacob-Filho W, Kramer JH, Gatchel JR, Grinberg LT (2018) Neuropathologic Correlates of Psychiatric Symptoms in Alzheimer's Disease. J Alzheimers Dis 66:115-126.

Ehrenberg AJ, Nguy AK, Theofilas P, Dunlop S, Suemoto CK, Di Lorenzo Alho AT, Leite RP, Diehl Rodriguez R, Mejia MB, Rub U, Farfel JM, de Lucena Ferretti-Rebustini RE, Nascimento CF, Nitrini R, Pasquallucci CA, Jacob-Filho W, Miller B, Seeley WW, Heinsen H, Grinberg LT (2017) Quantifying the accretion of hyperphosphorylated tau in the locus coeruleus and dorsal raphe nucleus: the pathological building blocks of early Alzheimer's disease. Neuropathol Appl Neurobiol 43:393-408.

Ehrenberg AJ et al. (2023) Priorities for research on neuromodulatory subcortical systems in Alzheimer's disease: Position paper from the NSS PIA of ISTAART. Alzheimers Dement 19:2182-2196.

Ehrminger M, Latimier A, Pyatigorskaya N, Garcia-Lorenzo D, Leu-Semenescu S, Vidailhet M, Lehericy S, Arnulf I (2016) The coeruleus/subcoeruleus complex in idiopathic rapid eye movement sleep behaviour disorder. Brain 139:1180-1188.

Elman JA, Panizzon MS, Hagler DJ, Jr., Eyler LT, Granholm EL, Fennema-Notestine C, Lyons MJ, McEvoy LK, Franz CE, Dale AM, Kremen WS (2017) Task-evoked pupil dilation and BOLD variance as indicators of locus coeruleus dysfunction. Cortex 97:60-69.

Elobeid A, Soininen H, Alafuzoff I (2012) Hyperphosphorylated tau in young and middle-aged subjects. Acta Neuropathol 123:97-104.

Elrod R, Peskind ER, DiGiacomo L, Brodkin KI, Veith RC, Raskind MA (1997) Effects of Alzheimer's disease severity on cerebrospinal fluid norepinephrine concentration. Am J Psychiatry 154:25-30.

Engels-Dominguez N, Koops EA, Prokopiou PC, Van Egroo M, Schneider C, Riphagen JM, Singhal T, Jacobs HIL (2023) State-of-the-art imaging of neuromodulatory subcortical systems in aging and Alzheimer's disease: Challenges and opportunities. Neurosci Biobehav Rev 144:104998.

Ennis M, Aston-Jones G (1988) Activation of locus coeruleus from nucleus paragigantocellularis: a new excitatory amino acid pathway in brain. J Neurosci 8:3644-3657.

Fagan AM, Roe CM, Xiong C, Mintun MA, Morris JC, Holtzman DM (2007) Cerebrospinal fluid tau/beta-amyloid(42) ratio as a prediction of cognitive decline in nondemented older adults. Arch Neurol 64:343-349.

Farrand A, Jacquemet V, Verner R, Owens M, Beaumont E (2023) Vagus nerve stimulation parameters evoke differential neuronal responses in the locus coeruleus. Physiol Rep 11.

Finlayson PG, Marshall KC (1988) Synchronous bursting of locus coeruleus neurons in tissue culture. Neuroscience 24:217-225.

Fitzgerald PJ, Giustino TF, Seemann JR, Maren S (2015) Noradrenergic blockade stabilizes prefrontal activity and enables fear extinction under stress. Proc Natl Acad Sci U S A 112:E3729-3737.

Flores-Aguilar L, Hall H, Orciani C, Foret MK, Kovecses O, Ducatenzeiler A, Cuello AC (2022) Early loss of locus coeruleus innervation promotes cognitive and neuropathological changes before amyloid plaque deposition in a transgenic rat model of Alzheimer's disease. Neuropath Appl Neuro 48.

Florin-Lechner SM, Druhan JP, Aston-Jones G, Valentino RJ (1996) Enhanced norepinephrine release in prefrontal cortex with burst stimulation of the locus coeruleus. Brain Res 742:89-97.

Foote SL, Aston-Jones G, Bloom FE (1980) Impulse activity of locus coeruleus neurons in awake rats and monkeys is a function of sensory stimulation and arousal. Proc Natl Acad Sci U S A 77:3033-3037.

Foster SL, Galaj E, Karne SL, Ferre S, Weinshenker D (2021) Cell-type specific expression and behavioral impact of galanin and GalR1 in the locus coeruleus during opioid withdrawal. Addict Biol 26:e13037.

Friard O, Gamba M (2016) BORIS: a free, versatile open-source event-logging software for video/audio coding and live observations. British Ecological Society 7:1325-1330.

Fritsch T, Smyth KA, Debanne SM, Petot GJ, Friedland RP (2005) Participation in novelty-seeking leisure activities and Alzheimer's disease. J Geriatr Psychiatry Neurol 18:134-141.

Fujio K, Sato M, Uemura T, Sato T, Sato-Harada R, Harada A (2007) 14-3-3 proteins and protein phosphatases are not reduced in tau-deficient mice. Neuroreport 18:1049-1052.

Gannon M, Che P, Chen Y, Jiao K, Roberson ED, Wang Q (2015) Noradrenergic dysfunction in Alzheimer's disease. Front Neurosci 9:220.

Gatchel JR, Donovan NJ, Locascio JJ, Schultz AP, Becker JA, Chhatwal J, Papp KV, Amariglio RE, Rentz DM, Blacker D, Sperling RA, Johnson KA, Marshall GA (2017) Depressive Symptoms and Tau Accumulation in the Inferior Temporal Lobe and Entorhinal Cortex in Cognitively Normal Older Adults: A Pilot Study. J Alzheimers Dis 59:975-985.

Gazarini L, Stern CA, Carobrez AP, Bertoglio LJ (2013) Enhanced noradrenergic activity potentiates fear memory consolidation and reconsolidation by differentially recruiting alpha1- and beta-adrenergic receptors. Learn Mem 20:210-219.

Gazarini L, Stern CA, Piornedo RR, Takahashi RN, Bertoglio LJ (2014) PTSD-like memory generated through enhanced noradrenergic activity is mitigated by a dual step pharmacological intervention targeting its reconsolidation. Int J Neuropsychopharmacol 18.

Gendron TF, Petrucelli L (2009) The role of tau in neurodegeneration. Mol Neurodegener 4:13.

German DC, Manaye KF, White CL, 3rd, Woodward DJ, McIntire DD, Smith WK, Kalaria RN, Mann DM (1992) Disease-specific patterns of locus coeruleus cell loss. Ann Neurol 32:667-676.

Ghacibeh GA, Shenker JL, Shenal B, Uthman BM, Heilman KM (2006) The influence of vagus nerve stimulation on memory. Cogn Behav Neurol 19:119-122.

Ghosh A, Torraville SE, Mukherjee B, Walling SG, Martin GM, Harley CW, Yuan Q (2019) An experimental model of Braak's pretangle proposal for the origin of Alzheimer's disease: the role of locus coeruleus in early symptom development. Alzheimers Research & Therapy 11.

Ghosh A, Massaeli F, Power KD, Omoluabi T, Torraville SE, Pritchett JB, Sepahvand T, Strong VD, Reinhardt C, Chen X, Martin GM, Harley CW, Yuan Q (2021) Locus Coeruleus Activation Patterns Differentially Modulate Odor Discrimination Learning and Odor Valence in Rats. Cereb Cortex Commun 2:tgab026.

Gilvesy A, Husen E, Magloczky Z, Mihaly O, Hortobagyi T, Kanatani S, Heinsen H, Renier N, Hokfelt T, Mulder J, Uhlen M, Kovacs GG, Adori C (2022) Spatiotemporal characterization of cellular tau pathology in the human locus coeruleus-pericoerulear complex by three-dimensional imaging. Acta Neuropathol 144:651-676.

Giustino TF, Maren S (2018) Noradrenergic Modulation of Fear Conditioning and Extinction. Front Behav Neurosci 12:43.

Goedert M, Jakes R (2005) Mutations causing neurodegenerative tauopathies. Bba-Mol Basis Dis 1739:240-250.

Golebiowski M, Barcikowska M, Pfeffer A (1999) Magnetic resonance imaging-based hippocampal volumetry in patients with dementia of the Alzheimer type. Dement Geriatr Cogn Disord 10:284-288.

Gomez-Isla T, Hollister R, West H, Mui S, Growdon JH, Petersen RC, Parisi JE, Hyman BT (1997) Neuronal loss correlates with but exceeds neurofibrillary tangles in Alzheimer's disease. Ann Neurol 41:17-24.

Gong L, Shi M, Wang J, Xu RH, Yu SY, Liu D, Ding X, Zhang B, Zhang XP, Xi CH (2021) The Abnormal Functional Connectivity in the Locus Coeruleus-Norepinephrine System Associated With Anxiety Symptom in Chronic Insomnia Disorder. Front Neurosci-Switz 15.

Goodman AM, Langner BM, Jackson N, Alex C, McMahon LL (2021) Heightened Hippocampal beta-Adrenergic Receptor Function Drives Synaptic Potentiation and Supports Learning

and Memory in the TgF344-AD Rat Model during Prodromal Alzheimer's Disease. J Neurosci 41:5747-5761.

Grace AA, Bunney BS (1983) Intracellular and extracellular electrophysiology of nigral dopaminergic neurons--3. Evidence for electrotonic coupling. Neuroscience 10:333-348.

Grace AA, Bunney BS (1984) The control of firing pattern in nigral dopamine neurons: burst firing. J Neurosci 4:2877-2890.

Grant SJ, Aston-Jones G, Redmond DE, Jr. (1988) Responses of primate locus coeruleus neurons to simple and complex sensory stimuli. Brain Res Bull 21:401-410.

Groves DA, Bowman EM, Brown VJ (2005) Recordings from the rat locus coeruleus during acute vagal nerve stimulation in the anaesthetised rat. Neurosci Lett 379:174-179.

Grueschow M, Stenz N, Thorn H, Ehlert U, Breckwoldt J, Brodmann Maeder M, Exadaktylos AK, Bingisser R, Ruff CC, Kleim B (2021) Real-world stress resilience is associated with the responsivity of the locus coeruleus. Nat Commun 12:2275.

Grzanna R, Molliver ME (1980) The locus coeruleus in the rat: an immunohistochemical delineation. Neuroscience 5:21-40.

Grzanna R, Berger U, Fritschy JM, Geffard M (1989) Acute Action of Dsp-4 on Central Norepinephrine Axons - Biochemical and Immunohistochemical Evidence for Differential-Effects. J Histochem Cytochem 37:1435-1442.

Guerin D, Sacquet J, Mandairon N, Jourdan F, Didier A (2009) Early locus coeruleus degeneration and olfactory dysfunctions in Tg2576 mice. Neurobiol Aging 30:272-283.

Guo T, Noble W, Hanger DP (2017) Roles of tau protein in health and disease. Acta Neuropathologica 133:665-704.

Hagan JJ et al. (1999) Orexin A activates locus coeruleus cell firing and increases arousal in the rat. Proc Natl Acad Sci U S A 96:10911-10916.

Hagena H, Hansen N, Manahan-Vaughan D (2016) beta-Adrenergic Control of Hippocampal Function: Subserving the Choreography of Synaptic Information Storage and Memory. Cereb Cortex 26:1349-1364.

Hamann SB, Monarch ES, Goldstein FC (2000) Memory enhancement for emotional stimuli is impaired in early Alzheimer's disease. Neuropsychology 14:82-92.

Hammack SE, Cheung J, Rhodes KM, Schutz KC, Falls WA, Braas KM, May V (2009) Chronic stress increases pituitary adenylate cyclase-activating peptide (PACAP) and brain-derived neurotrophic factor (BDNF) mRNA expression in the bed nucleus of the stria terminalis (BNST): roles for PACAP in anxiety-like behavior. Psychoneuroendocrinology 34:833-843.

Hammerer D, Callaghan MF, Hopkins A, Kosciessa J, Betts M, Cardenas-Blanco A, Kanowski M, Weiskopf N, Dayan P, Dolan RJ, Duzel E (2018) Locus coeruleus integrity in old age is selectively related to memories linked with salient negative events. P Natl Acad Sci USA 115:2228-2233.

Hamze R, Delangre E, Tolu S, Moreau M, Janel N, Bailbe D, Movassat J (2022) Type 2 Diabetes Mellitus and Alzheimer's Disease: Shared Molecular Mechanisms and Potential Common Therapeutic Targets. International Journal of Molecular Sciences 23.

Hanes J, Zilka N, Bartkova M, Caletkova M, Dobrota D, Novak M (2009) Rat tau proteome consists of six tau isoforms: implication for animal models of human tauopathies. Journal of Neurochemistry 108:1167-1176.

Hansen N (2017) The Longevity of Hippocampus-Dependent Memory Is Orchestrated by the Locus Coeruleus-Noradrenergic System. Neural Plasticity 2017.

Hansen N, Manahan-Vaughan D (2015) Locus Coeruleus Stimulation Facilitates Long-Term Depression in the Dentate Gyrus That Requires Activation of beta-Adrenergic Receptors. Cereb Cortex 25:1889-1896.

Hardy JA, Higgins GA (1992) Alzheimer's disease: the amyloid cascade hypothesis. Science 256:184-185.

Harper JD, Lansbury PT, Jr. (1997) Models of amyloid seeding in Alzheimer's disease and scrapie: mechanistic truths and physiological consequences of the time-dependent solubility of amyloid proteins. Annu Rev Biochem 66:385-407.

Hashimoto H, Nogi H, Mori K, Ohishi H, Shigemoto R, Yamamoto K, Matsuda T, Mizuno N, Nagata S, Baba A (1996) Distribution of the mRNA for a pituitary adenylate cyclase-activating polypeptide receptor in the rat brain: an in situ hybridization study. J Comp Neurol 371:567-577.

Hayat H, Regev N, Matosevich N, Sales A, Paredes-Rodriguez E, Krom AJ, Bergman L, Li Y, Lavigne M, Kremer EJ, Yizhar O, Pickering AE, Nir Y (2020) Locus coeruleus norepinephrine activity mediates sensory-evoked awakenings from sleep. Sci Adv 6:eaaz4232.

Heneka MT, Nadrigny F, Regen T, Martinez-Hernandez A, Dumitrescu-Ozimek L, Terwel D, Jardanhazi-Kurutz D, Walter J, Kirchhoff F, Hanisch UK, Kummer MP (2010) Locus ceruleus controls Alzheimer's disease pathology by modulating microglial functions through norepinephrine. Proc Natl Acad Sci U S A 107:6058-6063.

Heneka MT, Ramanathan M, Jacobs AH, Dumitrescu-Ozimek L, Bilkei-Gorzo A, Debeir T, Sastre M, Galldiks N, Zimmer A, Hoehn M, Heiss WD, Klockgether T, Staufenbiel M (2006) Locus ceruleus degeneration promotes Alzheimer pathogenesis in amyloid precursor protein 23 transgenic mice. J Neurosci 26:1343-1354.

Henjum K, Watne LO, Godang K, Halaas NB, Eldholm RS, Blennow K, Zetterberg H, Saltvedt I, Bollerslev J, Knapskog AB (2022) Cerebrospinal fluid catecholamines in Alzheimer's disease patients with and without biological disease. Transl Psychiatry 12:151.

Herkenham M, Nauta WJ (1979) Efferent connections of the habenular nuclei in the rat. J Comp Neurol 187:19-47.

Hernandez F, Merchan-Rubira J, Valles-Saiz L, Rodriguez-Matellan A, Avila J (2020) Differences Between Human and Murine Tau at the N-terminal End. Frontiers in Aging Neuroscience 12.

Herrero MT, Hirsch EC, Kastner A, Ruberg M, Luquin MR, Laguna J, Javoyagid F, Obeso JA, Agid Y (1993) Does Neuromelanin Contribute to the Vulnerability of Catecholaminergic Neurons in Monkeys Intoxicated with Mptp. Neuroscience 56:499-511.

Herve-Minvielle A, Sara SJ (1995) Rapid habituation of auditory responses of locus coeruleus cells in anaesthetized and awake rats. Neuroreport 6:1363-1368.

Hezemans FH, Wolpe N, O'Callaghan C, Ye R, Rua C, Jones PS, Murley AG, Holland N, Regenthal R, Tsvetanov KA, Barker RA, Williams-Gray CH, Robbins TW, Passamonti L, Rowe JB (2022) Noradrenergic deficits contribute to apathy in Parkinson's disease through the precision of expected outcomes. PLoS Comput Biol 18:e1010079.

Hikishima K, Ando K, Komaki Y, Kawai K, Yano R, Inoue T, Itoh T, Yamada M, Momoshima S, Okano HJ, Okano H (2015) Voxel-based morphometry of the marmoset brain: In vivo detection of volume loss in the substantia nigra of the MPTP-treated Parkinson's disease model. Neuroscience 300:585-592.

Hirata H, Aston-Jones G (1994) A novel long-latency response of locus coeruleus neurons to noxious stimuli: mediation by peripheral C-fibers. J Neurophysiol 71:1752-1761.

Hirschberg S, Li Y, Randall A, Kremer EJ, Pickering AE (2017) Functional dichotomy in spinal- vs prefrontal-projecting locus coeruleus modules splits descending noradrenergic analgesia from ascending aversion and anxiety in rats. Elife 6.

Holets VR, Hokfelt T, Rokaeus A, Terenius L, Goldstein M (1988) Locus coeruleus neurons in the rat containing neuropeptide Y, tyrosine hydroxylase or galanin and their efferent projections to the spinal cord, cerebral cortex and hypothalamus. Neuroscience 24:893-906.

Holmes PV, Yoo HS, Dishman RK (2006) Voluntary exercise and clomipramine treatment elevate prepro-galanin mRNA levels in the locus coeruleus in rats. Neurosci Lett 408:1-4.

Holth JK, Bomben VC, Reed JG, Inoue T, Younkin L, Younkin SG, Pautler RG, Botas J, Noebels JL (2013) Tau loss attenuates neuronal network hyperexcitability in mouse and Drosophila genetic models of epilepsy. J Neurosci 33:1651-1659.

Hoogendijk WJ, Feenstra MG, Botterblom MH, Gilhuis J, Sommer IE, Kamphorst W, Eikelenboom P, Swaab DF (1999) Increased activity of surviving locus ceruleus neurons in Alzheimer's disease. Ann Neurol 45:82-91.

Horvath TL, Peyron C, Diano S, Ivanov A, Aston-Jones G, Kilduff TS, van Den Pol AN (1999) Hypocretin (orexin) activation and synaptic innervation of the locus coeruleus noradrenergic system. J Comp Neurol 415:145-159.

Hott SC, Gomes FV, Fabri DR, Reis DG, Crestani CC, Correa FM, Resstel LB (2012) Both alpha1- and beta1-adrenoceptors in the bed nucleus of the stria terminalis are involved in the expression of conditioned contextual fear. Br J Pharmacol 167:207-221.

Howells FM, Stein DJ, Russell VA (2012) Synergistic tonic and phasic activity of the locus coeruleus norepinephrine (LC-NE) arousal system is required for optimal attentional performance. Metab Brain Dis 27:267-274.

Huang Y, Yu S, Wilson G, Park J, Cheng M, Kong X, Lu T, Kong J (2021) Altered Extended Locus Coeruleus and Ventral Tegmental Area Networks in Boys with Autism Spectrum Disorders: A Resting-State Functional Connectivity Study. Neuropsychiatr Dis Treat 17:1207-1216.

Huijbers W, Schultz AP, Papp KV, LaPoint MR, Hanseeuw B, Chhatwal JP, Hedden T, Johnson KA, Sperling RA (2019) Tau Accumulation in Clinically Normal Older Adults Is Associated with Hippocampal Hyperactivity. J Neurosci 39:548-556.

Hulsey DR, Riley JR, Loerwald KW, Rennaker RL, 2nd, Kilgard MP, Hays SA (2017) Parametric characterization of neural activity in the locus coeruleus in response to vagus nerve stimulation. Exp Neurol 289:21-30.

Hunsley MS, Palmiter RD (2003) Norepinephrine-deficient mice exhibit normal sleep-wake states but have shorter sleep latency after mild stress and low doses of amphetamine. Sleep 26:521-526.

Hunsley MS, Palmiter RD (2004) Altered sleep latency and arousal regulation in mice lacking norepinephrine. Pharmacol Biochem Behav 78:765-773.

Hunsley MS, Curtis WR, Palmiter RD (2006) Behavioral and sleep/wake characteristics of mice lacking norepinephrine and hypocretin. Genes Brain Behav 5:451-457.

Hussain LS, Reddy V, Maani CV (2023) Physiology, Noradrenergic Synapse. In: StatPearls. Treasure Island (FL).

Hutten DR, Bos JHJ, de Vos S, Hak E (2022) Targeting the Beta-2-Adrenergic Receptor and the Risk of Developing Alzheimer's Disease: A Retrospective Inception Cohort Study. J Alzheimers Dis 87:1089-1101.

Hwang DY, Carlezon WA, Jr., Isacson O, Kim KS (2001) A high-efficiency synthetic promoter that drives transgene expression selectively in noradrenergic neurons. Hum Gene Ther 12:1731-1740.

Hyun Joo Y, Kaoru N, Shubir D, Jungwon M, Christine C, Julian FT, Paul L, Catie C, Mara M (2023) Daily biofeedback to modulate heart rate oscillations affects structural volume in hippocampal subregions targeted by the locus coeruleus in older adults but not younger adults. medRxiv:2023.2003.2002.23286715.

Iannitelli AF, Segal A, Pare JF, Mulvey B, Liles LC, Sloan SA, McCann KE, Dougherty JD, Smith Y, Weinshenker D (2023a) Tyrosinase-induced neuromelanin accumulation triggers rapid dysregulation and degeneration of the mouse locus coeruleus. bioRxiv.

Iannitelli AF, Kelberman MA, Lustberg DJ, Korukonda A, McCann KE, Mulvey B, Segal A, Liles LC, Sloan SA, Dougherty JD, Weinshenker D (2023b) The Neurotoxin DSP-4 Dysregulates the Locus Coeruleus-Norepinephrine System and Recapitulates Molecular and Behavioral Aspects of Prodromal Neurodegenerative Disease. eNeuro 10.

Iba M, Guo JL, McBride JD, Zhang B, Trojanowski JQ, Lee VMY (2013) Synthetic Tau Fibrils Mediate Transmission of Neurofibrillary Tangles in a Transgenic Mouse Model of Alzheimer's-Like Tauopathy. Journal of Neuroscience 33:1024-1037.

Iba M, McBride JD, Guo JL, Zhang B, Trojanowski JQ, Lee VMY (2015) Tau pathology spread in PS19 tau transgenic mice following locus coeruleus (LC) injections of synthetic tau fibrils is determined by the LC's afferent and efferent connections. Acta Neuropathologica 130:349-362.

Il Jacobs H, Priovoulos N, Poser BA, Pagen LHG, Ivanov D, Verhey FRJ, Uludag K (2020) Dynamic behavior of the locus coeruleus during arousal-related memory processing in a multi-modal 7T fMRI paradigm. Elife 9.

Inutsuka A, Yamanaka A (2013) The physiological role of orexin/hypocretin neurons in the regulation of sleep/wakefulness and neuroendocrine functions. Front Endocrinol (Lausanne) 4:18.

Iro CM, Hamati R, El Mansari M, Blier P (2021) Repeated but Not Single Administration of Ketamine Prolongs Increases of the Firing Activity of Norepinephrine and Dopamine Neurons. Int J Neuropsychopharmacol 24:570-579.

Ishimatsu M, Williams JT (1996) Synchronous activity in locus coeruleus results from dendritic interactions in pericoerulear regions. J Neurosci 16:5196-5204.

Ittner LM, Ke YD, Delerue F, Bi M, Gladbach A, van Eersel J, Wolfing H, Chieng BC, Christie MJ, Napier IA, Eckert A, Staufenbiel M, Hardeman E, Gotz J (2010) Dendritic function of tau mediates amyloid-beta toxicity in Alzheimer's disease mouse models. Cell 142:387-397.

Jacobs HI, Wiese S, van de Ven V, Gronenschild EH, Verhey FR, Matthews PM (2015a) Relevance of parahippocampal-locus coeruleus connectivity to memory in early dementia. Neurobiol Aging 36:618-626.

Jacobs HI, Priovoulos N, Poser BA, Pagen LH, Ivanov D, Verhey FR, Uludag K (2020) Dynamic behavior of the locus coeruleus during arousal-related memory processing in a multi-modal 7T fMRI paradigm. Elife 9.

Jacobs HIL, Muller-Ehrenberg L, Priovoulos N, Roebroeck A (2018) Curvilinear locus coeruleus functional connectivity trajectories over the adult lifespan: a 7T MRI study. Neurobiology of Aging 69:167-176.

Jacobs HIL, Wiese S, van de Ven V, Gronenschild EHBM, Verhey FRJ, Matthews PM (2015b) Relevance of parahippocampal-locus coeruleus connectivity to memory in early dementia. Neurobiology of Aging 36:618-626.

Jacobs HIL, Becker JA, Kwong K, Engels-Dominguez N, Prokopiou PC, Papp KV, Properzi M, Hampton OL, d'Oleire Uquillas F, Sanchez JS, Rentz DM, El Fakhri G, Normandin MD, Price JC, Bennett DA, Sperling RA, Johnson KA (2021) In vivo and neuropathology data support locus coeruleus integrity as indicator of Alzheimer's disease pathology and cognitive decline. Sci Transl Med 13:eabj2511.

Janitzky K (2020) Impaired Phasic Discharge of Locus Coeruleus Neurons Based on Persistent High Tonic Discharge-A New Hypothesis With Potential Implications for Neurodegenerative Diseases. Front Neurol 11:371.

Janitzky K, Lippert MT, Engelhorn A, Tegtmeier J, Goldschmidt J, Heinze HJ, Ohl FW (2015) Optogenetic silencing of locus coeruleus activity in mice impairs cognitive flexibility in an attentional set-shifting task. Front Behav Neurosci 9:286.

Jankowsky JL, Zheng H (2017) Practical considerations for choosing a mouse model of Alzheimer's disease. Mol Neurodegener 12:89.

Jardanhazi-Kurutz D, Kummer MP, Terwel D, Vogel K, Dyrks T, Thiele A, Heneka MT (2010) Induced LC degeneration in APP/PS1 transgenic mice accelerates early cerebral amyloidosis and cognitive deficits. Neurochem Int 57:375-382.

Jeganathan S, von Bergen M, Mandelkow EM, Mandelkow E (2008) The natively unfolded character of Tau and its aggregation to Alzheimer-like paired helical filaments. Biochemistry-Us 47:10526-10539.

Jin M, Shepardson N, Yang T, Chen G, Walsh D, Selkoe DJ (2011) Soluble amyloid beta-protein dimers isolated from Alzheimer cortex directly induce Tau hyperphosphorylation and neuritic degeneration. Proc Natl Acad Sci U S A 108:5819-5824.

Jodo E, Aston-Jones G (1997) Activation of locus coeruleus by prefrontal cortex is mediated by excitatory amino acid inputs. Brain Res 768:327-332.

Johansson M, Stomrud E, Insel PS, Leuzy A, Johansson PM, Smith R, Ismail Z, Janelidze S, Palmqvist S, van Westen D, Mattsson-Carlgren N, Hansson O (2021) Mild behavioral impairment and its relation to tau pathology in preclinical Alzheimer's disease. Transl Psychiatry 11:76.

Jorm CM, Stamford JA (1993) Actions of the hypnotic anaesthetic, dexmedetomidine, on noradrenaline release and cell firing in rat locus coeruleus slices. Br J Anaesth 71:447-449.

Joshi S, Li Y, Kalwani RM, Gold JI (2016) Relationships between Pupil Diameter and Neuronal Activity in the Locus Coeruleus, Colliculi, and Cingulate Cortex. Neuron 89:221-234.

Ju YE, McLeland JS, Toedebusch CD, Xiong C, Fagan AM, Duntley SP, Morris JC, Holtzman DM (2013) Sleep quality and preclinical Alzheimer disease. JAMA Neurol 70:587-593.

Jul P, Volbracht C, de Jong IE, Helboe L, Elvang AB, Pedersen JT (2016) Hyperactivity with Agitative-Like Behavior in a Mouse Tauopathy Model. J Alzheimers Dis 49:783-795.

Juottonen K, Laakso MP, Partanen K, Soininen H (1999) Comparative MR analysis of the entorhinal cortex and hippocampus in diagnosing Alzheimer disease. AJNR Am J Neuroradiol 20:139-144.

Kadavath H, Hofele RV, Biernat J, Kumar S, Tepper K, Urlaub H, Mandelkow E, Zweckstetter M (2015) Tau stabilizes microtubules by binding at the interface between tubulin heterodimers. P Natl Acad Sci USA 112:7501-7506.

Kaitin KI, Bliwise DL, Gleason C, Nino-Murcia G, Dement WC, Libet B (1986) Sleep disturbance produced by electrical stimulation of the locus coeruleus in a human subject. Biol Psychiatry 21:710-716.

Kalwani RM, Joshi S, Gold JI (2014) Phasic activation of individual neurons in the locus ceruleus/subceruleus complex of monkeys reflects rewarded decisions to go but not stop. J Neurosci 34:13656-13669.

Kane GA, Vazey EM, Wilson RC, Shenhav A, Daw ND, Aston-Jones G, Cohen JD (2017) Increased locus coeruleus tonic activity causes disengagement from a patch-foraging task. Cogn Affect Behav Neurosci 17:1073-1083.

Kang SS, Ahn EH, Liu X, Bryson M, Miller GW, Weinshenker D, Ye K (2021) ApoE4 inhibition of VMAT2 in the locus coeruleus exacerbates Tau pathology in Alzheimer's disease. Acta Neuropathol 142:139-158.

Kang SS, Liu X, Ahn EH, Xiang J, Manfredsson FP, Yang X, Luo HR, Liles LC, Weinshenker D, Ye K (2020) Norepinephrine metabolite DOPEGAL activates AEP and pathological Tau aggregation in locus coeruleus. J Clin Invest 130:422-437.

Kang SS, Meng L, Zhang X, Wu Z, Mancieri A, Xie B, Liu X, Weinshenker D, Peng J, Zhang Z, Ye K (2022) Tau modification by the norepinephrine metabolite DOPEGAL stimulates its pathology and propagation. Nat Struct Mol Biol 29:292-305.

Karapetyan G, Fereshetyan K, Harutyunyan H, Yenkoyan K (2022) The synergy of beta amyloid 1-42 and oxidative stress in the development of Alzheimer's disease-like neurodegeneration of hippocampal cells. Sci Rep 12:17883.

Karch CM, Goate AM (2015) Alzheimer's disease risk genes and mechanisms of disease pathogenesis. Biol Psychiatry 77:43-51.

Kawahara Y, Hesselink MB, van Scharrenburg G, Westerink BH (2004) Tonic inhibition by orphanin FQ/nociceptin of noradrenaline neurotransmission in the amygdala. Eur J Pharmacol 485:197-200.

Kebschull JM, Garcia da Silva P, Reid AP, Peikon ID, Albeanu DF, Zador AM (2016) High-Throughput Mapping of Single-Neuron Projections by Sequencing of Barcoded RNA. Neuron 91:975-987.

Keehn B, Kadlaskar G, Bergmann S, McNally Keehn R, Francis A (2021) Attentional Disengagement and the Locus Coeruleus - Norepinephrine System in Children With Autism Spectrum Disorder. Front Integr Neurosci 15:716447.

Kelberman M, Keilholz S, Weinshenker D (2020) What's That (Blue) Spot on my MRI? Multimodal Neuroimaging of the Locus Coeruleus in Neurodegenerative Disease. Front Neurosci 14:583421.

Kelberman MA, Anderson CR, Chlan E, Rorabaugh JM, McCann KE, Weinshenker D (2022) Consequences of Hyperphosphorylated Tau in the Locus Coeruleus on Behavior and Cognition in a Rat Model of Alzheimer's Disease. J Alzheimers Dis 86:1037-1059.

Kelberman MA, Rorabaugh JM, Anderson CR, Marriott A, DePuy SD, Rasmussen K, McCann KE, Weiss JM, Weinshenker D (2023) Age-dependent dysregulation of locus coeruleus firing in a transgenic rat model of Alzheimer's disease. Neurobiol Aging 125:98-108.

Kelly L, Seifi M, Ma R, Mitchell SJ, Rudolph U, Viola KL, Klein WL, Lambert JJ, Swinny JD (2021) Identification of intraneuronal amyloid beta oligomers in locus coeruleus neurons of Alzheimer's patients and their potential impact on inhibitory neurotransmitter receptors and neuronal excitability. Neuropathol Appl Neurobiol 47:488-505.

Kelly SC, He B, Perez SE, Ginsberg SD, Mufson EJ, Counts SE (2017) Locus coeruleus cellular and molecular pathology during the progression of Alzheimer's disease. Acta Neuropathol Commun 5:8.

Kelly SC, McKay EC, Beck JS, Collier TJ, Dorrance AM, Counts SE (2019) Locus Coeruleus Degeneration Induces Forebrain Vascular Pathology in a Transgenic Rat Model of Alzheimer's Disease. Journal of Alzheimers Disease 70:369-386.

Kempadoo KA, Mosharov EV, Choi SJ, Sulzer D, Kandel ER (2016) Dopamine release from the locus coeruleus to the dorsal hippocampus promotes spatial learning and memory. Proc Natl Acad Sci U S A 113:14835-14840.

Khakpour-Taleghani B, Lashgari R, Motamedi F, Naghdi N (2009) Effect of reversible inactivation of locus ceruleus on spatial reference and working memory. Neuroscience 158:1284-1291.

Khoury R, Ghossoub E (2019) Diagnostic biomarkers of Alzheimer’s disease: A state-of-the-art review. Biomarkers in Neuropsychiatry 1:100005.

Kjaerby C, Andersen M, Hauglund N, Untiet V, Dall C, Sigurdsson B, Ding F, Feng J, Li Y, Weikop P, Hirase H, Nedergaard M (2022) Memory-enhancing properties of sleep depend on the oscillatory amplitude of norepinephrine. Nat Neurosci 25:1059-1070.

Klimek V, Stockmeier C, Overholser J, Meltzer HY, Kalka S, Dilley G, Ordway GA (1997) Reduced levels of norepinephrine transporters in the locus coeruleus in major depression. J Neurosci 17:8451-8458.

Klunk WE et al. (2004) Imaging brain amyloid in Alzheimer's disease with Pittsburgh Compound-B. Ann Neurol 55:306-319.

Knudsen K, Fedorova TD, Hansen AK, Sommerauer M, Otto M, Svendsen KB, Nahimi A, Stokholm MG, Pavese N, Beier CP, Brooks DJ, Borghammer P (2018) In-vivo staging of pathology in REM sleep behaviour disorder: a multimodality imaging case-control study. Lancet Neurol 17:618-628.

Kosel F, Pelley JMS, Franklin TB (2020) Behavioural and psychological symptoms of dementia in mouse models of Alzheimer's disease-related pathology. Neurosci Biobehav Rev 112:634-647.

Kreuzer M, Keating GL, Fenzl T, Hartner L, Sinon CG, Hajjar I, Ciavatta V, Rye DB, Garcia PS (2020) Sleep/Wake Behavior and EEG Signatures of the TgF344-AD Rat Model at the Prodromal Stage. Int J Mol Sci 21.

Kuo CC, Hsieh JC, Tsai HC, Kuo YS, Yau HJ, Chen CC, Chen RF, Yang HW, Min MY (2020) Inhibitory interneurons regulate phasic activity of noradrenergic neurons in the mouse locus coeruleus and functional implications. J Physiol 598:4003-4029.

Lacor PN, Buniel MC, Furlow PW, Clemente AS, Velasco PT, Wood M, Viola KL, Klein WL (2007) Abeta oligomer-induced aberrations in synapse composition, shape, and density provide a molecular basis for loss of connectivity in Alzheimer's disease. J Neurosci 27:796-807.

LaLumiere RT, Buen TV, McGaugh JL (2003) Post-training intra-basolateral amygdala infusions of norepinephrine enhance consolidation of memory for contextual fear conditioning. J Neurosci 23:6754-6758.

Lang R, Gundlach AL, Holmes FE, Hobson SA, Wynick D, Hokfelt T, Kofler B (2015) Physiology, signaling, and pharmacology of galanin peptides and receptors: three decades of emerging diversity. Pharmacol Rev 67:118-175.

Lauren J, Gimbel DA, Nygaard HB, Gilbert JW, Strittmatter SM (2009) Cellular prion protein mediates impairment of synaptic plasticity by amyloid-beta oligomers. Nature 457:1128-1132.

Lazzaro SC, Hou M, Cunha C, LeDoux JE, Cain CK (2010) Antagonism of lateral amygdala alpha1-adrenergic receptors facilitates fear conditioning and long-term potentiation. Learn Mem 17:489-493.

Lee A, Rosin DL, Van Bockstaele EJ (1998) alpha2A-adrenergic receptors in the rat nucleus locus coeruleus: subcellular localization in catecholaminergic dendrites, astrocytes, and presynaptic axon terminals. Brain Res 795:157-169.

Lei P, Ayton S, Finkelstein DI, Spoerri L, Ciccotosto GD, Wright DK, Wong BX, Adlard PA, Cherny RA, Lam LQ, Roberts BR, Volitakis I, Egan GF, McLean CA, Cappai R, Duce JA, Bush AI (2012) Tau deficiency induces parkinsonism with dementia by impairing APP-mediated iron export. Nat Med 18:291-295.

Leon WC, Canneva F, Partridge V, Allard S, Ferretti MT, DeWilde A, Vercauteren F, Atifeh R, Ducatenzeiler A, Klein W, Szyf M, Alhonen L, Cuello AC (2010) A Novel Transgenic Rat Model with a Full Alzheimer's-Like Amyloid Pathology Displays Pre-Plaque Intracellular Amyloid-beta-Associated Cognitive Impairment. Journal of Alzheimers Disease 20:113-126.

Leuner K, Muller WE, Reichert AS (2012) From mitochondrial dysfunction to amyloid beta formation: novel insights into the pathogenesis of Alzheimer's disease. Mol Neurobiol 46:186-193.

Levey AI et al. (2021) A phase II study repurposing atomoxetine for neuroprotection in mild cognitive impairment. Brain.

Levey AI et al. (2022) A phase II study repurposing atomoxetine for neuroprotection in mild cognitive impairment. Brain 145:1924-1938.

Li HW, Zhang L, Qin C (2019a) Current state of research on non-human primate models of Alzheimer's disease. Animal Model Exp Med 2:227-238.

Li S, Jin M, Zhang D, Yang T, Koeglsperger T, Fu H, Selkoe DJ (2013) Environmental novelty activates beta2-adrenergic signaling to prevent the impairment of hippocampal LTP by Abeta oligomers. Neuron 77:929-941.

Li S, Shi Y, Yao X, Wang X, Shen L, Rao Z, Yuan J, Liu Y, Zhou Z, Zhang Z, Liu F, Han S, Geng J, Yang H, Cheng L (2019b) Conversion of Astrocytes and Fibroblasts into Functional Noradrenergic Neurons. Cell Rep 28:682-697 e687.

Lin CC, Tung CS, Lin PH, Huang CL, Liu YP (2016) Traumatic stress causes distinctive effects on fear circuit catecholamines and the fear extinction profile in a rodent model of posttraumatic stress disorder. Eur Neuropsychopharmacol 26:1484-1495.

Liu KY, Kievit RA, Tsvetanov KA, Betts MJ, Duzel E, Rowe JB, Howard R, Hammerer D, Cam-CAN (2020) Noradrenergic-dependent functions are associated with age-related locus coeruleus signal intensity differences. Nature Communications 11.

Liu X, Ye KQ, Weinshenker D (2015) Norepinephrine Protects against Amyloid-beta Toxicity via TrkB. Journal of Alzheimers Disease 44:251-260.

Liu Y, Rodenkirch C, Moskowitz N, Schriver B, Wang Q (2017) Dynamic Lateralization of Pupil Dilation Evoked by Locus Coeruleus Activation Results from Sympathetic, Not Parasympathetic, Contributions. Cell Rep 20:3099-3112.

Liu Y, Yoo MJ, Savonenko A, Stirling W, Price DL, Borchelt DR, Mamounas L, Lyons WE, Blue ME, Lee MK (2008) Amyloid pathology is associated with progressive monoaminergic neurodegeneration in a transgenic mouse model of Alzheimer's disease. J Neurosci 28:13805-13814.

Liu YU, Ying Y, Li Y, Eyo UB, Chen T, Zheng J, Umpierre AD, Zhu J, Bosco DB, Dong H, Wu LJ (2019) Neuronal network activity controls microglial process surveillance in awake mice via norepinephrine signaling. Nat Neurosci 22:1771-1781.

Lopes S, Lopes A, Pinto V, Guimaraes MR, Sardinha VM, Duarte-Silva S, Pinheiro S, Pizarro J, Oliveira JF, Sousa N, Leite-Almeida H, Sotiropoulos I (2016) Absence of Tau triggers

age-dependent sciatic nerve morphofunctional deficits and motor impairment. Aging Cell 15:208-216.

Loughlin SE, Foote SL, Fallon JH (1982) Locus coeruleus projections to cortex: topography, morphology and collateralization. Brain Res Bull 9:287-294.

Loughlin SE, Foote SL, Grzanna R (1986) Efferent projections of nucleus locus coeruleus: morphologic subpopulations have different efferent targets. Neuroscience 18:307-319.

Lu J, Bjorkum AA, Xu M, Gaus SE, Shiromani PJ, Saper CB (2002) Selective activation of the extended ventrolateral preoptic nucleus during rapid eye movement sleep. J Neurosci 22:4568-4576.

Ludwig M, Wienke C, Betts MJ, Zaehle T, Hammerer D (2021) Current challenges in reliably targeting the noradrenergic locus coeruleus using transcutaneous auricular vagus nerve stimulation (taVNS). Auton Neurosci-Basic 236.

Luskin AT, Li L, Fu X, Barcomb K, Blackburn T, Li EM, Rana A, Simon RC, Sun L, Murry AD, Golden SA, Stuber GD, Ford CP, Gu L, Bruchas MR (2022) A diverse network of pericoerulear neurons control arousal states.2022.2006.2030.498327.

Lustberg D, Iannitelli AF, Tillage RP, Pruitt M, Liles LC, Weinshenker D (2020a) Central norepinephrine transmission is required for stress-induced repetitive behavior in two rodent models of obsessive-compulsive disorder. Psychopharmacology (Berl) 237:1973-1987.

Lustberg D, Tillage RP, Bai Y, Pruitt M, Liles LC, Weinshenker D (2020b) Noradrenergic circuits in the forebrain control affective responses to novelty. Psychopharmacology (Berl) 237:3337-3355.

Lustberg DJ, Liu JQ, Iannitelli AF, Vanderhoof SO, Liles LC, McCann KE, Weinshenker D (2022) Norepinephrine and dopamine contribute to distinct repetitive behaviors induced by novel odorant stress in male and female mice. Horm Behav 144:105205.

Ma QL, Zuo X, Yang F, Ubeda OJ, Gant DJ, Alaverdyan M, Kiosea NC, Nazari S, Chen PP, Nothias F, Chan P, Teng E, Frautschy SA, Cole GM (2014) Loss of MAP function leads to hippocampal synapse loss and deficits in the Morris Water Maze with aging. J Neurosci 34:7124-7136.

Maldonado R (1997) Participation of noradrenergic pathways in the expression of opiate withdrawal: biochemical and pharmacological evidence. Neurosci Biobehav Rev 21:91-104.

Mallo SC, Ismail Z, Pereiro AX, Facal D, Lojo-Seoane C, Campos-Magdaleno M, Juncos-Rabadan O (2018) Assessing Mild Behavioral Impairment with the Mild Behavioral Impairment-Checklist in People with Mild Cognitive Impairment. J Alzheimers Dis 66:83-95.

Manaye KF, Mcintire DD, Mann DMA, German DC (1995) Locus-Coeruleus Cell Loss in the Aging Human Brain - a Nonrandom Process. Journal of Comparative Neurology 358:79-87.

Manczak M, Anekonda TS, Henson E, Park BS, Quinn J, Reddy PH (2006) Mitochondria are a direct site of A beta accumulation in Alzheimer's disease neurons: implications for free radical generation and oxidative damage in disease progression. Hum Mol Genet 15:1437-1449.

Mandelkow EM, Mandelkow E (2012) Biochemistry and cell biology of tau protein in neurofibrillary degeneration. Cold Spring Harb Perspect Med 2:a006247.

Mann DMA, Yates PO (1974) Lipoprotein Pigments - Their Relationship to Aging in Human Nervous-System .2. Melanin Content of Pigmented Nerve-Cells. Brain 97:489-+.

Mansour A, Fox CA, Burke S, Meng F, Thompson RC, Akil H, Watson SJ (1994) Mu, delta, and kappa opioid receptor mRNA expression in the rat CNS: an in situ hybridization study. J Comp Neurol 350:412-438.

Mao P, Reddy PH (2011) Aging and amyloid beta-induced oxidative DNA damage and mitochondrial dysfunction in Alzheimer's disease: implications for early intervention and therapeutics. Biochim Biophys Acta 1812:1359-1370.

Maren S, Holmes A (2016) Stress and Fear Extinction. Neuropsychopharmacology 41:58-79.

Marinkovic P, Blumenstock S, Goltstein PM, Korzhova V, Peters F, Knebl A, Herms J (2019) In vivo imaging reveals reduced activity of neuronal circuits in a mouse tauopathy model. Brain 142:1051-1062.

Marino MD, Bourdelat-Parks BN, Cameron Liles L, Weinshenker D (2005) Genetic reduction of noradrenergic function alters social memory and reduces aggression in mice. Behav Brain Res 161:197-203.

Marner L, Soborg C, Pakkenberg B (2005) Increased volume of the pigmented neurons in the locus coeruleus of schizophrenic subjects: a stereological study. J Psychiatr Res 39:337-345.

Marquie M et al. (2017) Pathological correlations of [F-18]-AV-1451 imaging in non-alzheimer tauopathies. Annals of Neurology 81:117-128.

Martchek M, Thevarkunnel S, Bauman M, Blatt G, Kemper T (2006) Lack of evidence of neuropathology in the locus coeruleus in autism. Acta Neuropathol 111:497-499.

Martin-Belmonte A, Aguado C, Alfaro-Ruiz R, Itakura M, Moreno-Martinez AE, de la Ossa L, Molnar E, Fukazawa Y, Lujan R (2020) Age-Dependent Shift of AMPA Receptors From

Synapses to Intracellular Compartments in Alzheimer's Disease: Immunocytochemical Analysis of the CA1 Hippocampal Region in APP/PS1 Transgenic Mouse Model. Front Aging Neurosci 12:577996.

Martin L, Latypova X, Terro F (2011) Post-translational modifications of tau protein: implications for Alzheimer's disease. Neurochem Int 58:458-471.

Martinez G, Vernooij RW, Fuentes Padilla P, Zamora J, Bonfill Cosp X, Flicker L (2017) 18F PET with florbetapir for the early diagnosis of Alzheimer's disease dementia and other dementias in people with mild cognitive impairment (MCI). Cochrane Database Syst Rev 11:CD012216.

Marzo A, Totah NK, Neves RM, Logothetis NK, Eschenko O (2014) Unilateral electrical stimulation of rat locus coeruleus elicits bilateral response of norepinephrine neurons and sustained activation of medial prefrontal cortex. J Neurophysiol 111:2570-2588.

Mason ST, Fibiger HC (1979) Regional topography within noradrenergic locus coeruleus as revealed by retrograde transport of horseradish peroxidase. J Comp Neurol 187:703-724.

Matchett BJ, Grinberg LT, Theofilas P, Murray ME (2021) The mechanistic link between selective vulnerability of the locus coeruleus and neurodegeneration in Alzheimer's disease. Acta Neuropathol 141:631-650.

Mather M, Clewett D, Sakaki M, Harley CW (2016) Norepinephrine ignites local hotspots of neuronal excitation: How arousal amplifies selectivity in perception and memory. Behav Brain Sci 39:e200.

Matschke LA, Komadowski MA, Stohr A, Lee B, Henrich MT, Griesbach M, Rinne S, Geibl FF, Chiu WH, Koprich JB, Brotchie JM, Kiper AK, Dolga AM, Oertel WH, Decher N (2022)

Enhanced firing of locus coeruleus neurons and SK channel dysfunction are conserved in distinct models of prodromal Parkinson's disease. Sci Rep-Uk 12.

Matsumoto M, Nakamachi T, Watanabe J, Sugiyama K, Ohtaki H, Murai N, Sasaki S, Xu Z, Hashimoto H, Seki T, Miyazaki A, Shioda S (2016) Pituitary Adenylate Cyclase-Activating Polypeptide (PACAP) Is Involved in Adult Mouse Hippocampal Neurogenesis After Stroke. J Mol Neurosci 59:270-279.

Matthews KL, Chen CP, Esiri MM, Keene J, Minger SL, Francis PT (2002) Noradrenergic changes, aggressive behavior, and cognition in patients with dementia. Biol Psychiatry 51:407-416.

McBurney-Lin J, Vargova G, Garad M, Zagha E, Yang H (2022) The locus coeruleus mediates behavioral flexibility. Cell Rep 41:111534.

McCall JG, Al-Hasani R, Siuda ER, Hong DY, Norris AJ, Ford CP, Bruchas MR (2015) CRH Engagement of the Locus Coeruleus Noradrenergic System Mediates Stress-Induced Anxiety. Neuron 87:605-620.

McCormack AL, Di Monte DA, Delfani K, Irwin I, DeLanney LE, Langston WJ, Janson AM (2004) Aging of the nigrostriatal system in the squirrel monkey. Journal of Comparative Neurology 471:387-395.

McCune SK, Voigt MM, Hill JM (1993) Expression of multiple alpha adrenergic receptor subtype messenger RNAs in the adult rat brain. Neuroscience 57:143-151.

McMillan PJ, White SS, Franklin A, Greenup JL, Leverenz JB, Raskind MA, Szot P (2011) Differential response of the central noradrenergic nervous system to the loss of locus coeruleus neurons in Parkinson's disease and Alzheimer's disease. Brain Res 1373:240-252.

Megemont M, McBurney-Lin J, Yang H (2022) Pupil diameter is not an accurate real-time readout of locus coeruleus activity. Elife 11.

Mehla J, Lacoursiere SG, Lapointe V, McNaughton BL, Sutherland RJ, McDonald RJ, Mohajerani MH (2019) Age-dependent behavioral and biochemical characterization of single APP knock-in mouse (APP(NL-G-F/NL-G-F)) model of Alzheimer's disease. Neurobiol Aging 75:25-37.

Michailidis M, Moraitou D, Tata DA, Kalinderi K, Papamitsou T, Papaliagkas V (2022) Alzheimer's Disease as Type 3 Diabetes: Common Pathophysiological Mechanisms between Alzheimer's Disease and Type 2 Diabetes. International Journal of Molecular Sciences 23.

Miller MA, Kolb PE, Leverenz JB, Peskind ER, Raskind MA (1999) Preservation of noradrenergic neurons in the locus ceruleus that coexpress galanin mRNA in Alzheimer's disease. J Neurochem 73:2028-2036.

Minter MR, Taylor JM, Crack PJ (2016) The contribution of neuroinflammation to amyloid toxicity in Alzheimer's disease. J Neurochem 136:457-474.

Mittal S et al. (2017) beta2-Adrenoreceptor is a regulator of the alpha-synuclein gene driving risk of Parkinson's disease. Science 357:891-898.

Mouton PR, Pakkenberg B, Gundersen HJ, Price DL (1994) Absolute number and size of pigmented locus coeruleus neurons in young and aged individuals. J Chem Neuroanat 7:185-190.

Mukrasch MD, Biernat J, von Bergen M, Griesinger C, Mandelkow E, Zweckstetter M (2005) Sites of tau important for aggregation populate beta-structure and bind to microtubules and polyanions. J Biol Chem 280:24978-24986.

Mulvey B, Bhatti DL, Gyawali S, Lake AM, Kriaucionis S, Ford CP, Bruchas MR, Heintz N, Dougherty JD (2018) Molecular and Functional Sex Differences of Noradrenergic Neurons in the Mouse Locus Coeruleus. Cell Rep 23:2225-2235.

Munoz-Moreno E, Tudela R, Lopez-Gil X, Soria G (2018) Early brain connectivity alterations and cognitive impairment in a rat model of Alzheimer's disease. Alzheimers Res Ther 10:16.

Murchison CF, Zhang XY, Zhang WP, Ouyang M, Lee A, Thomas SA (2004) A distinct role for norepinephrine in memory retrieval. Cell 117:131-143.

Murphy PR, O'Connell RG, O'Sullivan M, Robertson IH, Balsters JH (2014) Pupil diameter covaries with BOLD activity in human locus coeruleus. Hum Brain Mapp 35:4140-4154.

Murray PS, Groves JL, Pettett BJ, Britton SL, Koch LG, Dishman RK, Holmes PV (2010) Locus coeruleus galanin expression is enhanced after exercise in rats selectively bred for high capacity for aerobic activity. Peptides 31:2264-2268.

Naegeli C, Zeffiro T, Piccirelli M, Jaillard A, Weilenmann A, Hassanpour K, Schick M, Rufer M, Orr SP, Mueller-Pfeiffer C (2018) Locus Coeruleus Activity Mediates Hyperresponsiveness in Posttraumatic Stress Disorder. Biol Psychiatry 83:254-262.

Nam H, Kerman IA (2016) A2 noradrenergic neurons regulate forced swim test immobility. Physiol Behav 165:339-349.

Nazarali AJ, Reynolds GP (1992) Monoamine neurotransmitters and their metabolites in brain regions in Alzheimer's disease: a postmortem study. Cell Mol Neurobiol 12:581-587.

Neal CR, Jr., Mansour A, Reinscheid R, Nothacker HP, Civelli O, Akil H, Watson SJ, Jr. (1999) Opioid receptor-like (ORL1) receptor distribution in the rat central nervous system: comparison of ORL1 receptor mRNA expression with (125)I-[(14)Tyr]-orphanin FQ binding. J Comp Neurol 412:563-605.

Neophytou SI, Aspley S, Butler S, Beckett S, Marsden CA (2001) Effects of lesioning noradrenergic neurones in the locus coeruleus on conditioned and unconditioned aversive behaviour in the rat. Prog Neuropsychopharmacol Biol Psychiatry 25:1307-1321.

Nestler EJ, Alreja M, Aghajanian GK (1999) Molecular control of locus coeruleus neurotransmission. Biol Psychiatry 46:1131-1139.

Nguyen TT, Ta QTH, Nguyen TKO, Nguyen TTD, Giau VV (2020) Type 3 Diabetes and Its Role Implications in Alzheimer's Disease. International Journal of Molecular Sciences 21.

Nitz D, Siegel JM (1997) GABA release in the locus coeruleus as a function of sleep/wake state. Neuroscience 78:795-801.

Noei S, Zouridis IS, Logothetis NK, Panzeri S, Totah NK (2022) Distinct ensembles in the noradrenergic locus coeruleus are associated with diverse cortical states. P Natl Acad Sci USA 119.

Noriega NC, Garyfallou VT, Kohama SG, Urbanski HF (2007) Glutamate receptor subunit expression in the rhesus macaque locus coeruleus. Brain Res 1173:53-65.

O'Brien JT, Herholz K (2015) Amyloid imaging for dementia in clinical practice. BMC Med 13:163.

O'Callaghan C, Hezemans FH, Ye R, Rua C, Jones PS, Murley AG, Holland N, Regenthal R, Tsvetanov KA, Wolpe N, Barker RA, Williams-Gray CH, Robbins TW, Passamonti L, Rowe JB (2021) Locus coeruleus integrity and the effect of atomoxetine on response inhibition in Parkinson's disease. Brain 144:2513-2526.

O'Dell TJ, Connor SA, Guglietta R, Nguyen PV (2015) beta-Adrenergic receptor signaling and modulation of long-term potentiation in the mammalian hippocampus. Learn Mem 22:461-471.

O'Neal HA, Van Hoomissen JD, Holmes PV, Dishman RK (2001) Prepro-galanin messenger RNA levels are increased in rat locus coeruleus after treadmill exercise training. Neurosci Lett 299:69-72.

O'Neil JN, Mouton PR, Tizabi Y, Ottinger MA, Lei DL, Ingram DK, Manaye KF (2007) Catecholaminergic neuronal loss in locus coeruleus of aged female dtg APP/PS1 mice. J Chem Neuroanat 34:102-107.

Oh J, Eser RA, Ehrenberg AJ, Morales D, Petersen C, Kudlacek J, Dunlop SR, Theofilas P, Resende E, Cosme C, Alho EJL, Spina S, Walsh CM, Miller BL, Seeley WW, Bittencourt JC, Neylan TC, Heinsen H, Grinberg LT (2019) Profound degeneration of wake-promoting neurons in Alzheimer's disease. Alzheimers Dement 15:1253-1263.

Ohtaki H, Nakamachi T, Dohi K, Aizawa Y, Takaki A, Hodoyama K, Yofu S, Hashimoto H, Shintani N, Baba A, Kopf M, Iwakura Y, Matsuda K, Arimura A, Shioda S (2006) Pituitary adenylate cyclase-activating polypeptide (PACAP) decreases ischemic neuronal cell death in association with IL-6. Proc Natl Acad Sci U S A 103:7488-7493.

Okawa H, Kudo M, Kudo T, Guerrini R, Lambert DG, Kushikata T, Yoshida H, Matsuki A (2001) Effects of nociceptinNH2 and [Nphe1]nociceptin(1-13)NH2 on rat brain noradrenaline release in vivo and in vitro. Neurosci Lett 303:173-176.

Olivieri P, Lagarde J, Lehericy S, Valabregue R, Michel A, Mace P, Caille F, Gervais P, Bottlaender M, Sarazin M (2019) Early alteration of the locus coeruleus in phenotypic variants of Alzheimer's disease. Ann Clin Transl Neur 6:1345-1351.

Olpe HR, Steinmann MW (1982) Age-related decline in the activity of noradrenergic neurons of the rat locus coeruleus. Brain Res 251:174-176.

Omoluabi T, Torraville SE, Maziar A, Ghosh A, Power KD, Reinhardt C, Harley CW, Yuan Q (2021) Novelty-like activation of locus coeruleus protects against deleterious human

pretangle tau effects while stress-inducing activation worsens its effects. Alzheimers Dement (N Y) 7:e12231.

Osorio-Forero A, Cherrad N, Banterle L, Fernandez LMJ, Luthi A (2022) When the Locus Coeruleus Speaks Up in Sleep: Recent Insights, Emerging Perspectives. Int J Mol Sci 23.

Ouyang M, Thomas SA (2005) A requirement for memory retrieval during and after long-term extinction learning. Proc Natl Acad Sci U S A 102:9347-9352.

Ovod V, Ramsey KN, Mawuenyega KG, Bollinger JG, Hicks T, Schneider T, Sullivan M, Paumier K, Holtzman DM, Morris JC, Benzinger T, Fagan AM, Patterson BW, Bateman RJ (2017) Amyloid beta concentrations and stable isotope labeling kinetics of human plasma specific to central nervous system amyloidosis. Alzheimers & Dementia 13:841-849.

Page ME, Abercrombie ED (1999) Discrete local application of corticotropin-releasing factor increases locus coeruleus discharge and extracellular norepinephrine in rat hippocampus. Synapse 33:304-313.

Pagliari R, Peyrin L (1995) Norepinephrine release in the rat frontal cortex under treadmill exercise: a study with microdialysis. J Appl Physiol (1985) 78:2121-2130.

Paiva HS, Filho IJZ, Cais C (2021) Using Prazosin to Treat Posttraumatic Stress Disorder and Associations: A Systematic Review. Psychiatry Investig 18:365-372.

Palmer AM, Francis PT, Bowen DM, Benton JS, Neary D, Mann DM, Snowden JS (1987) Catecholaminergic neurones assessed ante-mortem in Alzheimer's disease. Brain Res 414:365-375.

Palmqvist S, Mattsson N, Hansson O, Alzheimer's Disease Neuroimaging I (2016) Cerebrospinal fluid analysis detects cerebral amyloid-beta accumulation earlier than positron emission tomography. Brain 139:1226-1236.

Pamphlett R (2014) Uptake of environmental toxicants by the locus ceruleus: A potential trigger for neurodegenerative, demyelinating and psychiatric disorders. Med Hypotheses 82:97-104.

Pentkowski NS, Rogge-Obando KK, Donaldson TN, Bouquin SJ, Clark BJ (2021) Anxiety and Alzheimer's disease: Behavioral analysis and neural basis in rodent models of Alzheimer's-related neuropathology. Neurosci Biobehav Rev 127:647-658.

Pentkowski NS, Berkowitz LE, Thompson SM, Drake EN, Olguin CR, Clark BJ (2018) Anxiety-like behavior as an early endophenotype in the TgF344-AD rat model of Alzheimer's disease. Neurobiol Aging 61:169-176.

Peskind ER, Tsuang DW, Bonner LT, Pascualy M, Riekse RG, Snowden MB, Thomas R, Raskind MA (2005) Propranolol for disruptive behaviors in nursing home residents with probable or possible Alzheimer disease: a placebo-controlled study. Alzheimer Dis Assoc Disord 19:23-28.

Pichet Binette A, Vachon-Presseau E, Morris J, Bateman R, Benzinger T, Collins DL, Poirier J, Breitner JCS, Villeneuve S, Dominantly Inherited Alzheimer N, Group P-AR (2021) Amyloid and Tau Pathology Associations With Personality Traits, Neuropsychiatric Symptoms, and Cognitive Lifestyle in the Preclinical Phases of Sporadic and Autosomal Dominant Alzheimer's Disease. Biol Psychiatry 89:776-785.

Pietrzak RH, Gallezot JD, Ding YS, Henry S, Potenza MN, Southwick SM, Krystal JH, Carson RE, Neumeister A (2013) Association of posttraumatic stress disorder with reduced in vivo norepinephrine transporter availability in the locus coeruleus. JAMA Psychiatry 70:1199-1205.

Pietrzak RH, Lim YY, Neumeister A, Ames D, Ellis KA, Harrington K, Lautenschlager NT, Restrepo C, Martins RN, Masters CL, Villemagne VL, Rowe CC, Maruff P, Australian

Imaging B, Lifestyle Research G (2015) Amyloid-beta, anxiety, and cognitive decline in preclinical Alzheimer disease: a multicenter, prospective cohort study. JAMA Psychiatry 72:284-291.

Pirhajati Mahabadi V, Movahedin M, Semnanian S, Mirnajafi-Zadeh J, Faizi M (2015) In vitro differentiation of neural stem cells into noradrenergic-like cells. Int J Mol Cell Med 4:22-31.

Pletnikova O, Kageyama Y, Rudow G, LaClair KD, Albert M, Crain BJ, Tian J, Fowler D, Troncoso JC (2018) The spectrum of preclinical Alzheimer's disease pathology and its modulation by ApoE genotype. Neurobiol Aging 71:72-80.

Poe GR, Foote S, Eschenko O, Johansen JP, Bouret S, Aston-Jones G, Harley CW, Manahan-Vaughan D, Weinshenker D, Valentino R, Berridge C, Chandler DJ, Waterhouse B, Sara SJ (2020) Locus coeruleus: a new look at the blue spot. Nat Rev Neurosci 21:644-659.

Pompeiano M, Palacios JM, Mengod G (1992) Distribution and cellular localization of mRNA coding for 5-HT1A receptor in the rat brain: correlation with receptor binding. J Neurosci 12:440-453.

Porter-Stransky KA, Centanni SW, Karne SL, Odil LM, Fekir S, Wong JC, Jerome C, Mitchell HA, Escayg A, Pedersen NP, Winder DG, Mitrano DA, Weinshenker D (2019) Noradrenergic Transmission at Alpha1-Adrenergic Receptors in the Ventral Periaqueductal Gray Modulates Arousal. Biol Psychiatry 85:237-247.

Preskorn SH, Zeller S, Citrome L, Finman J, Goldberg JF, Fava M, Kakar R, De Vivo M, Yocca FD, Risinger R (2022) Effect of Sublingual Dexmedetomidine vs Placebo on Acute Agitation Associated With Bipolar Disorder: A Randomized Clinical Trial. JAMA 327:727-736.

Prokopiou PC, Engels-Dominguez N, Papp KV, Scott MR, Schultz AP, Schneider C, Farrell ME, Buckley RF, Quiroz YT, El Fakhri G, Rentz DM, Sperling RA, Johnson KA, Jacobs HIL (2022) Lower novelty-related locus coeruleus function is associated with Abeta-related cognitive decline in clinically healthy individuals. Nat Commun 13:1571.

Rapoport M, Dawson HN, Binder LI, Vitek MP, Ferreira A (2002) Tau is essential to beta -amyloid-induced neurotoxicity. Proc Natl Acad Sci U S A 99:6364-6369.

Rash JE, Olson CO, Davidson KG, Yasumura T, Kamasawa N, Nagy JI (2007) Identification of connexin36 in gap junctions between neurons in rodent locus coeruleus. Neuroscience 147:938-956.

Raskind MA, Peskind ER, Hoff DJ, Hart KL, Holmes HA, Warren D, Shofer J, O'Connell J, Taylor F, Gross C, Rohde K, McFall ME (2007) A parallel group placebo controlled study of prazosin for trauma nightmares and sleep disturbance in combat veterans with post-traumatic stress disorder. Biol Psychiatry 61:928-934.

Raskind MA et al. (2013) A trial of prazosin for combat trauma PTSD with nightmares in active-duty soldiers returned from Iraq and Afghanistan. Am J Psychiatry 170:1003-1010.

Rasmussen H, Rosness TA, Bosnes O, Salvesen Ø, Knutli M, Stordal E (2018) Anxiety and Depression as Risk Factors in Frontotemporal Dementia and Alzheimer’s Disease: The HUNT Study. Dementia and Geriatric Cognitive Disorders Extra 8:414-425.

Reimer J, McGinley MJ, Liu Y, Rodenkirch C, Wang Q, McCormick DA, Tolias AS (2016) Pupil fluctuations track rapid changes in adrenergic and cholinergic activity in cortex. Nat Commun 7:13289.

Reinikainen KJ, Paljarvi L, Huuskonen M, Soininen H, Laakso M, Riekkinen PJ (1988) A post-mortem study of noradrenergic, serotonergic and GABAergic neurons in Alzheimer's disease. J Neurol Sci 84:101-116.

Reyes BA, Drolet G, Van Bockstaele EJ (2008) Dynorphin and stress-related peptides in rat locus coeruleus: contribution of amygdalar efferents. J Comp Neurol 508:663-675.

Reyes BA, Fox K, Valentino RJ, Van Bockstaele EJ (2006) Agonist-induced internalization of corticotropin-releasing factor receptors in noradrenergic neurons of the rat locus coeruleus. Eur J Neurosci 23:2991-2998.

Risacher SL, Fandos N, Romero J, Sherriff I, Pesini P, Saykin AJ, Apostolova LG (2019) Plasma amyloid beta levels are associated with cerebral amyloid and tau deposition. Alzh Dement-Dadm 11:510-519.

Ritchie C, Smailagic N, Noel-Storr AH, Takwoingi Y, Flicker L, Mason SE, McShane R (2014) Plasma and cerebrospinal fluid amyloid beta for the diagnosis of Alzheimer's disease dementia and other dementias in people with mild cognitive impairment (MCI). Cochrane Database Syst Rev 2014:CD008782.

Rittenhouse PA, Lopez-Rubalcava C, Stanwood GD, Lucki I (2002) Amplified behavioral and endocrine responses to forced swim stress in the Wistar-Kyoto rat. Psychoneuroendocrinology 27:303-318.

Roberson ED, Scearce-Levie K, Palop JJ, Yan F, Cheng IH, Wu T, Gerstein H, Yu GQ, Mucke L (2007) Reducing endogenous tau ameliorates amyloid beta-induced deficits in an Alzheimer's disease mouse model. Science 316:750-754.

Robert A, Scholl M, Vogels T (2021) Tau Seeding Mouse Models with Patient Brain-Derived Aggregates. Int J Mol Sci 22.

Robertson IH (2013) A noradrenergic theory of cognitive reserve: implications for Alzheimer's disease. Neurobiology of Aging 34:298-308.

Rorabaugh JM, Chalermpalanupap T, Botz-Zapp CA, Fu VM, Lembeck NA, Cohen RM, Weinshenker D (2017) Chemogenetic locus coeruleus activation restores reversal learning in a rat model of Alzheimer's disease. Brain 140:3023-3038.

Ruffoli R, Giorgi FS, Pizzanelli C, Murri L, Paparelli A, Fornai F (2011) The chemical neuroanatomy of vagus nerve stimulation. J Chem Neuroanat 42:288-296.

Ryan SD, Whitehead SN, Swayne LA, Moffat TC, Hou W, Ethier M, Bourgeois AJ, Rashidian J, Blanchard AP, Fraser PE, Park DS, Figeys D, Bennett SA (2009) Amyloid-beta42 signals tau hyperphosphorylation and compromises neuronal viability by disrupting alkylacylglycerophosphocholine metabolism. Proc Natl Acad Sci U S A 106:20936-20941.

Safaai H, Neves R, Eschenko O, Logothetis NK, Panzeri S (2015) Modeling the effect of locus coeruleus firing on cortical state dynamics and single-trial sensory processing. Proc Natl Acad Sci U S A 112:12834-12839.

Saint-Aubert L, Lemoine L, Chiotis K, Leuzy A, Rodriguez-Vieitez E, Nordberg A (2017) Tau PET imaging: present and future directions. Mol Neurodegener 12:19.

Salehi A, Ashford JW, Mufson EJ (2016) The Link between Alzheimer's Disease and Down Syndrome. A Historical Perspective. Curr Alzheimer Res 13:2-6.

Sander K, Lashley T, Gami P, Gendron T, Lythgoe MF, Rohrer JD, Schott JM, Revesz T, Fox NC, Arstad E (2016) Characterization of tau positron emission tomography tracer [F-18]AV-1451 binding to postmortem tissue in Alzheimer's disease, primary tauopathies, and other dementias. Alzheimers & Dementia 12:1116-1124.

Sara SJ (2009) The locus coeruleus and noradrenergic modulation of cognition. Nat Rev Neurosci 10:211-223.

Sara SJ, Segal M (1991) Plasticity of sensory responses of locus coeruleus neurons in the behaving rat: implications for cognition. Prog Brain Res 88:571-585.

Sara SJ, Bouret S (2012) Orienting and reorienting: the locus coeruleus mediates cognition through arousal. Neuron 76:130-141.

Sare RM, Cooke SK, Krych L, Zerfas PM, Cohen RM, Smith CB (2020) Behavioral Phenotype in the TgF344-AD Rat Model of Alzheimer's Disease. Front Neurosci 14:601.

Sasaki M, Shibata E, Tohyama K, Takahashi J, Otsuka K, Tsuchiya K, Takahashi S, Ehara S, Terayama Y, Sakai A (2006) Neuromelanin magnetic resonance imaging of locus ceruleus and substantia nigra in Parkinson's disease. Neuroreport 17:1215-1218.

Sathyanesan A, Ogura T, Lin W (2012) Automated measurement of nerve fiber density using line intensity scan analysis. J Neurosci Methods 206:165-175.

Savtchouk I, Volterra A (2018) Gliotransmission: Beyond Black-and-White. J Neurosci 38:14-25.

Scattoni ML, Gasparini L, Alleva E, Goedert M, Calamandrei G, Spillantini MG (2010) Early behavioural markers of disease in P301S tau transgenic mice. Behav Brain Res 208:250-257.

Scherer HJ (1939) Melanin pigmentation of the substantia nigra in primates. Journal of Comparative Neurology 71:91-98.

Schiff HC, Johansen JP, Hou M, Bush DE, Smith EK, Klein JE, LeDoux JE, Sears RM (2017) beta-Adrenergic Receptors Regulate the Acquisition and Consolidation Phases of Aversive Memory Formation Through Distinct, Temporally Regulated Signaling Pathways. Neuropsychopharmacology 42:895-903.

Schwalbe M, Ozenne V, Bibow S, Jaremko M, Jaremko L, Gajda M, Jensen MR, Biernat J, Becker S, Mandelkow E, Zweckstetter M, Blackledge M (2014) Predictive Atomic

Resolution Descriptions of Intrinsically Disordered hTau40 and alpha-Synuclein in Solution from NMR and Small Angle Scattering. Structure 22:238-249.

Schwarz LA, Luo L (2015) Organization of the locus coeruleus-norepinephrine system. Curr Biol 25:R1051-R1056.

Schwarz LA, Miyamichi K, Gao XJ, Beier KT, Weissbourd B, DeLoach KE, Ren J, Ibanes S, Malenka RC, Kremer EJ, Luo L (2015) Viral-genetic tracing of the input-output organization of a central noradrenaline circuit. Nature 524:88-92.

Sciolino NR, Holmes PV (2012) Exercise offers anxiolytic potential: a role for stress and brain noradrenergic-galaninergic mechanisms. Neurosci Biobehav Rev 36:1965-1984.

Sciolino NR, Dishman RK, Holmes PV (2012) Voluntary exercise offers anxiolytic potential and amplifies galanin gene expression in the locus coeruleus of the rat. Behav Brain Res 233:191-200.

Sciolino NR, Hsiang M, Mazzone CM, Wilson LR, Plummer NW, Amin J, Smith KG, McGee CA, Fry SA, Yang CX, Powell JM, Bruchas MR, Kravitz AV, Cushman JD, Krashes MJ, Cui G, Jensen P (2022) Natural locus coeruleus dynamics during feeding. Sci Adv 8:eabn9134.

Sears RM, Fink AE, Wigestrand MB, Farb CR, de Lecea L, Ledoux JE (2013) Orexin/hypocretin system modulates amygdala-dependent threat learning through the locus coeruleus. Proc Natl Acad Sci U S A 110:20260-20265.

Segal SK, Cotman CW, Cahill LF (2012) Exercise-induced noradrenergic activation enhances memory consolidation in both normal aging and patients with amnestic mild cognitive impairment. J Alzheimers Dis 32:1011-1018.

Seita Y, Morimura T, Watanabe N, Iwatani C, Tsuchiya H, Nakamura S, Suzuki T, Yanagisawa D, Tsukiyama T, Nakaya M, Okamura E, Muto M, Ema M, Nishimura M, Tooyama I (2020)

Generation of Transgenic Cynomolgus Monkeys Overexpressing the Gene for Amyloid-beta Precursor Protein. J Alzheimers Dis 75:45-60.

Seutin V, Verbanck P, Massotte L, Dresse A (1989) Galanin decreases the activity of locus coeruleus neurons in vitro. Eur J Pharmacol 164:373-376.

Shamoto-Nagai M, Maruyama W, Akao Y, Osawa T, Tribl F, Gerlach M, Zucca FA, Zecca L, Riederer P, Naoi M (2004) Neuromelanin inhibits enzymatic activity of 26S proteasome in human dopaminergic SH-SY5Y cells. J Neural Transm 111:1253-1265.

Shelby LB, Steve C, Hyun Joo Y, Kaoru N, Jungwon M, Noah M, Padideh N, Julian FT, Paul L, Mara M (2022) Daily heart rate variability biofeedback training decreases locus coeruleus MRI contrast in younger adults. medRxiv:2022.2002.2004.22270468.

Shen HL, Fuchino Y, Miyamoto D, Nomura H, Matsuki N (2012) Vagus nerve stimulation enhances perforant path-CA3 synaptic transmission via the activation of beta-adrenergic receptors and the locus coeruleus. Int J Neuropsychoph 15:523-530.

Shi G, Xing L, Wu D, Bhattacharyya BJ, Jones CR, McMahon T, Chong SYC, Chen JA, Coppola G, Geschwind D, Krystal A, Ptacek LJ, Fu YH (2019) A Rare Mutation of beta(1)-Adrenergic Receptor Affects Sleep/Wake Behaviors. Neuron 103:1044-1055 e1047.

Shibata E, Sasaki M, Tohyama K, Otsuka K, Sakai A (2007) Reduced signal of locus ceruleus in depression in quantitative neuromelanin magnetic resonance imaging. Neuroreport 18:415-418.

Shibata E, Sasaki M, Tohyama K, Otsuka K, Endoh J, Terayama Y, Sakai A (2008) Use of neuromelanin-sensitive MRI to distinguish schizophrenic and depressive patients and healthy individuals based on signal alterations in the substantia nigra and locus ceruleus. Biol Psychiat 64:401-406.

Shimojo M, Takuwa H, Takado Y, Tokunaga M, Tsukamoto S, Minatohara K, Ono M, Seki C, Maeda J, Urushihata T, Minamihisamatsu T, Aoki I, Kawamura K, Zhang MR, Suhara T, Sahara N, Higuchi M (2020) Selective Disruption of Inhibitory Synapses Leading to Neuronal Hyperexcitability at an Early Stage of Tau Pathogenesis in a Mouse Model. J Neurosci 40:3491-3501.

Shipton OA, Leitz JR, Dworzak J, Acton CE, Tunbridge EM, Denk F, Dawson HN, Vitek MP, Wade-Martins R, Paulsen O, Vargas-Caballero M (2011) Tau protein is required for amyloid beta-induced impairment of hippocampal long-term potentiation. J Neurosci 31:1688-1692.

Shu YS, Zhao ZQ, Li MY, Zhou GM (1998) Orphanin FQ/nociceptin modulates glutamate- and kainic acid-induced currents in acutely isolated rat spinal dorsal horn neurons. Neuropeptides 32:567-571.

Singh B, Hughes AJ, Mehta G, Erwin PJ, Parsaik AK (2016) Efficacy of Prazosin in Posttraumatic Stress Disorder: A Systematic Review and Meta-Analysis. Prim Care Companion CNS Disord 18.

Singh C, Oikonomou G, Prober DA (2015) Norepinephrine is required to promote wakefulness and for hypocretin-induced arousal in zebrafish. Elife 4:e07000.

Sommerauer M, Fedorova TD, Hansen AK, Knudsen K, Otto M, Jeppesen J, Frederiksen Y, Blicher JU, Geday J, Nahimi A, Damholdt MF, Brooks DJ, Borghammer P (2018) Evaluation of the noradrenergic system in Parkinson's disease: an C-11-MeNER PET and neuromelanin MRI study. Brain 141:496-504.

Srivastava H, Lasher AT, Nagarajan A, Sun LY (2023) Sexual dimorphism in the peripheral metabolic homeostasis and behavior in the TgF344-AD rat model of Alzheimer's disease. Aging Cell:e13854.

Stern Y (2012) Cognitive reserve in ageing and Alzheimer's disease. Lancet Neurol 11:1006-1012.

Sterpenich V, D'Argembeau A, Desseilles M, Balteau E, Albouy G, Vandewalle G, Degueldre C, Luxen A, Collette F, Maquet P (2006) The locus ceruleus is involved in the successful retrieval of emotional memories in humans. Journal of Neuroscience 26:7416-7423.

Stowell RD, Sipe GO, Dawes RP, Batchelor HN, Lordy KA, Whitelaw BS, Stoessel MB, Bidlack JM, Brown E, Sur M, Majewska AK (2019) Noradrenergic signaling in the wakeful state inhibits microglial surveillance and synaptic plasticity in the mouse visual cortex. Nat Neurosci 22:1782-1792.

Sulkes Cuevas JN, Watanabe M, Uematsu A, Johansen JP (2023) Whole-brain afferent input mapping to functionally distinct brainstem noradrenaline cell types. Neurosci Res.

Sun LH, Perakyla J, Holm K, Haapasalo J, Lehtimaki K, Ogawa KH, Peltola J, Hartikainen KM (2017) Vagus nerve stimulation improves working memory performance. J Clin Exp Neuropsyc 39:954-964.

Swanson LW (1976) The locus coeruleus: a cytoarchitectonic, Golgi and immunohistochemical study in the albino rat. Brain Res 110:39-56.

Swift KM, Gross BA, Frazer MA, Bauer DS, Clark KJD, Vazey EM, Aston-Jones G, Li Y, Pickering AE, Sara SJ, Poe GR (2018) Abnormal Locus Coeruleus Sleep Activity Alters Sleep Signatures of Memory Consolidation and Impairs Place Cell Stability and Spatial Memory. Curr Biol 28:3599-3609 e3594.

Szakaly P, Laszlo E, Kovacs K, Racz B, Horvath G, Ferencz A, Lubics A, Kiss P, Tamas A, Brubel R, Opper B, Baba A, Hashimoto H, Farkas J, Matkovits A, Magyarlaki T, Helyes Z, Reglodi D (2011) Mice deficient in pituitary adenylate cyclase activating polypeptide (PACAP)

show increased susceptibility to in vivo renal ischemia/reperfusion injury. Neuropeptides 45:113-121.

Szot P, White SS, Greenup JL, Leverenz JB, Peskind ER, Raskind MA (2006) Compensatory changes in the noradrenergic nervous system in the locus ceruleus and hippocampus of postmortem subjects with Alzheimer's disease and dementia with Lewy bodies. J Neurosci 26:467-478.

Szot P, White SS, Greenup JL, Leverenz JB, Peskind ER, Raskind MA (2007) Changes in adrenoreceptors in the prefrontal cortex of subjects with dementia: evidence of compensatory changes. Neuroscience 146:471-480.

Szot P, Leverenz JB, Peskind ER, Kiyasu E, Rohde K, Miller MA, Raskind MA (2000) Tyrosine hydroxylase and norepinephrine transporter mRNA expression in the locus coeruleus in Alzheimer's disease. Brain Res Mol Brain Res 84:135-140.

Szot P, Miguelez C, White SS, Franklin A, Sikkema C, Wilkinson CW, Ugedo L, Raskind MA (2010) A Comprehensive Analysis of the Effect of Dsp4 on the Locus Coeruleus Noradrenergic System in the Rat. Neuroscience 166:279-291.

Szot P, Knight L, Franklin A, Sikkema C, Foster S, Wilkinson CW, White SS, Raskind MA (2012) Lesioning Noradrenergic Neurons of the Locus Coeruleus in C57bl/6 Mice with Unilateral 6-Hydroxydopamine Injection, to Assess Molecular, Electrophysiological and Biochemical Changes in Noradrenergic Signaling. Neuroscience 216:143-157.

Takahashi K, Kayama Y, Lin JS, Sakai K (2010) Locus coeruleus neuronal activity during the sleep-waking cycle in mice. Neuroscience 169:1115-1126.

Takeuchi T, Duszkiewicz AJ, Sonneborn A, Spooner PA, Yamasaki M, Watanabe M, Smith CC, Fernandez G, Deisseroth K, Greene RW, Morris RG (2016) Locus coeruleus and dopaminergic consolidation of everyday memory. Nature 537:357-362.

Takigawa M, Mogenson GJ (1977) A study of inputs to antidromically identified neurons of the locus coeruleus. Brain Res 135:217-230.

Teri L, Ferretti LE, Gibbons LE, Logsdon RG, McCurry SM, Kukull WA, McCormick WC, Bowen JD, Larson EB (1999) Anxiety of Alzheimer's disease: prevalence, and comorbidity. J Gerontol A Biol Sci Med Sci 54:M348-352.

Thal DR, Rub U, Orantes M, Braak H (2002) Phases of A beta-deposition in the human brain and its relevance for the development of AD. Neurology 58:1791-1800.

Theofilas P, Dunlop S, Heinsen H, Grinberg LT (2015) Turning on the Light Within: Subcortical Nuclei of the Isodentritic Core and their Role in Alzheimer's Disease Pathogenesis. J Alzheimers Dis 46:17-34.

Theofilas P, Ehrenberg AJ, Dunlop S, Di Lorenzo Alho AT, Nguy A, Leite REP, Rodriguez RD, Mejia MB, Suemoto CK, Ferretti-Rebustini REL, Polichiso L, Nascimento CF, Seeley WW, Nitrini R, Pasqualucci CA, Jacob Filho W, Rueb U, Neuhaus J, Heinsen H, Grinberg LT (2017) Locus coeruleus volume and cell population changes during Alzheimer's disease progression: A stereological study in human postmortem brains with potential implication for early-stage biomarker discovery. Alzheimers Dement 13:236-246.

Theofilas P et al. (2018) Probing the correlation of neuronal loss, neurofibrillary tangles, and cell death markers across the Alzheimer's disease Braak stages: a quantitative study in humans. Neurobiol Aging 61:1-12.

Theron CN, Devilliers AS, Taljaard JJF (1993) Effects of Dsp-4 on Monoamine and Monoamine Metabolite Levels and on Beta-Adrenoceptor Binding-Kinetics in Rat-Brain at Different Times after Administration. Neurochem Res 18:1321-1327.

Thomas SA, Palmiter RD (1997) Impaired maternal behavior in mice lacking norepinephrine and epinephrine. Cell 91:583-592.

Tillage RP, Wilson GE, Liles LC, Holmes PV, Weinshenker D (2020a) Chronic Environmental or Genetic Elevation of Galanin in Noradrenergic Neurons Confers Stress Resilience in Mice. J Neurosci 40:7464-7474.

Tillage RP, Foster SL, Lustberg D, Liles LC, McCann KE, Weinshenker D (2021) Co-released norepinephrine and galanin act on different timescales to promote stress-induced anxiety-like behavior. Neuropsychopharmacology 46:1535-1543.

Tillage RP, Sciolino NR, Plummer NW, Lustberg D, Liles LC, Hsiang M, Powell JM, Smith KG, Jensen P, Weinshenker D (2020b) Elimination of galanin synthesis in noradrenergic neurons reduces galanin in select brain areas and promotes active coping behaviors. Brain Struct Funct 225:785-803.

Tkaczynski JA, Borodovitsyna O, Chandler DJ (2022) Delta Opioid Receptors and Enkephalinergic Signaling within Locus Coeruleus Promote Stress Resilience. Brain Sci 12.

Toll L, Bruchas MR, Calo G, Cox BM, Zaveri NT (2016) Nociceptin/Orphanin FQ Receptor Structure, Signaling, Ligands, Functions, and Interactions with Opioid Systems. Pharmacol Rev 68:419-457.

Totah NK, Neves RM, Panzeri S, Logothetis NK, Eschenko O (2018) The Locus Coeruleus Is a Complex and Differentiated Neuromodulatory System. Neuron 99:1055-1068 e1056.

Trinchese F, Liu S, Battaglia F, Walter S, Mathews PM, Arancio O (2004) Progressive age-related development of Alzheimer-like pathology in APP/PS1 mice. Ann Neurol 55:801-814.

Tsoi KK, Chan JY, Hirai HW, Wong SY, Kwok TC (2015) Cognitive Tests to Detect Dementia: A Systematic Review and Meta-analysis. JAMA Intern Med 175:1450-1458.

Tu S, Okamoto S, Lipton SA, Xu H (2014) Oligomeric Abeta-induced synaptic dysfunction in Alzheimer's disease. Mol Neurodegener 9:48.

Uematsu A, Tan BZ, Ycu EA, Cuevas JS, Koivumaa J, Junyent F, Kremer EJ, Witten IB, Deisseroth K, Johansen JP (2017) Modular organization of the brainstem noradrenaline system coordinates opposing learning states. Nat Neurosci 20:1602-1611.

Ulm BS, Borchelt DR, Moore BD (2021) Remodeling Alzheimer-amyloidosis models by seeding. Mol Neurodegener 16:8.

Valentino RJ, Foote SL (1988) Corticotropin-releasing hormone increases tonic but not sensory-evoked activity of noradrenergic locus coeruleus neurons in unanesthetized rats. J Neurosci 8:1016-1025.

Valentino RJ, Reyes B, Van Bockstaele E, Bangasser D (2012) Molecular and cellular sex differences at the intersection of stress and arousal. Neuropharmacology 62:13-20.

Van Bockstaele EJ, Colago EE, Valentino RJ (1996) Corticotropin-releasing factor-containing axon terminals synapse onto catecholamine dendrites and may presynaptically modulate other afferents in the rostral pole of the nucleus locus coeruleus in the rat brain. J Comp Neurol 364:523-534.

Van Bockstaele EJ, Reyes BA, Valentino RJ (2010) The locus coeruleus: A key nucleus where stress and opioids intersect to mediate vulnerability to opiate abuse. Brain Res 1314:162-174.

Van Dam D, De Deyn PP (2006) Drug discovery in dementia: the role of rodent models. Nat Rev Drug Discov 5:956-970.

van Hooren RWE, Verhey FRJ, Ramakers I, Jansen WJ, Jacobs HIL (2021) Elevated norepinephrine metabolism is linked to cortical thickness in the context of Alzheimer's disease pathology. Neurobiol Aging 102:17-22.

Vankov A, Herve-Minvielle A, Sara SJ (1995) Response to novelty and its rapid habituation in locus coeruleus neurons of the freely exploring rat. Eur J Neurosci 7:1180-1187.

Vargas-Caballero M, Warming H, Walker R, Holmes C, Cruickshank G, Patel B (2022) Vagus Nerve Stimulation as a Potential Therapy in Early Alzheimer's Disease: A Review. Front Hum Neurosci 16.

Vaudry D, Hamelink C, Damadzic R, Eskay RL, Gonzalez B, Eiden LE (2005) Endogenous PACAP acts as a stress response peptide to protect cerebellar neurons from ethanol or oxidative insult. Peptides 26:2518-2524.

Vazey EM, Aston-Jones G (2014) Designer receptor manipulations reveal a role of the locus coeruleus noradrenergic system in isoflurane general anesthesia. Proc Natl Acad Sci U S A 111:3859-3864.

Vazquez-Oliver A, Brambilla-Pisoni C, Domingo-Gainza M, Maldonado R, Ivorra A, Ozaita A (2020) Auricular transcutaneous vagus nerve stimulation improves memory persistence in naive mice and in an intellectual disability mouse model. Brain Stimul 13:494-498.

Vermeiren C, Motte P, Viot D, Mairet-Coello G, Courade JP, Citron M, Mercier J, Hannestad J, Gillard M (2018) The Tau Positron-Emission Tomography Tracer AV-1451 Binds With Similar Affinities to Tau Fibrils and Monoamine Oxidases. Movement Disord 33:273-281.

Wagatsuma A, Okuyama T, Sun C, Smith LM, Abe K, Tonegawa S (2018) Locus coeruleus input to hippocampal CA3 drives single-trial learning of a novel context. Proc Natl Acad Sci U S A 115:E310-E316.

Wagner-Altendorf TA, Fischer B, Roeper J (2019) Axonal projection-specific differences in somatodendritic alpha2 autoreceptor function in locus coeruleus neurons. Eur J Neurosci 50:3772-3785.

Wahis J, Holt MG (2021) Astrocytes, Noradrenaline, alpha1-Adrenoreceptors, and Neuromodulation: Evidence and Unanswered Questions. Front Cell Neurosci 15:645691.

Waldvogel HJ, Baer K, Eady E, Allen KL, Gilbert RT, Mohler H, Rees MI, Nicholson LF, Faull RL (2010) Differential localization of gamma-aminobutyric acid type A and glycine receptor subunits and gephyrin in the human pons, medulla oblongata and uppermost cervical segment of the spinal cord: an immunohistochemical study. J Comp Neurol 518:305-328.

Walsh DM, Klyubin I, Fadeeva JV, Cullen WK, Anwyl R, Wolfe MS, Rowan MJ, Selkoe DJ (2002) Naturally secreted oligomers of amyloid beta protein potently inhibit hippocampal long-term potentiation in vivo. Nature 416:535-539.

Wang HW, Pasternak JF, Kuo H, Ristic H, Lambert MP, Chromy B, Viola KL, Klein WL, Stine WB, Krafft GA, Trommer BL (2002) Soluble oligomers of beta amyloid (1-42) inhibit long-term potentiation but not long-term depression in rat dentate gyrus. Brain Res 924:133-140.

Wang J, Li Y, Huang Z, Wan W, Zhang Y, Wang C, Cheng X, Ye F, Liu K, Fei G, Zeng M, Jin L (2018a) Neuromelanin-sensitive magnetic resonance imaging features of the substantia nigra and locus coeruleus in de novo Parkinson's disease and its phenotypes. European Journal of Neurology 25:949-+.

Wang JZ, Xia YY, Grundke-Iqbal I, Iqbal K (2013) Abnormal hyperphosphorylation of tau: sites, regulation, and molecular mechanism of neurofibrillary degeneration. J Alzheimers Dis 33 Suppl 1:S123-139.

Wang LY, Shofer JB, Rohde K, Hart KL, Hoff DJ, McFall YH, Raskind MA, Peskind ER (2009) Prazosin for the treatment of behavioral symptoms in patients with Alzheimer disease with agitation and aggression. Am J Geriatr Psychiatry 17:744-751.

Wang X, Smith K, Pearson M, Hughes A, Cosden ML, Marcus J, Hess JF, Savage MJ, Rosahl T, Smith SM, Schachter JB, Uslaner JM (2018b) Early intervention of tau pathology

prevents behavioral changes in the rTg4510 mouse model of tauopathy. PLoS One 13:e0195486.

Wang XM, Zhang KM, Mokha SS (1996) Nociceptin (orphanin FQ), an endogenous ligand for the QRL1 (opioid-receptor-like1) receptor; modulates responses of trigeminal neurons evoked by excitatory amino acids and somatosensory stimuli. J Neurophysiol 76:3568-3572.

Waterhouse BD, Chandler DJ (2016) Heterogeneous organization and function of the central noradrenergic system. Brain Res 1641:v-x.

Weber L, Divecha HR, Tran MN, Kwon SH, Spangler A, Montgomery KD, Tippani M, Bharadwaj R, Kleinman JE, Page SC, Hyde TM, Collado-Torres L, Maynard KR, Martinowich K, Hicks SC (2022) The Gene Expression Landscape of the Human Locus Coeruleus Revealed by Single-Nucleus and Spatially-Resolved Transcriptomics. Neuropsychopharmacology 47:328-329.

Weingarten MD, Lockwood AH, Hwo SY, Kirschner MW (1975) A protein factor essential for microtubule assembly. Proc Natl Acad Sci U S A 72:1858-1862.

Weinshenker D (2018) Long Road to Ruin: Noradrenergic Dysfunction in Neurodegenerative Disease. Trends Neurosci 41:211-223.

Weinshenker D, Schroeder JP (2007) There and back again: a tale of norepinephrine and drug addiction. Neuropsychopharmacology 32:1433-1451.

Weinshenker D, Holmes PV (2016) Regulation of neurological and neuropsychiatric phenotypes by locus coeruleus-derived galanin. Brain Res 1641:320-337.

Weinshenker D, White SS, Javors MA, Palmiter RD, Szot P (2002) Regulation of norepinephrine transporter abundance by catecholamines and desipramine in vivo. Brain Res 946:239-246.

West CH, Boss-Williams KA, Ritchie JC, Weiss JM (2015) Locus coeruleus neuronal activity determines proclivity to consume alcohol in a selectively-bred line of rats that readily consumes alcohol. Alcohol 49:691-705.

Williams DR (2006) Tauopathies: classification and clinical update on neurodegenerative diseases associated with microtubule-associated protein tau. Intern Med J 36:652-660.

Williams JT, North RA, Shefner SA, Nishi S, Egan TM (1984) Membrane properties of rat locus coeruleus neurones. Neuroscience 13:137-156.

Wilson RS, Nag S, Boyle PA, Hizel LP, Yu L, Buchman AS, Schneider JA, Bennett DA (2013) Neural reserve, neuronal density in the locus ceruleus, and cognitive decline. Neurology 80:1202-1208.

Winsky-Sommerer R, de Oliveira P, Loomis S, Wafford K, Dijk DJ, Gilmour G (2019) Disturbances of sleep quality, timing and structure and their relationship with other neuropsychiatric symptoms in Alzheimer's disease and schizophrenia: Insights from studies in patient populations and animal models. Neurosci Biobehav Rev 97:112-137.

Wittmann CW, Wszolek MF, Shulman JM, Salvaterra PM, Lewis J, Hutton M, Feany MB (2001) Tauopathy in Drosophila: neurodegeneration without neurofibrillary tangles. Science 293:711-714.

Wu C, Yang L, Li Y, Dong Y, Yang B, Tucker LD, Zong X, Zhang Q (2020) Effects of Exercise Training on Anxious-Depressive-like Behavior in Alzheimer Rat. Med Sci Sports Exerc 52:1456-1469.

Xu S, Chen M, Feng T, Zhan L, Zhou L, Yu G (2021) Use ggbreak to Effectively Utilize Plotting Space to Deal With Large Datasets and Outliers. Front Genet 12:774846.

Xu ZQ, Zheng K, Hokfelt T (2005) Electrophysiological studies on galanin effects in brain--progress during the last six years. Neuropeptides 39:269-275.

Yamazaki Y, Painter MM, Bu G, Kanekiyo T (2016) Apolipoprotein E as a Therapeutic Target in Alzheimer's Disease: A Review of Basic Research and Clinical Evidence. CNS Drugs 30:773-789.

Yang B, Sanches-Padilla J, Kondapalli J, Morison SL, Delpire E, Awatramani R, Surmeier DJ (2021) Locus coeruleus anchors a trisynaptic circuit controlling fear-induced suppression of feeding. Neuron 109:823-838 e826.

Yang L, Wu C, Li Y, Dong Y, Wu CY-C, Lee RH-C, Brann DW, Lin HW, Zhang Q (2022) Long-term exercise pre-training attenuates Alzheimer’s disease–related pathology in a transgenic rat model of Alzheimer’s disease. GeroScience 44:1457-1477.

Ye R, O'Callaghan C, Rua C, Hezemans FH, Holland N, Malpetti M, Jones PS, Barker RA, Williams-Gray CH, Robbins TW, Passamonti L, Rowe J (2022) Locus Coeruleus Integrity from 7 T MRI Relates to Apathy and Cognition in Parkinsonian Disorders. Mov Disord 37:1663-1672.

Yesavage JA, Friedman L, Kraemer H, Tinklenberg JR, Salehi A, Noda A, Taylor JL, O'Hara R, Murphy G (2004) Sleep/wake disruption in Alzheimer's disease: APOE status and longitudinal course. J Geriatr Psychiatry Neurol 17:20-24.

Yoo HJ, Nashiro K, Min J, Cho C, Bachman SL, Nasseri P, Porat S, Dutt S, Grigoryan V, Choi P, Thayer JF, Lehrer PM, Chang C, Mather M (2022) Heart rate variability (HRV) changes and cortical volume changes in a randomized trial of five weeks of daily HRV biofeedback in younger and older adults. Int J Psychophysiol 181:50-63.

Yoshitake S, Ijiri S, Kehr J, Yoshitake T (2013) Concurrent modulation of extracellular levels of noradrenaline and cAMP during stress and by anxiogenic- or anxiolytic-like neuropeptides in the prefrontal cortex of awake rats. Neurochem Int 62:314-323.

Yoshiyama Y, Higuchi M, Zhang B, Huang SM, Iwata N, Saido TC, Maeda J, Suhara T, Trojanowski JQ, Lee VM (2007) Synapse loss and microglial activation precede tangles in a P301S tauopathy mouse model. Neuron 53:337-351.

Zamalloa T, Bailey CP, Pineda J (2009) Glutamate-induced post-activation inhibition of locus coeruleus neurons is mediated by AMPA/kainate receptors and sodium-dependent potassium currents. Br J Pharmacol 156:649-661.

Zarow C, Lyness SA, Mortimer JA, Chui HC (2003) Neuronal loss is greater in the locus coeruleus than nucleus basalis and substantia nigra in Alzheimer and Parkinson diseases. Arch Neurol 60:337-341.

Zecca L, Mecacci C, Seraglia R, Parati E (1992) The Chemical Characterization of Melanin Contained in Substantia-Nigra of Human Brain. Biochimica Et Biophysica Acta 1138:6-10.

Zecca L, Youdim MBH, Riederer P, Connor JR, Crichton RR (2004) Iron, brain ageing and neurodegenerative disorders. Nature Reviews Neuroscience 5:863-873.

Zecca L, Tampellini D, Gerlach M, Riederer P, Fariello RG, Sulzer D (2001) Substantia nigra neuromelanin: structure, synthesis, and molecular behaviour. J Clin Pathol-Mol Pa 54:414-418.

Zecca L, Bellei C, Costi P, Albertini A, Monzani E, Casella L, Gallorini M, Bergamaschi L, Moscatelli A, Turro NJ, Eisner M, Crippa PR, Ito S, Wakamatsu K, Bush WD, Ward WC, Simon JD, Zucca FA (2008) New melanic pigments in the human brain that accumulate in aging and block environmental toxic metals. P Natl Acad Sci USA 105:17567-17572.

Zerbi V, Floriou-Servou A, Markicevic M, Vermeiren Y, Sturman O, Privitera M, von Ziegler L, Ferrari KD, Weber B, De Deyn PP, Wenderoth N, Bohacek J (2019) Rapid

Reconfiguration of the Functional Connectome after Chemogenetic Locus Coeruleus Activation. Neuron 103:702-718 e705.

Zhang F, Gannon M, Chen Y, Yan S, Zhang S, Feng W, Tao J, Sha B, Liu Z, Saito T, Saido T, Keene CD, Jiao K, Roberson ED, Xu H, Wang Q (2020) beta-amyloid redirects norepinephrine signaling to activate the pathogenic GSK3beta/tau cascade. Sci Transl Med 12.

Zhang S, Smailagic N, Hyde C, Noel-Storr AH, Takwoingi Y, McShane R, Feng J (2014) (11)C-PIB-PET for the early diagnosis of Alzheimer's disease dementia and other dementias in people with mild cognitive impairment (MCI). Cochrane Database Syst Rev 2014:CD010386.

Zhang W, Phillips K, Wielgus AR, Liu J, Albertini A, Zucca FA, Faust R, Qian SY, Miller DS, Chignell CF, Wilson B, Jackson-Lewis V, Przedborski S, Joset D, Loike J, Hong JS, Sulzer D, Zecca L (2011) Neuromelanin Activates Microglia and Induces Degeneration of Dopaminergic Neurons: Implications for Progression of Parkinson's Disease. Neurotox Res 19:63-72.

Zhao S, Rangaprakash D, Venkataraman A, Liang P, Deshpande G (2017) Investigating Focal Connectivity Deficits in Alzheimer's Disease Using Directional Brain Networks Derived from Resting-State fMRI. Front Aging Neurosci 9:211.

Zhu MY, Klimek V, Dilley GE, Haycock JW, Stockmeier C, Overholser JC, Meltzer HY, Ordway GA (1999) Elevated levels of tyrosine hydroxylase in the locus coeruleus in major depression. Biol Psychiatry 46:1275-1286.

Zhu Y, Zhan GX, Fenik P, Brandes M, Bell P, Francois N, Shulman K, Veasey S (2018) Chronic Sleep Disruption Advances the Temporal Progression of Tauopathy in P301S Mutant Mice. Journal of Neuroscience 38:10255-10270.

Zucca FA, Bellei C, Giannelli S, Terreni MR, Gallorini M, Rizzio E, Pezzoli G, Albertini A, Zecca L (2006) Neuromelanin and iron in human locus coeruleus and substantia nigra during aging: consequences for neuronal vulnerability. J Neural Transm 113:757-767.